Dottorato in Biotecnologie
Università di Napoli Federico II

Protein-Based Bioplastics From Seed Oilcakes

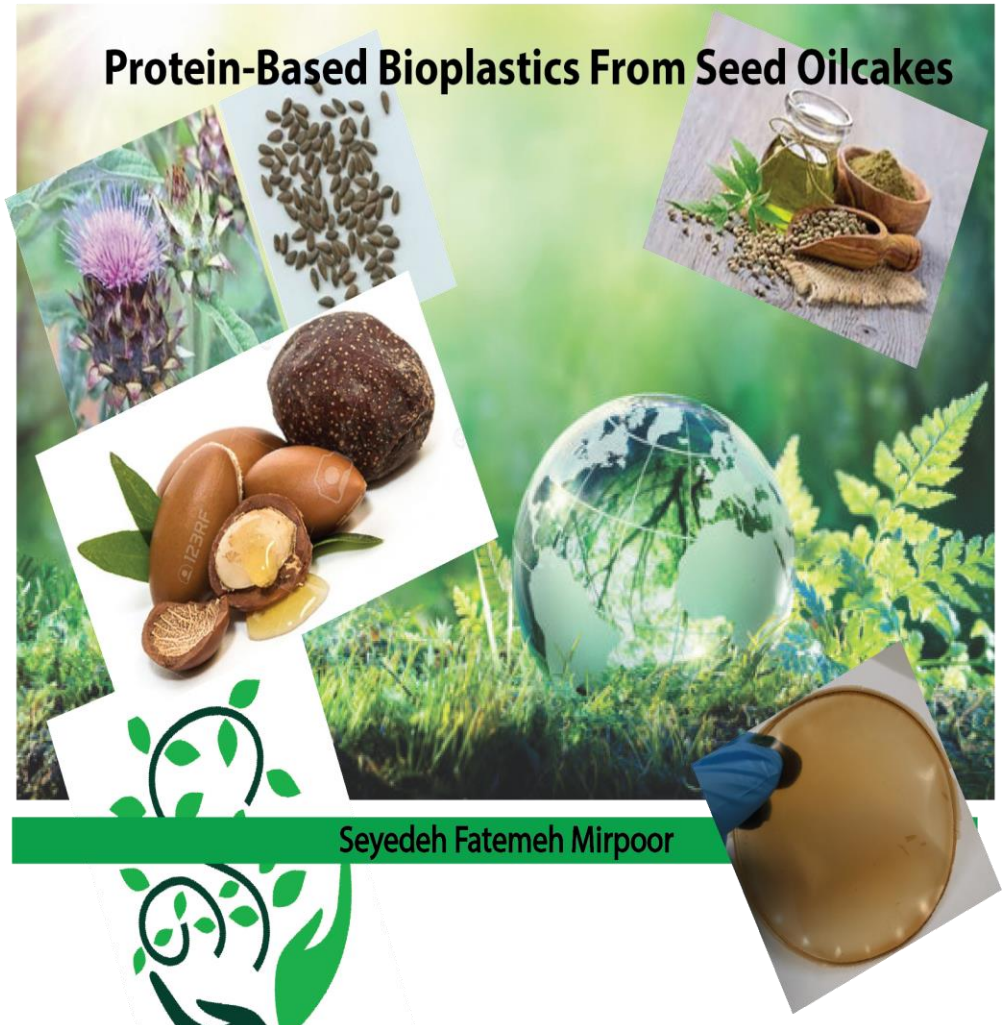

Seyedeh Fatemeh Mirpoor

XXXIV ciclo 2018-2022

Dottorato in Biotecnologie- ***XXXIV ciclo***
Università di Napoli Federico II

Protein-based bioplastics from seed oilcakes

BY

SEYEDEH FATEMEH MIRPOOR

Dottorando:	Seyedeh Fatemeh Mirpoor
Relatore:	Prof. Raffaele Porta
Co-Tutore:	Prof. C. Valeria L. Giosafatto
Coordinatore:	Prof. Marco Moracci
Settore Scientifico Disciplinare:	BIO/10

(Nov 2018 – Jan 2022)

To my supportive husband...

Acknowledgments

Table of Content

TABLE OF ABBREVIATIONS

Abbreviations	Description
ADSA	Axisymmetric Drop Shape Analysis
ADSA-P	Axisymmetric Drop Shape Analysis- Profile
AP	Argan Protein
CLE	Cardoon Leaf Extract
CP	Cardoon Proteins
DF	Dilution Factor
DPPH	1,1-DiPhenyl-2-Picryl Hydrazyl
EB	Elongation at Break
FFS	Film Forming Solution
FT-IR	Fourier Transform Infrared
GC-MS	Gas Chromatography-Mass Spectroscopy
GLY	GLYcerol
HP	Hemp Protein
HPAEC-PAD	High Performance Anion-Exchange Chromatography with Pulsed Amperometric Detection
LDPE	Low Density PolyEthylene
LF	Lignin containing Fraction
mTGase	Microbial TransGlutaminase
MW	Molecular Weight
NC	Nanocrystalline Cellulose
NMR	Nuclear Magnetic Resonance
PAGE	PolyAcrylamide Gel Electrophoresis

PDI	PolyDispersity Index
PO	Posidonia Oceanica
PV	Peroxide Value
RH	Relative Humidity
RI	Refractive Index
SDS-PAGE	Sodium Dodecyl Sulfate PolyAcrylamide Gel Electrophoresis
SEC-TDA	Size-Exclusion Chromatography with Triple Detector Array
SEM	Scanning Electron Microscopy
SOC	Seed Oil Cake
TS	Tensile Strength
WC	Water Content
WV	Water Vapor
WVP	Water Vapor Permeability
YM	Young's Module

TABLE OF FIGURES

LIST OF TABLES

SUMMARY

The use of petroleum-based plastics in different fields, such as food and pharmaceutical sectors, has increased significantly in the last 50 years, being the durability of the plastic materials, as well as their outstanding features, the main reason of their success. However, their worldwide applications led to huge waste-disposal problems and, as a consequence, to a dramatic environmental pollution. These issues have encouraged innovation and research activities in the field of biodegradable plastics, offering alternatives for conventional plastics. One potential option to pursue would be to explore agri-food wastes and by-products for bioplastic production. Numerous different seeds are utilized for edible and non-edible oil extraction and seed by-products following oil extraction. These by-products are known as seed oil cakes (SOCs) and represent roughly 50% of the original seed weight. Since SOCs are rich in fibers, proteins and secondary metabolites, they are considered as promising candidates to be raw material consumed in a biorefinery for the production of bioplastics. In this scenario the present thesis provides insights into the production and characterization of bioplastics obtained by using the proteins extracted from hemp (*Cannabis sativa*), cardoon (*Cynara cardunculus*) and argan (*Argania spinosa* L.) SOCs. Different conditions, such as *i)* change in pH, *ii)* protein amount and *iii)* plasticizer concentration were exploited in order to find the best conditions to develop these protein-based films. To achieve innovative films with improved features the films showing the best characteristics were also modified by adding different additives. Hemp proteins (HPs) and cardoon proteins (CPs) were preliminarily cross-linked by means of microbial transglutaminase (mTGase) and an improvement in both mechanical and barrier properties of the derived films was observed. The results obtained from wrapping peanuts revealed that films prepared with enzyme-modified CPs are able to prolong the shelf life of the oily food. Moreover, nanocrystalline cellulose (NC) and the lignin fraction (LF), obtained from egagropili and added to the HP-based film forming solutions, enhanced the film technological properties. To develop an active bioplastic, cardoon leaf extract (CLE) was tested as additive of CP-based films and a further enhancement of the mechanical, barrier properties and antioxidant activity of the obtained materials was observed. Finally the interfacial properties of the SOC proteins and the surface wetting of the

obtained bioplastics were studied in the period of stay at the Department of Applied Physics of the University of Granada (Spain).

RIASSUNTO

La plastica è diventata parte integrante della vita umana, essendo un materiale economico, leggero e durevole, e potendo essere facilmente modellata in una varietà di prodotti che trovano uso in una vasta gamma di applicazioni. Circa il 4% della produzione mondiale di petrolio e gas, risorsa non rinnovabile, viene utilizzato come materia prima della plastica e un ulteriore 3-4% viene speso per fornire energia per la loro produzione. Vari studi indicano, inoltre, che circa l'80% della plastica che viene prodotta torna nell'ambiente come rifiuti, e una parte significativa di questi rifiuti viene sversata nei mari provocando uno stato di inquinamento delle acque che cresce in maniera esponenziale. La lunga esposizione alla luce e all'acqua salata porta le differenti plastiche a scomporsi in micro- e nano-plastiche, che hanno impatti letali sulla vita marina. La plastica è uno dei maggiori protagonisti del modello di economia lineare che prevede produzione, utilizzo e smaltimento di risorse nell'ambiente. Sempre più spazio sta raggiungendo, invece, l'economia circolare che rappresenta un modello alternativo e più sostenibile: secondo la definizione data dalla Ellen MacArthur Foundation, si parla di un'economia progettata per auto-rigenerarsi, in cui i materiali biologici sono destinati ad essere reintegrati nell'atmosfera, e quelli tecnici devono essere rivalorizzati senza entrare nella biosfera. Le bioplastiche svolgono un ruolo chiave nella transizione verso un'economia circolare attraverso la sostituzione dei fossili con risorse rinnovabili, ed aumentando gli obiettivi di riciclo e l'efficienza nella gestione dei rifiuti. Attualmente, le bioplastiche rappresentano circa l'1% dei 368 milioni di tonnellate di plastica prodotte ogni anno ma, con l'aumento della domanda e l'emergere di materiali, applicazioni e prodotti più sofisticati, il mercato delle bioplastiche va via via crescendo in modo molto dinamico. In questo lavoro sperimentale ci si è focalizzati sulla preparazione di bioplastiche rivolgendo l'attenzione verso l'utilizzo di risorse sostenibili, quali alcune proteine derivanti da scarti alimentari o da lavorazione industriale. La ricerca, infatti, si è incentrata sulle proteine contenute nei pannelli di semi oleosi *(seed oil cakes, SOCs*), la cui produzione mondiale è destinata

principalmente alla generazione di olio alimentare. L'attività sperimentale è stata preceduta da un attento studio della letteratura scientifica che ha portato alla stesura di una rivista sintetica pubblicata recentemente sulla rivista *Trends in Food Science & Technology* (Mirpoor et al., 2021). I SOC rappresentano circa il 50% del peso del seme originario e sono ricchi in fibre, antiossidanti, vitamine, minerali nonché acidi grassi mono- e poli-insaturi. Tali *byproducts* industriali sono stati a lungo sotto i riflettori per le loro molteplici utilizzazioni, come la produzione di mangimi per animali, oli vegetali funzionali, prodotti farmaceutici, biocarburanti e altri usi industriali, e tutto ciò ha portato ad un aumento delle aree di coltivazione dei semi oleosi. La composizione chimica dei SOC è influenzata da diversi fattori, principalmente dalla varietà vegetale e dalle condizioni di crescita ma, poiché i SOC sono ricchi di diverse molecole bioattive di basso e alto peso molecolare, come polifenoli, flavonoidi, proteine e fibre, essi sono stati esplorati soprattutto come possibili fonti biologiche in diverse bioraffinerie. In particolare, le proteine estratte da SOC, prima o dopo la loro purificazione, potrebbero rappresentare una potenziale materia prima per la produzione di bioplastiche, in quanto abbondanti, biodegradabili e poco costose. Le colture più diffuse riguardano la soia (*Glicina max*), il cotone (*Gossypium hirsutum L*.), il girasole (*Helianthus annuus*), le arachidi (*Arachis ipogea*), ma anche il sesamo (*Sesamum indicum*), la canapa (*Cannabis sativa*), il cardo (*Cynara cardunculus*) e l'argan (*Argania spinosa*). Le proteine estratte da questi ultimi tre SOC, ovvero cardo (CP), canapa (HP) e argan (AP) sono state utilizzate in questa tesi per la produzione di bioplastiche. In tutti i casi, per ottenere i SOC, l'olio è stato estratto dai semi mediante *Soxhlet* e le proteine estratte mediante precipitazione isoelettrica. I film sono stati preparati utilizzando il metodo del *casting* ossia versando le soluzioni filmanti (FFS), preparate in presenza di glicerolo (GLY) come plasticizzante, in piastre di Petri. Le FFS venivano preliminarmente sottoposte a studi di stabilità mediante valutazione della dimensione dei colloidi e del potenziale Z, e poi essiccate in una camera climatica a temperatura e umidità controllate. Al fine di poter valutare le possibili applicazioni di tali film in campo industriale, le bioplastiche preparate in diverse condizioni sperimentali sono state analizzate per le loro proprietà meccaniche, di barriera ai gas ed al vapore acqueo e di idrofobicità. Le analisi chimico-fisiche delle FFS hanno dimostrato che per tutte le proteine considerate il pH 12 era un pH ottimale per ottenere soluzioni stabili dal punto di vista del potenziale Z, e che tutte le FFS preparate a tale pH producevano film manipolabili e dotati

di buone proprietà tecnologiche in presenza di GLY. Di seguito sono riportate le caratteristiche dei film ottenuti in diverse condizioni sperimentali da questi 3 tipi di *byproduct*. Alcune di queste proprietà sono state studiate presso il Dipartimento di Fisica Applicata dell'Università di Granada in Spagna. I risultati ottenuti incoraggiano ulteriori indagini poiché i SOC sembrano una potenziale fonte rinnovabile in grado di sostituire, almeno in parte, gli altamente inquinanti polimeri derivati dal petrolio. Infatti lo *scale-up* di questi nuovi materiali potrebbe aprire nuovi orizzonti per produrre bioplastiche innovative adatte all'imballaggio alimentare e non solo.

1) Film ottenuti da proteine provenienti da SOC di cardo (CP): la concentrazione minima di GLY utile per ottenere film manipolabili nelle migliori condizioni sperimentali identificate era del 30% (*w/w* di CP), poiché i film preparati in assenza o in quantità inferiore (10 e 20%) di plasticizzante si erano dimostrati fragili e non potevano essere staccati dalle piastre. I film manipolabili sono stati quindi caratterizzati per il loro spessore e per le loro proprietà meccaniche. Come previsto, è stato riscontrato che lo spessore del film aumentava incrementando la concentrazione delle CP, indipendentemente dalla quantità di GLY presente nelle FFS. Al contrario, tutti i parametri che caratterizzano le proprietà meccaniche dei film risultarono diversi variando sia le concentrazioni di CP che di plasticizzante. Infatti, la resistenza alla trazione (TS) ed il modulo di Young (YM) diminuivano mentre l'allungamento a rottura (EB) aumentava incrementando le quantità di GLY a tutte le concentrazioni di CP utilizzate. Inoltre, è stato dimostrato che le CP agivano efficacemente come substrato della transglutaminasi microbica (mTGasi, EC.2.3.2.13), un enzima capace di catalizzare la formazione di legami isopeptidici, intra- o inter-molecolari, tra residui endoproteici di glutammina e lisina. La modifica delle CP da parte della mTGasi rafforzava la matrice delle bioplastiche ottenute producendo dei materiali con migliorate proprietà meccaniche e di barriera ai gas (O_2 e CO_2) ed al vapore acqueo. Il preventivo trattamento delle CP con l'enzima diminuiva, inoltre, anche l'idroficilità delle biopastiche ottenute. Inoltre la capacità di sigillatura dei film ottenuti con le CP trattate preventivamente con la mTGasi, ed il loro colore verdastro scuro, li rende candidati adatti per il confezionamento di diversi tipi di alimenti la cui *shelf-life* puo' essere negativamente influenzata dalla luce. Infatti in questa tesi è stato dimostrato che tali film, quando rinforzati mediante mTGasi, erano in grado di prevenire l'ossidazione e l'irrancidimento dei lipidi delle arachidi, prolungando la durata di conservazione di questo alimento confezionato mediante tale

packaging. I film di CP sono stati anche funzionalizzati con estratti fenolici delle foglie di cardo stesse (CLE). I CLE, che si sono dimostrati dotati di proprietà antiossidanti, quando aggiunti alle FFS di CP hanno dato origine a materiali con un significativo miglioramento di tutte le proprietà testate. I film contenenti CLE apparivano più omogenei, e mostravano anche un'attività antiossidante più elevata e duratura che conferiva un valore aggiunto alle bioplastiche ottenute.

2) Film ottenuti da proteine provenienti da SOC di canapa (HP): il concentrato proteico ottenuto dai SOC di canapa è stato utilizzato come possibile fonte di biopolimeri per produrre film biodegradabili a diversi valori di pH in assenza o presenza di differenti concentrazioni di GLY (utilizzato come plasticizzante). Esperimenti preliminari hanno mostrato che solo a pH > 6, ed in presenza di almeno il 30% di GLY, è stato possibile ottenere film, di colore giallo/marrone, in grado di essere manipolati. Pertanto, le proprietà meccaniche dei film, preparati sia a pH 7 che a pH 12 con 400 mg HP, sono state determinate in presenza di 30, 40 o 50% GLY. I risultati hanno dimostrato che i film a base di HP, preparati a pH 12, avevano valori di TS ed EB sempre più elevati e, in particolare, quelli contenenti il 50% di GLY esibivano migliori prestazioni meccaniche, essendo abbastanza resistenti ed estremamente flessibili e plastici. Le proprietà meccaniche osservate, diminuendo le concentrazioni di HP da 400 a 300 e 200 mg, hanno confermato che i film contenenti 400 mg di proteine e preparati a pH 12 in presenza del 50% GLY erano i materiali più promettenti e degni di ulteriori studi. Anche le HP hanno mostrato di agire come substrato della mTGasi. Vale la pena precisare che, anche in questo caso, per ottenere film manipolabili, è stato necessario aggiungere GLY (almeno il 30%) alle FFS contenenti HP reticolate dalla mTGasi. Le proprietà meccaniche di tali film, inoltre, erano significativamente influenzate dalla presenza dei legami isopeptidici prodotti dalla mTGasi. I film ottenuti con HP sono stati analizzati anche per determinare la loro capacità di termosaldatura, poiché, come è noto, questa caratteristica è fondamentale per le loro potenziali applicazioni industriali come sistema di confezionamento di alimenti. Le analisi effettuate hanno dimostrato che tutti i film potevano essere termosaldati e che la forza di sigillatura delle pellicole ottenute con le HP trattate con l'enzima era maggiore raggiungendo un valore di 30 N/m usando 20 U/g di enzima. Con tale quantità di enzima anche l'idrofilicità dei film risultava diminuita. Inoltre, alcuni film sono stati anche rinforzati mediante nanocellulosa cristallina (NC) o frazione di lignina (LF) ottenute da egagropili,

agglomerati sferici o ovali di colore marrone chiaro e di consistenza feltrosa, costituiti da residui fibrosi di piante del genere *Posidonia,* che si accumulano sulle spiagge portate a riva dalle onde e dalle correnti. I risultati hanno indicato che la microstruttura di tali materiali, quando preparati in presenza di NC e LF, erano molto omogenei, indicando una buona dispersione di questi due additivi nella matrice dei film. Pertanto, i biocompositi rafforzati con questi additivi hanno mostrato proprietà meccaniche e di barriera migliorate, nonché una maggiore capacità di resistenza all'acqua, indicando una possibile utilizzazione degli egagropili, finora considerati un rifiuto da eliminare dalle spiagge dove si accumulano.

3) Film ottenuti da proteine provenienti da SOC di argan (AP): per il SOC proveniente dall'argan, è stata preliminarmente osservata la particolarità che, data la grande quantità di olio presente nei semi di questa pianta, il materiale ottenuto dopo l'estrazione di olio ne conservava ancora una notevole quantità, evidente anche macroscopicamente durante la manipolazione dei film prodotti. La minima quantità di proteina per ottenere film manipolabili era di 300 mg con una concentrazione di GLY pari al 40% (*w/w* di AP). Tuttavia, i risultati ottenuti hanno messo in evidenza che l'uso di 600 mg di AP con l'aggiunta del 50% di GLY, consentivano l'ottenimento di una bioplastica con proprietà meccaniche superiori e, in particolare, tali film esibivano una buona estensibilità (allungamento a rottura pari a circa l'80%). Sono stati inoltre valutati sia il loro contenuto d'acqua che la loro capacità di assorbirne; tali valori si attestavano rispettivamente intorno al 14% e 12%, dati in linea con i risultati ottenuti su altri materiali idrocolloidali di origine proteica. Lo studio delle proprietà barriera ai gas ed al vapore acqueo ha dimostrato che i materiali ottenuti hanno caratteristiche paragonabili ed in alcuni casi anche migliori a quelle delle bioplastiche già presenti sul mercato, quali Mater-Bi® e Viscofan. Esperimenti condotti presso il Dipartimento di Fisica Applicata dell'Università di Granada, volti allo studio delle proprietà di superfice e di assorbimento dell'acqua, hanno dimostrato che tali materiali hanno la superficie più idrofoba degli altri materiali analizzati, e che presentano un maggior angolo di contatto dovuto alla presenza di lipidi nel concentrato proteico estratto.

INTRODUCTION

1. Introduction

1.1. Plastics and plastic pollution

The use of petroleum-based plastics in different fields, such as food and pharmaceutical sectors, has increased significantly in the last years, being the durability of the plastic materials, as well as their outstanding features, the main reason of their success. However, their worldwide applications led to huge waste-disposal problems and, as a consequence, to a dramatic environmental pollution. Every year 300 million tons of plastic wastes are generated and only less than 10% of them are recycled. The remaining part of plastic materials are disposed in landfills and oceans releasing toxic petro-polymers, which are swallowed by marine animals killing more than 100,000 of them each year (Porta, 2019; Geyer, Jambeck, & Law, 2017). Therefore, the replacement of fossil-based packaging materials with the ones based on renewable and biodegradable polymeric sources are on the rise (Letcher, 2020; Jiang et al., 2020).

1.2. Bioplastics

Bioplastics seem an attractive eco-friendly alternative to petroleum-based plastics since they can be easily degraded by the enzymes present in different microorganisms. The main polymers used so far to prepare these innovative biomaterials are aliphatic polyesters (e.g. polylactic acid and polyhydroxyalkanoates), proteins (e.g. soy proteins, collagen, gelatin, zein) and numerous polysaccharides (e.g. cellulose, starch, chitin, pectins) obtained from plant or animal feedstocks (Porta, 2019).

1.3. Proteins from Seed Oil Cakes (SOCs)

Numerous different seeds are utilized mainly for edible oil extraction and seed by-products following oil extraction, known as seed oil cakes (SOCs), represent roughly 50% of the original seed weight. Since SOCs are rich in fibers, proteins and secondary metabolites, they are considered as promising candidates to be raw material for the production of high-value added products such as bioplastics.

As the COVID-19 pandemic led to the lockdown at the very beginning of the 34th PhD cycle, thus preventing to log into and experimentally work in the lab, an extensive study of the existing bibliography about the utilizations of SOCs in different sectors was carried out at home by using remote connection. This investigation led to the publication of an extensive review paper on SOCs from the most cultivated oilseed crops all over the world as well as from cardoon (*Cynara cardunculus*) and hemp (*Cannabis sativa*) that are part of the subject of the present thesis (*Mirpoor, S. F., Giosafatto, C. V. L., & Porta, R. (2021). Biorefining of seed oil cakes as industrial co-streams for production of innovative bioplastics. A review. Trends in Food Science & Technology*).

Writing this review also gave some good ideas to work with hemp and cardoon SOCs, as well as to focus the attention also on non-conventional SOCs such as from *Argania spinosa*, a very popular plant for the outstanding properties of the oil contained in its seeds as described below. *Argania spinosa* L. (*Sapotaceae* family), known as Argan, is a plant cultivated in abundance in desert and semi-desert regions such as Morocco and the south-west of Algeria. The fruit is 2-4 cm long and 1.5-3 cm broad, with a sweet-smelling but unpleasantly flavoured layer of pulpy pericarp surrounded by a thick and bitter peel. This also surrounds the very hard nut which contains one to three small oil-rich seeds (Haloui, & Meniai, 2017) (Figure 1). The average oil content varies between 3.05% and 3.67% on dry fruit basis. However, the average kernel oil content is around 47% (Aithammou et al., 2019) but, for the incredibly low extraction yields (2 to 3.2 kilos of oil per 100 kilos of dried fruit), this oil is very expensive. Its dietary applications are the most important: it is described that such oil prevents cardiovascular risks, acts as a choleretic and hepatoprotective agent, as well as it helps to prevent hypercholesterolemia and atherosclerosis (El Abbassi et al., 2014). It is eaten directly and used also for cooking. Other applications include its use as a cosmetic product. The SOC resulting from oil extraction is generally used to feed animals (Cherki et al., 2006). It has been reported that the SOC has high levels (91%) of dry matter (48.4% protein, 17.6% fiber, 18.9% fat and ash (3.6%). In addition, it contains significant levels of calcium (6.9 g/kg), phosphorus (6.4 g/kg), potassium (10.4 g/kg), and magnesium (3.3 g/kg) (Lakram et al., 2019).

Figure 1. Argan seeds

1.4. Additives and processing aids for protein-based film improvement

1.4.1. Plasticizers

Protein-based films generally exhibit poor mechanical and water vapor (WV) barrier properties, so that their application in food packaging sector is still quite limited. Therefore, in order to improve the protein-based film properties, different preliminary treatments of the protein sources, such as gamma-irradiation, heating or cross-linking, have been often performed, as well as the protein blending with other biopolymers or additives (Xu et al., 2012; Amadori et al., 2015; Haghighi et al., 2020; Jiménez-Rosado et al., 2020; Wihodo and Moraru, 2013).

Plasticizers are added to polymers to reduce brittleness and improve the flexibility of the polymer matrix (De Groote et al., 2002). Plasticization reduces the relative number of polymer–polymer contacts, thereby decreasing the rigidity of the three-dimensional structure and allowing the material deformation without rupture (Varughese and Tripathy, 1993). Water is considered the most powerful ‘‘natural’’ plasticizer of hydrocolloid-based films since it is able to reduce the glass transition temperature and to increase the free volume of biomaterials (Cheng et al., 2006; Karbowiak et al., 2006). Several studies have been carried out on the application of different chemical plasticizers such as glycerol (GLY), ethylene glycol, diethylene glycol, triethylene glycol, tetraethylene glycol, polyethylene glycol and sorbitol

(Fitri et al., 2018; Suyatma et al., 2005; Cao et al., 2009; Escamilla-García et al., 2017).

1.4.2. Microbial transglutaminase (mTGase)

One of the most extensively used tool to reinforce protein-based films is represented by microbial transglutaminase (mTGase; EC.2.3.2.13), a calcium independent enzyme responsible for catalysing the formation of intermolecular ε-(γ-glutamyl)-lysine cross-links into proteins via an acyl transfer reaction (Giosafatto et al., 2020). The transamidation reaction occurs either in the same (Figure 2, panel A) or in a different polypeptide chain (Figure 2, panel B) between an acyl acceptor substrate (ε-amino group of an endoprotein lysine residue) and an acyl donor substrate (ɣ-carboxamide group of an endoprotein glutamine residue). mTGase is active in a wide range of pH (4-9), resistant between 4 and 60°C, commercially available, food grade and useful to modify *in vitro* protein structure and biological properties (Giosafatto et al., 2020; Kieliszek and Misiewicz, 2014).

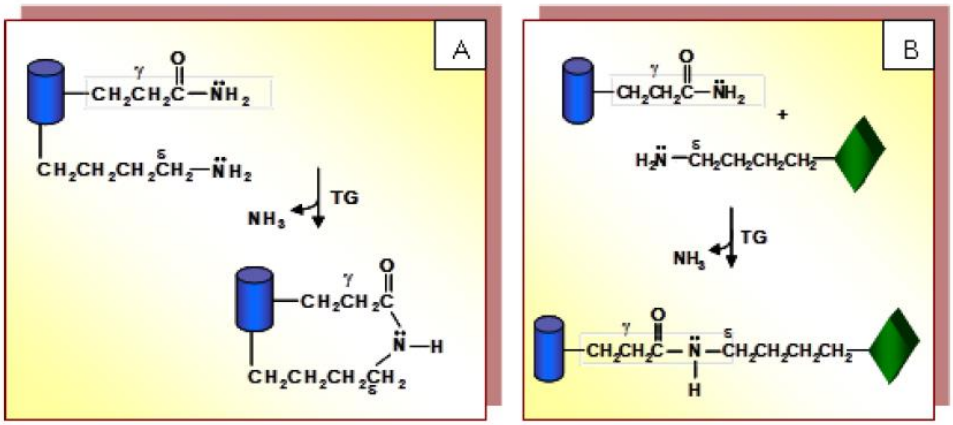

Figure 2: Intramolecular (A) and intermolecular (B) cross-linking reaction catalysed by microbial transglutaminase.

1.4.3. Nanocrystalline cellulose (NC) and lignin fraction (LF) from egagropili

Biocomposites containing plant- or wood- based fibers have been exploited thus far in an increasing range of items to reinforce plastics, since they have several advantages over synthetic additives. *Posidonia oceanica* (PO) is one of the most abundant Mediterranean endemic

species, covering 60% of the seabed from 0 to 40 m depth (Den Hartog and Kuo, 2007) and about fifty thousand km^2 of coastal sandy areas (Fornes et al., 2006). Fibre-like leaves of PO that are at the base of rhizomes and stems, cluster together very closely and generate these characteristic free-floating and brown coloured balls, called “egagropili”. Since egagropili represent a problem, first of all for their negative visual impact (Balestri et al., 2006), the municipalities are forced to remove and dispose them in landfills as municipal wastes with non-negligible costs. Therefore, egagropili can be considered as a lignocellulosic resource potentially useful to be added to the biodegradable materials as a reinforcement additive.

1.4.4. Cardoon leaf extract

Aiming to further improve food packaging materials, many studies have exploited natural additives with antimicrobial and antioxidant activity to produce bio-active food packaging (Shojaee-Aliabadi et al., 2013). In this regard, the cardoon leaf extract (CLE) is known for its therapeutic potential as a diuretic, choleretic, cardiotonic, antidiabetic and anti-hemorrhoidal agent (Ramos et al., 2017; Velez et al., 2012). Several studies have focused on the antioxidant activity of CLE, strictly related to the polyphenol fraction, mainly composed of hydroxycinnamic derivatives, such as mono- and dicaffeoylquinic acids, and flavonoids, such as apigenin and luteolin (Dias et al., 2018; Scavo et al., 2019).

1.5. Application of cardoon-based bioplastics for peanut wrapping

One of the important legumes that are consumed worldwide are peanuts (*Arachis hypogea*) (Rossi-Márquez et al., 2021) that contain approximately 50% oil, mostly composed of unsaturated fatty acids. Peanuts are a good source of tocopherols, natural antioxidants soluble in lipids. They contribute to the free radical scavenging activity protecting against lipid oxidation. However, these antioxidants degrade in the presence of oxygen molecules and/or high temperature and, as a consequence, the degraded products formed lead to sensory or nutritional deterioration (Christopoulos & Tsantili, 2011). Several factors can affect the lipid oxidation in peanuts such as storage condition, temperature, oxygen, light and humidity (Torres et al., 2014). In this context, a suitable packaging able to act as a gas and light barrier might help to reduce lipid oxidation rate during peanut storage.

1.6. Surface properties and wetting of protein-based bioplastics

This part of experimental work was carried out at the Department of Applied Physics of University of Granada (Spain), under the supervision of Prof. Julia Maldonado Valderrama, where experiments related to the investigations of the properties of the protein concentrates obtained from SOCs were performed. It is well known that proteins can stabilize the emulsions since they are amphiphilic molecules able to interact with both lipidic and aqueous phases. In this case, there are some important factors that should be investigated to determine the physical stability of the emulsion stabilized by proteins, such as the interfacial tension, the interfacial elasticity and viscosity (Aguilera-Garrido et al., 2021). In fact, the reduction in protein interfacial tension as a function of time specifies its surface activity (Zhou et al., 2021). During the adsorption into the interface film, proteins change their conformations and unfold to the more desired energy level. Viscoelastic interfacial films, produced as a result of intermolecular interactions, occur among the proteins that are adsorbed at the interface (Kim et al., 2005; Lam & Nickerson, 2013).

The second part of these experiments focused on the characterization of the surface of the obtained protein-based films by measuring the advancing and receding contact angles of water droplet on the surface of the films. Advancing contact angle is the maximum observable contact angle, whereas the minimum observable contact angle referred to as receding contact angle (Ruiz-Cabello et al., 2011). The contact angle depends on several parameters including the technique of measurement, the solid surface quality, the liquid purity, the size and creation of the liquid–vapor interface (Moraila-Martínez et al., 2012). It is reported that the surface heterogeneity or roughness can affect the hysteresis contact angles (Eral et al., 2013). In fact, the roughness of a hydrophobic surface decreases the ratio between the real solid-liquid area and the apparent contact area (Ruiz-Cabello et al., 2018).

1.7. Aim of PhD project

The objective of the present thesis was the development and characterization of novel films obtained from proteins contained in by-products of oil industry, namely SOCs. All the films were obtained in the presence of GLY as plasticizer. Further additives or processing aids were preliminarily used to covalently modify the protein structure (mTGase) or grafted into the film matrix (NC, LF or CLE) in order to reinforce or to render bioactive the films. The mechanical and barrier

properties as well as the hydrophobicity of the obtained films were investigated. Finally, peanuts were wrapped in the cardoon-based bioplastics and the ability of the obtained biomaterials to improve the shelf-life and prevent lipid oxidation of food was investigated. Some of experimental work was carried out at the Department of Applied Physics of University of Granada (Spain), where the interfacial properties of the protein concentrates from SOCs were investigated.

2. Materials and methods

2.1. Materials

Hemp seeds, purchased from Consorzio Goji Italia (Andria, Italy), were a generous gift of prof. Daniele Naviglio. Cardoon seeds were recovered in April 2019, from a field experiment made in Sant'Angelo dei Lombardi (Avellino, Italy), a hilly area about 700 m above sea level, characterized by cold and rainy winters and low-fertility soil. Argan seeds were purchased from a local market in Marrakech (Morocco). Egagropili sea balls were collected in the sardinian Poetto beach (Cagliari, Italy) and stored at 4 °C until used. mTGase from Streptoverticillium sp. (Activa WM; specific activity 90 Units/g) was supplied by Prodotti Gianni SpA (Milano, Italy). The enzyme solution was prepared by dissolving the commercial preparation in distilled water at a concentration of 100 mg/mL. Roasted unsalted peanuts (Virginia variety) were purchased from a local market in Naples (Italy). Cardoon leaves were separated from fresh plants obtained from Sant'Angelo dei Lombardi (Avellino, Italy) and stored in vacuum sealed plastic bags at −20 °C. Then, 40 g of cut cardoon leaves were placed in a filter bag (porosity 100 μm) and CLE was obtained by inserting it into the Naviglio® extractor chamber (Lab. model 500 cm^3 capacity). MaterBi, as well as low density polyethylene (LDPE), were from local market shopping bags, (Naples, Italy). All other reagents and solvents were of the highest purity from Carlo Erba (Milan, Italy).

2.2. Protein concentrates from seed oilcakes (SOCs)

Oil seeds were grinded at a speed of 1000 *x g* for 3 min in a Knife Mill Grindomix GM 200 (Grindomix GM200, Retsch GmbH, Haan, Germany) and then defatted for 6 h by using a soxhlet apparatus (3:1, v/w hexane:grinded seeds) and, finally, the obtained hemp, cardoon and argan seed oilcakes (SOCs) were dried at 50°C in an oven for 2 h. Isoelectric-precipitation technique was used for extracting SOC proteins according to Dapčević-Hadnađev et al. (2018) with minor modifications. SOCs were suspended in water at 1:10 ratio (w/v) and 1.0 N NaOH was added under constant stirring to adjust the pH to 11. After 1 h of stirring, the suspension was centrifuged for 15 min at 5000

rpm and the pH of the collected supernatant was adjusted to pH 5.4 using 1.0 N HCl. Then, the precipitate was separated by another centrifugation at 5000 *x g* for 15 min and the obtained pellet collected and dried in an environmental chamber at 25 ºC and 45% relative humidity (RH). The protein content of the obtained protein concentrate powder was determined by the Kjeldahl's method (AACC, 2003) using a nitrogen conversion factor of 6.25.

2.3. NC and LF from egagropili

Egagropili balls were reshaped to rhizome fibers by hands, then washed and rinsed vigorously in distilled water in order to remove sand, salts and other soil contaminants, and finally dried in an oven at 80 °C for 24 h. The dried egagropili fibers were grinded in a rotary mill (Grindomix GM200, Retsch GmbH, Haan, Germany) at a speed of 1000 *x g* for 3 min to a 60-mesh sieve size. Cellulose extraction was carried out as reported by Ilyas et al., 2018, with some modifications. In the first step, 20 g of grinded egagropili fibers were dewaxed by means of Soxhlet apparatus with 440 mL of toluene/ethanol (2:1 *v/v*) during 24 h and oven dried overnight at 105 °C. Afterwards, delignification process has been carried out by dispersing at 70 °C for 2 h the dewaxed egagropili powder in 600 mL of 1.7% sodium chlorite solution brought at pH 3.5 by acetic acid. This process was repeated 3 times consecutively until the color changed from brown to white/yellowish. The resulted bleached fibers, known as holocellulose, were filtered by using a filter paper and washed with distilled water until the filtrate became neutral. The first filtrate obtained in the delignification step was referred as the lignin containing fraction (LF). A quantitative analysis, carried out by calculating the dry weight of LF, indicated that 152 mg of LF were obtained from 1 g of grinded egagropili powder. To remove hemicellulose and residual pectin, the obtained holocellulose was treated with 5% potassium hydroxide for 24 h at room temperature followed by an exposure for 2 h at 90 °C. Finally, the obtained cellulose fraction was filtered and washed several times until pH neutralization, and finally dried at 55 °C for 18 h. NC was obtained by sulfuric acid hydrolysis of the egagropili cellulose fraction according to the procedure described by Sanyang et al., 2016. Acid hydrolysis started by adding 1 g of cellulose fraction into 10 mL of sulfuric acid solution (65%, *w/w*) and by stirring the reaction mixture at 45 °C for 45 min in order to totally hydrolyze the amorphous regions of cellulose. Hydrolysis reaction was stopped by diluting ten-times the suspension by cold distilled water,

followed by repeated washing of the pellet obtained by centrifugation at 10,000 *x g* for 10 min, until the neutral pH was reached. The resulting precipitate containing NC was finally freeze-dried and, then, the obtained powder was dispersed in distilled water and subjected to ultrasonication for 10 min at 400 W to stabilize NC dispersion by eliminating its excessive aggregation. The quantitative gravimetric determination indicated that 225 mg of NC were obtained from 1 g of grinded egagropili powder. The entire extraction process, summarized in Figure 3, was monitored by Fourier-transform infrared spectroscopy analysis using a model ALPHA spectrometer (Bruker, Leipzig, Germany) equipped with an attenuated total reflectance accessory.

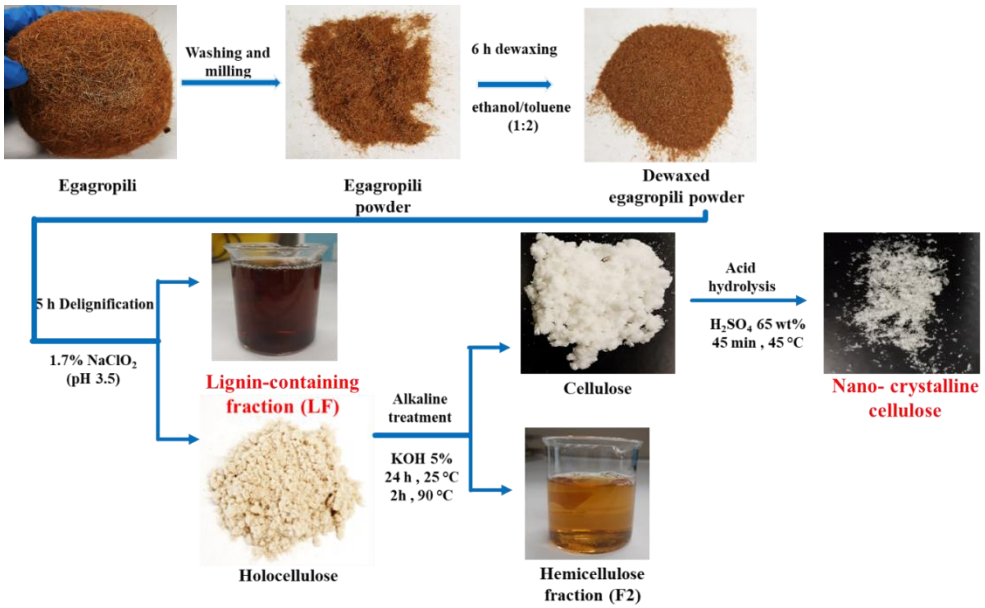

Figure 3. Scheme of the extraction procedure of nanocrystalline cellulose (NC) and lignin containing fraction (LF) from egagropili.

2.4. Determination of zeta potential and particle size

Zeta potential and Z-average values of the FFSs containing the different SOC protein concentrates were determined by a Zetasizer Nano-ZSP (Malvern®, Worcestershire, UK) equipped with an automatic titrator unit (MPT-2) to study the effect of both pH and additives. The device was equipped with a helium-neon laser of 4 mW output power operating at the fixed wavelength of 633 nm (wavelength of laser red emission). The instrument software programmer calculated the zeta potential through the electrophoretic mobility by applying a voltage of 200 mV using the

Henry equation. The zeta potential and Z-average were studied in triplicate samples immediately after their preparation to prevent possible alterations in molecular interaction during their storage (Schmid et al., 2015).

2.5. Two-dimensional polyacrylamide gel electrophoresis (2D PAGE)

2D PAGE was carried out by analyzing 100 µg of protein onto 7-cm IPG strips (pH 3–10) previously dissolved in 125 µL of sample rehydration buffer (Bio-Rad). 2 mL of mineral oil were added to each strip in order to prevent the evaporation during the 24 h protein separation. In the second step, protein separation according to molecular mass has been carried out by placing the gel horizontally into the precast SDS-PAGE gel (12%, Mini-protein gels, Bio-Rad) and performed at a current of 220 V for 40 min. The gel was finally stained with Coomassie Brilliant Blue R250 (Bio-Rad, Segrate, Milan, Italy).

2.6. Sodium dodecyl sulphate polyacrylamide gel electrophoresis (SDS-PAGE)

The protein pattern of SOC protein concentrates (100 µg protein) incubated at 37 °C and pH 7.5 for different times (5, 10, 20, 40, 60 min and 2, 4 and 24 h), in the presence of 80 mM Tris-HCl buffer and different concentrations of mTGase (0, 5, 10, 20, 40 U/g of protein concentrates), was analyzed by 12% SDS-PAGE as described by Laemmli (Laemmli, 1970). 25 µL of sample buffer (62.5 mM Tris-HCl, pH 6.8, containing 4 % (w/v) SDS, 30 % (v/v) GLY, 10% (v/v) β-mercaptoethanol, and 0.05 % (w/v) bromophenol blue) was added to each sample and all the samples were then heated for 5 min in a boiling water bath to inactivate the enzyme. 25 µL of each sample were loaded into each well and the electrophoresis was performed at a constant voltage (80 V). Subsequently, protein bands were stained with Coomassie Brilliant Blue R250 (Bio-Rad, Segrate, Milan, Italy) and, then, the gel was placed in destaining solution (acetic acid: methanol: water 10: 10: 80 (v/v/v)). Bio-Rad Precision Protein Standards were run as molecular weight markers.

2.7. Protein-based film forming solution (FFS) and film preparation

2.7.1. Preparation of hemp protein (HP)-based FFS

Preliminary experiments were carried out to find the best conditions for developing HP-based films. HP stock solution (2% w/v) was prepared by dissolving the HP concentrate in distilled water and by adding 1 N NaOH, under constant stirring at room temperature, until the pH of the solution was brought at pH 7 or 12. Finally, different FFSs (25 mL), containing 200, 300 or 400 mg of HPs and different concentrations of GLY (10-50%, w/w of proteins), were prepared.

2.7.2. HP-based FFSs prepared in the presence of mTGase

Some FFSs were prepared in the presence of mTGase as follows: 400 mg HPs were incubated for 2 h, at 37°C and pH 7.5, in the absence or presence of different amounts of mTGase (5, 10, 20, 40 U/g HPs). At the end of incubation, the pH was adjusted to pH 12 by 1 N NaOH addition and all the samples were heated at 80°C in a water bath for 20 min to deactivate the enzyme. After cooling of the samples at room temperature, 0.2 g GLY were added to 25 mL of FFS to obtain a concentration of plasticizer of 50% (w/w of proteins).

2.7.3. HP-based FFSs prepared in the presence of egagropili-derived nanocrystalline cellulose or lignin fraction

FFSs (25 mL), containing 400 mg of HPs and 50% GLY (w/w protein), were prepared at two different pHs in the presence of different amounts of either NC (2, 4, 6% w/w of proteins), at pH 9, or the extensively dialyzed LF (3, 6, 9% w/w of proteins), at pH 12.

2.7.4. Cardoon protein (CP)-based FFSs preparation

To find out the best conditions for developing the CP-based films, FFSs containing 200, 300 and 400 mg of CPs were prepared at pH 12 in the presence of different concentrations of GLY (0, 10, 20, 30, 40, 50%, w/w of protein). Further experiments have been conducted with a FFS prepared at pH 12 in the presence of 400 mg of CPs and 50% GLY (w/w protein).

2.7.5. CP-based FFSs prepared in the presence of mTGase

CP-based FFSs were incubated, in the presence of different amounts of mTGase (0, 10, 20, 40 U/g CP), at pH 7.5 for 2 h at 37 °C. Then, the pH of the reaction mixtures was adjusted to 12 with 1 N NaOH, the samples heated at 80 °C in a water bath for 20 min to deactivate the

enzyme and, finally, cooled down to room temperature before GLY addition (50% w/w protein).

2.7.6. Bioactive CP-based protein FFS preparation

CP concentrate was dispersed in distilled water (2% w/v), the pH was adjusted to pH 12 by 1 N NaOH and the dispersion was stirred for 2 h at room temperature for complete CP dissolution. Then, CLE (16 mg/mL) was added to the CP solution at different concentrations (15 and 30% w/w of CPs) and the mixture was stirred for 1 h. GLY was then added to obtain a final concentration of 50% (w/w protein) and the obtained FFS was stirred for further 30 min.

2.7.7. Argan protein (AP)-based FFS preparation

FFSs of AP concentrate were prepared by using 300, 500, 600 and 800 mg of argan proteins dissolved at pH 12 and added with different concentrations of GLY (0, 10, 20, 30, 40, 50%, w/w of protein).

2.7.8. FFS casting

All the above mentioned FFSs were cast onto 8 cm diameter polycarbonate Petri dishes (Figure 4) and allowed to dry in an environmental chamber at 25 °C and 45% RH for 24 h. The dried films were peeled, intact, from the casting surface and analyzed after their conditioning at 53% RH and 25 °C by placing them in a desiccator over a saturated solution of $Mg(NO_3)_2 \cdot 6H_2O$ for 24 h. Finally, each film was characterized for their physicochemical, morphological, and biological properties.

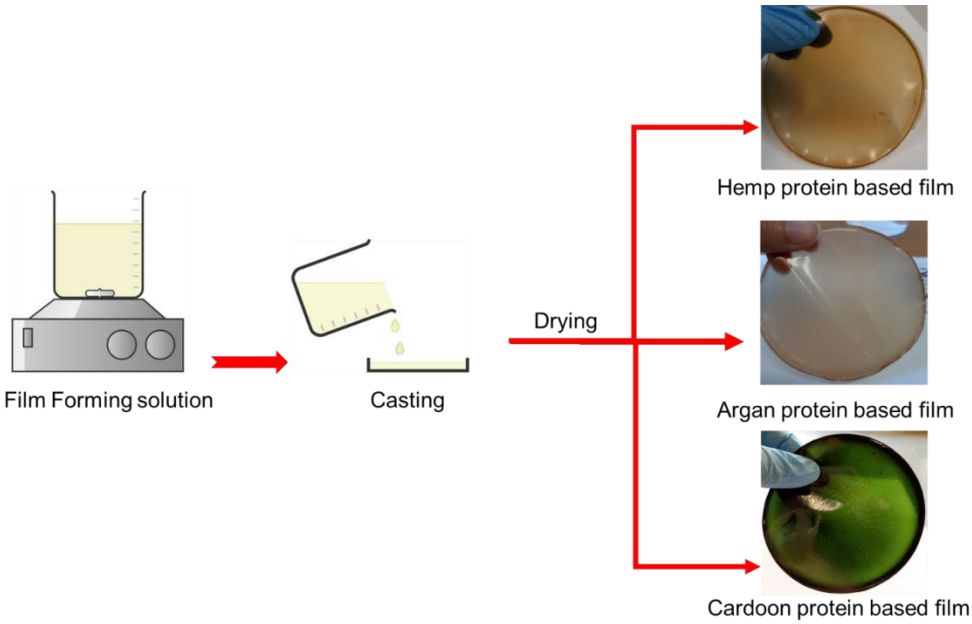

Figure 4. Scheme of film preparation method

2.8. Film physicochemical and morphological characterization

2.8.1. Mechanical properties of films

Film thickness was determined randomly in five different locations by using a micrometer (IP65 Alpa Exacto) with a precision of 0.001 mm. The tensile strength (TS), elongation at break (EB) and Young's modulus (YM) of the manufactured films were analyzed by an Instron universal testing instrument model no. 5543A (Instron Engineering Corp., Norwood, MA, USA). The conditioned films were cut into strips with a width of 10 mm and a length of 60 mm and five specimens of each film (1 kN load and 5 mm/min speed) were then tested according to the ASTM D882-97 (1997). The film seal strength, evaluated according to ASTM E88-07a (ASTM, 2007), was determined by reducing each film into strips of 5 × 2.5 cm, and one strip was placed onto another one of the same sample. Then, all the samples were placed into an automatic heat sealer (MagicVac®Axolute Mod: P0608ED, Italy) and heat-sealed at 100°C for 10 seconds at 0.7 bar. The seal strength (N/m), was measured by means of the above mentioned dynamometer by dividing the maximum peak force detected to the film width.

2.8.2. Film hydrophilicity properties

2.8.2.1. *Moisture content*

Film moisture content was analyzed according to the method described by Zahedi et al., 2018, with slight modifications. The film specimens (3×3 cm^2) were placed on the aluminum plates and weighed after drying at 105 °C for 24 h in an oven. Moisture content of the films was evaluated by calculating the difference between the initial and final weight of each sample before and after drying using the following equation:

$$\text{Moisture content} = [(W_i - W_d) / W_i] \times 100 \quad (1)$$

where W_i and W_d represent the weights of the initial and dried film, respectively.

2.8.2.2. *Water solubility*

In order to determine the film water solubility, the initial weight (W_i) of each film sample (3x3 cm^2) was determined after oven drying at 105 ℃ for 24 h. The dried samples were then immersed in 30 mL of distilled water and stirred in a shaker incubator at 25 °C for 24 h. After that, the final weight (W_f) of each sample was obtained by removing and drying in oven at 105 °C for another 24 h. Finally, water solubility was calculated using the following equation:

$$\text{Water solubility (\%)} = (W_i - W_f) * 100 / W_i \quad (2)$$

2.8.2.3. *Swelling ratio*

Film swelling ratio was examined using a gravimetric method as reported by Roy and Rhim (2020). Each film sample (3×3 cm^2) was pre-weighed (W_i) and then immersed in 30 mL of distilled water at 25°C for 1 h. After film surface drying by an absorbent paper, the films were finally weighed again (W_s). The swelling ratio was calculated using the following equation**:**

$$\text{Swelling ratio} = [(W_s - W_i) / W_i] \times 100 \quad (3)$$

All the above mentioned experiments of film water resistance were repeated three times.

2.8.2.4. *Contact angle*

The surface hydrophobicity of the films was measured using a homemade water contact analyzer. The film strips were placed on the horizontal stage and, then, 10 µL of distilled water was dropped on the film surfaces. The image of water drop was captured using a fixed digital microscopic camera after 30 sec. Five measurements were reported as the average of the contact angle values.

2.8.3. Film density

To determine the density, the film samples were cut (2x2 cm) and their weight and thickness at three random places were measured. Density of films was calculated as the proportion between the weight and volume of each films (thickness x film surface area).

2.8.4. Film opacity

Film opacity values were recorded by measuring light transmission through the films at a wavelength of 600 nm divided by the film thickness (mm), using a UV visible Spectrophotometer (SmartSpec 3000 Bio-Rad, Segrate, Milan, Italy), according to the method previously described by Jahed et al. 2017. Four strips of each film were cut (1cm × 4cm) and put in a quartz cuvette and air was considered as a blank reference.

2.8.5. Film scanning electron microscopy (SEM)

The surface and cross-section microstructure of the films were observed by scanning electron microscopy (Nova NanoSem 450-FEI-Thermo Fisher, Scientific, Waltham, MA, USA). The samples were coated with thin layers of gold and platinum using a sputter coater at a current of 20 mA for 90 sec and, then, the images were taken at an accelerating voltage of 3 kV, (4.4–5.2) mm.

2.8.6. Film color measurement

The colour parameters of CP-based films prepared in the absence or presence of different concentrations of CLEs were measured using a Mightex® HRS series compact CCD spectrometer HRS-VIS-025 (Mightex, Toronto, ON). All measurements were made at 5 random positions of each film. The color parameters, including “L” as well as “a” and “b” values, indicate lightness/darkness (0–100),

greenness/redness (-60 to +60) and blueness/yellowness (-60 to +60), respectively, of the materials tested. The total color difference (ΔE) was determined by the following equation:

$$\Delta E = \sqrt{(L* - L)^2 + (a* - a)^2 + (b* - b)^2} \quad (4)$$

where L* (99.94), a* (-1.07) and b* (3.74) were the color parameter values of the standard white tile (Bai et al., 2019).

2.8.7. Film water vapor and gas permeability

Measurements of film water vapor (WV) and gas (CO_2 and O_2) permeability were performed in duplicate for each film (50% RH, 25 °C and 101 kPa for gas permeability; 90% RH, 38 °C and 6 kPa for WV permeability) by using a Total Perm apparatus (ExtraSolution s.r.l., Pisa, Italy) according to the Standard Methods ASTM D3985-05 (2010), ASTM F2476-13 (2013), ASTM F1249-13 (2013). The measurements were carried out after conditioning the film specimens for 24 h at 50% RH and placing them in the aluminum masks to reduce the film test area to 2 cm^2.

2.9. Peanut (*Arachis hypogea*) packaging by CP-based films

2.9.1. Experimental design of peanut packaging, sampling and storage conditions

Peanut samples (8 g) were divided into four groups and three of them were wrapped with three different packaging materials (CP-based and mTGase (20U/g of CPs) cross-linked CP-based films, low density polyethylene (LDPE). One peanut sample was not packed and kept in an open Petri dish as control (Figure 5).

Figure 5. Peanut wrapping with cardoon protein (CP)-based films (A), cross-linked CP-based film(B) or LDPE (C); unwrapped peanuts (D)

Each group was replicated 8 times. Experiments were carried out during July 2021 in the lab in Naples (Italy), where the room temperature was 33±2.5 °C and the RH 65±5 %. After 0, 4, 8, 12, 16, 20, 24 and 28 days samples were withdrawn from each group to be analyzed.

2.9.2. Peanut peroxide value (PV)

Peanuts were crushed by mortar and pestle until a creamy texture was obtained. Hence, the peanut oil was extracted by using cold hexane in the ratio of 1:4 (w/v) peanuts/hexane. After 1 hour of stirring the mixture of extracted oil and hexane was removed and the hexane was evaporated using rotary evaporator. PV was evaluated according to AOAC (1990) and expressed as milliequivalents of active oxygen per kg of oil ($meqO_2/kg$).

2.9.3. Peanut water content

The unwrapped and wrapped peanut moisture content was determined according to AOAC (2010) method. Peanuts were kept in a convection oven at 105 °C for 24 h and the water content (WC) was calculated by dividing the difference of the weight detected before and after oven drying divided by the initial weight of the peanuts after opening the peanuts package multiplied by 100.

2.10 OTHER METHODS

2.10.1. Antioxidant activity

2.10.1.1. 1,1-Diphenyl-2-picrylhydrazyl radical scavenging activity of egagropili lignin fraction

The antioxidant activity measurement of extensively dialyzed LF to scavenge 1,1-diphenyl-2-picrylhydrazyl (DPPH) was carried out according to Parveen et al. (2019) with some modifications. Methanol DPPH solution (0.005 %, w/v) was prepared and 0.1 mL of LF containing different amounts of lignin (0.15 - 0.03 mg) were mixed with 0.9 mL of methanol DPPH solution and the resulting mixture was incubated in the dark at room temperature for different times (5 - 90 min). Moreover, the antioxidant activity of LF (0.15 mg) was studied during 6 months, by adding 0.1 mL of the sample to 0.9 mL of freshly prepared DPPH solution and by incubating the aliquots in dark for 90

min. Absorbance was recorded at 517 nm using UV/visible spectrophotometer (SmartSpec 3000 Bio-Rad, Segrate, Milan, Italy). 1 mL methanol was used as blank, while 100 µL of water in 900 µL of DPPH solution were used as control.

DPPH radical scavenging activity was calculated by the following equation:

$$\text{DPPH scavenging activity (\%)} = (A_0 - A_s)/A_0 \times 100 \quad (5)$$

Where A_0 is the absorbance of the control (methanol DPPH solution), and A_s is the absorbance of the sample.

2.10.1.2. 1,1-Diphenyl-2-picrylhydrazyl radical scavenging activity of protein-based FFSs and films

The antioxidant activity of the protein-based FFSs and the derived films was evaluated by mixing 0.01 mL of FFS in 1 mL of methanol or by dissolving 20 mg of film in 1 mL of methanol; 0.1 mL of the two different solutions were mixed with 0.9 mL of DPPH solution (0.005 % (w/v). Absorbance of each sample was measured at 517 nm after incubation in darkness for 30, 60 and 90 min at room temperature according to the Equation 5.

2.10.2. Fourier Transform Infrared spectroscopy

NC and LF was extracted from egagropili as previously described (Mirpoor et al. 2020). Fourier Transform Infrared (FT-IR) spectrum was recorded for washed and milled egagropilli fibers, holocellulose (after LF removal) and cellulose (after hemicellulose removal) at room temperature by using FT-IR Nicolet 5700 spectrophotometer (Thermo Fisher Scientific, Waltham, MA, USA). Infrared spectra analysis was performed using the Omnic software, in the range of 4000–500 cm^{-1} with a spectral resolution of 2 cm^{-1} and by 64 average scan.

2.10.3. Phenol, flavonoid and anthocyanin determination

The total phenolic content was investigated by the Folin-Ciocalteau method as described by Velderrain-Rodríguez et al. (2021) with some modifications. 0.1 mL of different concentrations of gallic acid solution (0.01–0.25 mg/mL) were mixed with 0.75 mL of Folin-Ciocalteau (2 N) reagent and 0.65 mL of 7.5% (w/v) Na_2CO_3 freshly prepared solution to develop a calibration curve for quantifying total phenolic content. Absorbance of the samples was measured after 30 min at 765 nm using

UV/visible Spectrophotometer (SmartSpec 3000 Bio-Rad, Segrate, Milan, Italy). 100 µL of sample were mixed with the same reagents and incubated for 30 min, as performed for the calibration curve, and the absorbance was determined at 765 nm.

The total flavonoid content was performed by the aluminum chloride colorimetric method (Sagar et al., 2020). Two solutions of 3.5 mg/mL of $NaNO_2$ (solution A) and of 18.18 mg/mL of NaOH (solution B) were prepared and then 0.1mL of either the sample or quercetin solution at different concentrations (0.01- 2.5 mg/mL) were added to 0.43 mL of solution A followed by 5 min incubation. Then, 30 µL of anhydrous $AlCl_3$ solution (10%) were added to the mixture and incubated for further 1 min. Finally, 0.44 mL of solution B were added and the absorbance of the samples were measured at 415 nm using UV/visible Spectrophotometer (SmartSpec 3000 Bio-Rad, Segrate, Milan, Italy). The total flavonoid content was determined from a quercetin calibration curve and expressed as mg of quercetin/g of dried sample.

The total anthocyanin content was measured by pH-differential method (Teix´e- Roig et al., 2018). Two different buffers of 0.025 M potassium chloride and 0.4 M sodium acetate were prepared at pH 1.0 and 4.5, respectively. Sample was mixed with these two different buffers at a 3:1 buffer/sample ratio and the absorbance was measured at 515 nm and 700 nm, respectively, while distilled water was used as blank. The anthocyanin content (mg of cyanidin-3-gucoside/g of extract), expressed as equivalents of cyanidin-3-glucoside, was calculated on the base of the following equation:

$$\text{Total anthocyanins} = [(A_{515} - A_{700})_{\text{pH 1.0}} - (A_{515} - A_{700})_{\text{pH 4.5}}] \times MW \times DF \times 1000/ \varepsilon \times L \quad (6)$$

where MW is the molecular weight of cyanidin-3-glucoside (449.2 g/mol), DF is the dilution factor, L is the path length of cell (cm), and ε is the molar extinction coefficient for cyanidin-3-glucoside (26900 L mol^{-1} cm^{-1}).

2.10.4. Light barrier properties

Light-barrier properties of LF were analyzed by measuring sample absorbance at different wavelengths ranging from 200 nm to 800 nm by using a Spectrophotometer SmartSpec 3000 Bio-Rad (Segrate, Milan, Italy).

2.10.5. ^{1}H NMR analysis

20 mg sample of the LF was dissolved in 600 µL of deuterated water (D_2O) at pH 12 and the ^{1}H NMR spectrum was recorded at 298 K with a Varian Inova 500 spectrometer (HDO δ 4.8 as internal reference).

2.10.6. Molecular weight determination by size-exclusion chromatography with triple detector array

Analyses were performed by using a high performance size-exclusion chromatography (Viscotek, Malvern, Italy), equipped with a triple detector array module (SEC-TDA), that included a refractive index detector (RI), a four-bridge viscosimeter (VIS), and a laser detector (LS) made of a right-angle light scattering (RALS) and a low-angle light scattering (LALS) detector. Runs were performed by injecting, as previously described (Tolbert et al., 2014), 0.1 mL of the sample onto two gel-permeation columns (TSK-GEL GMPWXL, 7.8 × 30.0 cm, Tosoh Bioscience, Italy), equipped with a guard column put in series, and by eluting with 0.1 M $NaNO_3$, pH 7.0, at 40 °C for 50 minutes (flow rate of 0.6 ml·min^{-1}). Data were acquired by using a OmniSEC software program (Viscotek, Malvern, Italy). The instrument was calibrated by using a polyethylene oxide (PEO) standard (22 kDa PolyCAL, Viscotek, Malvern, Italy) (Tolbert et al., 2014). The values of the average MW of the sample component(s), as well as of both sample polidispersity index (MW/Mn) and intrinsic viscosity, were determined on the base of all the detector signals by applying the equations reported by the manufacturer (data from Viscotek) and on the base of the lignin dn·dc^{-1} (refractive index increment) value (0.1875) reported in literature (data from Viscotek).

2.10.7. Monosaccharide determination by high performance anion-exchange chromatography with pulsed amperometric detection

The monosaccharide composition of egagropili fibers and of LF, hollocellulose and cellulose fractions was determined by high performance anion-exchange chromatography with pulsed amperometric detection (HPAEC-PAD) by improving a previously reported method (Rencoret et al., 2020). The samples were hydrolyzed by 5 M HCl treatment for 6 h at 100 °C and 600 rpm (Thermomixer comfort, Eppendorf, Germany) and then analyzed by using a high-pressure ion chromatography system (ICS3000; Thermo Fisher Scientific, Italy), equipped with an anion exchange column (Carbopac

PA1; Thermo Fisher Scientific, Italy) and a pulsed amperometric detector. Runs were performed by eluting in gradient conditions with 1 to 4 mM NaOH and 100 mM NaOH containing 20 mM sodium acetate at a flow rate of 1 mL/min for 41 min. The identity of each monosaccharide peak was determined on the base of the elution times by comparison with standard solutions of different monosaccharides. Calibration curves of the monosaccharide standards were built in the range from 0.002 to 0.008 g/L (for fucose, galactose, glucosamine, glucose), from 0.02 to 0.08 g/L (for arabinose, rhamnose, xylose), and from 0.2 to 0.8 g/L (for glucuronic acid) after their acid hydrolysis performed at 2.5 mg/mL as described above. The percentage of representativity of each monosaccharide was calculated according to the following formula:

$$\%X = \%[X(g/L)/(\Sigma Xn(g/L)*100] \quad (7)$$

where X is the single monosaccharide, whereas the total carbohydrate content percentage with respect to the dry weight of the samples was calculated according to the following formula:

$$\%\text{carbohydrate content} = \%[\ \Sigma Xn\ (g)/(\text{dry weight}\ (g)*100] \quad (8)$$

2.10.8. Gas chromatography–mass spectrometry

The sample was prepared by dissolving 1 mg of CLE obtained by Naviglio® method in 1 mL of diethyl ether and gas chromatography–mass spectrometry (GC-MS) analysis was carried out by a Shimazu gas chromatograph. The gas chromatograph was equipped with a 30 m x 0.25 mm fused-silica capillary column (SLB5ms) coated with 0.25 µm film of poly(5% phenyl, 95% dimethyl siloxane). The temperature was monitored from 50°C to 280°C.

The mass spectrometer was set to scan 33-700 m/z. Samples were injected (1µL) with a splitting ratio 1:20 and the injector temperature was set to 280 °C. The temperature of the column oven was initially at 50 °C and was held for 2 min at 50 °C after the injection, followed by the temperature ramping at 8 °C/min up to 250 °C, and 250-280 °C at 3 °C/min. The total run time was 63.33 minute (Mathe et al., 2004).

2.10.9. Interfacial characterisation

2.10.9.1. Preparation of SOC protein solutions

SOC proteins were dissolved in ultrapure water produced through a purification Milli-Q water system (0.054 μS). The prepared solutions were stirred for 6 h at 500 rpm and the pH adjusted to either pH 10 or 12 by using 1 N NaOH. The solutions were kept overnight at 4 °C and the day after kept at room temperature before analysis. Solutions at different protein concentrations (0.002, 0.02, 0.1, 0.2, 2 and 20 mg/mL) were prepared at both pH 10 and 12 by using all SOC protein concentrates. Glass wares were washed extensively by isopropanol, deionized water and ultrapure water (Del Castillo-Santaella et al., 2014). All the solutions were prepared in triplicate.

2.10.9.2. Interfacial tension

Interfacial tension and dilatational rheology of water solutions of proteins were measured by OCTOPUS, a pendant drop tensiometer designed at the University of Granada (patent ES 2 153 296 B1/WO 2012/080536 A, ES) as described previously by Maldonado-Valderrama et al. (2015). This system was composed of 4 basic subsystems: an illumination system, image acquisition, a flow controller and an antivibration system. The illumination system consisted of a light source and a diffusor that was utilized to have an uniform illumination of the drop.

Digital images were captured with a resolution of 1280 × 1024 pixels with 256 gray scales by a video camera CCD (Pixelink®) connected to an optical microscope (Edmund Optics®). The drop was formed by pumping a specified drop volume with a constant speed into a Teflon tip through a micro-injector. In order to prevent any vibration during the experiment, all the system was placed on an antivibratory table 'Kinetic System Inc. Vibraplane'. All the experiments carried out with this equipment were controlled by DINATEN© and CONTACTO©, computer softwares that were developed at the University of Granada. Axisymmetric Drop Shape Analysis (ADSA) of the experimental drop profiles obtained from the DINATEN© that processed the digitized images of pendant drops was carried out on the base of the following Young-Laplace capillarity equation (Ruiz-Álvarez, et al., 2022):

$$\Delta P = \gamma \left(\frac{1}{R1} + \frac{1}{R2}\right) \quad (9)$$

where ΔP is the pressure difference, R1 and R2 are the two principal radii of curvature of the drop and γ is the surface tension of the liquid surrounded by the surface active substance. The adsorption process was performed at a constant interfacial area of 27 mm^2 for 1700s and the drop volume was adjusted to 14 mL. The outputs of the programme are the drop volume V, the interfacial tension γ, and the interfacial area A.

2.10.9.3. Dilatational viscoelasticity analysis

Dilatational rheology measurements were performed at the end of the adsorption process. In this regard, a periodic turbulence was created by oscillations applied to the interfacial surface and the response of the surface tension to a triangular area deformation was recorded. The dilatational viscoelastic modulus is a complex quantity consisting of two parts, a real and an imaginary part that were calculated according to the following equation:

$$E = E' + iE'' = \varepsilon d + if\, \eta d \quad (10)$$

where (E) is the dilatational viscoelastic modulus and (E′) is the real part or the storage modulus which is the elasticity of the interfacial layer (εd). The imaginary part or loss component equivalent to the viscosity of the interfacial layer (ηd) and 'if' is the angular frequency of the applied oscillation. The dilatational viscoelastic modulus (E) was measured during 100 sec by applying 10 cycles to the drop (each of them takes 10 sec) at 0.1 Hz frequency and at amplitude values of less than 5% to remain in the linear viscoelastic range and prevent extreme turbulence of the interfacial layer (Tian et al., 2021; Maldonado-Valderrama et al., 2014). The DINATEN© software recorded the images obtained from the experiment that was the response of interfacial tension to the area deformation. The software CONTACTO® calculated the interfacial dilatational modulus (E) by using all the outputs that this software provided (Maldonado-Valderrama et al., 2013).

2.10.9.4. Desorption profile

Reversibility and desorption profile of the protein concentrates were studied by the OCTOPUS, that is an upgraded version of pendant drop instrument, designed in UGR (Maldonado-Valderrama et al., 2015). OCTOPUS was equipped with a multi-exchange that had two micro-

injection systems (PSD/3 syringe pumps, Hamilton Company) and each of them were connected to 8 channels. These syringes that worked independently, exchanged the subphase of the drop completely by water at the same pH that the stock solution of protein concentrate was prepared. In this subphase exchange step, the drop volume and the surface area were constant. Similarly to the surface tension measurements, all the experiments were monitored by the DINATEN© software.

2.10.10. Solid surface characterization

2.10.10.1. Surface preparation

In order to prepare the samples for the surface characterization, the protein-based bioplastics were cut to circle pieces (2 cm diameter) and a hole of 1 mm diameter was formed in the middle of the circle pieces by a syringe. Later, the film circles were attached perfectly to the plastic discs (PDMS) with the same dimension using a two face tape. Before each experiment, the plastic discs were cleaned ultrasonically in a 70% ethanol solution for 10 min and then rinsed by Milli-Q.

2.10.10.2. Contact angle measurements

Advancing and receding contact angles were measured by using the experimental set-up previously described by Montes Ruiz-Cabello et al. (2011). The experiments were carried out by increasing or decreasing the volume of a sessile drops (70µL) by injecting/suctioning Milli-Q water, at a flow rate of 5 µL/s, through the hole that was formed in the middle of the surface of each sample with a microinjector (Hamilton ML500). To measure the advancing and receding contact angles, the side view drop images were captured and the contact angle was calculated from Axisymmetric Drop Shape Analysis- Profile (ADSA-P) (Moraila-Martínez et al., 2012). The software outputs were contact angle, contact radius, area, volume and surface tension. The experiments were carried out at 25 ^{o}C and 40–55% RH. Each measurement on each protein-based film was repeated five times on different parts of the same film.

2.10.10.3. Roughness measurements

Film surface roughness was investigated using a white light confocal microscope (PLµ, Sensofar©-Tech S.L.). In order to fix the films and prevent their probable movement, the films were attached to glass

slides by a two face tape. The roughness of the air-side dried films was analyzed. The topographies were collected using an objective of 20x magnification. The topographies were taken 5 times for each sample from different parts of the film surface.

2.11. Statistical Analysis

SPSS19 (Version 19, SPSS Inc., Chicago, IL, USA) software was used for all statistical analyses. One-way analysis of variance (ANOVA) and Duncan's multiple range tests ($p < 0.05$) were used to determine the significant difference among the samples. All treatments were analyzed in triplicate.

3. Results and discussion

It seemed crucial to preliminarily study the production of films by using different SOC protein concentrates under different experimental conditions, such as different protein amounts, pH values and GLY concentrations. Afterwards, several additives were tested in order to improve the features of the selected films.

3.1. Developing HP-based films: effect of mTGase-induced protein cross-linking

Proteins obtained from wastes of vegetable origin are potential candidates for producing biodegradable/edible plastics. Among the various oilseed plants, special attention should be given to the hemp (*Cannabis sativa L*.), a multipurpose, sustainable, and low environmental impact crop belonging to the Cannabaceae family and containing low levels of Δ9-tetrahydrocannabinol (THC, <0.1–1%), that is cultivated for producing textiles, food, paper, biofuel, medicine and hygiene products (Fike, 2016). However, protein-based films generally exhibit poor mechanical and WV barrier properties and, thus, in order to improve these properties, HPs were enzymatically cross-linked by different amounts of mTGase before FFS drying. The morphological characterization of the obtained films demonstrated that mTGase treatment was effective to produce more homogeneous and smoother materials with improved properties, being more resistant, still flexible and exhibiting a higher heat-sealing strength. In addition, the enzymatic treatment of HPs gave rise to bioplastics with a higher gas and WV permeability (WVP) and a greater hydrophobicity. All these results are described in the published paper reported in the appendix of this thesis (*Mirpoor, S. F., Giosafatto, C. V. L., Di Girolamo, R., Famiglietti, M., & Porta, R. (2022). Hemp (Cannabis sativa) seed oilcake as a promising by-product for developing protein-based films: Effect of transglutaminase-induced crosslinking. Food Packaging and Shelf Life, 31, 100779*.

3.2. HP-based films grafted with NC and LF extracted from egagropili

NC and LF were isolated in good yield from egagropili, better known as sea balls, and used as reinforcement additives of the HP-based film matrix. Film microstructure analysis indicated a good interaction of the two additives tested, as both were properly dispersed in the protein film matrix. The improved mechanical and barrier properties, as well as the weakened water trapping ability, exhibited by the grafted biocomposites suggest a potential use of egagropili as a valuable renewable source for reinforcing agents of protein-based films as described in the published article reported in the appendix of the present thesis (*Mirpoor, S. F., Giosafatto, C.V.L., Di Pierro, P., Di Girolamo, R., Regalado-González, C., & Porta, R., 2020. Valorisation of Posidonia oceanica Sea Balls (Egagropili) as a Potential Source of Reinforcement Agents in Protein-Based Biocomposites. Polymers, 12(12), 2788.*

3.3. Characterization of LF and investigation of antioxidant activity of HP-based film grafted with LF

LF extracted from egagropili was extensively dialyzed and characterized by FT-IR, NMR analyses, antioxidant activity, phenolic content and light barrier properties. LF, containing a lignin/carbohydrate complex exhibiting a remarkable and stable antioxidant activity, was demonstrated to be incorporated into HP-based films from which it was easily released over time, as it was described in the published paper reported in the appendix of the thesis (*Mirpoor, S. F., Restaino, O. F., Schiraldi, C., Giosafatto, C.V.L., Ruffo, F., & Porta, R., 2021. Lignin/Carbohydrate Complex Isolated from Posidonia oceanica Sea Balls (Egagropili): Characterization and Antioxidant Reinforcement of Protein-Based Films. International Journal of Molecular Sciences, 22(17), 9147*.

3.4. Developing active CP-based films

CLE was added to the CP-based FFSs and the characterization of the derived films showed a significant improvement of all the properties, both technological and biological, of the manufactured materials. Film microstructure observed by SEM revealed a good compatibility of CPs and CLE, showing a uniform distribution of the leaf extract components throughout the film network that reflected, in turn, an improvement of the mechanical and barrier properties of the obtained material. In

addition, the CLE containing films exhibited higher hydrophobicity, as indicated by the contact angle measurement and by the evaluation of water solubility and swelling degree experiments. Finally, CLE-containing films showed a marked antioxidant activity, as reported in the published article reported in the appendix of the thesis (*Mirpoor, S. F., Varriale, S., Porta, R., Naviglio, D., Spennato, M., Gardossi, L., Giosafatto, C.V.L., & Pezzella, C., 2022. A biorefinery approach for the conversion of Cynara cardunculus biomass to active films. Food Hydrocolloids, 122, 107099*.

3.5. Development and characterization of argan AP-based films

3.5.1. Protein characterization of argan seed oilcake

Argan seeds are a good source of proteins, accounting for about 50% of the oilcake composition. Therefore, a preliminary study was carried out on APs to qualitatively and quantitatively characterize them after partial oil removal from the argan seeds by means of a Soxhlet apparatus using n-hexane. Protein determination was carried out using the Kjeldhal method on the AP concentrate obtained by treating the defatted argan seed flour under acidic/alkaline protein extraction. The results have shown that samples containing 55% of protein were achieved following this kind of extraction. In addition, a protein profile was obtained by SDS-PAGE (Figure 6) showing that the extracted APs had molecular masses ranging from 15 to 30 kDa.

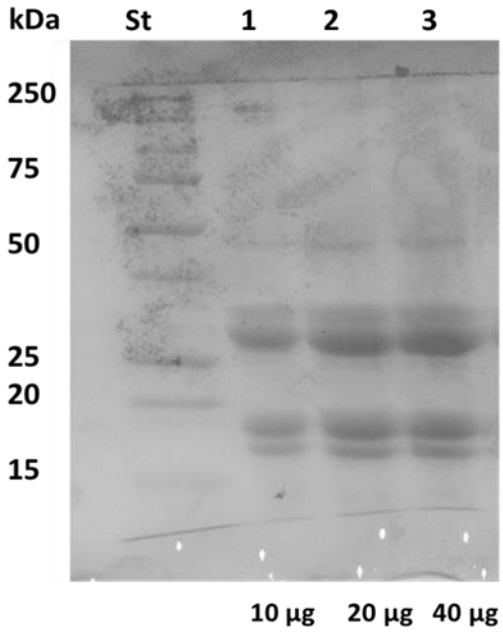

Figure 6. SDS-PAGE (12%) of different amounts of protein extracted from argan seeds

The data reported in Figure 7 show that APs were positively charged in the acidic pH range, since the detected zeta potential was found to progressively increase from a value of about -35.00 mV at pH 12 to a 0 mV value under pH 5.0, as a result of the gradual deprotonation of carboxyl groups and protonation of the amino groups occurring in the lateral chains of each protein present in the sample.

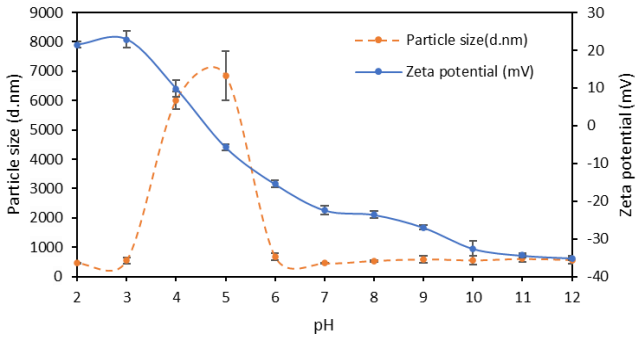

Figure 7. Titration of proteins extracted from argan seed oilcakes

As far as the AP particle size, it also varied during the sample titration. In fact, at pH $\leq$ 6 high molecular mass protein species were present in the solution, likely because the isoelectric point of APs was between pH 5 and 6 where the zeta potential value was around 0 mV.

3.5.2. Zeta potential and particle size of argan protein AP-based FFSs

In order to evaluate the stability of FFSs containing different concentrations of APs and GLY, measurements of zeta potential and Z-average were carried out.

Table 1. Zeta potential, Z-average and polydispersity Index values of FFSs prepared with increasing amounts of argan proteins (AP) in the presence of different concentrations of GLY.Different small letters (a-g) indicate significant differences among the values reported in each column ($p < 0.05$).

AP (mg)	GLY concentration (%)	Zeta potential (mV)	Z - Average (nm)	Polydispersity index
300	30	-34.80 ± 1.90^{a}	409.90 ± 42.10^{d}	0.75 ± 0.02^{b,c}
	40	-30.00 ± 2.00^{a}	519.30 ± 45.40^{c}	0.78 ± 0.06^{b,c}
	50	-34.00 ± 2.00^{a}	726.00 ± 10.20^{a}	0.90 ± 0.08^{a}
500	30	-36.20 ± 4.90^{a}	302.20 ± 11.50^{e}	0.69 ± 0.07^{d,e}
	40	-34.80 ± 3.70^{a}	320.40 ± 14.60^{e}	0.52 ± 0.02^{f}
	50	-35.30 ± 3.60^{a}	394.50 ± 13.50^{e}	0.58 ± 0.02^{f,g}
600	30	-35.90 ± 5.80^{a}	327.40 ± 4.60^{e}	0.65 ± 0.02^{e,f}
	40	-35.60 ± 5.70^{a}	338.80 ± 14.80^{e}	0.66 ± 0.01^{d,e}
	50	-34.90 ± 5.00^{a}	579.00 ± 17.00^{b}	0.76 ± 0.08^{b,c}
800	30	-20.30 ± 1.30^{a}	495.50 ± 10.70^{c}	0.78 ± 0.02^{b,c}
	40	-20.80 ± 0.90^{a}	488.20 ± 25.90^{c}	0.75 ± 0.05^{b,c}
	50	-20.30 ± 0.04^{a}	590.00 ± 41.00^{b}	0.81 ± 0.09^{b}

The data reported in Table 1 indicate that FFSs prepared with APs were markedly stable, as the zeta potential values were always lower than -20 mV at all GLY concentrations even at higher protein concentrations. The drop down in Zeta potential recorded for FFSs prepared with 800 mg of AP is due to the high protein concentration that, in turn, may cause the precipitation of the macromolecules, thus, affecting the stability of the system.

Moreover, the FFS particle size measurements indicated Z-average values, between about 300 and 700 nm, that increased by increasing the GLY concentration. Finally, FFSs showed polydispersity index

values between 0.5 and 0.8, indicating that particles in solution occurred in a non-uniform size.

3.5.3. Evaluation of casting conditions of AP-containing FFSs

The development of AP-based films started with the identification of the best GLY and protein concentrations to prepare the FFSs for casting and drying. In this regard FFSs (25 mL) containing 300 mg of APs and different concentrations of GLY (0-50% w/w of AP) were prepared at pH 12. This AP amount was chosen because it was the minimum concentration necessary to obtain peelable and handleable films. All FFSs were casted in Petri dishes and placed in the climatic chamber for 24 hours at 25 °C and 45% RH. It was observed that the minimum GLY concentration needed to obtain a peelable and handleable film by using 300 mg of AP was 40% (Figure 8). In addition, some films were also prepared by using 500, 600 and 800 mg of APs in the presence of 30, 40 and 50% GLY. The obtained results demonstrated that also under these experimental conditions it was possible to obtain homogeneous and manipulable films by adding at least 30% GLY.

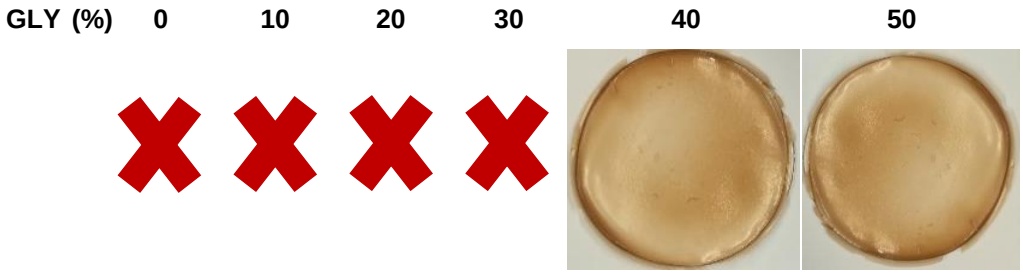

Figure 8. Films obtained at pH 12 by using 300 mg argan proteins in the presence of different concentrations of glycerol (GLY)

3.5.4. Film mechanical properties

Figure 9 shows the mechanical properties of AP-based films prepared under different experimental conditions (Figure 9). It is worthy to note that, among all the films prepared with different concentrations of APs and GLY, the film prepared by using 600 mg of APs and 50% of GLY seemed to have the highest EB value. The influence of GLY on EB has been previously reported by Farahnaky et al. 2013. Conversely, both TS and YM were found to decrease by increasing GLY concentration, a lower YM indicating a reduced stiffness and a lower TS being related to a poor resistance.

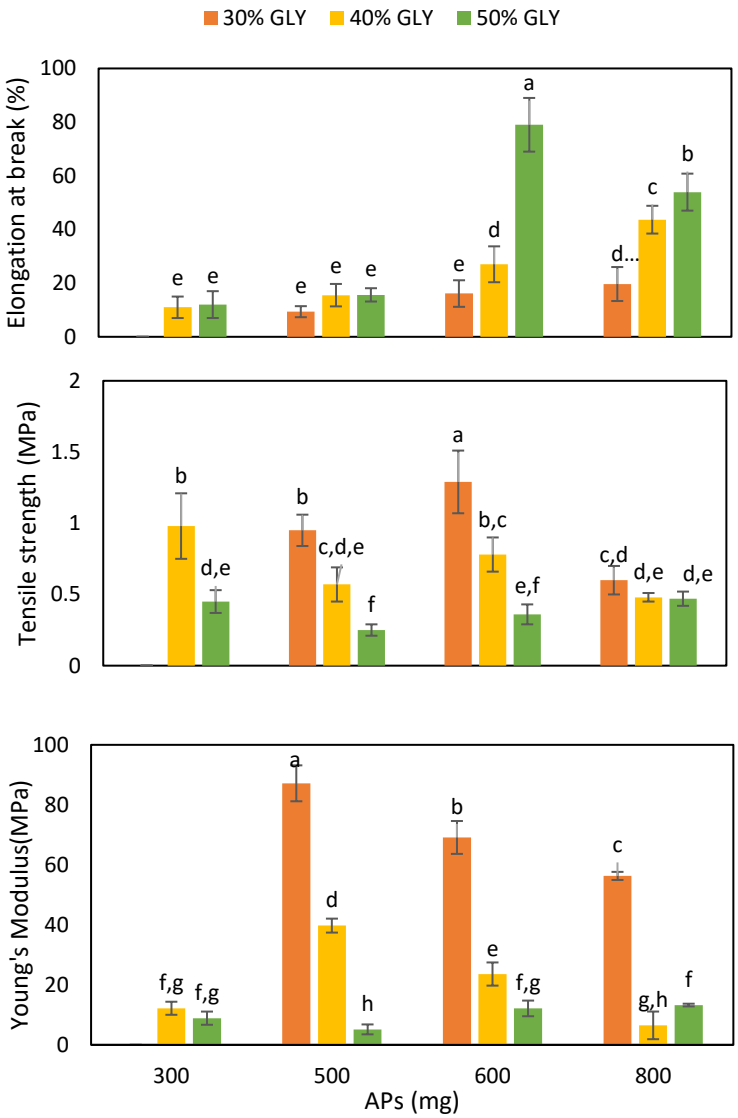

Figure 9. Mechanical properties of argan protein (AP)-based films. Different small letters (a-h) indicate significant differences among the values reported ($p < 0.05$).

3.5.5. Film water content (WC) and uptake

AP-based films were also analysed for WC and water uptake, as these features are important for food packaging applications, particularly when the water activity is high or when the film is manufactured as a food protective barrier (Vejdan et al., 2016). In fact, a high water content of the coating material considerably limits its use for packaging foods.

The results reported in Table 2 show that both WC and water uptake do not seem to significantly change in all films, thus suggesting that neither the amount of APs nor the amount of GLY added can affect these properties for this kind of material.

Table 2. Water content (WC) and water uptake of argan protein (AP)-based films prepared with different amounts of APs and concentrations of glycerol (GLY). Different small letters (a-d) indicate significant differences among the values reported ($p < 0.05$).

APs (mg)	GLY (%)	WC (%)	Water uptake (%)
500	30	10.03 ± 0.31^{d}	9.16 ± 0.12^{b}
	40	$10.48 \pm 0.28^{c,d}$	9.77 ± 1.34^{b}
	50	$10.12 \pm 2.77^{c,d}$	9.22 ± 1.01^{b}
600	30	$12.11 \pm 0.31^{b,c}$	12.74 ± 1.32^{a}
	40	$12.62 \pm 0.29^{b,c}$	12.02 ± 0.97^{a}
	50	14.20 ± 0.70^{a}	12.23 ± 1.46^{a}
800	30	$11.43 \pm 0.43^{b,c,d}$	12.99 ± 0.25^{a}
	40	$12.66 \pm 1.18^{a,b}$	13.57 ± 1.06^{a}
	50	$12.10 \pm 0.30^{b,c}$	12.21 ± 0.41^{a}

3.5.6. Film barrier properties, antioxidant activity and opacity

The ability of AP-based films to act as barrier towards WV and gases (CO_2 and O_2) has been studied (Table 3) and compared to that exhibited by two commercial bioplastics, namely Mater Bi®, based on the polysaccharide starch, and Viscofan®, based on the protein gelatin. As far as WVP, the AP-based films seemed to be less permeable to WV than Mater Bi®, while they showed a barrier behaviour similar to that exhibited by Viscofan®. On the other hand, the values of permeability toward CO_2 and O_2 were lower than those exhibited by the two commercial plastics. I n addition in Table 3, the antioxidant activity as well as the opacity of the AP films are reported. The opacity values (2.6 ± 0.56 mm^{-1}) of the AP-based films were quite lower than those of CP-based films (14.89±0.17) and similar to the ones of HP-based film (2.39±0.27). Finally, AP-based films were found to possess a significant antioxidant activity (12.37 ± 1.33) suggesting their potential application in protecting foods from oxidation.

Table 3. Barrier properties, antioxidant activity and opacity of the films manufactured with 600 mg APs and 50% (w/w of APs) GLY. Different small letters (a-c) indicate significant differences among the values reported ($p < 0.05$).

	WVP	CO_2	O_2	Antioxidant activity	Opacity
	$cm^3\ mm\ m^{-2}\ d^{-1}\ kPa^{-1}$			(%)	mm^{-1}
AP film	7.52 ± 0.62^b	0.46 ± 0.08^c	0.02 ± 0.001^b	12.37±1.33	2.6±0.56
Mater Bi®	15.5 ± 1.24^a	1.45 ± 0.12^b	0.72 ± 0.16^a	-----	-----
Viscofan®	4.96 ± 0.63^c	3.71 ± 0.16^a	0.03 ± 0.01^b	-----	-----

4. Conclusions

Petroleum based plastic are non-degradable and their wide spread application over the past few decades has caused serious environmental pollution. Hence, the development of protein-based films is receiving an increasing attention for their possible industrial application as alternatives to oil-derived polymers. In this regard, the residues of oilseed crops, known as SOCs, are extremely rich in valuable ingredients, such as proteins, fiber and various bioactive compounds, that are by-products mostly consumed so far as animal feed supplementation, food additives or fertilizers. Therefore, the relatively high protein content and their inexpensive cost make SOCs an adequate source to develop novel bioplastic materials. In this work HPs, CPs and APs, obtained from the respective SOCs were used as renewable resources to prepare innovative biodegradable and edible films. Preliminary experiments have been carried out to find the best conditions for developing hydrocolloidal films and the obtained results suggested that pH 12 was the best pH to produce manipulable materials with all the proteins tested. In addition, it was found out that the best protein concentration for developing samples to be studied was 400 mg for HP- and CP-based films, and 600 mg for AP-based films. All the films were produced in the presence of glycerol (GLY) used as plasticizer and it was found out that the best material performances were obtained with 50% (w/w of protein) of GLY. In order to improve the film properties, HP-based films were reinforced by the protein preliminary treatment with microbial transglutaminase (mTGase) or by adding to the FFSs either nanocellulose (NC) or lignin fraction (LF) extracted from egagropili, brown colored balls free-floating in the sea-waters derived from fibre-like leaves of rhizomes and stems of *Posidonia Oceanica*. In fact, improved mechanical and/or barrier properties, as well as the weakened water trapping ability were exhibited by these two biotechnological processes.
Furthermore, it was also focused the attention on the cardoon leaf extract (CLE) in order to use them to functionalize CP-based films. CLE was demonstrated to be endowed with antioxidant properties and, when added to CP-based FFS, gave rise to materials with a significant improvement of all the tested properties. In fact, CLE-containing films

appeared smoother and more homogenous, and showed also a higher and lasting antioxidant activity that conferred a higher value to the obtained bio-plastics. Furthermore, also CPs were demonstrated to effectively act *in vitro* as acyl donor and acceptor substrates for mTGase, and the heat-sealing ability exhibited by the enzyme-crosslinked CP films, as well as their dark greenish color, suggested them as suitable candidates for wrapping peanuts, preventing lipid oxidation and rancidity and prolonging their shelf life.

The third SOC protein concentrate object of this study was that derived from argan seeds. Among all the films prepared with different concentrations of APs and GLY, those prepared by using 600 mg of APs and 50% of GLY showed to exhibit a particularly high extensibility property. Moreover, as far as WVP, the AP-based films showed to be less permeable to WV than Mater Bi® with a behavior similar to that exhibited by Viscofan®, whereas the values of permeability toward CO_2 and O_2 were lower than those exhibited by the two commercial plastics. Finally, AP-based films were found to possess also a significant antioxidant activity, suggesting their potential application in protecting foods from oxidation.

The last part of the experimental work was performed at the University of Granada (Spain) and was focused on the interfacial properties and surface characterization of the HP, CP and AP-based bioplastics. The obtained results demonstrated that APs had the highest and CPs the lowest surface elasticity features, and that APs was irreversibly adsorbed. Furthermore, the surface characterization indicated that APs possessed the most hydrophobic surface and the highest advancing contact angle, probably as a consequence of the high lipid content of the extracted protein concentrate.

In conclusion, for what stated above, an early transition to renewable sources, as those represented by hemp, cardoon and argan SOCs, for preparing eco-friendly bioplastics might be a timely, valuable and innovative milestone at least for some specific sectors of food packaging industry. Obviously, the film with the best characteristics will be chosen on the basis of the kind of food product the material will be applied for. An industrial scale up will be necessary after feedback from companies working in the specific sector. Furthermore, in the next future feasibility studies together with the risk for consumers will have to be undoubtedly evaluated.

5. References

AACC. (2003). Approved methods of AACC. St. Paul, MN, USA: The Association. Available at: https://methods.aaccnet.org/default.aspx. (Accessed 5 May 2021).

Aguilera-Garrido, A., del Castillo-Santaella, T., Yang, Y., Galisteo-Gonz´alez, F., G´alvez- Ruiz, M. J., Molina-Bolívar, J. A., et al. (2021). Applications of serum albumins in delivery systems: Differences in interfacial behaviour and interacting abilities with polysaccharides. Advances in Colloid and Interface Science, 290, 102365.

Aithammou, R., Harrouni, C., Aboudlou, L., Hallouti, A., Mlouk, M., Elasbahani, A., & Daoud, S. (2019). Effect of clones, year of harvest and geographical origin of fruits on quality and chemical composition of Argan oil. Food Chemistry, 297, 124749.

Amadori, S., Torricelli, P., Rubini, K., Fini, M., Panzavolta, S., & Bigi, A. (2015). Effect of sterilization and crosslinking on gelatin films. Journal of Materials Science: Materials in Medicine, 26(2), 69.

AOAC. (1990). Official Methods of Analysis of the Association of Official Analytical Chemists, 15th edn (edited by K. Helrich). Arlington, VA: Association of Official Analytical Chemists

AOAC. (2010). Official methods of analysis of the AOAC. Gaithersburg, MD: AOAC International.

ASTM D3985-05 (2010). Standard test method for oxygen gas transmission rate through plastic film and sheeting using a colorimetric sensor; West Conshohocken, PA, USA .

ASTM D882-97 (1997). Standard test method for tensile properties of thin plastic sheeting; Philadelphia, PA, USA .

ASTM E88-07a (2007). Standard test method for seal strength of flexible barrier materials. F88-07. Annual book of American standard testing method (pp.768-777); Philadelphia, PA :

ASTM F1249-13 (2013). Standard test method for water vapor transmission rate through plastic film and sheeting using a modulated infrared sensor; West Conshohocken, PA, USA .

ASTM F2476-13 (2013). Standard test method for the determination of carbon dioxide gas transmission rate through barrier materials using an infrared detector; West Conshohocken, PA, USA .

Bai, R., Zhang, X., Yong, H., Wang, X., Liu, Y., & Liu, J. (2019). Development and characterization of antioxidant active packaging and intelligent Al 3+ -sensing films based on carboxymethyl chitosan and quercetin. International Journal of Biological Macromolecules, 126, 1074–1084. https://doi.org/10.1016/j.ijbiomac.2018.12.264

Bakkalbaşı, E., Yılmaz, Ö. M., Javidipour, I., & Artık, N. (2012). Effects of packaging materials, storage conditions and variety on oxidative stability of shelled walnuts. LWT-Food Science and Technology, 46(1), 203-209.

Balestri, E., Vallerini, F., & Lardicci, C. (2006). A qualitative and quantitative assessment of the reproductive litter from Posidonia oceanica accumulated on a sand beach following a storm. Estuarine, Coastal and Shelf Science, 66(1-2), 30-34.

Cao, N., Yang, X., & Fu, Y. (2009). Effects of various plasticizers on mechanical and water vapor barrier properties of gelatin films. Food Hydrocolloids, 23(3), 729-735.

Cheng, L. H., Karim, A. A., & Seow, C. C. (2006). Effects of water-glycerol and water-sorbitol interactions on the physical properties of konjac glucomannan films. Journal of Food Science, 71(2), E62-E67.

Cherki, M., Berrougui, H., Drissi, A., Adlouni, A., & Khalil, A. (2006). Argan oil: which benefits on cardiovascular diseases?. Pharmacological Research, 54(1), 1-5.

Christopoulos, M. V., & Tsantili, E. (2011). Effects of temperature and packaging atmosphere on total antioxidants and colour of walnut (Juglans regia L.) kernels during storage. Scientia Horticulturae, 131, 49e57.

Dapˇcevi´c-Hadnađev, T., Hadnađev, M., Lazaridou, A., Moschakis, T., & Biliaderis, C. G. (2018). Hempseed meal protein isolates

prepared by different isolation techniques. Part II. gelation properties at different ionic strengths. Food Hydrocolloids, 81, 481–489. https://doi.org/10.1016/j.foodhyd.2018.03.022

De Groote, P. H., Devaux, J., & Godard, P. (2002). Effect of benzenesulfonamide plasticizers on the glass-transition temperature of semicrystalline polydodecamide. Journal of Polymer Science Part B: Polymer Physics, 40(19), 2208-2218.

Del Castillo-Santaella, T., Cebrí´an, R., Maqueda, M., G´alvez-Ruiz, M. J., & Maldonado- Valderrama, J. (2018). Assessing in vitro digestibility of food biopreservative AS-48. Food Chemistry, 246, 249–257. https://doi.org/10.1016/j.foodchem.2017.10.149

Del Castillo-Santaella, T., Sanmartín, E., Cabrerizo-Vílchez, M. A., Arboleya, J. C., & Maldonado-Valderrama, J. (2014). Improved digestibility of β-lactoglobulin by pulsed light processing: A dilatational and shear study. Soft Matter, 10(48), 9702–9714. https://doi.org/10.1039/c4sm01667j.

Delahaije, R. J. B. M., Gruppen, H., Giuseppin, M. L. F., & Wierenga, P. A. (2014). Quantitative description of the parameters affecting the adsorption behaviour of globular proteins. Colloids and Surfaces B: Biointerfaces, 123, 199–206.

Den Hartog, C., & Kuo, J. (2007). Taxonomy and biogeography of seagrasses. In Seagrasses : biology, ecologyand conservation (pp. 1-23). Springer, Dordrecht.

Dias, M. I., Barros, L., Barreira, J. C. M., Alves, M. J., Barracosa, P., & Ferreira, I. C. F. R. (2018). Phenolic profile and bioactivity of cardoon (Cynara cardunculus L.) inflorescence parts: Selecting the best genotype for food applications. Food Chemistry, 268(March), 196–202. https://doi.org/10.1016/j.foodchem.2018.06.081

El Abbassi, A., Khalid, N., Zbakh, H., & Ahmad, A. (2014). Physicochemical characteristics, nutritional properties, and health benefits of argan oil: A review. Critical Reviews in Food Science and Nutrition, 54(11), 1401-1414.

Eral, H. B., t Mannetje, D. J. C. M., & Oh, J. M. (2013). Contact angle hysteresis: a review of fundamentals and applications. Colloid and Polymer Science, 291(2), 247-260.

Escamilla-García, M., Calderón-Domínguez, G., Chanona-Pérez, J. J., Mendoza-Madrigal, A. G., Di Pierro, P., García-Almendárez, B. E., ... & Regalado-González, C. (2017). Physical, structural, barrier, and antifungal characterization of chitosan–zein edible films with added essential oils. International Journal of Molecular Sciences, 18(11), 2370.

Fan, Y., Peng, G., Pang, X., Wen, Z., & Yi, J. (2021). Physicochemical, emulsifying, and interfacial properties of different whey protein aggregates obtained by thermal treatment. LWT, 111904.

Faradilla, R. F., Lee, G., Roberts, J., Martens, P., Stenzel, M., & Arcot, J. (2018). Effect of glycerol, nanoclay and graphene oxide on physicochemical properties of biodegradable nanocellulose plastic sourced from banana pseudo-stem. Cellulose, 25(1), 399-416.

Farahnaky, A., Saberi, B., & Majzoobi, M. (2013). Effect of glycerol on physical and mechanical properties of wheat starch edible films. Journal of Texture Studies, 44(3), 176-186.

Fike, J. (2016). Industrial hemp: renewed opportunities for an ancient crop. Critical Reviews in Plant Sciences, 35, 406–424.

Fornes, A., Basterretxea, G., Orfila, A., Jordi, A., Álvarez, A., & Tintoré, J. (2006). Mapping Posidonia oceanica from IKONOS. ISPRS Journal of Photogrammetry and Remote Sensing, 60(5), 315-322.

Geyer, R., Jambeck, J. R., & Law, K. L. (2017). Production, use, and fate of all plastics ever made. Science Advances, 3(7), e1700782.

Giosafatto, C. V. L., Fusco, A., Al-Asmar, A., & Mariniello, L. (2020). Microbial transglutaminase as a tool to improve the features of hydrocolloid-based bioplastics. International Journal of Molecular Sciences, 21(10), 3656.

Gonzalez-Gutierrez, J., Partal, P., Garcia-Morales, M., & Gallegos, C. (2010). Development of highly-transparent protein/starch-based bioplastics. *Bioresource technology*, *101*(6), 2007-2013.

Haghighi, H., Leugoue, S. K., Pfeifer, F., Siesler, H. W., Licciardello, F., Fava, P., & Pulvirenti, A. (2020). Development of antimicrobial films based on chitosan-polyvinyl alcohol blend enriched with

ethyl lauroyl arginate (LAE) for food packaging applications. Food Hydrocolloids, 100, 105419.

Haloui, I., & Meniai, A. H. (2017). Supercritical CO2 extraction of essential oil from Algerian Argan (Argania spinosa L.) seeds and yield optimization. International Journal of Hydrogen Energy, 42(17), 12912-12919.

Ilyas, R. A., Sapuan, S. M., & Ishak, M. R. (2018). Isolation and characterization of nanocrystalline cellulose from sugar palm fibres (Arenga Pinnata). Carbohydrate Polymers, 181, 1038-1051.

Jagadeesh, D., Kumar, B. P., Sudhakara, P., Prasad, C. V., Rajulu, A. V., & Song, J. I. (2013). Preparation and properties of propylene glycol plasticized wheat protein isolate novel green films. Journal of Polymers and the Environment, 21(4), 930-936.

Jahed, E., Khaledabad, M. A., Bari, M. R., & Almasi, H. (2017). Effect of cellulose and lignocellulose nanofibers on the properties of Origanum vulgare ssp. gracile essential oil-loaded chitosan films. Reactive and Functional Polymers, 117, 70-80.

Jiang, S., Zou, L., Hou, Y., Qian, F., Tuo, Y., Wu, X., Zhu, X., & Mu, G. (2020). The influence of the addition of transglutaminase at different phase on the film and film forming characteristics of whey protein concentrate-carboxymethyl chitosan composite films. Food Packaging and Shelf Life, 25, 100546.

Jiménez-Rosado, M., Bouroudian, E., Perez-Puyana, V., Guerrero, A., & Romero, A. (2020). Evaluation of different strengthening methods in the mechanical and functional properties of soy protein-based bioplastics. Journal of Cleaner Production, 262, 121517.

Karbowiak, T., Hervet, H., Léger, L., Champion, D., Debeaufort, F., & Voilley, A. (2006). Effect of plasticizers (water and glycerol) on the diffusion of a small molecule in iota-carrageenan biopolymer films for edible coating application. Biomacromolecules, 7(6), 2011-2019.

Kieliszek, M., & Misiewicz, A. (2014). Microbial transglutaminase and its application in the food industry. A review. Folia Microbiologica, 59(3), 241-250.

Kim, D. A., Cornec, M., & Narsimhan, G. (2005). Effect of thermal treatment on interfacial properties of beta-lactoglobulin. Journal of Colloid and Interface Science, 285(1), 100–109. https://doi.org/10.1016/j.jcis.2004.10.044

Laemmli, U. K. (1970). Cleavage of structural proteins during the assembly of the head of bacteriophage T4. Nature, 227(5259), 680-685.

Lakram, N., Moutik, S., MERCHA, I., EL HAJ, E. M., KABBOUR, R., DOUAIK, A., ... & NACIRI, M. (2019). Effects of the inclusion of detoxified argan press cake in the diet of dairy goats on milk production and milk quality. Turkish Journal of Veterinary and Animal Sciences, 43(3), 323-333.

Lam, R. S. H., & Nickerson, M. T. (2013). The effect of pH and heat pre-treatments on the physicochemical and emulsifying properties of β-lactoglobulin. Food Biophysics, 9(1), 20–28. https://doi.org/10.1007/s11483-013-9313-4

Letcher, T.M. (ed.) (2020). Plastic Waste and Recycling: Environmental Impact, Societal Issues, Academic Press, pp. 1-664, doi.org/10.1016/B978-0-12-817880-5.00004-9.

li Zhai, J., Day, L., Aguilar, M. I., & Wooster, T. J. (2013). Protein folding at emulsion oil / water interfaces. Current Opinion in Colloid & Interface Science, 18(4), 257-271.

Liu, Y., Liu, Y., Xu, Z., Shan, M., Ge, X., Zhang, Y., Shao, S., Huang, L., Wang, W & Lu, F. (2019). Effects of Bacillus subtilis transglutaminase treatment on the functional properties of whey protein. LWT, 116, 108559.

Maldonado-Valderrama, J., Martín-Rodriguez, A., G´alvez-Ruiz, M. J., Miller, R., Langevin, D., & Cabrerizo-Vílchez, M. A. (2008). Foams and emulsions of β-casein examined by interfacial rheology. Colloids and Surfaces A: Physicochemical and Engineering Aspects, 323(1–3), 116–122. https://doi.org/10.1016/j. colsurfa.2007.11.003

Maldonado-Valderrama, J., Muros-Cobos, J. L., Holgado-Terriza, J. A., & Cabrerizo-Vílchez, M. A. (2014). Bile salts at the air–water interface: adsorption and desorption. Colloids and Surfaces B: Biointerfaces, 120, 176-183.

Maldonado-Valderrama, J., Terriza, J. A. H., Torcello-G´omez, A., & Cabrerizo- Vílchez, M. A. (2013). In vitro digestion of interfacial protein structures. Soft Matter, 9(4), 1043–1053. https://doi.org/10.1039/c2sm26843d

Maldonado-Valderrama, J., Torcello-G´omez, A., Del Castillo-Santaella, T., Holgado- Terriza, J. A., & Cabrerizo-Vílchez, M. A. (2015). Subphase exchange experiments with the pendant drop technique. Advances in Colloid and Interface Science, 222, 488–501. https://doi.org/10.1016/j.cis.2014.08.002

Martín, M. P., Nepote, V., & Grosso, N. R. (2016). Chemical, sensory, and microbiological stability of stored raw peanuts packaged in polypropylene ventilated bags and high barrier plastic bags. LWT-Food Science and Technology, 68, 174-182.

Mathe, C., Culioli, G., Archier, P., & Vieillescazes, C. (2004). Characterization of archaeological frankincense by gas chromatography-mass spectrometry. Journal of Chromatography A, 1023(2), 277–285. https://doi.org/10.1016/j.chroma.2003.10.016

Mirpoor, S. F., Giosafatto, C. V. L., Di Pierro, P., Di Girolamo, R., Regalado-González, C., & Porta, R. (2020). Valorisation of Posidonia oceanica Sea Balls (Egagropili) as a Potential Source of Reinforcement Agents in Protein-Based Biocomposites. Polymers, 12(12), 2788.

Montes Ruiz-Cabello, F. J., Rodríguez-Valverde, M. A., & Cabrerizo-Vílchez, M. A. (2011). Comparison of the relaxation of sessile drops driven by harmonic and stochastic mechanical excitations. Langmuir, 27(14), 8748-8752.

Moraila-Martínez, C. L., Ruiz-Cabello, F. J. M., Cabrerizo-Vílchez, M. A., & Rodríguez-Valverde, M. A. (2012). The effect of contact line dynamics and drop formation on measured values of receding contact angle at very low capillary numbers. Colloids and Surfaces A: Physicochemical and Engineering Aspects, 404, 63-69.

Neumann, A. W., & Good, R. J. (1972). Thermodynamics of contact angles. I. Heterogeneous solid surfaces. Journal of Colloid and Interface Science, 38(2), 341-358.

Ortega-Toro, R., Jiménez, A., Talens, P., & Chiralt, A. (2014). Properties of starch–hydroxypropyl methylcellulose based films obtained by compression molding. Carbohydrate Polymers, 109, 155-165.

Padial-Domínguez, M., Espejo-Carpio, F. J., García-Moreno, P. J., Jacobsen, C., & Guadix, E. M. (2020). Protein derived emulsifiers with antioxidant activity for stabilization of omega-3 emulsions. Food Chemistry, 329(May), 127148.

Parveen, S., Chaudhury, P., Dasmahapatra, U., & Dasgupta, S. (2019). Biodegradable protein films from gallic acid and the cataractous eye protein isolate. International Journal of Biological Macromolecules, 139, 12-20.

Porta, R. (2019). The plastics sunset and the bio-plastics sunrise. Coatings, 9, 526. doi: 10.3390/coatings9080526.

Porta, R., Di Pierro, P., Rossi-Marquez, G., Mariniello, L., Kadivar, M., & Arabestani, A. (2015). Microstructure and properties of bitter vetch (Vicia ervilia) protein films reinforced by microbial transglutaminase. Food Hydrocolloids, 50, 102-107.

Ramos, P. A. B., Guerra, Â. R., Guerreiro, O., Santos, S. A. O., Oliveira, H., Freire, C. S. R., Silvestre, A. J.D., Duarte, M. F. (2017). Antiproliferative effects of cynara cardunculus L. Var. altilis (DC) lipophilic extracts. International Journal of Molecular Sciences, 18(1). https://doi.org/10.3390/ijms18010063

Rencoret, J., Marques, G., Serrano, O., Kaal, J., Martínez, A. T., del Río, J. C., & Gutiérrez, A. (2020). Deciphering the unique structure and acylation pattern of Posidonia oceanica lignin. ACS Sustainable Chemistry & Engineering, 8(33), 12521-12533.

Rossi-Márquez, G., Helguera, M., Briones, M., Dávalos-Saucedo, C. A., & Di Pierro, P. (2021). Edible Coating from Enzymatically Reticulated Whey Protein-Pectin to Improve Shelf Life on Roasted Peanuts. Coatings, 11(3), 329.

Roy, S., & Rhim, J. W. (2020). Preparation of carbohydrate-based functional composite films incorporated with curcumin. Food Hydrocolloids, 98, 105302.

Ruiz-Álvarez, J. M., del Castillo-Santaella, T., Maldonado-Valderrama, J., Guadix, A., Guadix, E. M., & García-Moreno, P. J. (2022). pH

influences the interfacial properties of blue whiting (M. poutassou) and whey protein hydrolysates determining the physical stability of fish oil-in-water emulsions. Food Hydrocolloids, 122, 107075.

Ruiz-Cabello, F. M., Ibañez-Ibañez, P., Paz-Gomez, G., Cabrerizo-Vilchez, M., & Rodriguez-Valverde, M. A. (2018). Fabrication of superhydrophobic metal surfaces for anti-icing applications. JoVE (Journal of Visualized Experiments), (138), e57635.

Ruiz-Cabello, F. M., Rodríguez-Valverde, M. A., & Cabrerizo-Vilchez, M. A. (2011). Contact angle hysteresis on polymer surfaces: an experimental study. Journal of Adhesion Science and Technology, 25(16), 2039-2049.

Sagar, N. A., Pareek, S., & Gonzalez-Aguilar, G. A. (2020). Quantification of flavonoids, total phenols and antioxidant properties of onion skin: a comparative study of fifteen Indian cultivars. Journal of Food Science and Technology, 57(7), 2423-2432.

Sanyang, M. L., Sapuan, S. M., Jawaid, M., Ishak, M. R., & Sahari, J. (2016). Effect of sugar palm-derived cellulose reinforcement on the mechanical and water barrier properties of sugar palm starch biocomposite films. BioResources, 11(2), 4134-4145.

Scavo, A., Pandino, G., Restuccia, C., Parafati, L., Cirvilleri, G., & Mauromicale, G. (2019). Antimicrobial activity of cultivated cardoon (Cynara cardunculus L. var. altilis DC.) leaf extracts against bacterial species of agricultural and food interest. Industrial Crops and Products, 129(December 2018), 206–211.

Schmid, M., Reichert, K., Hammann, F., & Stäbler, A. (2015). Storage time-dependent alteration of molecular interaction–property relationships of whey protein isolate-based films and coatings. Journal of Materials Science, 50(12), 4396-4404.

Shi, X., Davis, J. P., Xia, Z., Sandeep, K. P., Sanders, T. H., & Dean, L. O. (2017). Characterization of peanuts after dry roasting, oil roasting, and blister frying. LWT, 75, 520-528

Shojaee-Aliabadi, S., Hosseini, H., Mohammadifar, M. A., Mohammadi, A., Ghasemlou, M., Ojagh, S. M., Hosseini, S.M., & Khaksar, R. (2013). Characterization of antioxidant-antimicrobial κ-

carrageenan films containing Satureja hortensis essential oil. International Journal of Biological Macromolecules, 52, 116-124.

Sorde, K. L., & Ananthanarayan, L. (2019). Effect of transglutaminase treatment on properties of coconut protein-guar gum composite film. LWT, 115, 108422.

Suyatma, N. E., Tighzert, L., Copinet, A., & Coma, V. (2005). Effects of hydrophilic plasticizers on mechanical, thermal, and surface properties of chitosan films. Journal of Agricultural and Food Chemistry, 53(10), 3950-3957.

Teixé-Roig, J., Oms-Oliu, G., Velderrain-Rodríguez, G. R., Odriozola-Serrano, I., & Martín-Belloso, O. (2018). The effect of sodium carboxymethylcellulose on the stability and bioaccessibility of anthocyanin water-in-oil-in-water emulsions. Food and Bioprocess Technology, 11(12), 2229-2241.

Tian, Y., Taha, A., Zhang, P., Zhang, Z., Hu, H., & Pan, S. (2021). Effects of protein concentration, pH, and NaCl concentration on the physicochemical, interfacial, and emulsifying properties of β-conglycinin. Food Hydrocolloids, 118, 106784.

Tolbert, A., Akinosho, H., Khunsupat, R., Naskar, A. K., & Ragauskas, A. J. (2014). Characterization and analysis of the molecular weight of lignin for biorefining studies. Biofuels, Bioproducts and Biorefining, 8(6), 836-856.

Torres, A. M., Barros, G. G., Palacios, S. A., Chulze, S. N., & Battilani, P. (2014). Review on pre- and post-harvest management of peanuts to minimize aflatoxin contamination. Food Research International, 62, 11e19.

Torres, A. M., Barros, G. G., Palacios, S. A., Chulze, S. N., & Battilani, P. (2014). Review on pre-and post-harvest management of peanuts to minimize aflatoxin contamination. Food Research International, 62, 11-19.

Varughese, S., & Tripathy, D. K. (1993). Effect of plasticizer type and concentration on the dynamic mechanical properties of epoxidized natural rubber vulcanizates. Journal of Elastomers & Plastics, 25(4), 343-357.

Vejdan, A., Ojagh, S. M., Adeli, A., & Abdollahi, M. (2016). Effect of TiO2 nanoparticles on the physico-mechanical and ultraviolet

light barrier properties of fish gelatin/agar bilayer film. LWT-Food Science and Technology, 71, 88-95.

Velderrain-Rodríguez, G. R., Salvia-Trujillo, L., González-Aguilar, G. A., & Martín-Belloso, O. (2021). Interfacial activity of phenolic-rich extracts from avocado fruit waste: Influence on the colloidal and oxidative stability of emulsions and nanoemulsions. Innovative Food Science & Emerging Technologies, 69, 102665.

Velez, Z., Campinho, M. A., Guerra, Â. R., García, L., Ramos, P., Guerreiro, O., Felício, L., Schmitt, F., Duarte, M. (2012). Biological characterization of cynara cardunculus l. Methanolic extracts: Antioxidant, anti-proliferative, anti-migratory and anti-angiogenic activities. Agriculture (Switzerland), 2(4), 472–492. https://doi.org/10.3390/agriculture2040472

Wan, Z., Yang, X., & Sagis, L. M. C. (2016). Contribution of long fibrils and peptides to surface and foaming behavior of soy protein fibril system. Langmuir, 32(32), 8092–8101.

Wihodo, M., & Moraru, C.I. (2013). Physical and chemical methods used to enhance the structure and mechanical properties of protein films: A review. Journal of Food Engineering, 114, 292–302.

Xu, W., Liu, B., Yang, H., Liu, K., Jia, S., & Chen, F. (2012). Effect of γ-irradiation on the physicochemical properties of mixed soy protein isolate/starch material. African Journal of Biotechnology, 11(28), 7238-7246.

Zahedi, Y., Fathi-Achachlouei, B., & Yousefi, A. R. (2018). Physical and mechanical properties of hybrid montmorillonite/zinc oxide reinforced carboxymethyl cellulose nanocomposites. International Journal of Biological Macromolecules, 108, 863-873.

Zhou, B., Tobin, J. T., Drusch, S., & Hogan, S. A. (2021). Dynamic adsorption and interfacial rheology of whey protein isolate at oil-water interfaces: Effects of protein concentration, pH and heat treatment. Food Hydrocolloids, 116, 106640.

APPENDIX

6. Appendix

- **Experience in foreign laboratories**

1. **Department of Applied Physics,** University of Granada, Spain
   Supervisor: Prof. Julia Maldonado-Valderrama
   Topic: Studying the interfacial properties of HP,CP and AP obtained from seed oilcake as well as investigating the wettability and surface properties of bioplastics obtained from these proteins
   Date: September-November 2021

- **Courses**

1. Protein structure visualization, analysis and molding (Prof. Eugenio Notomista), 2019
2. First step in writing and publishing a scientific manuscript (Prof. Viola Calabro, Dr. Daria Monti), 2019
3. Microscopic methodologies for life and material science (Dr. Angelo Arciello, Dr. Rocco di Girolamo, Dr. Fabio Borbone),2019
4. Enzymes as additives or processing aids (Dr.Giosafatto Valeria), 2019
5. Carbohydrate active enzymes for biorefineris (Prof. Marco Moracci, Dr. Andrea Strazzulli), 2019
6. Immunology as a tool in Biotechnology (Dr. Andrea Fulgione), 2019
7. Matlab fundamentals (Agostino De Marco - Stefano Marrone), 2020
8. Bioactive molecules from natural sources: purification and applications (Daria Maria Monti), 2021

9. Discovery of carbohydrate active enzymes from hyperthermophiles: genomic and metagenomic approaches (Dr. Andrea Strazzulli), 2021
10. Bioplastic for a sustainable development (Prof. Loredana Mariniello), 2021

- **List of Publications**

1- **Mirpoor, S. F.,** Giosafatto, C. V. L., & Porta, R. (2021). Biorefining of seed oil cakes as industrial co-streams for production of innovative bioplastics. A review. Trends in Food Science & Technology, https://doi.org/10.1016/j.tifs.2021.01.014

Trends in Food Science & Technology 109 (2021) 259–270

Contents lists available at ScienceDirect

Trends in Food Science & Technology

journal homepage: www.elsevier.com/locate/tifs

Biorefining of seed oil cakes as industrial co-streams for production of innovative bioplastics. A review

Seyedeh Fatemeh Mirpoor, C. Valeria L. Giosafatto, Raffaele Porta *

Department of Chemical Sciences, University of Naples "Federico II", Naples, Italy

ARTICLE INFO

Keywords:
Seed oil cakes
Renewable materials
Bioplastics
Protein-based films
Biorefinery

ABSTRACT

Background: Numerous different seeds are utilized for edible oil extraction and seed by-products following oil extraction, known as seed oil cakes, represent roughly 50% of the original seed weight. Since seed oil cakes are rich in fibers, proteins and secondary metabolites, they are considered as promising candidates to be raw material to be consumed in a biorefinery for the production of high-value added products according to circular economy paradigms. Several studies have been performed on the potential uses of seed oil cakes derived from different plant species.

Scope and approach: This review, resulting from a collection of experimental results by databases, as well as by topic and keyword search, summarizes the current use of most seed oil cakes so far utilized, as well as that of additional four seed cakes obtained from plants having an economically significant relevance due to their food, nutraceutical or pharmaceutical properties: sesame (*Sesamum indicum* L.), hemp (*Cannabis sativa*), cardoon (*Cynara cardunculus*) and black cumin (*Nigella sativa*). Various attempts have been done to convert their protein content into a renewable source for producing biodegradable and edible plastics, potentially attractive mainly for food and agricultural industries, as substitutes of the highly polluting petroleum-based plastics.

Key findings and conclusions: Seed oil cakes are generally used as animal feed supplementation, plant fertilizer or soil compost due to their high protein, carbohydrate and nitrogen contents. More recently, novel exploitations of the seed oil cakes are under study, such as the production of biofuels and bioplastics. Therefore, seed oil cakes may represent an attractive feedstock for the development of biorefineries through the edible or not edible oil production.

1. Introduction

Oilseed crops, considered as energy dense foods, are grown all over the world mainly for the oil production. They are rich in fibers, antioxidants, vitamins (e.g. vitamin E, niacin, folate), minerals (e.g. phosphorus, iron, magnesium), as well as monounsaturated and polyunsaturated fatty acids. There is, generally, a deficiency of lysine and of sulfur amino acids in oilseed proteins in comparison with animal proteins and, in some cases, the presence of anti-nutritional factors is also observed. However, these limits could be easily counteracted by both integration of other proteins and physicochemical treatments.

Oilseeds have long been in the spotlight due to their multiple applications, such as producing functional vegetable oils, as well as animal feeds, pharmaceuticals, biofuels and other industrial usages, that led to an increase in oilseed crop cultivation areas. In fact, it was registered over the last thirty years 82% expansion of cultivation areas and about 240% increase in total oilseed world production (Rahman & de Jiménez, 2016).

The most cultivated oilseed crops all over the world are soybean (*Glycine max*), rapeseed (*Brassica napus*), cotton (*Gossypium hirsutum* L.), sunflower (*Helianthus annuus*), and groundnut (*Arachis hypogaea*), even though to soybean it is dedicated almost 60% of the world's oilseed production (Gaonkar & Rosentrater, 2019) (Fig. 1). Further oilseed types have an economically significant relevance due to their food, nutraceutical or pharmaceutical properties. Among these, the seeds obtained from sesame (*Sesamum indicum* L.) (over 5 million tons/year produced worldwide), hemp (*Cannabis sativa*) (about 150 thousand tons/year produced worldwide), cardoon (*Cynara cardunculus* var. altilis), a native crop of the Mediterranean region, produced in few thousands tons/year, that has gained interest due to its multipurpose

Abbreviations: SOC, seed oil cake; FFS, film forming solution.

* Corresponding author.
E-mail address: raffaele.porta@unina.it (R. Porta).

https://doi.org/10.1016/j.tifs.2021.01.014
Received 22 May 2020; Received in revised form 11 November 2020; Accepted 2 January 2021
Available online 20 January 2021
0924-2244/© 2021 Elsevier Ltd. All rights reserved.

applications (FAOSTAT, 2020) have been selected. In addition, also several oilseed plants traditionally known to give rise to culinary spices deserve particular attention for their increasing spread even as sources of bioactive compounds. One of these is black cumin (*Nigella sativa*), the seeds of which are widely used in Indian and middle east cuisine, as well as drug in traditional medicine (Srinivasan, 2018). The fatty acids content of the different oilseeds under study is reported in Table 1.

The global production of oilseeds, mainly intended for edible oil production, reached almost 600 million tons in 2018/2019 (USDA, 2018b) but the generation of by-products after the oil extraction, known as seed oil cake (SOC), accounts generally for about 50% of the original seed total weight.

The world SOC market is dominated, of course, by those derived from the five major oilseed plants cultivated (e.g. soybean, rapeseed, cotton, sunflower and groundnut). Among these soybean SOC occupies more than 50% of the total production volume followed by rapeseed (10%) and cotton SOCs (10%). SOC chemical composition is affected by different factors, primarily by the plant variety and growing conditions. Table 2 indicates that, among the nine oilseeds examined, sesame- and black cumin-derived SOCs still contain, despite the seed defatting process, high amounts of oil (11.9–27.8 and 15.5–16.5, respectively). Conversely, hemp and sunflower SOCs are particularly rich in fiber and total carbohydrates, whereas the protein content is particularly high in all SOCs, varying from a minimum of 16.5% in cardoon SOC to a maximum of 54% and 55.3% in soybean and groundnut, respectively. Finally, also the oil extraction process can significantly influence SOC properties. For instance, different amino acids, particularly lysine, methionine, arginine, tryptophan and cysteine might be destroyed under intense heat treatments.

Since SOCs are rich in different small and high molecular weight bioactive molecules, such as polyphenols, flavonoids, proteins and fibers, they have been explored as candidates of biological sources in a biorefinery (Teh & Bekhit, 2015). In fact, biomass biorefining can improve the economy of oil production by obtaining from SOCs multiple value-added products. In this regard several attempts have been done with the different SOCs and some innovative strategies are under study and are here discussed.

2. SOC production and utilization

The consumption of vegetable proteins in food products has been increasing over the years because of economic as well as religious reasons, global shortage of animal proteins, and increasing demand for wholesome food. Therefore, oilseed request, as well as that of grain legumes, have been enhanced to be utilized to manufacture and market high quantities of protein foods at reasonably low prices. The potential commercial relevance of proteins present in SOCs was recognized starting from early 60's, since before oilseeds were valued only for their oil content. Since then industries, in addition to supplying oil, started to produce vegetable protein enriched meals, at beginning only for animal feed and, then, also for human consumption. However, although SOCs are used as food for animals, the potential impact of a use change of them on other productive chains should not create significant concerns. In fact, it must be taken into consideration that the exploitation of SOCs as animal feed has some drawbacks that limit its use. The high water content, which often exceeds 80%, makes their handling difficult and can accelerate the growth of microbiological contamination. In addition, the analytical composition of the different SOCs vary thus meaning that animal feed manufacturers have to change their feed formulations depending on the composition. Finally, their digestibility is often limited and somewhat also complicated by anti-nutritional factors present within the material. Consequently, SOC-based diets are only partially used and the addition of other ingredients is almost always required. Due to their considerable protein, fiber and mineral content, SOCs are used today also as plant fertilizers or soil composts and, more recently, there is a strong interest to utilize them also as human food, because of the alarming increase of the world population and the attractive emerging nutritional properties of numerous of these by-products. However SOCs, mainly those produced in tropical and subtropical areas, are often infected by various microorganisms during plant growth, as well as during seed storage and transport, and are consequently contaminated by aflatoxins (Fink-Gremmels, 2012). Moreover, as mentioned before, also the high water activity in oilseeds can also promote growth of fungi and production of toxins. Therefore, SOCs need to be often heated or chemically treated to make them suitable for human food use, and a careful control of SOC safety is a must before any use.

SOCs, mostly those derived from soybean, rapeseed, cotton, sunflower and groundnut crops, account for the largest proportion of annual protein production, together with legumes, over the world. Removal of carbohydrates and other components from SOCs allows to obtain enriched protein concentrates. Therefore, protein extraction procedures from the various SOCs have been refined to obtain maximum protein yield from each source. A complex mixture of different proteins characterizes the different SOC protein concentrates, and some of them are structurally related, playing a role in equipping the seed for survival.

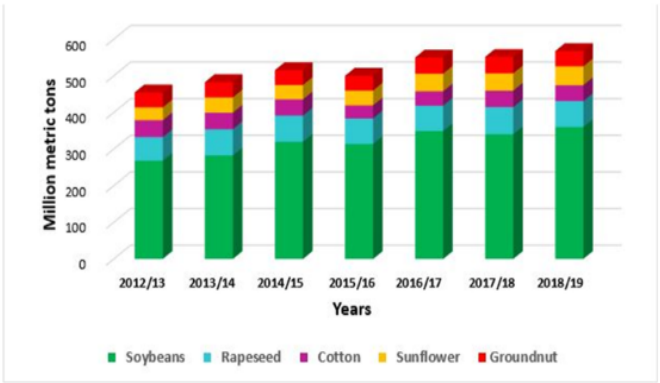

Fig. 1. Global production of the five main oilseeds over the last eight years. Source: World Agricultural Supply and Demand Estimates. USDA, Washington, DC. (USDA, 2018a).

Table 1
Fatty acid content in different seed oils (%, w/w).

	Saturated	Mono-unsaturated	Poly-unsaturated	Omega-6	Omega-3	*Omega-6/Omega-3*
Soybean[a]	13.9–15.7	24.2–30.0	56.1–59.8	47.1–52.1	7.8–9.1	5.7–6.7
Rapeseed[a]	6.8–8.0	60.6–62.4	31.5–32.7	20.6–23.2	9.5–11.6	2.0–2.2
Cotton[b]	26.1–28.0	17.6–18.5	53.4–56.1	53.2–55.8	0.2–0.3	186.0–266.0
Sunflower[b]	11.3–12.8	20.6–22.4	66.0–68.2	65.1–65.5	0.4–0.5	130.0–162.0
Groundnut[b]	18.3–20.3	48.1–49.6	30.8–31.5	30.3–31.4	0.1–0.4	76.0–78.5
Sesame[b]	16.4–22.0	26.1–36.2	45.7–47.6	45.3–47.3	0.3–0.4	113.0–119.0
Black cumin[c]	24.8–27.0	21.0–22.3	50.7–52.4	48.3–49	2.4–2.7	18.0–20.0
Hemp[d]	18.0–20.0	10.45–12.1	79.1–80.4	56.9–59.4	19.7–23.5	2.5–2.8
Cardoon[e]	13.2–13.4	21.1–21.3	65.3–65.5	64.8–65.0	0.5–0.6	109–130

[a] Gunstone, 2002; Dubois, Breton, Linder, Fanni, & Parmentier, 2007.
[b] Gunstone, 2002; Dubois et al., 2007.
[c] Atta, 2003; Dubois et al., 2007.
[d] Teh & Birch, 2013; Dubois et al., 2007.
[e] Petropoulos, Pereira, Tzortzakis, Barros, & Ferreira, 2018.

Table 2
Chemical composition of different SOCs[a].

	Protein	Oil	Fiber	Total carbohydrates	Starch	Ash
Soybean[b]	46.0–54.0	1.8–6.0	14.0–23.3	29.0–36.0	0.0–2.7	6.0–6.4
Rapeseed[c]	38.0–48.0	2.3–6.4	9.7–13.9	38.5–41.3	0.7–2.3	6.3–7.9
Cotton[d]	40.3–43.0	1.4–2.9	12.5–15.7	32.5–33.0	0.7–2.9	6.5–6.9
Sunflower[c]	32.0–42.6	1.5–2.9	29.0–43.0	44.8–51.7	0.1–1.5	6.5–8.0
Groundnut[f]	45.0–55.3	2.5–10.1	5.3–9.0	22.0–33.6	7.7–8.8	4.5–5.0
Sesame[g]	30.6–40.9	11.9–27.8	6.2–8.1	25.8–30.5	1.1–2.1	5.3–7.9
Black cumin[h]	19.0–27.0	15.5–16.5	5.9–7.8	22.9–28.4	ND	5.0–10
Hemp[i]	34.0–47.9	5.2–11.1	39.2–56.2	43.0–66.7	1.5–5.6	7.2–7.5
Cardoon[j]	16.5–21.0	2.9–6.9	12.4–28.1	45.3–48.9	3.3–5.9	5.5–6.3

[a] Reported values are given as grams per 100 g of dry matter. The used analytical methods for analyzing each component are described by Kyntäjä, Partanen, Siljander-Rasi, and Jalava (2014). Further data are reported in INRA-CIRAD-AFZ Feed tables (https://feedtables.com/content/table-dry-matter, accessed on July 17th, 2020).
[b] Lee & Min, 2014; Pettersson & Pontoppidan, 2013.
[c] Pettersson & Pontoppidan, 2013; Kyntäjä et al., 2014.
[d] Yu et al., 2020; Pettersson & Pontoppidan, 2013.
[e] Lomascolo, Uzan-Boukhris, Sigoillot, & Fine, 2012; Pettersson & Pontoppidan, 2013.
[f] Ghosh & Mandal, 2015; Sunil, Appaiah, Kumar, & Krishna, 2015.
[g] Sibt-e-Abbas et al., 2020; Sunil et al., 2015.
[h] Thilakarathne, Madhusankha, & Navaratne, 2018; Gharby et al., 2015.
[i] Hadnadev et al., 2018; Serrapica et al., 2019.
[j] Genovese et al., 2015; Serrapica et al., 2019.

SOC proteins are traditionally classified into four groups on the basis of their extraction and solubility in water (albumins), dilute saline (globulins), alcohol/water mixtures (prolamins), and dilute acid or alkali (glutelins).

The main proteins present in the analyzed oilseeds are listed in Table 3.

Furthermore, the specific applications reported so far for the five main SOCs, as well as for four additional SOCs, are summarized in Table 4, whereas the primary features of each oilseed are described below.

Table 3
Main proteins present in different oilseeds.

	Main Protein	References
Soybean	glycinin; β-conglycinin	Pettersson and Pontoppidan (2013)
Rapeseed	12 S globulin cruciferin; 1.7–2 S albumin napin	Fetzer, Hintermayr, Schmid, Stäbler, & Eisner (2020)
Cotton	gossypin (11 S); congossypin (7 S)	Yue, Cui, Shuttleworth, and Clark (2012)
Sunflower	helianthinin (11 S globulin)	Salgado, López-Caballero, Gómez-Guillén, Mauri, and Montero (2012)
Groundnut	arachin; conarachin	Wang et al. (2014)
Sesame	11 S globulin; 2 S albumin	Onsaard (2012)
Black cumin	albumin; glutelin	Atta, 2003; Dubois et al., 2007
Hemp	albumin; edestin	Hadnadev et al., 2018; Kitryté, Bagdonaité, & Venskutonis, 2018
Cardoon	not detected	

2.1. Soybean

Soybean is the most cultivated oilseed crop in the world (USDA, 2018b), because of its high nutritional value, short crop cycle and oil-enriching profitable crop. Therefore, it offers rapid economic return and provides health benefits to the consumers as component of nutraceutical and functional food-grade produce (Zhang, Li, Chin, & Qi, 2017). According to the Food and Agriculture Organization of the United Nations (FAOSTAT, 2020), USA and Brazil are the countries with the highest soybean production (more than 200 million tons from 2015 to 2018).

Soybean seeds are an excellent source of plant-based proteins containing all the essential amino acids and have the distinction of generating the highest amount of SOCs with respect to other plants (Teh & Bekhit, 2015). Soybean SOCs have been utilized until now for producing different value-added products. Several studies indicate that the soybean SOCs are also rich sources of phenolic compounds, including isoflavones (Esaki, Watanabe, Hishikawa, Osawa, & Kawakishi, 2004), that possess antioxidant properties. In this respect, a functional protein-carbohydrate extract with high antioxidant activity, potentially

Table 4
Main current utilizations of SOCs.

Seed oil cake	Utilization	References
Soybean	Animal feed and human food additive	Gerliani, Hammami, and Aïder (2020)
	Enzyme production	Prabaningtyas, Putri, Utami, and Hermansyah (2018)
	Green adhesive	Tous, Ruseckaite, & Ciannamea, 2019 ì
	Antioxidant agent	Gerliani et al. (2020)
Rapeseed	Animal feed and human food additive	Sibt-e-Abbas et al. (2020)
	Antioxidant and antimicrobial agent	Teh and Bekhit (2015)
	Biofuel	Özçimen and Karaosmanoğlu (2004)
	Fertilizer	Bonjean, Dequidt, Sang, and Limagrain (2016)
	Blood pressure-lowering activity	He et al. (2013)
Cotton	Animal feed and human food additive	Ma et al. (2018)
	Fertilizer	He et al. (2014)
	Enzyme production	Aguieiras, de Barros, Fernandez-Lafuente, and Freire (2019)
	Green adhesive	He, Cheng, Klasson, Ford, and Barroso (2019)
Sunflower	Animal feed and human food additive	Salgado, Drago, et al., 2012; Dabbour, He, Mintah, Xiang, & Ma, 2019
	Antioxidant and antimicrobial agent	Dabbour et al. (2019)
	Biofuel	Havrysh, Kalinichenko, Mentel, Mentel, and Vasbieva (2020)
Groundnut	Animal feed and human food additive	Bansal and Kochhar (2014)
	Fertilizer	Bansal and Kochhar (2014)
	Production of protein beverage	Ye, Liao, Sun, and Zhao (2015)
	Antioxidant agent	Hu et al. (2019)
Sesame	Animal feed and human food additive	Cano-Medina et al., 2011; Yasothai, 2014a,b; Machado, Benelli, & Tessaro, 2017
	Antioxidant agent	Sarkis, Michel, Tessaro, and Marczak (2014)
Black cumin	Animal feed and food additive	Kadam and Lele (2017)
Hemp	Animal feed and human food additive	Hadnadev et al. 2018; Mamone, Picariello, Ramondo, Nicolai, & Ferranti, 2019
	Antioxidant agent	Kitryté et al. (2018)
Cardoon	Animal feed additive	Genovese et al., 2015; Cabiddu et al., 2019
	Soil modification	De Corato, De Bari, Viola, and Pugliese (2018)
	Antioxidant agent	Genovese et al. (2015)

exploitable in food industry, was obtained from soybean SOC (Gerliani et al., 2020). Moreover, different researches were carried out on producing enzymes, such as lipase by *Aspergillus niger* by using soybean SOC as a solid substrate (Prabaningtyas et al., 2018). Finally, a new biodegradable adhesive was also developed by replacing 50% of polycaprolactone with soybean protein isolate and castor oil added as plasticizer (Tous et al., 2019).

2.2. Rapeseed

Although rapeseed is often used as annual forage and, mainly in USA, as cover crop during the winter, being able to suppress weeds and to improve cultivation with its root system, it represents the second largest source of protein meal in the world, after soybean, and the third largest source of vegetable oil after soybean and palm oil (FAOSTAT, 2020). In fact, rapeseed oil is one of the oldest known vegetable oils, although its use is limited because of the high content in erucic acid (2% by weight allowed in the USA and 5% in the EU) and glucosinolate.

Rapeseed is mainly grown in Canada (over 20 million tons produced/year) (FAOSTAT, 2020), where the largest amount of rapeseed SOC biomass originates after soybean. A big challenge of profitable rapeseed production is just the limited use for the SOC remaining after oil extraction, despite the fact that this by-product is a high-protein animal feed (about 35–36%), competitive with soybean and possessing a balanced amino acid profile compared to other oilseed proteins. It contains also polysaccharides, such as pectin, hemicellulose and cellulose (Kdidi et al., 2019). Due to its favorable amino acid profile, as well as to its high content of fibers and antioxidant/antimicrobial compounds, rapeseed cake has been proposed as a human food additive or as nutraceutical in food manufacture (Kdidi et al., 2019; Sibt-e-Abbas et al., 2020; Teh & Bekhit, 2015). In this respect, He et al. (2013) demonstrated that rapeseed protein hydrolysates have also a pharmacological activity being able to reduce blood-pressure, whereas Rivera, Rommi, Fernandes, Lantto, and Tzanov (2015) proposed their use as raw materials for skincare applications.

Conversely in China, the world's second most important producer of rapeseed after Canada, rapeseed cake is mostly used as soil fertilizer rather than for animal feed supplementation (Bonjean et al., 2016). Finally, Özçimen and Karaosmanoğlu (2004) produced from rapeseed cakes a biodiesel, either alone or blended with fossil-fuel diesel, with a high heating value and the potential to become a candidate as a non-polluting solid biofuel.

2.3. Cotton

China and India are the countries with the highest cottonseed production with about 10 million tons each per year (FAOSTAT, 2020). Cottonseed oil is obtained from the seeds of plants of various species, mainly *Gossypium hirsutum* and *Gossypium herbaceum*, and is used as cooking oil because of its flavor stability. Cottonseed oil ranks third in volume, behind soybean and corn oil, representing about 5–6% of the total domestic oil supply. However, as edible product, cottonseed oil must be processed and refined to eliminate gossypol, a natural seed pigment able to act as a natural defense against insects, but acting as a toxin towards humans. The fine quality oil extracted from cottonseed is also used in cosmetics, such as component of bath soaps and moisturizing lotions.

SOC, the second most valuable product of cottonseed, is a good protein source for animal feed additive and fertilizer applications, having an amino acid composition similar to that of soy proteins (He et al., 2014). In particular, cottonseed cake is mostly used to feed the adult ruminants, which are relatively tolerant to gossypol. Recently, Webb, Bernard, and Tao (2019) studied the effects of replacing soybean meal with cottonseed cake on the performance of lactating cows, whereas (Yu et al., 2020) investigated the effects of cottonseed meal, compared to soybean meal, on the meat chemical composition and quality in Jiangnan White goslings. The reported results did not indicate significant differences, demonstrating that the meal substitution had no effects on milk yield and its composition, as well as on the meat quality in geese, altering only the amino acid and fatty acid composition of their breast muscle. Similar results were obtained by replacing dietary soybean meal with cottonseed cake, in order to decrease total feed costs, on the growth performance and meat chemical composition of ostriches (Dalle Zotte et al., 2013). Furthermore, Ma et al. (2018) showed that cottonseed cake proteins exhibited high water/oil absorption capacity, as well as emulsifying property, suggesting their potential as functional ingredients in the food industry. More recently, Aguieiras et al. (2019) added value to cottonseed cake through the production of *Rhizomucor miehei* lipases and application of the dry fermented solid in esterification reactions between oleic acid and alcohol and transesterification of a vegetable oil. A conversion higher than 85% was obtained in few hours, demonstrating that fermented solids produced in cottonseed meal can be used as biocatalyst of esterification and transesterification reactions. Finally, cottonseed cake was also proposed as a capable candidate for being used as a source of a "green" adhesive with acceptable bonding performance, comparable to that of wood-based composites, either

blended with guanidine hydrochloride and sodium dodecyl sulfate or with urea and formaldehyde (He et al., 2019).

2.4. Sunflower

The global sunflower seed production was about 50 million tons in 2018, more than half in Ukraine and Russia with 14.1 and 12,7 million tons annual production in each of these countries, respectively (FAOSTAT, 2020). The oil extracted from sunflower seeds is commonly used in food sector as a frying oil or processed into polyunsaturated margarines. In addition, it is an emollient component of some cosmetic formulations and, mixed with diesel, increases fuel viscosity at cold temperatures (Lim, 2013).

The by-product of sunflower oil extraction are the pressed seeds, typically referred to as sunflower SOC, which is rich in dietary fiber and proteins (roughly 500 g of protein/Kg of SOC) and used as animal feed supplementation, fertilizer or fuel (Lomascolo et al., 2012). In terms of production, it is the 4th most important SOC after those derived from soybean, rapeseed and cottonseed. However, due to its relatively high content in phenolic compounds, especially chlorogenic and caffeic acids, the use of sunflower SOC as a feedstuff is quite limited (Salgado, Drago, et al., 2012). Hence, polyphenols must be removed by protein isoelectric precipitation in order to improve the SOC functional properties, such as emulsifying, foaming, surface hydrophobicity and water-holding activities, and consequently to increase protein digestibility (Salgado, Drago, et al., 2012). Furthermore, Dabbour et al. (2019) demonstrated that enzymatic hydrolysis and ultrasonication treatments improve solubility, foaming properties and emulsion stability of the sunflower protein isolate, allowing its use as a natural additive in both food and pharmacological sectors. Finally, sunflower oil and SOC have captured the attention also as possible sources of a clean fuel (Havrysh et al., 2020).

2.5. Groundnut

Groundnut is native to South America where Incas, in the 14th century, already used its seeds. Then, after the arrival of Europeans, groundnut was spread worldwide. However, it acquired economic importance, both in the more developed and developing countries, only as late as at beginning of last century. Today, groundnut is the fifth largest oilseed produced in the world after soybean, rapeseed, cottonseed and sunflower accounting for around 46 million tons, and China is the country with the highest production (more than 17 million tons annually) followed by India with about 7 million tons/year (FAOSTAT, 2020). The extracted oil has a strong groundnut flavor and aroma and is used for general cooking, as a massage oil, to make soap and as a source of fuel for diesel engines.

Oil production gives rise to a large amount of by-products, containing up to 40–50% proteins with high essential amino acid content, that are normally used as feed ingredient for animals and as fertilizers (Bansal & Kochhar, 2014). Groundnut meal is the sixth oilseed meal produced in the world after soybean, rapeseed, sunflower, cottonseed and palm kernel meals and is generally considered as an excellent feed ingredient, due not only to its high protein content but also to low fiber, high oil and relative absence of anti-nutritional factors. Defatted groundnut flour, easily produced from cake blends, is used to enrich the nutritive value of wheat and other flours (Purohit & Rajyalakshmi, 2011). Groundnut SOC is, thus, a potential alternative to soybean and cottonseed meals for ruminants and there are no restrictions on the use of it provided that it is not contaminated by aflatoxins, since groundnuts are particularly vulnerable to contamination by fungi *Aspergillus flavus* and *Aspergillus parasiticus*. Further studies assessed the value of groundnut SOC in fish and crustacean diets, even though it seems that only part of fish meal can be replaced by it (Cai et al., 2013).

The functional properties of proteins obtained from groundnut SOC are affected by the different methods of extraction. Protein concentrates are used in the production of protein beverages to replace animal proteins (Ye et al., 2015). However their applying in beverages is limited because of the protein instability under harsh temperature of pasteurization or sterilization (Hu et al., 2019). Finally, since groundnut SOC is a rich, but also cheap, source of protein, it was suggested for preparing added-value products for children finalized to counteract the malnutrition phenomenon (Bansal & Kochhar, 2014; Srivastava, Mathur, & Shirshat, 2018).

2.6. Sesame

Sesame is one of the oldest oilseed crops, domesticated over 3000 years ago. Its production for seed oil extraction has tripled in the past years reaching in total more than 5 million tons in five largest producer countries (Sudan, Myanmar, India, Nigeria and Tanzania) (FAOSTAT, 2020). Sesame is a rich source also of micronutrients such as polyphenols, the main of which were identified as lignans, including sesamin, sesamolin and lignan glycosides, that provide an exceptional oxidative stability compared to other edible seed oils (Kuo, Lin, Chen, Yiu, & Tzen, 2011). Sesame seed oil is a common ingredient in cuisines across the world, whereas the by-product that remains after oil extraction, sesame SOC, is a protein meal rich in sulfur-amino acids generally used as feed for poultry and livestock (Yasothai, 2014a, 2014b). Unlike other SOCs, sesame SOC is usually obtained by only mechanical extraction without solvent addition and, thus, its residual oil content remains quite high.

Extracted proteins from sesame SOC have excellent functional properties, like foaming capacity, emulsifying activity, water- and oil-holding capacity, as well as solubility, useful for many food applications (Cano-Medina et al., 2011). In addition to food component, sesame SOC is also used as additive of drugs, cosmetics, soaps, drugs and lubricants.

2.7. Black cumin

Black cumin (*Nigella sativa*) is an annual flowering plant the seeds of which are used as spice in Indian and middle east cuisine and as drug in traditional medicine. The nutritional value of black cumin seeds is linked to its content in substantial amount of proteins and fiber. Seed proteins are rich in glutamate, arginine, and aspartate, while they are poor in cysteine and methionine (Srinivasan, 2018; Yimer, Tuem, Karim, Ur-Rehman, & Anwar, 2019).

Black cumin seed oil, representing 35–40% of the total seeds, contains a variety of chemicals (linoleic, oleic and palmitic acids, as well as trans-anethole, p-cymene, carvacrol, α-thujene, thymol, α- and β-pinene), but most of the pharmacological properties of black cumin are attributed to the presence of quinine compounds, of which thymoquinone is the most abundant (Yimer et al., 2019; Srinivasan, 2018).

The presence of large number of essential nutrients and a variety of pharmacologically active compounds made black cumin seeds successfully suitable for their use as animal feed ingredient (Kumar & Patra, 2017), as well as additive to extend fish shelf life and quality during cold storage (Ozpolat & Duman, 2017). Finally, the potential of black cumin seed oil as a cosmetic ingredient was also suggested (Sudhir, Deshmukh, & Verma, 2016).

The black cumin SOC, obtained from the seeds by cold pressing, contains considerable amount of protein that can be utilized in different ways with the aim to search new market opportunities (Thilakarathne, Madushanka, & Navaratne, 2018). In addition to its exploitation as food ingredient and animal feed, black cumin SOC has been proposed as a protein, phenolic, and carbohydrate-rich meal able to improve the immune system (Kadam & Lele, 2017), as well as a biomass feedstock for conversion, by pyrolysis process, into a bio oil suitable for the production of fuels and chemicals by further upgrading (Şen & Kar, 2011).

2.8. Hemp

Hemp is certainly one of the earliest plants to have been cultivated and its fibers have been used extensively throughout history. Although its cultivation was prohibited for a certain period of time because of its high content in narcotic substances, since 2003 hemp strains with low concentrations of Δ-9-tetrahydrocannabinol (less than 0.2%, as described in Council Regulation (EC) No 1420/98) were once again allowed to be grown in the European Union (EU Council Directive, 2003). Today hemp is grown specifically for manufacturing of a variety of industrial products, including textiles, food, paper, and biofuel, and France is the country with the highest production (about 150 thousand tons per year) followed by China (FAOSTAT, 2020).

It is of utmost importance to consider that hemp properties are strictly related to its chemical composition, which varies depending not only on the manufacturing method, but also on the hemp variety employed. In fact, as mentioned before, hemp is well known for its characteristics to produce a class of terpenophenolic compounds (more than one hundred identified to date according to the most recent cannabinoid inventory) named phytocannabinoids (Hanuš, Meyer, Muñoz, Taglialatela-Scafati, & Appendino, 2016). Cultivation of industrial hemp with low levels of Δ9-tetrahydrocannabinol has an increasing rate due to its multipurpose utilization for a wide variety of products, such as cellulose and fiber for paper and textile, hemp seed oil and SOC for food, cosmetics and pharmaceutical industries (Kitrytė et al., 2018). Hemp seed oil is not widespread on the market and, thus, it is considered a niche product characterized by a high content of polyunsaturated fatty acids. In this respect, it is well known for its nutraceutical, cosmetic and pharmaceutical potential, due to a perfectly balanced content of ω-3 and ω-6 polyunsaturated fatty acids (Crescente et al., 2018). But, just because of its high content of unsaturated fatty acids, hemp seed oil is very susceptible to oxidative deterioration by light and heat, turning rancid within a short period of time if not properly stored. However, when oxidized, hemp seed oil becomes solid and can be used for cooking or manufacturing of oil-based paints. Furthermore, also a specific biodiesel can be obtained from hemp oil, even though such kind of fuel production is at moment very limited (Afif & Biradar, 2019). Hemp SOC, similarly to the other SOCs, is generally used as animal feed. Protein concentration in cold-pressed hempseed cake is higher than in pea and rapeseed cakes and its amino acid profile is comparable with that of other protein sources, such as meat, milk, eggs and soy. Functional properties of proteins isolated from hemp SOC, such as solubility as well as emulsifying and foaming capacities, make hemp protein isolate suitable to be used as valuable additive in food industry (Hadnađev et al., 2018; Teh & Bekhit, 2015). In particular, the digestibility and allergenicity analyses of the hemp protein isolate demonstrated that hemp SOC-derived protein can be successfully used as an ingredient for hypoallergenic foods (Mamone et al., 2019). Finally, hemp SOC exhibits a marked antioxidant activity due to the presence of specific phytochemicals that could be refined by different methods of extraction (Kitrytė et al., 2018).

2.9. Cardoon

Although cardoon (*Cynara cardunculus* L.), a native crop belonging to the Mediterranean region, is a minor vegetable crop in most countries (except in Italy, Spain and France where it is produced in few thousands of tons/year and used in traditional dishes) (FAOSTAT, 2020), it has recently achieved increasing interest and economic value due to its multipurpose applications. In particular, Mauromicale, Sortino, Pesce, Agnello, and Mauro (2014) valued that cardoon is well suited to the Mediterranean climate as a perennial crop with high biomass and yields and, as such, they classified cardoon as a promising competitive bioenergy crop representing a good opportunity of development of marginal Mediterranean areas. Moreover, cardoon leaves and flowers are used as a vegetarian source of protease for cheese production (Almeida & Simões, 2018; Esposito, Di Pierro, Dejonghe, Mariniello, & Porta, 2016). Cardoon seed oil exhibits a very nutritious profile that deserves to be further valorized for the production of alternative vegetable oils and herbal formulations for human consumption. In fact, the extracted oil is a rich source of unsaturated fatty acids, such as linoleic and oleic acids (44.5 and 42.6%, respectively), whereas only two phenolic acids (e.g. trans 3,5-O-dicaffeoylquinic acid and 5-O-caffeoylquinic acid), probably responsible for the high antioxidant activity observed, were identified (Petropoulos et al., 2018).

The remaining by-product after oil extraction, the cardoon SOC, is a valuable source of fiber, proteins and bioactive compounds, such as polyphenols and unsaturated fatty acids (Genovese et al., 2015), largely used for animal feeding (Cabiddu et al., 2019; Genovese et al., 2015; Serrapica et al., 2019) or soil modification to control soil-borne plant pathogens (De Corato et al., 2018). Since cardoon SOC is a promising material also for the pharmaceutical and cosmetics industries, there is a growing interest for the economic and environmental valorization of the whole cardoon biomass, following an integrated biorefinery framework.

3. SOCs as biopolymer sources of protein-based materials

World public opinion is becoming increasingly aware that fossil raw material is a not infinite resource and that it is crucial to find out not only new energy sources but also innovative materials alternative to the petroleum-based plastics (Letcher, 2020). In addition, the resistance and durability of the traditional plastics, which make them ideal for a variety of applications, led to huge waste disposal problems and a consequent environmental pollution (Porta, 2019). The most interesting renewable sources to replace the fossil sources of the plastic materials are the biobased and biodegradable natural polymers (Letcher, 2020). In this respect a glossary of biorefinery, biomass and different bioplastics is reported in Table S1.

Although the number of scientific papers on this topic is increasingly growing, nowadays the produced bioplastics still represent a little percentage of the total oil-based materials (Porta, 2019). In this scenario, biopolymers from agricultural sources are an interesting option for biodegradable/edible plastics production since agricultural industry generates a high quantity of different by-products containing biomacromolecules, such as proteins and polysaccharides, potentially able to mimic the oil-derived polymeric matrices.

But, despite the huge worldwide production of agricultural biomass, only a small fraction of it is today utilized for applications different from those finalized to animal feed or human nutrition.

SOCs, by-products of vegetable oil industries, are known to contain high amount of fiber, polysaccharides and proteins that can be extracted and that may represent a renewable source to produce innovative biobased materials. In this respect, natural fibers have been successfully investigated as a sustainable source for the production of biocomposite matrices, having potential as outstanding reinforcing fillers. In fact, the agricultural biomass derived materials found, thus far, a wide reutilization, from the pulp and paper industries to the automotive and construction industries, as well as in various biomedical applications. On the other hand, when SOCs are used to raise the protein level of animal diets, they must be complemented by legume seeds, as well as animal by-products and synthetic amino acids because they are normally deficient in some essential amino-acids. Therefore, among the biopolymers derived from renewable resources, SOC-extracted proteins, without or after purification, could be a potential raw material for bioplastic products since they are abundant, biodegradable and inexpensive (Fig. 2).

These plastic films made with proteins derived from oilseeds could be successfully employed to manufacture one time or short-term use items, mostly in food packaging sector, replacing at least a portion of non-biodegradable materials currently used (Rouilly & Vaca-Garcia, 2013). However, the low mechanical and water vapor barrier properties of protein films are general drawbacks with respect to synthetic

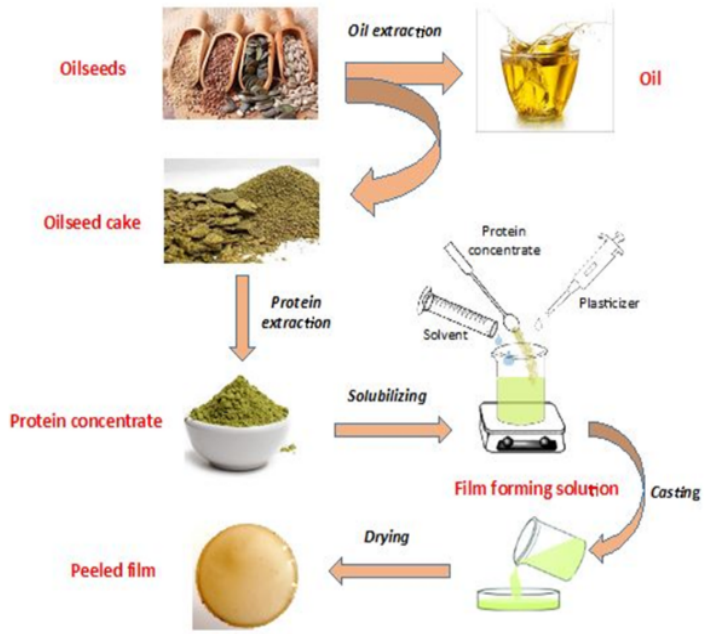

Fig. 2. Flowchart of the possible production of a biodegradable film by using as raw material the by-products of oil extraction from oilseeds.

films. Various methods to improve protein film performance have been investigated, such as appropriate film formulation and preparation conditions, plasticization, irradiation, protein cross-linking induced by heat, chemical or enzymes, protein acylation, incorporation of nano-composites, blending with different biopolymers (Wihodo & Moraru, 2013).

The main findings obtained during the last ten years in this field with the nine oil seeds previously discussed, together with some additional unpublished and promising results obtained with hemp- and cardoon-derived proteins, are here summarized.

3.1. Soybean protein-based materials

Soy proteins are a mixture of β-conglycinin (35%) and glycinin (52%) with an effective film-forming ability in the presence of plasticizers. The main drawbacks of the soy protein-based films are the same of those generally exhibited by all the protein-based materials, mainly weak mechanical properties and high sensitivity to moisture (Calva-Estrada, Jiménez-Fernández, & Lugo-Cervantes, 2019). Therefore, several methodological strategies were utilized to improve soy protein-based film performances, as indeed those of all protein-based materials, including plasticization, cross-linking, nanotechnology, and blending to obtain composite films (Zink, Wyrobnik, Prinz, & Schmid, 2016). Among the most significant results reported in the last five years, cross-linking is one of the proposed techniques to improve the performance of protein-based films as food contact materials, especially concerning their high water sensitivity, which hinders many of their potential applications in food packaging. In this field, Xu et al. (2015) proposed a biodegradable film made of soy protein cross-linked with polyacrylamide and 1,2,3-propanetriol-diglycidyl-ether. Both tensile strength and water barrier property of the cross-linked films were found markedly increased compared to those of soy protein films simply plasticized with glycerol. More recently, Yamada, Morimitsu, Hosono, and Yamada (2020) produced soy protein films cross-linked by formaldehyde. After hand pressed the proteins under 600 MPa pressure for 15 min, the obtained pellets were immersed in formaldehyde solutions at different concentrations for 24 h at room temperature. The pellets were then rinsed with water, dried at room temperature for 12 h and then heated for 2 h at 80 °C. Soy protein film cross-linked with 1% formaldehyde exhibited the same bending strength value as polyethylene with thermal stability at temperatures below 200 °C. Furthermore, pronase tests confirmed that cross-linked films were completely biodegradable and, thus, potential candidates to be used in agricultural fields as mulching sheets, seedling pots, and disposable poles.

Furthermore, protein–polysaccharide composites have been also known to show a wide range of applications in biomedical and green chemical fields. In this respect, a soy hull hemicellulose–soy protein conjugate, stable and emulsified successfully, was produced, giving rise to a biomaterial suitable for food and pharmaceutical applications (Wang, Wu, & Liu, 2017). Also the interaction of soy proteins with pectin resulted useful to tailor coatings for various applications, such as to carry and protect bioactive compounds. In fact, when pectin was added to soy protein isolate films, their elasticity, solubility, and permeability to water vapor were not significantly altered, but the film tensile strength and permeability to oxygen increased (Ravazzi Amado, de Souza Silva, & Mauro, 2019). In addition, glycerol-plasticized nanocomposite films were prepared from SPI grafted with cellulose nanofibers and nano-silica particles in order to reinforce film mechanical properties as well as to reduce its water vapor permeability. Also in this case the obtained results demonstrated that both tensile strength and water resistance of the obtained films were markedly increased compared to the control ones (Qin, Mo, Liao, He, & Sun, 2019).

Finally, protein-based films finalized to act as antimicrobial packaging are designed to be able to transfer incorporated antimicrobial compounds to the surface of different foods with the aim to extend their shelf life. The addition of peppermint essential oil to soy protein FFS was shown to significantly enhance water vapor barrier property of the derived film and to confer antimicrobial activity to the coating, without negatively modifying the material physic-mechanical properties. This kind of packaging was demonstrated to be able to extend the shelf life of raw hamburger stored under refrigerated condition without altering meat organoleptic characteristics (Karimian, Tabatabaee Bafroee, & Sharifan, 2019).

3.2. Rapeseed protein-based materials

Jang, Lim, and Song (2011) obtained edible films from rapeseed cake by adding sorbitol and sucrose as plasticizers and polysorbate as emulsifier, as well as SOC/gelatin blends to markedly increase the physical properties of the films, mainly their tensile strength. The manufactured rapeseed cake/gelatin blend films were suggested suitable for applications in food packaging. In particular, rapeseed cake/gelatin films containing the antimicrobial grapefruit seed extract were demonstrated suitable for packaging strawberries being able to extend their shelf life (Jang, Shin, & Song, 2011). However, rapeseed protein-based bioplastics generally exhibit low mechanical properties, thus various factors were explored to improve their features, including controlled protein denaturation, cross-linking, acylation and blending with synthetic polymers (Zhang, Liu, & Rempel, 2017).

Shi and Dumont (2014) obtained rapeseed protein isolate-based films in the presence of 10% SDS (as a protein denaturant), glycerol (as plasticizer) and stearic acid (as a co-plasticizer). The mechanical, thermal and water absorption properties of the prepared films were found significantly improved. The films possessed also a very high elongation at break (551%) and a water absorption capacity (1115%) that conferred them the potential to be used in the manufacture of super-absorbents. Furthermore, dough-like blends were produced from rapeseed meal, added with glycerol, by an injection molding process at three different temperatures (80, 100 and 120 °C) (Delgado, Felix, & Bengoechea, 2018). Biocomposites of rapeseed meal blended with different concentrations of polycaprolactone (up to 20%) were also prepared using the same method and experimental conditions except for the mold temperature which was constantly held at 100 °C. The obtained results showed a 50% increase in the viscoelastic properties of the produced material and a significant decrease in its water uptake capacity. In addition, a clear enhancement in the viscoelastic properties (200%) of the obtained bioplastics was also observed.

More recently (Fetzer, Hintermayr, Schmid, Stäbler, & Eisner, 2020), described the preparation of a rapeseed protein concentrate by dissolving rapeseed meal in a saline solution at 30 °C under alkaline conditions and by treating the obtained supernatant at acidic pH and with phytase followed by ultrafiltration. The prepared protein concentrate was then modified by addition of lauryl chloride or oleoyl chloride at 40 °C and the reaction mixture was then brought to pH 9.5 and finally dialyzed and lyophilized. The dried proteins were washed with ethanol, in order to remove the excess of fatty acids and dried again at room temperature. FFSs containing either modified or unmodified rapeseed proteins were prepared at pH 3.0 in the presence of glycerol, then cast and finally dried. The analyses of the obtained films showed a significant reduction in hydrophilicity and water solubility of the acylated films, as well as an increase in their tensile strength as a function of the acylation degree, while film elongation at break decreased in parallel. The new material obtained with rapeseed acylated proteins was proposed to realize biodegradable adhesives, edible coatings and biodetergents.

3.3. Cottonseed protein-based materials

Notoriously, cottonseed proteins possess good film-forming properties in the presence of plasticizers like glycerol. To improve the features of the cottonseed protein-based films (Yue et al., 2012), modified proteins chemically, after their preliminary denaturation by adding urea to cottonseed flour solution, adjusting the pH to 11.0, and heating the mixture at 70 °C. Then, denatured proteins were treated with a cross-linking reagent (formaldehyde, glyoxal or glutaraldehyde) and the mixture subjected to vacuum-drying for 10 h at 80 °C. Finally, hot-press molding has been applied to the homogenized mixture after glycerol addition and the modified cottonseed protein preparation was conditioned in a desiccator for 24 h at room temperature. A marked improvement was observed in both mechanical and thermal properties, as well as in water absorption resistance, of the bioplastics derived from cottonseed proteins modified in this way, so much to be considered potential materials to be used in agriculture as well as in packaging. With the same strategy, Yue, Fernandez-Blazquez, Shuttleworth, Cui, and Ellis (2014) studied the effect of different aldehydes as cross-linking agents of proteins extracted from cotton SOC.

A different biomaterial has been prepared, more recently, by blending either washed cottonseed meal or cottonseed protein isolate with polycapronolactone in the presence of cottonseed oil, coconut oil or polyethylene glycol used as plasticizers (Cheng, Ford, & He, 2019). The analyses of the mechanical properties of the cottonseed protein films plasticized with cottonseed oil indicated a higher elongation at break with the same tensile strength, whereas the blending of cottonseed protein or (Dalle Zotte et al., 2013) cottonseed oil with polycaprolactone had no effect on adhesive property of the derived material.

Finally, de Oliveira Filho et al. (2019) developed an active packaging by incorporating cottonseed protein hydrolysates into alginate films. An increase in film antioxidant and antimicrobial activities, together with a lipid barrier acceptable property and a controlled peptide release (up to 60% in 30 min) in aqueous media, was observed by increasing the protein amount incorporated into alginate blends. Therefore, such bioplastics might be used as bioactive packaging of fatty foods sensitive to oxidation and/or microbial growth.

3.4. Sunflower protein-based materials

Salgado, López-Caballero, Gómez-Guillén, Mauri, and Montero (2012) produced protein-based films with protein concentrates obtained from sunflower SOC by casting methods in the presence of glycerol as plasticizer and drying the obtained FFSs at 60 °C for 5 h. These bioplastics contained different amounts of polyphenols, mainly chlorogenic and caffeic acids, possessing antioxidant properties and naturally present in the sunflower SOC, and exhibited physicochemical properties suitable for packaging products sensitive to oxidation. The same authors (Salgado, López-Caballero, Gómez-Guillén, Mauri, & Montero, 2013) developed an active packaging for the preservation of fish patties by exploiting sunflower protein concentrate incorporated with clove essential oil. Films were prepared by FFS casting at pH 11.0 in the presence of glycerol and clove essential oil and drying at 60 °C for 5 h. The obtained films showed a reduction both in water solubility and glass transition temperature, without significant changes in moisture content, water vapor permeability, and mechanical properties, and exhibited antioxidant and antimicrobial properties. Applying the films to the refrigerated sardine patties retarded the lipid auto-oxidation as well as the total mesophyll growth. Rouilly and Vaca-Garcia (2013) confirmed that sunflower SOC is a valuable candidate to make 100% natural thermoplastic composites, demonstrating that thermomechanical twin-screw extrusion processing of the raw SOC is a way to carry out the plasticization of the protein matrix, the defibration of the husk and the compounding of the thermoplastic composite. A preindustrial study of the process was also proposed by indicating some examples of industrial materials, such as agricultural transplanting pots, developed in terms of economic feasibility and environmental benefits.

3.5. Groundnut protein-based materials

The functional properties of groundnut SOC, such as emulsification, and water absorption, are important in food processing. But, despite the fact that groundnut SOC has a great potential in food formulations, its reutilization remain limited. Groundnut protein concentrate prepared from defatted flour is effective to give rise by casting to edible films in the presence of plasticizers such as glycerol. As it generally happens for the majority of the protein-based films, the tensile strength decreases with the increase in FFS glycerol concentration, whereas the elongation at break increases correspondingly. Compared to solution casting, compression molding was demonstrated to be more effective, providing improved properties of the films (Reddy, Chen, & Yang, 2013). Groundnut SOC proteins have been used also to prepare films blended with polysaccharides to improve their properties. Li et al. (2015) studied the effect of the groundnut proteins conjugated with gum Arabic in the presence of glycerol and observed higher tensile strength, lower water vapor permeability and elongation at break of the obtained films. Moreover, Zhong et al. (2017) developed an active packaging by incorporating thymol in a matrix prepared with transglutaminase-modified groundnut proteins. The resulting film has weakened its mechanical properties but, however, its water vapor permeability decreased and acquired antioxidant and antimicrobial activities. Finally, a defatted groundnut flour-based film was developed and its efficacy for preserving the quality of sunflower oil during storage evaluated. The resulted film possessed suitable physicochemical, optical, barrier and mechanical properties and allowed the chemical stability of sunflower oil stored (Riveros, Martin, Aguirre, & Grosso, 2018).

3.6. Sesame protein-based materials

Proteins extracted from sesame seeds seem an appropriate source for preparing bioplastics because of their good heat stability and low hydrophilicity. Therefore, various studies have been recently performed to develop innovative sesame protein-based films. Sharma and Singh (2016) prepared edible films with protein isolates obtained from defatted sesame meal showing, under optimized conditions of protein and plasticizer concentrations, pH and temperature, a suitable low solubility and water vapor permeability and satisfying tensile strength. More recently, glycerol-plasticized films were prepared from sesame protein isolate following a preliminary protein cross-linking with different concentrations of malic acid, citric acid and succinic acid. The obtained films exhibited markedly improved mechanical and water barrier properties, as well as thermal stability and uniform morphology, mostly when succinic acid was used as cross-linking agent (Sharma, Sharma, & Saini, 2018). The same authors developed composite films by blending sesame proteins with different amounts of gum rosin in the presence of glycerol as a plasticizer. They observed that moisture resistance, water vapor permeability, mechanical, thermal, and morphological properties were improved in comparison with films obtained from native sesame protein isolates (Sharma & Singh, 2018).

Furthermore, Fathi, Almasi, and Pirouzifard (2018) analyzed the effect of the treatment of sesame protein isolate FFS with UV light type "A, B, C", by examining the properties of the derived films obtained in the presence of glycerol. The results of these experiments demonstrated that UV light type C irradiation improved the mechanical properties as well as the hydrophobicity of the obtained film, the structure of which showed also more compact compared to that of control film. The same authors (Fathi, Almasi, & Pirouzifard, 2019) obtained glycerol-plasticized and UV-irradiated sesame protein films containing different amounts of TiO_2 nanoparticles. Film tensile strength and water contact angle were observed to increase, whereas their water vapor transmission rate and water solubility decreased in bionanocomposite films containing 3% TiO_2. Moreover, the films containing 5% TiO_2 nanoparticles exhibited good O_2 scavenging activity and also acceptable level of dye photo-degradation potential. Thus, the obtained bionano-composite film was proposed as a suitable candidate for active food packaging as well as for photo-decolorization purposes.

Finally, baked foams based on cassava starch added with sesame SOC were developed and the morphological, physical and mechanical properties of these materials were evaluated (Machado et al., 2017). The addition of sesame SOC was found to improve mechanical properties and to reduce water capacity absorption in comparison to foams made using only starch. Furthermore, foams developed with concentrations >20% of sesame SOC exhibited most suitable combination of mechanical properties when compared to commercial expanded polystyrene. The authors concluded that the starch-based foams incorporated with sesame SOC might represent a valid alternative for packing foods with low moisture content.

3.7. Black cumin protein-based materials

There is only one recent report (Sabbah, Altamimi, Di Pierro, Schiraldi, Cammarota, & Porta, 2020) in the literature about the exploitation of the proteins extracted from black cumin defatted seeds to obtain novel biomaterials. In this study, edible films were prepared by using a protein concentrate, in the presence of glycerol as plasticizer, and characterized in comparison with films obtained with the same proteins previously treated with transglutaminase. In fact, SDSPAGE analysis showed a progressive attenuation of all proteins when the reaction mixtures were incubated in the presence of the enzyme, while a concomitant formation of protein polymers became detectable at the top of the gel. These results clearly indicated the transglutaminase-catalyzed formation of cross-linked polymers of the black cumin SOC proteins, the monomeric forms of which have low molecular weights ranging between 20 and 50 kDa.

Casting and drying of the different FFSs, prepared at pH values between 6.0 and 12.0 in the absence or presence of different concentrations of glycerol, showed that handleable films were obtained only when the plasticizer was present at a concentration at least of 20%. More in particular, the presence of 20% glycerol into FFSs cast at pH 8.0 generated a peculiar positive effect on the mechanical properties of the films obtained with the transglutaminase-treated proteins, producing films more resistant and at the same time flexible. In addition, all the produced films exhibited a clear antimicrobial activity, probably due to the diffusion of bioactive agents, such as polyphenols, tannins, and flavonoids contained in the black cumin seed protein extract.

Therefore, the enzymatically cross-linked proteins gave rise to dark biodegradable films, endowed with antimicrobial activity, exploitable not only for food packaging but also for mulching. In fact, the black color of these films would be helpful not only to protect packaged drugs or food products from a variety of photo-oxidative agents, but also to be used as mulching sheets. Indeed, their permeability properties confirmed the possible application of the obtained material in agriculture, since a marked decrease in the barrier effect to both carbon dioxide and oxygen should allow an active gas exchange without significantly influencing their poor water vapor permeability.

3.8. Hemp protein-based materials

Mirpoor et al. (2020) recently prepared FFSs with a protein concentrate obtained from hemp SOC and added with different egagropili-derived fractions. FFSs were then characterized by determining zeta potential and the size of the dispersed particles. As shown in Table 3, no significant differences in both FFS zeta potential and Z-average were revealed at the different plasticizer concentrations. These results indicated that all FFSs were stable in the range of glycerol tested (30–50%, w/w protein), being the zeta potential values measured always lower than −30 mV. In addition, no aggregation was detected in the different FFSs since the particle Z-average remained between 340 and 360 nm at all glycerol concentrations tested. Fig. S1 (left panel) shows the SDSPAGE profile of hemp seed proteins, of molecular mass

between 20 and 50 kDa and the derived brown films obtained by FFS casting and drying. The tensile strength, elongation at break and Young's module values reported in Table S2 indicate that the seed hemp protein films possessed mechanical properties similar to those generally exhibited by the majority of the other seed protein-based films.

In fact, similarly to what observed by analyzing other protein-based films, the tensile strength and Young' module of hemp protein films decreased by enhancing glycerol concentrations, whereas the elongation at break concurrently increased. These findings strongly encourage further investigations with the aim to improve hemp protein film features and, consequently, to consider also hemp SOCs as a potential renewable source for preparing edible materials suitable for food packaging.

3.9. Cardoon protein-based materials

Cardoon is the feedstock utilized from the first biorefinery in the world, located in Porto Torres (Sardinia, Italy), in which the installations of a petrochemical plant provide plant oil and biomass destined to give rise to building blocks of an innovative bioplastics. Recently, Mirpoor, Giosafatto and Porta (unpublished results) extracted proteins from the cardoon seeds and prepared FFSs in the presence of different glycerol concentrations, as well as the derived films by casting procedure. The SDSPAGE protein profile and the image of a typical film made of cardoon seed proteins are shown in the right panel of Fig. S1. The obtained films had a typical dark green color, due to the concurrent extraction of specific pigments present in the biological source, whereas the protein electrophoretic pattern showed a marked band at very high molecular weight in addition to further three bands between 20 and 50 kDa. Table S2 reports the characterization of the FFSs prepared at different glycerol concentrations and the mechanical properties and thickness of the derived films. The data showed that both FFS zeta potential and the average size of the particles dispersed did not significantly change by varying glycerol concentrations, indicating the stability of the FFSs and the lack of protein aggregation. Furthermore, according to the values of tensile strength, elongation at break and Young's module detected, the mechanical properties of the obtained films indicated that the films containing 50% glycerol acquired more flexible and plastic features without loosing their resistance. Therefore, these results stimulate further investigations to obtain also from defatted cardoon seed protein biomaterials with higher performance to be exploited in food packaging sector.

4. Conclusions

Bioeconomy includes, as one of its core activities, the development of new commodities in the processing industry by using the by-products of the main process. Waste-less biorefinery solutions, thus, aim at using the by-products in connection with the primary output to realize new business opportunities. However, even though from both economic and ecological aspects, biomass conversion into high added-value products has been getting an ever-increasing attention, its success is generally assessed in terms of techno-economic feasibility, raw material efficiency and environmental impacts. SOCs are voluminous food-grade industrial by-products and novel biotechnological approaches are needed to valorize the different industrial co-streams containing high amounts not only of oil but also of SOC. Even though the residues of oilseed crops are known to be extremely rich in valuable ingredients, such as proteins, fiber and various bioactive compounds, these by-products are so far mostly consumed as animal feed supplementation, food additives or fertilizers in their production areas. The relatively high protein content and its inexpensive cost make SOC an adequate source also to develop bioplastic materials. Although the functional properties of protein-based films are still not comparable to those of petroleum-derived materials, extensive work has been done in the past decade to improve their properties. Bioplastics are produced by several different procedures and techniques according to the final purpose of the desired material. However, the issue to process production of any bioplastics into large scale remains ongoing because the development of the majority of bioplastics so far proposed is still limited to the laboratory scale. Moreover, although the recent scientific advances in industrial biotechnology have diminished the costs of converting organic material into polymers and despite the fast expansion of biobased chemicals in the 2000s, the chemical companies continue to tackle with several drawbacks in switching to a new raw material. The development of bioplastics is, thus, mainly exposed to the reliability achieved by the new materials and the availability of the companies in encouraging, manufacturing and marketing a new sustainable technology. Consequently, traditional plastics actually continue to dominate the market not only because oil-based production benefits from mature technologies, as well as from evident economies of scale, but also because of the existing difficulties in scaling small-scale biotechnologies to industrial levels by substituting the conventional plastics with new untried materials. Finally, it is still not fully accepted that bioplastics can be profitable due to the costs required both to expand R&D activities and create new infrastructures. Thus, only developing better feedstock supplies, increasing yields, reducing costs and including societal actors in the efforts to define sustainability, will allow to the industrial sector to guarantee the success of bioplastics in the future market (Iles & Martin, 2013).

The present review represents, thus, an overview of the most abundant SOCs worldwide produced, as well as of some by-products of niche oilseeds, and the most advanced results obtained in the attempt to utilize SOC protein content to produce novel biodegradable/edible materials in an eco-sustainable oilseed biorefinery.

Funding

This research was funded by the grant PRIN: Progetti di Ricerca di Interesse Nazionale –Bando 2017– "CARDoon valorization by InteGrAted biorefiNery (CARDIGAN)" of Italian Ministero dell'Università e della Ricerca (COD. 2017KBTK93).

Appendix A. Supplementary data

Supplementary data to this article can be found online at https://doi.org/10.1016/j.tifs.2021.01.014.

References

Afif, M. K., & Biradar, C. H. (2019). Production of biodiesel from *Cannabis sativa* (hemp) seed oil and its performance and emission characteristics on DI engine fueled with biodiesel blends. *International Research Journal of Engineering and Technology, 6*, 246–253.

Aguieiras, E. C., de Barros, D. S., Fernandez-Lafuente, R., & Freire, D. M. (2019). Production of lipases in cottonseed meal and application of the fermented solid as biocatalyst in esterification and transesterification reactions. *Renewable Energy, 130*, 574–581.

Almeida, C. M., & Simões, I. (2018). Cardoon-based rennets for cheese production. *Applied Microbiology and Biotechnology, 102*, 4675–4686.

Atta, M. B. (2003). Some characteristics of nigella (*Nigella sativa* L.) seed cultivated in Egypt and its lipid profile. *Food Chemistry, 83*, 63–68.

Bansal, P., & Kochhar, A. (2014). Sensory and nutritional evaluation of value added products using peanut flour for nutritional and health benefits. *International Journal of Agriculture Innovations and Research, 3*, 27–32.

Bonjean, A. P., Dequidt, C., Sang, T., & Limagrain, G. (2016). Rapeseed in China. *Oilseed and Crop Lipids, 23*, D605. https://doi.org/10.1051/ocl/2016045

Cabiddu, A., Contini, S., Gallo, A., Lucini, L., Bani, P., Decandia, M., … Sulas, L. (2019). *In vitro* fermentation of cardoon seed press cake - a valuable byproduct from biorefinery as a novel supplement for small ruminants. *Industrial Crops and Products, 130*, 420–427.

Cai, C., Song, L., Wang, Y., Wu, P., Ye, Y., Zhang, Z., et al. (2013). Assessment of the feasibility of including high levels of rapeseed meal and peanut meal in diets of juvenile crucian carp (*Carassius auratus gibelio*♀× *Cyprinus carpio*♂): Growth, immunity, intestinal morphology, and microflora. *Aquaculture, 410*, 203–215.

Calva-Estrada, S. J., Jiménez-Fernández, M., & Lugo-Cervantes, E. (2019). Protein-based films: Advances in the development of biomaterials applicable to food packaging. *Food Engineering Reviews*. https://doi.org/10.1007/s12393-019-09189-w

Cano-Medina, A., Jiménez-Islas, H., Dendooven, L., Herrera, R. P., González-Alatorre, G., & Escamilla-Silva, E. M. (2011). Emulsifying and foaming capacity and emulsion and

foam stability of sesame protein concentrates. *Food Research International, 44*, 684–692.
Cheng, H. N., Ford, C. V., & He, Z. (2019). Evaluation of polyblends of cottonseed protein and polycaprolactone plasticized by cottonseed oil. *International Journal of Polymer Analysis and Characterization, 24*, 389–398.
Crescente, G., Piccolella, S., Esposito, A., Scognamiglio, M., Fiorentino, A., & Pacifico, S. (2018). Chemical composition and nutraceutical properties of hempseed: An ancient food with actual functional value. *Phytochemistry Reviews, 17*, 733–749.
Dabbour, M., He, R., Mintah, B., Xiang, J., & Ma, H. (2019). Changes in functionalities, conformational characteristics and antioxidative capacities of sunflower protein by controlled enzymolysis and ultrasonication action. *Ultrasonics Sonochemistry, 58*, 104625.
Dalle Zotte, A., Brand, T. S., Hoffman, L. C., Schoon, K., Cullere, M., & Swart, R. (2013). Effect of cottonseed oilcake inclusion on ostrich growth performance and meat chemical composition. *Meat Science, 93*, 194–200.
De Corato, U., De Bari, I., Viola, E., & Pugliese, M. (2018). Assessing the main opportunities of integrated biorefining from agro-bioenergy co/by-products and agro industrial residues into high-value added products associated to some emerging markets: A review. *Renewable and Sustainable Energy Reviews, 88*, 326–346.
Delgado, M., Felix, M., & Bengoechea, C. (2018). Development of bioplastic materials: From rapeseed oil industry by products to added-value biodegradable biocomposite materials. *Industrial Crops and Products, 125*, 401–407.
Dubois, V., Breton, S., Linder, M., Fanni, J., & Parmentier, M. (2007). Fatty acid profiles of 80 vegetable oils with regard to their nutritional potential. *European Journal of Lipid Science and Technology, 109*, 710–732.
Esaki, H., Watanabe, R., Hishikawa, N., Osawa, T., & Kawakishi, S. (2004). Utility of isoflavone preparations from soy sauce cake as antioxidant materials. *Nippon Shokuhin Kagaku Kogaku Kaishi, 51*, 47–53.
Esposito, M., Di Pierro, P., Dejonghe, W., Mariniello, L., & Porta, R. (2016). Enzymatic milk clotting activity in artichoke (*Cynara scolymus*) leaves and alpine thistle (*Carduus defloratus*) flowers. Immobilization of alpine thistle aspartic protease. *Food Chemistry, 204*, 115–121.
Faostat. (2020). Food and agriculture organization of the united Nations. Countries by commodity http://www.fao.org/faostat/en/#rankings/countries_by_commodity. (Accessed 25 April 2020).
Fathi, N., Almasi, H., & Pirouzifard, M. K. (2018). Effect of ultraviolet radiation on morphological and physicochemical properties of sesame protein isolate based edible films. *Food Hydrocolloids, 85*, 136–143.
Fathi, N., Almasi, H., & Pirouzifard, M. K. (2019). Sesame protein isolate based bionanocomposite films incorporated with TiO_2 nanoparticles: Study on morphological, physical and photocatalytic properties. *Polymer Testing, 77*, 105919. https://doi.org/10.1016/j.polymertesting.2019.105919
Fetzer, A., Hintermayr, C., Schmid, M., Stäbler, A., & Eisner, P. (2020). Effect of acylation of rapeseed proteins with lauroyl and oleoyl chloride on solubility and film-forming properties. *Waste and Biomass Valorization*. https://doi.org/10.1007/s12649-020-01012-6
Fink-Gremmels, J. (Ed.). (2012). *Animal feed contamination: Effects on livestock and food safety* (pp. 1–704). Cambridge, UK: Woodhead Publishing Series in Food Science, Technology and Nutrition.
Gaonkar, V., & Rosentrater, K. A. (2019). Soybean. In *Integrated processing technologies for food and agricultural by-products* (pp. 73–104). Academic Press.
Genovese, C., Platania, C., Venticinque, M., Calderaro, P., Argento, S., Scandurra, S., et al. (2015). Evaluation of cardoon seeds presscake for animal feeding. In *IX international symposium on artichoke, cardoon and their wild relatives* (Vol. 1147, pp. 323–328).
Gerliani, N., Hammami, R., & Aïder, M. (2020). A comparative study of the functional properties and antioxidant activity of soybean meal extracts obtained by conventional extraction and electro-activated solutions. *Food Chemistry, 307*, 125547. https://doi.org/10.1016/j.foodchem.2019.125547
Gharby, S., Harhar, H., Guillaume, D., Roudani, A., Boulbaroud, S., Ibrahimi, M., et al. (2015). Chemical investigation of *Nigella sativa* L. seed oil produced in Morocco. *Journal of the Saudi Society of Agricultural Sciences, 14*, 172–177.
Ghosh, K., & Mandal, S. (2015). Nutritional evaluation of groundnut oil cake in formulated diets for rohu, *Labeo rohita* (Hamilton) fingerlings after solid state fermentation with a tannase producing yeast, *Pichia kudriavzevii* (GU939629) isolated from fish gut. *Aquaculture Reports, 2*, 82–90.
Gunstone, F. D. (Ed.). (2002). *Vegetable oils in food technology, composition, properties and uses* (pp. 1–337). Oxford (UK): Blackwell Publishing Ltd.
Hadnađev, M., Dapčević-Hadnađev, T., Lazaridou, A., Moschakis, T., Michaelidou, A. M., Popović, S., et al. (2018). Hempseed meal protein isolates prepared by different isolation techniques. Part I. Physicochemical properties. *Food Hydrocolloids, 79*, 526–533.
Hanuš, L. O., Meyer, S. M., Muñoz, E., Taglialatela-Scafati, O., & Appendino, G. (2016). Phytocannabinoids: A unified critical inventory. *Natural Product Reports, 33*, 1357–1392.
Havrysh, V., Kalinichenko, A., Mentel, G., Mentel, U., & Vasbieva, D. G. (2020). Husk energy supply systems for sunflower oil mills. *Energies, 13*, 361.
He, R., Alashi, A., Malomo, S. A., Girgih, A. T., Chao, D., Ju, X., et al. (2013). Antihypertensive and free radical scavenging properties of enzymatic rapeseed protein hydrolysates. *Food Chemistry, 141*, 153–159.
He, Z., Cheng, H. N., Klasson, K. T., Ford, C., & Barroso, V. A. (2019). Optimization and practical application of cottonseed meal-based wood adhesive formulations for small wood item bonding. *International Journal of Adhesion and Adhesives, 95*, 102448.
He, Z., Zhang, H., Olk, D. C., Shankle, M., Way, T. R., & Tewolde, H. (2014). Protein and fiber profiles of cottonseed from upland cotton with different fertilizations. *Modern Applied Science, 8*, 97.
Hu, Y., Sun-Waterhouse, D., Liu, L., He, W., Zhao, M., & Su, G. (2019). Modification of peanut protein isolate in glucose-containing solutions during simulated industrial thermal processes and gastric-duodenal sequential digestion. *Food Chemistry, 295*, 120–128.
Iles, A., & Martin, A. N. (2013). Expanding bioplastics production: Sustainable business innovation in the chemical industry. *Journal of Cleaner Production, 45*, 38–49.
Inra-Cirad-Afz, & Feed tables. Composition and nutritive values of feeds for cattle, sheep, goats, pigs, poultry, rabbits, horses and salmonids. Oil byproducts Table data (dry matter) accessed on July 17th 2020 https://feedtables.com/content/table-dry-matter.
Jang, S. A., Lim, G. O., & Song, K. B. (2011a). Preparation and mechanical properties of edible rapeseed protein films. *Journal of Food Science, 76*, C218–C223. https://doi.org/10.1111/j.1750-3841.2010.02026.x
Jang, S. A., Shin, Y.-J., & Song, K. B. (2011). Effect of rapeseed protein-gelatin film containing grapefruit seed extract on 'Maehyang' strawberry quality. *International Journal of Food Science and Technology*. https://doi.org/10.1111/j.1365-2621.2010.02530.x, 2011.
Kadam, D., & Lele, S. S. (2017). Extraction, characterization and bioactive properties of *Nigella sativa* seedcake. *Journal of Food Science & Technology, 54*, 3936–3947.
Karimian, Z., Tabatabaee Bafroee, A. S., & Sharifan, A. (2019). Physico-mechanical and antimicrobial properties of isolated soy protein film incorporated with peppermint essential oil on raw hamburger. *Journal of Agricultural Science and Technology A, 21*, 1145–1159.
Kdidi, S., Vaca-Medina, G., Peydecastaing, J., Oukarroum, A., Fayoud, N., & Barakat, A. (2019). Electrostatic separation for sustainable production of rapeseed oil cake protein concentrate: Effect of mechanical disruption on protein and lignocellulosic fiber separation. *Powder Technology, 344*, 10–16.
Kitryté, V., Bagdonaitė, D., & Venskutonis, P. R. (2018). Biorefining of industrial hemp (*Cannabis sativa* L.) threshing residues into cannabinoid and antioxidant fractions by supercritical carbon dioxide, pressurized liquid and enzyme-assisted extractions. *Food Chemistry, 267*, 420–429.
Kumar, P., & Patra, A. K. (2017). Beneficial uses of black cumin (*Nigella sativa* L.) seeds as a feed additive in poultry nutrition. *World's Poultry Science Journal, 73*, 872–885.
Kuo, P. C., Lin, M. C., Chen, G. F., Yiu, T. J., & Tzen, J. T. (2011). Identification of methanol-soluble compounds in sesame and evaluation of antioxidant potential of its lignans. *Journal of Agricultural and Food Chemistry, 59*, 3214–3219.
Kyntäjä, S., Partanen, K., Siljander-Rasi, H., & Jalava, T. (2014). MTT Reports 164. Tables of composition and nutritional values of organically produced feed materials for pigs and poultry accessed on July 17th 2020 https://orgprints.org/28116/3/28116.pdf.
Lee, H., & Min, S. C. (2014). Development of antimicrobial defatted soybean meal-based edible films incorporating the lactoperoxidase system by heat pressing. *Journal of Food Engineering, 120*, 183–190.
Letcher, T. M. (Ed.). (2020). *Plastic waste and recycling: Environmental impact, societal issues* (pp. 1–664). Academic Press. https://doi.org/10.1016/B978-0-12-817880-5.00004-9.
Lim, T. K. (Ed.). (2013). *Edible medicinal and non-medicinal plants : Flowers* (Vol. 7, pp. 1–1102). Springer Science & Business Media.
Li, C., Zhu, W., Xue, H., Chen, Z., Chen, Y., & Wang, X. (2015). Physical and structural properties of peanut protein isolate-gum Arabic films prepared by various glycation time. *Food Hydrocolloids, 43*, 322–328.
Lomascolo, A., Uzan-Boukhris, E., Sigoillot, J. C., & Fine, F. (2012). Rapeseed and sunflower meal: A review on biotechnology status and challenges. *Applied Microbiology and Biotechnology, 95*, 1105–1114.
Machado, C. M., Benelli, P., & Tessaro, I. C. (2017). Sesame cake incorporation on cassava starch foams for packaging use. *Industrial Crops and Products, 102*, 115–121.
Mamone, G., Picariello, G., Ramondo, A., Nicolai, M. A., & Ferranti, P. (2019). Production, digestibility and allergenicity of hemp (*Cannabis sativa* L.) protein isolates. *Food Research International, 115*, 562–571.
Ma, M., Ren, Y., Xie, W., Zhou, D., Tang, S., Kuang, M., et al. (2018). Physicochemical and functional properties of protein isolate obtained from cottonseed meal. *Food Chemistry, 240*, 856–862.
Mauromicale, G., Sortino, O., Pesce, G. R., Agnello, M., & Mauro, R. P. (2014). Suitability of cultivated and wild cardoon as a sustainable bioenergy crop for low input cultivation in low quality Mediterranean soils. *Industrial Crops and Products, 57*, 82–89.
Mirpoor, S. F., Giosafatto, C. V. L., Di Pierro, P., Di Girolamo, R., Regalado-González, C., & Porta, R. (2020). Valorisation of Posidonia oceanica Sea Balls (Egagropili) as a potential source of reinforcement agents in protein-based biocomposites. *Polymers, 12*, 2788.
de Oliveira Filho, J. G., Rodrigues, J. M., Valadares, A. C. F., de Almeida, A. B., de Lima, T. M., Takeuchi, K. P., et al. (2019). Active food packaging: Alginate films with cottonseed protein hydrolysates. *Food Hydrocolloids, 92*, 267–275.
Onsaard, E. (2012). Sesame proteins. *International Food Research Journal, 19*, 1287–1295.
Ozpolat, E., & Duman, M. (2017). Effect of black cumin oil (*Nigella sativa* L.) on fresh fish (*Barbus grypus*) fillets during storage at 2±1 °C. *Food Science and Technology, 37*, 148–152.
Özçimen, D., & Karaosmanoğlu, F. (2004). Production and characterization of bio-oil and biochar from rapeseed cake. *Renewable Energy, 29*, 779–787.
Petropoulos, S. A., Pereira, C., Tzortzakis, N., Barros, L., & Ferreira, I. C. (2018). Nutritional value and bioactive compounds characterization of plant parts *from Cynara cardunculus* L. (Asteraceae) cultivated in central Greece. *Frontiers of Plant Science, 9*, 459.
Pettersson, D., & Pontoppidan, K. (2013). Soybean meal and the potential for upgrading its feeding value by enzyme supplementation. In *Soybean-bio-active compounds* (pp. 288–307). IntechOpen: Hany A. El-Shemy. https://doi.org/10.5772/52607.

Porta, R. (2019). The plastics sunset and the bio-plastics sunrise. *Coatings, 9*, 526. https://doi.org/10.3390/coatings9080526

Prabaningtyas, R. K., Putri, D. N., Utami, T. S., & Hermansyah, H. (2018). Production of immobilized extracellular lipase from *Aspergillus niger* by solid state fermentation method using palm kernel cake, soybean meal, and coir pith as the substrate. *Energy Procedia, 153*, 242–247.

Purohit, C., & Rajyalakshmi, P. (2011). Quality of products containing defatted groundnut cake flour. *Journal of Food Science & Technology, 48*, 26–35.

Qin, Z., Mo, L., Liao, M., He, H., & Sun, J. (2019). Preparation and characterization of soy protein isolate-based nanocomposite films with cellulose nanofibers and nano-silica via silane grafting. *Polymers, 11*, 1835.

Rahman, M., & de Jiménez, M. M. (2016). Designer oil crops. In S. Gupta (Ed.), *Breeding oilseed crops for sustainable production* (pp. 361–376). Academic Press.

Ravazzi Amado, L., de Souza Silva, K., & Mauro, M. A. (2019). Effects of interactions between soy protein isolate and pectin on properties of soy protein-based films. *Journal of Applied Polymer Science, 137*, 48732.

Reddy, N., Chen, L., & Yang, Y. (2013). Thermoplastic films from peanut proteins extracted from peanut meal. *Industrial Crops and Products, 43*, 159–164.

Rivera, D., Rommi, K., Fernandes, M. M., Lantto, R., & Tzanov, T. (2015). Biocompounds from rapeseed oil industry co-stream as active ingredients for skin care applications. *International Journal of Cosmetic Science, 37*, 496–505.

Riveros, C. G., Martin, M. P., Aguirre, A., & Grosso, N. R. (2018). Film preparation with high protein defatted peanut flour: Characterization and potential use as food packaging. *International Journal of Food Science and Technology, 53*, 969–975.

Rouilly, A., & Vaca-Garcia, C. (2013). Industrial use of oil cakes for material applications. In A. Kazmi, & P. Shuttleworth (Eds.), *The economic utilization of food Co-products* (pp. 185–213). Royal Society of Chemistry Publ.. https://doi.org/10.1039/9781849737326

Sabbah, M., Altamimi, M., Di Pierro, P., Schiraldi, C., Cammarota, M., & Porta, R. (2020). Black edible films from protein-containing defatted cake of *Nigella sativa* seeds. *International Journal of Molecular Sciences, 21*, 832. https://doi.org/10.3390/ijms21030832

Salgado, P. R., Drago, S. R., Ortiz, S. E. M., Petruccelli, S., Andrich, O., González, R. J., et al. (2012). Production and characterization of sunflower (*Helianthus annuus* L.) protein-enriched products obtained at pilot plant scale. *LWT-Food Science and Technology, 45*, 65–72.

Salgado, P. R., López-Caballero, M. E., Gómez-Guillén, M. C., Mauri, A. N., & Montero, M. P. (2012a). Exploration of the antioxidant and antimicrobial capacity of two sunflower protein concentrate films with naturally present phenolic compounds. *Food Hydrocolloids, 29*, 374–381.

Salgado, P. R., López-Caballero, M. E., Gómez-Guillén, M. C., Mauri, A. N., & Montero, M. P. (2013). Sunflower protein films incorporated with clove essential oil have potential application for the preservation of fish patties. *Food Hydrocolloids, 33*, 74–84.

Sarkis, J. R., Michel, I., Tessaro, I. C., & Marczak, L. D. F. (2014). Optimization of phenolics extraction from sesame seed cake. *Separation and Purification Technology, 122*, 506–514.

Şen, N., & Kar, Y. (2011). Pyrolysis of black cumin seed cake in a fixed-bed reactor. *Biomass and Bioenergy, 35*, 4297–4304.

Serrapica, F., Masucci, F., Raffrenato, E., Sannino, M., Vastolo, A., Barone, C. M. A., et al. (2019). High fiber cakes from Mediterranean multipurpose oilseeds as protein sources for ruminants. *Animals, 9*, 918.

Sharma, L., Sharma, H. K., & Saini, C. S. (2018). Edible films developed from carboxylic acid cross-linked sesame protein isolate: Barrier, mechanical, thermal, crystalline and morphological properties. *Journal of Food Science & Technology, 55*, 532–539.

Sharma, L., & Singh, C. (2016). Sesame protein based edible films: Development and characterization. *Food Hydrocolloids, 61*, 139–147.

Sharma, L., & Singh, C. (2018). Composite film developed from the blends of sesame protein isolate and gum rosin and their properties thereof. *Polymer Composites, 39*, 1480–1487.

Shi, W., & Dumont, M. J. (2014). Processing and physical properties of canola protein isolate-based films. *Industrial Crops and Products, 52*, 269–277.

Sibt-e-Abbas, M., Butt, M. S., Khan, M. R., Tauseef, M., Sultan, M. S. S., & Shahid, M. (2020). Nutritional and functional characterization of defatted oilseed protein isolates. *Pakistan Journal of Agricultural Sciences, 57*, 219–228.

Srinivasan, K. (2018). Cumin (*Cuminum cyminum*) and black cumin (*Nigella sativa*) seeds: Traditional uses, chemical constituents, and nutraceutical effects. *Food Quality and Safety, 2*, 1–16.

Srivastava, D., Mathur, A. N., & Shirshat, M. K. (2018). Use of de-oiled groundnut cake flour as an alternate source of nutrition. *International Journal of Agricultural Engineering, 11*, 150–152.

Sudhir, S. P., Deshmukh, V. O., & Verma, H. N. (2016). *Nigella sativa* seed, a novel beauty care ingredient: A review. *International Journal of Pharmaceutical Sciences and Research, 7*, 3185–3196.

Sunil, L., Appaiah, P., Kumar, P. P., & Krishna, A. G. (2015). Preparation of food supplements from oilseed cakes. *Journal of Food Science & Technology, 52*, 2998–3005.

Teh, S. S., & Bekhit, A. E. D. A. (2015). Utilization of oilseed cakes for human nutrition and health benefits. In *Agricultural biomass based potential materials* (pp. 191–229). Cham: Springer.

Teh, S. S., & Birch, J. (2013). Physicochemical and quality characteristics of cold-pressed hemp, flax and canola seed oils. *Journal of Food Composition and Analysis, 30*, 26–31.

Thilakarathne, R. C. N., Madushanka, G. D. M. P., & Navaratne, S. B. (2018). Comparison of physico-chemical properties of Indian and Ethiopian origin black cumin (*Nigella sativa*) seed cake. *International Journal of Food Sciences & Nutrition, 3*, 30–31.

Tous, L., Ruseckaite, R. A., & Ciannamea, E. M. (2019). Sustainable hot-melt adhesives based on soybean protein isolate and polycaprolactone. *Industrial Crops and Products, 135*, 153–158.

USDA. (2018a). *World agricultural supply and demand Estimates*. Washington, DC: USDA. Available online: http://www.usda.gov/oce/commodity/wasde/. (Accessed 20 April 2020).

USDA. (2018b). *Economic Research Service using data from USDA, Foreign Agricultural Service, Oilseeds: World Markets and Trade*. https://www.ers.usda.gov/data-products/oil-crops-yearbook.aspx. (Accessed 20 April 2020).

Wang, L., Liu, H., Liu, L., Wang, Q., Li, Q., Du, Y., et al. (2014). Protein contents in different peanut varieties and their relationship to gel property. *International Journal of Food Properties, 17*, 1560–1576.

Wang, L., Wu, M., & Liu, H.-M. (2017). Emulsifying and physicochemical properties of soy hull hemicelluloses-soy protein isolate conjugates. *Carbohydrate Polymers, 163*, 181–190.

Webb, N. W., Bernard, J. K., & Tao, S. (2019). Production responses to diets supplemented with soybean meal, expeller soybean meal, or dry-extruded cottonseed cake by lactating dairy cows. *Applied Animal Science, 35*, 543–549.

Wihodo, M., & Moraru, C. I. (2013). Physical and chemical methods used to enhance the structure and mechanical properties of protein films: A review. *Journal of Food Engineering, 114*, 292–302.

Xu, F., Dong, Y., Zhang, W., Zhang, S., Li, L., & Li, J. (2015). Preparation of cross-linked soy protein isolate-based environmentally-friendly films enhanced by PTGE and PAM. *Industrial Crops and Products, 67*, 373–380.

Yamada, M., Morimitsu, S., Hosono, E., & Yamada, T. (2020). Preparation of bioplastic using soy protein. *International Journal of Biological Macromolecules, 149*, 1077–1083.

Yasothai, R. (2014a). Chemical composition of sesame oil cake–review. *International Journal of Science, Environment and Technology, 3*, 827–835.

Yasothai, R. (2014b). Processing method and composition of sesame oil cake – a review. *International Journal of Science, Environment and Technology, 3*, 993–996.

Ye, L., Liao, Y., Sun, W., & Zhao, M. (2015). Effect of protein oxidation on the stability of peanut beverage. *CyTA - Journal of Food, 13*, 49–55.

Yimer, E. M., Tuem, K. B., Karim, A., Ur-Rehman, N., & Anwar, F. (2019). *Nigella sativa* L. (black cumin): A promising natural remedy for wide range of illnesses. *Evidence-based Complementary and Alternative Medicine*. https://doi.org/10.1155/2019/1528635. Article ID 1528635.

Yue, H. B., Cui, Y. D., Shuttleworth, P. S., & Clark, J. H. (2012). Preparation and characterization of bioplastics made from cottonseed protein. *Green Chemistry, 14*, 2009–2016.

Yue, H. B., Fernandez-Blazquez, J. P., Shuttleworth, P. S., Cui, Y. D., & Ellis, G. (2014). Thermomechanical relaxation and different water states in cottonseed protein derived bioplastics. *RSC Advances, 4*, 32320–32326.

Yu, J., Yang, H. M., Wan, X. L., Chen, Y. J., Yang, Z., Liu, W. F., et al. (2020). Effects of cottonseed meal on slaughter performance, meat quality, and meat chemical composition in Jiangnan White goslings. *Poultry Science, 99*, 207–213.

Zhang, Q., Li, Y., Chin, K. L., & Qi, Y. (2017b). Vegetable soybean: Seed composition and production research. *Italian Journal of Agronomy, 12*, 276–282.

Zhang, Y., Liu, Q., & Rempel, C. (2017). Processing and characteristics of canola protein-based biodegradable packaging: A review. *Critical Reviews in Food Science and Nutrition, 58*. https://doi.org/10.1080/10408398.2016.1193463

Zhong, T., Liang, Y., Jiang, S., Yang, L., Shi, Y., Guo, S., et al. (2017). Physical, antioxidant and antimicrobial properties of modified peanut protein isolate based films incorporating thymol. *RSC Advances, 7*, 41610–41618.

Zink, J., Wyrobnik, T., Prinz, T., & Schmid, M. (2016). Physical, chemical and biochemical modifications of protein-based films and coatings: An extensive review. *International Journal of Molecular Sciences, 17*, 1376–1420.

2- **Mirpoor, S. F.,** Giosafatto, C. V. L., Di Girolamo, R., Famiglietti, M., & Porta, R. (2022). Hemp (Cannabis sativa) seed oilcake as a promising by-product for developing protein-based films: Effect of transglutaminase-induced crosslinking. Food Packaging and Shelf Life, 31, 100779 https://doi.org/10.1016/j.fpsl.2021.100779

Food Packaging and Shelf Life 31 (2022) 100779

Contents lists available at ScienceDirect

Food Packaging and Shelf Life

journal homepage: www.elsevier.com/locate/fpsl

Hemp (*Cannabis sativa*) seed oilcake as a promising by-product for developing protein-based films: Effect of transglutaminase-induced crosslinking

Seyedeh Fatemeh Mirpoor, C. Valeria L. Giosafatto *, Rocco Di Girolamo, Michela Famiglietti, Raffaele Porta

Department of Chemical Sciences, University of Naples "Federico II", Montesantangelo Campus, Via Cintia 4, 80126 Naples, Italy

ARTICLE INFO

Keywords:
Seed oilcake
hemp proteins
microbial transglutaminase
film properties

ABSTRACT

Protein concentrates were obtained from hemp seed oilcakes (OCs) and investigated as potential waste-derived source of biodegradable films at different protein and glycerol concentrations and at different pH values. These studies indicated that hemp protein (HP) film forming solutions gave rise to higher performance films when cast at pH 12 in the presence of 50% glycerol (w/w protein) used as plasticizer. Since HPs were demonstrated to act as both acyl donor and acceptor substrates of microbial transglutaminase (mTGase), they have been used as raw material to obtain films also after enzyme treatment. Film morphological characterization demonstrated that mTGase treatment was effective to produce more homogeneous and smoother films, influencing in turn positively their properties. In fact, mTGase-crosslinked films were shown to be more resistant, still flexible and exhibited a higher heat-sealing strength. In addition, the enzymatic treatment of HPs originated bio-plastics with a higher gas permeability and a greater hydrophobicity. These findings suggest the possibility to exploit the mTGase-crosslinked proteins derived from hemp OC as a promising source to produce bio-based materials useful as packaging systems for protecting food products from physical contamination and, thus, for extending their shelf-life.

1. Introduction

The use of petroleum-based plastics in different fields, such as food and pharmaceutical sectors, has increased significantly in the last years, being the durability of the plastic materials, as well as their outstanding features, the main reason of their success. However, their worldwide applications led to huge waste-disposal problems and, as a consequence, to a dramatic environmental pollution. Every year 300 million tons of plastic wastes are generated and only less than 10% of them are recycled. The remaining part of plastic materials are disposed off in landfills and oceans releasing small and toxic petro-polymers, which are swallowed by marine animals killing more than 100,000 of them each year (Porta, 2019; Geyer, Jambeck, & Law, 2017). Therefore, the replacement of fossil-based packaging materials with the ones based on renewable and biodegradable polymeric sources are on the rise (Letcher, 2020; Jiang et al., 2020). Among these biopolymers, several researchers are being focused on developing bio-plastics from residual protein sources since they are cheap, biodegradable, abundant and possess promising film forming capacities (Wittaya, 2012; Jiménez-Rosado, Bouroudian, Perez-Puyana, Guerrero & Romero, 2020; González, Gastelú, Barrera, Ribotta & Igarzabal, 2019; Kaewprachu, Osako, Benjakul, Tongdeesoontorn & Rawdkuen, 2016; Sorde & Ananthanarayan, 2019; Kaewprachu, Osako, Tongdeesoontorn & Rawdkuen, 2017). In this context, plant proteins obtained from wastes of vegetable origin are potential candidates for producing biodegradable/edible plastics and, in particular, several attempts have been done for developing bio-plastics from proteins contained in different seed OCs, such those derived from soybean, rapeseed, cottonseed, sunflower, groundnut, sesame, bitter vetch and black cumin (Karimian, Tabatabaee Bafroee, & Sharifan, 2019; Fetzer, Hintermayr, Schmid, Stäbler & Eisner,2020; de Oliveira Filho et al., 2019; Rouilly & Vaca-Garcia, 2013; Riveros, Martin, Aguirre & Grosso, 2018; Fathi, Almasi, & Pirouzifard, 2019; Sabbah, Altamimi, Di Pierro, Schiraldi, Cammarota & Porta, 2020; Porta, Di Pierro, Rossi-Marquez, Mariniello, Kadivar & Arabestani, 2015).

Among the various oilseed plants, special attention should be given to the hemp (*Cannabis sativa L.*), a multipurpose, sustainable, and low

* Corresponding author.
E-mail address: giosafat@unina.it (C.V.L. Giosafatto).

https://doi.org/10.1016/j.fpsl.2021.100779
Received 1 March 2021; Received in revised form 23 June 2021; Accepted 16 November 2021
Available online 3 December 2021
2214-2894/© 2021 Elsevier Ltd. All rights reserved.

environmental impact crop belonging to the Cannabaceae family and containing low levels of Δ9-tetrahydrocannabinol (THC, <0.1–1%), that is cultivated for producing textiles, food, paper, biofuel, medicine and hygiene products (Fike, 2016; Kitrytė, Bagdonaitė, & Venskutonis, 2018). Due to its ability to grow under a wide range of conditions, *Cannabis sativa* L. can be found at different latitudes (Zhao, Xu, Wang, Griffin, Roozeboom & Wang, 2020). The world production of hemp seeds was around 110 × 10^3 tons/year in the last 25 years and France was the country with the highest production (about 65 ×10^3 tons per year) followed by China (about 35 ×10^3 tons/year) (FAOSTAT, 2020). The yield of hempseed oil extracted from 1 kg of seeds can reach up to 300 mL and, being not widespread on the market, it is considered a niche product characterized by a high content of polyunsaturated fatty acids. In particular, hemp seeds contain oil (25–35%) with important nutritional and functional properties. Hemp seed oil is indeed a rich source of polyunsaturated fatty acids including linoleic acid (18:2 ω-6) and α-linolenic acid (18:3 ω − 3), with a favorable balance ratio of ω-6 to ω-3 that makes it a potential candidate to be used in food and cosmetics (Crescente, Piccolella, Esposito, Scognamiglio, Fiorentino & Pacifico, 2018; Callaway, 2004; Pojić et al., 2014). Differently from most of the oilseeds, hemp seeds contain also low concentrations of antinutritional compounds, such as phytic acid, condensed tannins and trypsin inhibitors (Russo & Reggiani, 2015). In addition to lipids, hemp seeds contain proteins (20–30%), carbohydrates (10–15%) and insoluble fibers, vitamins and different minerals, such as phosphorus, potassium, magnesium, sulfur, calcium, iron, and zinc (Callaway, 2004; House, Neufeld, & Leson, 2010). The main protein content of hemp seeds consists of albumin and edestin, polypeptides with high amounts of arginine, glutamic acid, as well as of sulfur-containing amino acids, which makes their amino acid profiles comparable with those of soybean, egg and meat proteins (Tang, Ten, Wang & Yang, 2006; Dapčević-Hadnađev, Dizdar, Pojić, Krstonošić, Zychowski & Hadnađev, 2019; Callaway, 2004).

However, protein-based films generally exhibit poor mechanical and water vapor barrier properties, so that their application in food packaging sector is still quite limited. Therefore, in order to improve the protein-based film properties, different preliminary treatments of the protein sources, such as gamma-irradiation, heating or crosslinking, have been often performed, as well as the protein blending with other biopolymers or additives (Xu, Liu, Yang, Liu, Jia & Chen, 2012; Amadori, Torricelli, Rubini, Fini, Panzavolta & Bigi, 2015; Haghighi et al., 2020; Jiménez-Rosado et al., 2020; Wihodo and Moraru, 2013). Among these procedures, enzymatic crosslinking has received an increasing attention, due to its nontoxicity and the higher level of acceptance by consumers (Gaspar & Góes-Favoni, 2015; Kaewprachu et al., 2017). The most extensively used tool to reinforce protein-based films is represented by microbial transglutaminase (mTGase; EC.2.3.2.13), enzyme responsible for catalysing the formation of intermolecular ε-(γ-glutamyl)-lysine crosslinks into proteins via an acyl transfer reaction (Giosafatto, Fusco, Al-Asmar & Mariniello, 2020; Zink, Wyrobnik, Prinz & Schmid, 2016).

Despite the numerous researches carried out on developing protein-based films, information about hemp protein (HP)-derived films is still very scarce. Therefore, the present study was carried out to investigate the possibility to use hemp seed oilcakes (OCs) as an effective source to obtain bio-plastics. In addition, the ability of HPs to act as mTGase substrates was also tested with the aim to reinforce HP-based films and improve their properties.

2. Experimental section

2.1. Materials

Hemp OCs purchased from Consorzio Goji Italia (Andria, Italy) were a generous gift of prof. Daniele Naviglio; mTGase (Activa WM, containing 1% of mTGase and 99% of maltodextrins), obtained from the culture of *Streptoverticillium* sp., was supplied by Prodotti Gianni SpA (Milano, Italy). Chemical reagents used for electrophoresis were from Bio-Rad (Segrate, Milano, Italy). Sodium hydroxide, hydrochloric acid and glycerol (GLY) were purchased from Sigma Chemical Co (USA). All other chemicals and reagents utilized in this study were of analytical grade.

2.2. Extraction of hemp proteins (HPs)

HPs were extracted from the hemp OC according to acid precipitation method as described previously with some slight modification (Arabestani, Kadivar, Shahedi, Goli & Porta, 2013; Dapčević-Hadnađev et al., 2019; Hadnađev et al., 2018). Hemp OC flour (150 g) was added to 1.5 L of distilled water adjusted to pH 11 by 1 N NaOH, and the mixture stirred for 1 h at room temperature. The supernatant was collected after centrifugation at 5000 rpm for 15 min and the proteins were precipitated at pH 5.4 by adding 1 N HCl, and the suspension was then centrifuged at 5000 rpm for 15 min. The obtained pellet was finally dried in a plastic plate at 25 °C and 45% relative humidity (RH). The obtained protein concentrate was grinded in a Knife Mill Grindomix GM 200 (Grindomix GM200, Retsch GmbH, Haan, Germany) at a speed of 1000 rpm for 3 min. The protein content of the derived final HP concentrate was determined by the Kjeldahl's method (AACC, 2003), using a nitrogen conversion factor of 6.25.

2.3. Determination of zeta potential and particle size

HP concentrate was dissolved in distilled water (0.1 mg/mL) under constant stirring and the pH was then adjusted to 12.0 by using 0.1 N NaOH. Zeta potential and particle size values of HP solution were measured by titration from pH 12.0 to pH 2.0, adding 1.0, 0.1, and 0.01 N HCL under constant stirring at 25 °C (Gómez-Estaca, Gavara, Catalá & Hernández-Muñoz, 2016; Sabbah et al., 2017), with a Zetasizer Nano-ZSP (Malvern®, Worcestershire, UK) in the wavelength of 633 nm using a helium-neon laser of 4 mW output power. Zeta potential was calculated by the instrument software programmer trough the electrophoretic mobility at a voltage of 200 mV using the Henry equation, and all the results were reported as mean ± standard deviation. Zeta potential and particle size measurements were performed at each pH in triplicate. The effect of different concentrations of mTGase on zeta potential and particle size of the HP containing Film Forming Solutions (FFSs) at pH 12 was also studied. To this aim, each FFS (1.0 mL) containing 50% GLY and 16 mg HPs was previously incubated for 2 h at 37 °C and pH 7.5 in the absence or presence of different amounts of mTGase. At the end of incubation the pH of the FFSs was brought at 12 and, then, the samples were introduced in the measurement vessel. Each analysis took approximately 10 min.

2.4. Two-dimensional polyacrylamide gel electrophoresis (2D-PAGE)

2D-PAGE was carried out by analyzing 100 μg of HPs onto 7-cm IPG strips (pH 3–10) previously dissolved in 125 μL of sample rehydration buffer (Bio-Rad). 2 mL of mineral oil were added to each strip in order to prevent the evaporation during the 24 h protein separation. In the second step, protein separation according to molecular mass has been carried out by placing the gel horizontally into the precast SDS-PAGE gel (12%, Mini-protein gels, Bio-Rad) and performed at a current of 220 V for 40 min. The gel was finally stained with Coomassie Brilliant Blue R250 (Bio-Rad, Segrate, Milan, Italy).

2.5. Sodium dodecyl sulfate polyacrylamide gel electrophoresis (SDS-PAGE)

HPs (100 μg) were incubated at 37 °C in the presence of 80 mM Tris-HCl buffer, pH 7.5, and different concentration of mTGase (0, 5, 10, 20, 40 U/g protein) for two hours, as well as for different times (5, 10, 20,

40, 60 min and 2, 4 and 24 h) in the presence of 40 U/g of enzyme (100 μL final volume). 25 μL of sample buffer (62.5 mM Tris-HCl, pH 6.8, containing 4% (w/v) SDS, 30% (v/v) GLY, 10% (v/v) β-mercaptoethanol, and 0.05% (w/v) bromophenol blue) were added to the reaction mixtures at the end of incubation, then the samples were heated for 5 min in a boiling water bath and, finally, 25 μL of each sample finally analyzed by 12% SDS-PAGE as described by Laemmli (Laemmli, 1970). Bio-Rad Precision Protein Standards were run as molecular weight markers.

2.6. Preparation and casting of FFSs

HP stock solution (2g in 100 mL) was prepared by dissolving the HP concentrate in distilled water and by adding 1 N NaOH, under constant stirring at room temperature, until the pH of the solution was brought at 12. To find out the best conditions for developing HPs-based films, different FFSs (25 mL), containing 200, 300 and 400 mg of HPs and different concentrations of GLY (10-50%, w/w protein) used as plasticizer, were prepared at two different pH values (pH 7 and 12). Further FFSs were also prepared after incubation of HPs (400 mg) for 2 h, at 37 °C and pH 7.5, in the absence or presence of different amounts of mTGase (5, 10, 20, 40 U/g HPs). At the end of incubation, the pH was adjusted to 12 by 1 N NaOH addition and the mTGase-treated HP samples were heated at 80 °C in a water bath for 20 min to deactivate the enzyme. After cooling of the samples at room temperature, GLY was added to obtain FFSs containing a concentration of plasticizer of 50% (w/w protein). All the prepared FFSs were cast onto 8 cm diameter polycarbonate Petri dishes and allowed to dry in an environmental chamber at 25 °C and 45% RH for 24 h. The dried films were peeled intact from the casting surface and analyzed after their conditioning at 50% RH and 25 °C by placing them in a desiccator over a saturated solution of $Mg(NO_3)_2.6\ H_2O$ for 24 h.

2.7. Film properties

2.7.1. Opacity

The opacity values of the HP-based films were recorded by measuring the absorbance of the films, at a wavelength of 600 nm, divided by the film thickness (mm), using a UV/visible Spectrophotometer (SmartSpec 3000 Bio-Rad, Segrate, Milan, Italy), according to the method described previously by Jahed, Khaledabad, Bari, and Almasi (2017). Four strips of each film were cut (1 cm × 4 cm) and put in a spectrophotometer quartz cuvette; air was considered as a blank reference.

2.7.2. Density

Film density (ρ_s) was calculated according to the following equation. (Zahedi, Fathi-Achachlouei, & Yousefi, 2018; Cruz-Diaz, Cobos, Fernández-Valle, Díaz & Cambero, 2019):

$$\rho_s = (m/A \times \delta) \quad (1)$$

where m is the film dry mass after conditioning (g), A is the film area (2 ×2 cm^2), δ is the film thickness (cm) and ρ_s is the density of the film (gcm^{-3}). Three specimens of different points of each film were randomly selected.

2.7.3. Morphology

The surface microstructure and cross-sections of the films were studied by scanning electron microscopy (SEM) (Nova NanoSem 450-FEI-Thermo Fisher, Scientific, Waltham, MA, USA). The samples were coated with thin layers of gold and platinum using a sputter coater at a current of 20 mA for 90 s and then the images were taken at an accelerating voltage of 3 kV, (4.4–5.2) mm working.

2.7.4. Moisture content, swelling ratio and solubility

Film moisture content was analyzed according to the method described by Zahedi, Fathi-Achachlouei, & Yousefi, (2018) with some modifications. The film specimens (3 ×3 cm^2) were placed in the aluminum plates and dried at 105 °C in an oven for 24 h. Moisture content was evaluated by calculating the difference between their initial and final weight, before and after drying, using the following equation:

$$\text{Moisture content} = [(W_i - W_d)/W_i] \times 100 \quad (2)$$

Where, W_i and W_d represent the weights of the initial and dried film, respectively.

Film swelling ratio was examined using a gravimetric method as reported by Roy, Rhim, & Jaiswal (2019). Each film sample (3 ×3 cm^2) was pre-weighed (W_i) and then immersed in 30 mL of distilled water at 25 °C for 1 h. After film surface drying by an absorbent paper, the films were finally weighed again (W_s). The swelling ratio was calculated using the following equation:

$$\text{Swelling ratio} = [(W_s - W_i)/W_i] \times 100 \quad (3)$$

For the determination of film solubility in water, the dried film samples were weighed (W_i), immersed in 30 mL distilled water and then shaken for 24 h at 25 °C. The undissolved film residues were collected and dried in the oven at 105 °C to calculate their final dry weight (W_f). Film solubility was determined as the percentage of total weight by using the following equation (Roy and Rhim, 2020):

$$\text{Solubility}(\%) = \left[\left(W_i - W_f\right)/W_i\right] \times 100 \quad (4)$$

All the experiments were repeated three times.

2.7.5. Contact angle

Measurements of contact angle between water and HP-based films were carried out by using a homemade contact angle goniometer. Five droplets (10 μL) of distilled water were deposited on both sides of each film at different points and the photo was captured at the moment that the drop was in contact with the film surface. The mean value of contact angle was acquired with ImageJ software (González et al., 2019).

2.7.6. Thickness and mechanical properties

Film thickness was determined randomly in five different locations by using a micrometer (IP65 Alpa exacto) with a precision of 0.001 mm. Film tensile strength (TS), elongation at break (EB) and Young's modulus (YM) were determined by a dynamometer (Instron universal testing instrument model no. 5543 A, Instron Engineering Corp., Norwood, MA, USA). The conditioned films were cut into strips with a width of 10 mm and a length of 60 mm and five specimens of each film (1 kN load and 5 mm/min speed) were then tested as previously described according to the.

Film seal strength, evaluated according to (Amadori et al., 2015; Arabestani, Kadivar, Shahedi, Goli, & Porta, 2013; ASTM E88-07a, 2007a; AACC, 2003), was determined by reducing each film into strips of 5 × 2.5 cm, and placing each strip onto another one of the same sample. All the samples were previously conditioned at 25 °C and 50% RH for 24 h and, then, the two overlapped strips were placed into an automatic heat sealer (MagicVac®Axolute Mod: P0608ED, Italy). The seal strength (N/m), quantified by means of the above mentioned dynamometer, was calculated by dividing the maximum peak force to the film width.

2.7.7. Water vapor and gas permeability

HP-based film water vapor (WV) and gas (CO_2 and O_2) permeabilities were investigated and compared to the values obtained by analyzing two commercial materials, *i.e* low density polyethylene (LDPE), an oil-based plastic, and Mater-Bi, a starch-based bio-plastic, both purchased from a local supermarket. The measurements were performed in duplicate for each film (50% RH, 25°C and 101 kPa for gas

permeability; 90% RH, 38°C and 6 kPa for WV permeability) by using a Total Perm apparatus (ExtraSolution s.r.l., Pisa, Italy) according to the Standard Methods (ASTM D3985–05, 2010; ASTM F-2476-13, 2013). The measurements were carried out after conditioning the film specimens for 24h at 50% RH and placing them in the aluminum masks to reduce the film test area to 2 cm^2. The gas transmission rate was the actual measured volume converted into its value at standard temperature and pressure (STP) conditions.

2.8. Statistical analysis

SPSS19 (Version 19, SPSS Inc., Chicago, IL, USA) software was used for all statistical analyses. One-way analysis of variance (ANOVA) and Duncan's multiple range tests ($p < 0.05$) were used to determine the significant difference among the samples. All treatments were analyzed in triplicate.

3. Results and discussion

3.1. HP solution stability

Zeta potential values of a protein solution is affected by different factors, such as its pH and ionic strength, as well as the nature and composition of the solvent and the concentration of the dispersed particles (Bhattacharjee, 2016). It is an indicator of the colloidal stability of the solution, since values higher than ± 25 mV (in absolute value) indicate that the solution is relatively stable (Bhattacharjee, 2016). Thus, zeta potential of the aqueous solution of HP concentrate (72% HPs) obtained from hemp OCs was monitored at different pH values (2–12) in order to detect the best experimental conditions for preparing stable FFSs of HPs (Giosafatto, Al-Asmar, D'Angelo, Roviello, Esposito & Mariniello, 2018).

Panel A of Fig. 1 indicates that HP solution was quite stable between pH 8.0 and 12.0 and as demonstrated by the slight decrease in the zeta potential value from − 31 mV to − 24 mV. By further lowering the pH, the zeta potential values were observed to markedly decrease up to − 17 mV and − 4 mV at pH 6.0 and 5.0, respectively. Moreover, panel A of Fig. 1 also shows that, during the titration, the diameter (d.) of particle size values of the proteins were about 400–500 nm in the range of pH between 12.0 and 8.0, whereas they sharply increased over 1000 nm under pH 7.0. It is worthy to note that HP solution lost stability and began to flocculate around pH 6.0, as shown by the marked increase in the Z-average size of the protein particles, because this pH value is close to the isoelectric point (pI) of the majority of HPs as demonstrated by 2D-PAGE profile reported in the panel B of Fig. 1.

3.2. HP-based films

(ASTM E88–07a, 2007) the protein concentrate obtained from the hemp OCs was used as possible biopolymer source to produce biodegradable films at different pH values in the absence or presence of different concentrations of GLY used as plasticizer (Basiak, E., Lenart, A., & Debeaufort, F., 2018).

3.3. HPs as mTGase substrates

Panel A of Fig. 2 shows the HP SDS-PAGE profile following protein incubation with increasing amounts of mTGase. It is possible to note that HPs act as both acyl donor and acyl acceptor substrates of the enzyme as demonstrated by the decrease in intensity of the low molecular mass protein bands and the concomitant appearance of high molecular mass polymer(s), some of them unable to enter the stacking gel. Conversely, HP samples incubated in the absence of enzyme (lane 1) exhibited only three major bands with molecular masses of ~35 kDa, ~19 kDa, and ~16 kDa, identified as the main proteins occurring in the HP concentrate.

It is worthy to point out that the HP polymerization rate increased with the increase of mTGase concentration and that the most prominent disappearance of the HP bands was observed in lane 4 and lane 5 where the highest concentration of mTGase was used. These results are consistent with those reported by Giosafatto et al. (2018), Porta et al. (2015), Zhong et al. (2017) and Sabbah et al. (2020), who demonstrated that proteins extracted from several other seeds are able to act as mTGase substrates. Further experiments were carried out by incubating HPs at different times in the presence of the same amount of mTGase (40 U/g) (Fig. 2, **panel B**). In this case it was possible to observe that HPs started being polymerized by the enzyme after only 10 min and that the highest degree of polymerization was achieved after 2 h. Therefore, all the subsequent experiments were performed by incubating HPs for 2 h in the presence of different mTGase amounts.

3.4. Characterization of HP containing FFS treated with mTGase

Mean particle size and zeta potential of HPs, previously incubated at pH 7.5 for 2 h either in the absence or presence of different amounts of mTGase, were measured after GLY addition under alkaline conditions

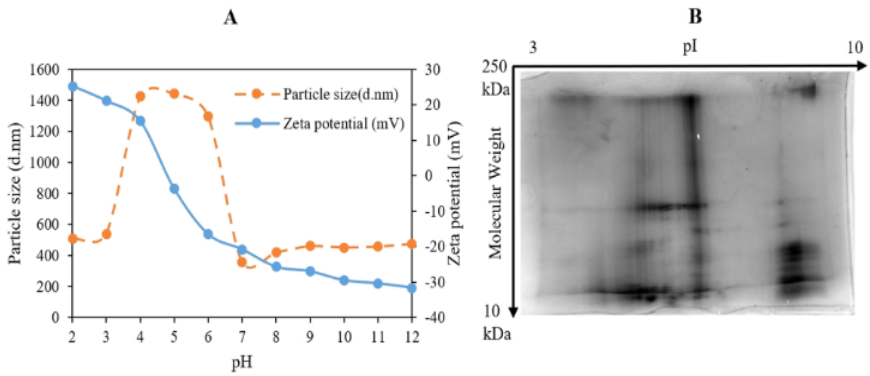

Fig. 1. Hemp protein zeta potential and particle size measurements at different pH values (A) and hemp protein 2D-PAGE (12%) profile (B). Further experimental details are given in the text.

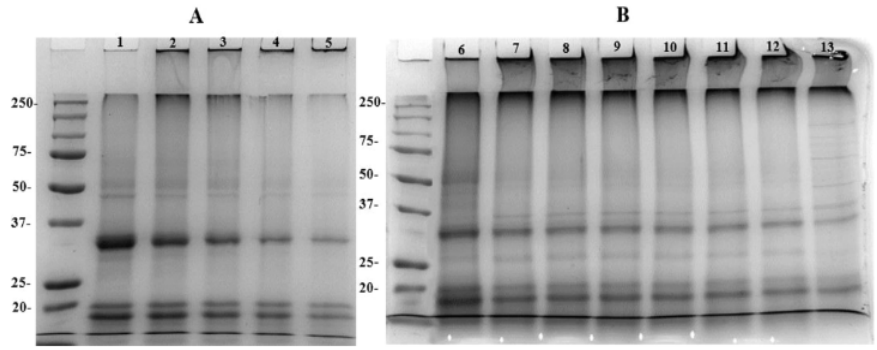

Fig. 2. SDS-PAGE analysis of hemp proteins (100 mg) incubated for 2 h in the absence (A1) or presence of different concentrations of microbial transglutaminase (A2, 5 U/g; A3, 10 U/g; A4, 20 U/g; A5, 40 U/g), or in the presence of 40 U/g of enzyme at different incubation times (B6, time 0; lane B7, 10 min; B8; 20 min; B9, 40 min; B10, 1 h; B11, 2 h; B12, 4 h; B13, 24 h). Further experimental details are given in the text.

(pH 12).

The results reported in Table 1 show that the negative zeta potential values of the FFSs slightly and progressively decreased with the increasing amounts of mTGase. However, all FFSs were quite stable exhibiting zeta potential values between − 30.3 and − 26.9 mV. Conversely, the mean particle size was observed to significantly increase by increasing mTGase concentration. This result seems to confirm the formation of HP polymers, already observed by SDS-PAGE (Fig. 2), and justify the observed linear increase of polydispersity index (PDI) value, that is an indicator of the relative variance in particle size distribution in the different FFS samples. Similar results have been recently reported by Liu et al. (2019), who investigated the particle size of mTGase-crosslinked whey proteins, and by Giosafatto et al. (2018) who studied the effect of the enzyme on the grass pea protein particle size.

3.5. mTGase-crosslinked HP-based films

Previous characterization of the FFSs containing HPs crosslinked by mTGase suggested the best experimental conditions to produce HP-based films following protein treatment with the crosslinking enzyme. It is worth to point out that, also in this case, it was necessary to add GLY (at least 30%) as plasticizer to the FFSs containing crosslinked HPs in order to obtain handleable films. Therefore, to compare the results obtained with the crosslinked HPs to the ones previously obtained with unmodified HPs, 50% GLY concentration was added to each FFS after enzyme treatment, as well as the FFS pH value was adjusted to pH 12 before casting. After drying, the films were peeled off intact from the plates and, after equilibration in a saturated solution of Mg $(NO_3)_2$·6 H_2O, their properties were investigated.

3.5.1. Thickness, opacity, density and morphology

Table 2 shows the values of thickness, opacity and density of the films produced with HPs previously incubated in the absence or presence of increasing mTGase concentrations. The thickness of crosslinked HP-based films was found to enhance as a function of mTGase amount used, ranging from about 97 μm for the uncrossliked films to 133 μm for the films derived from FFSs containing the maximal concentration of enzyme (40 U/g). Similar results have been previously reported by Porta et al. (2015) for bitter vetch protein-based films and by Giosafatto et al. (2018) for grass pea-based films.

The optical properties of the prepared films were also investigated because it is known that the appearance of the packaged products may influence the consumer acceptance of them (Shojaee-Aliabadi et al., 2014; Hosseini, Rezaei, Zandi & Ghavi, 2013). As reported in Table 2, the transparency of the mTGase-crosslinked films significantly decreased with the increase of the amount of enzyme used to modify HPs. The observed opacity enhancement is most probably due to the formation of protein aggregation consequent to the covalent crosslinks produced among the HP chains causing an hamperement to the light transmission through the film and changing of the refractive index (Ortega-Toro, Jiménez, Talens & Chiralt, 2014). Similar results were previously reported by Yilmaz, Turhan, Saricaoglu, and Tural (2020) for anchovy by-product protein films and by Rostamzad, Paighambari, Shabanpour, Ojagh, and Mousavi (2016) for fish protein-based films.

These data were also confirmed by the increase of film density of the films produced with crosslinked HPs that indicates the existence of a more compact film matrix network. Same results were obtained by Fathi, Almasi, & Pirouzifard, (2018) who reported that the density of sesame protein isolate films increased after crosslink formation due to

Table 1
Mean particle size, zeta potential and polydispersity index (PDI) of hemp protein film forming solutions incubated for 2 h in the presence of different amounts of microbial transglutaminase (mTGase)*.

mTGase (U/g of protein)	Mean particle size (nm)	Zeta potential (mV)	PDI (%)
0	368.33 ± 8.45^{d}	-30.30 ± 0.46^{d}	0.45 ± 0.03^{d}
5	432.27 ± 12.60^{c}	-29.63 ± 1.10^{cd}	0.53 ± 0.02^{c}
10	460.20 ± 12.40^{c}	-28.80 ± 0.46^{bc}	0.56 ± 0.03^{c}
20	533.16 ± 6.48^{b}	-27.73 ± 0.50^{ab}	0.67 ± 0.03^{b}
40	652.17 ± 37.54^{a}	-26.86 ± 0.35^{a}	0.76 ± 0.12^{a}

* Different small letters (a-d) indicate significant differences among the values reported in each column ($p < 0.05$). Further experimental details are given in text.

Table 2
Thickness, density and opacity of films containing 50% glycerol and prepared at pH 12 with hemp proteins previously incubated for 2 h in the absence or presence of different amounts of microbial transglutaminase (mTGase)*.

mTGase (U/g of protein)	Thickness (μm)	Density (g/cm^3)	Opacity (mm^{-1})
0	97.63 ± 7.09^{d}	1.31 ± 0.03^{d}	2.39 ± 0.27^{c}
5	106.00 ± 5.57 ^{cd}	1.45 ± 0.03^{c}	2.60 ± 0.21^{bc}
10	108.00 ± 6.25^{c}	1.50 ± 0.02^{b}	2.87 ± 0.19^{bc}
20	122.33 ± 2.08^{b}	1.61 ± 0.02^{a}	3.00 ± 0.30^{b}
40	133.33 ± 1.15^{a}	1.63 ± 0.03^{a}	3.77 ± 0.38^{a}

* Different small letters (a-d) indicate significant differences among the values reported in each column ($p < 0.05$). Values are given as mean ± standard deviation from triplicate determinations. Further experimental details are given in the text.

UV exposure.

Although the visual inspection of crosslinked HP-films (Fig. 3, A2–5) indicated that they were macroscopically similar to the ones produced with unmodified HPs (Fig. 3, **A1**) with a brownish color, SEM analyses of film cross-sections and surfaces showed significant differences. As far as the cross-section analyses, the films appeared more porous when manufactured with unmodified HPs (Fig. 3, **B1**) with respect to the films prepared with crosslinked HPs (Fig. 3, B2–5), as well as their surface resulted quite rough (Fig. 3, **C1**) in comparison with the smoother and more homogeneous surface observed in the films obtained with mTGase-crosslinked HPs (Fig. 3, C2–5), even though by using 20 U/g of mTGase the surface structure of the materials seems even more compact, thus influencing the film mechanical properties (Fig. 3, **C4**). Similar results have been previously reported by Porta et al. (2015), who observed a more compact microstructure of the films made with bitter vetch proteins when these proteins had been pretreated with mTGase.

3.5.2. Mechanical properties

As it is illustrated in Fig. 4, mechanical properties were significantly affected by the presence in the film matrix of isopeptide bonds produced by mTGase. TS of HP-based films was higher when enzymatically crosslinked proteins were used, reaching a value more than double, with respect to control films, by using 20 U/g of mTGase in the protein pretreatment. A similar trend was observed in the film YM change, thus indicating a more resistant and rigid feature of the material obtained following the treatment of HPs with mTGase (Sorde & Ananthanarayan, 2019; Kaewprachu et al., 2017; Yilmaz et al., 2020; Yayli, Turhan, & Saricaoglu, 2017). Conversely, and unexpectedly, only a slight decrease of the EB of the film produced by using crosslinked HPs was detected, indicating that the mobility of the protein chains and, consequently, the film flexibility were only slightly reduced following the enzyme catalyzed protein crosslinking.

Finally, HP-based films were also examined to determine their heat sealing ability, as this feature is fundamental for their potential

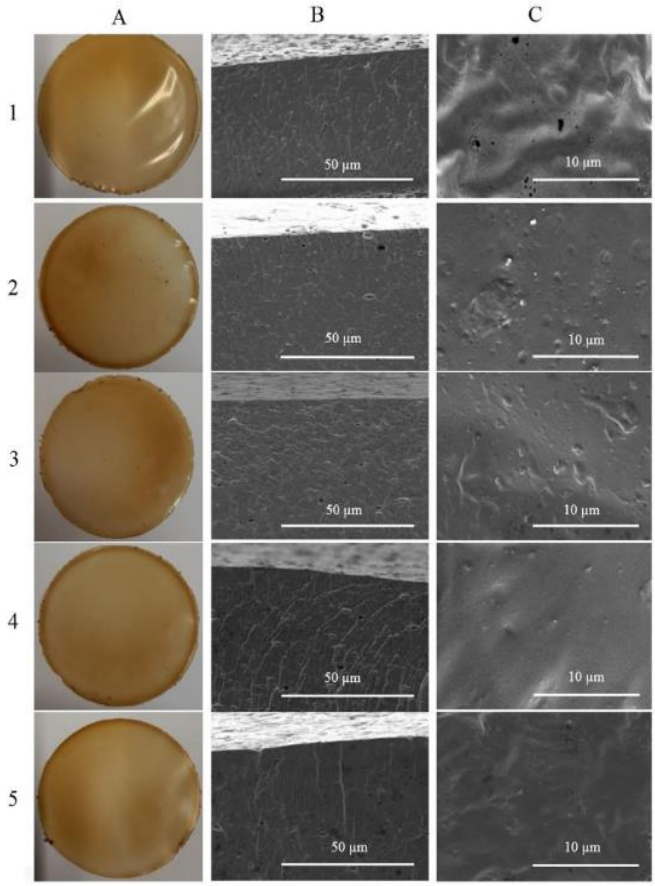

Fig. 3. Images of films (A), and of their SEM cross sections (B, magnification 2000 ×) and surfaces (C, magnification 8000 ×), containing 50% glycerol and prepared at pH 12 with hemp proteins previously incubated for 2 h in the absence (1) or presence of 5 (2), 10 (3) 20 (4), and 40 (5) U/g of microbial transglutaminase (mTGase).

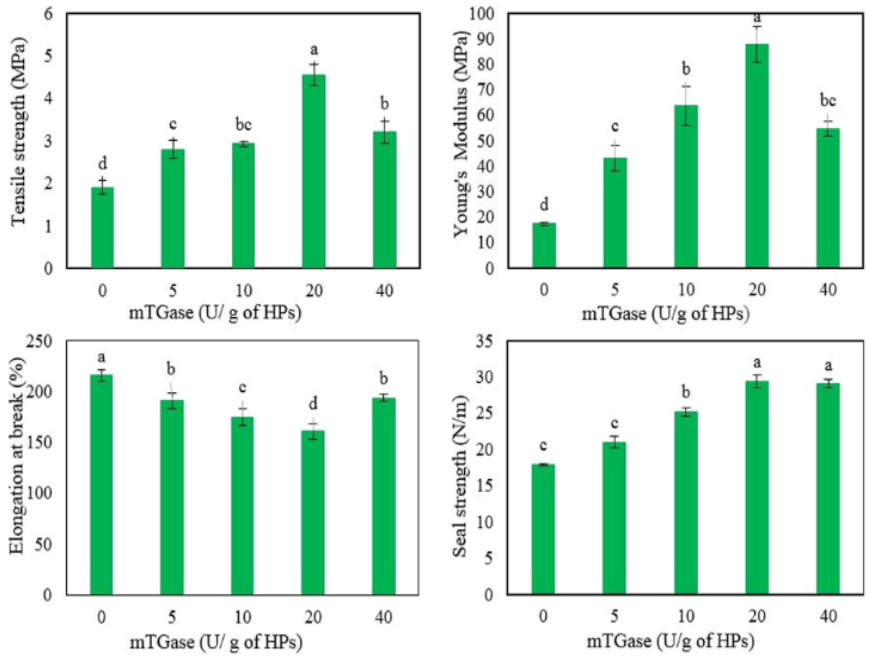

Fig. 4. Mechanical properties of films containing 50% glycerol and prepared at pH 12 with hemp proteins previously incubated for 2 h in the absence or presence of different amounts of microbial transglutaminase (mTGase). Different small letters (a-d) indicate significant differences among the values reported in each bar ($p < 0.05$).

industrial applications as food wrapping system. The analyses have shown that all the films were able to be heat-sealed and that the presence of mTGase-catalysed isopeptide bonds in HP matrix markedly increased the heat-sealing strength of the produced films, that almost doubled reaching a value of 30 N/m by using 20 U/g of enzyme (Fig. 4). This effect was probably due to the more compact structure of the films obtained with mTGase-crosslinked HPs and to the consequent increase of film hydrophobicity.

3.5.3. Moisture content, water solubility, swelling ratio and contact angle

Further investigations were carried out to determine moisture content, solubility, swelling ratio, as well as contact angle, of the films prepared with both unmodified and crosslinked HPs. Fig. 5 shows that the moisture content of HP films was higher and that it gradually decreased with the increase of mTGase concentration from 0 to 20 U/g (Fig. 5). This result could be explained with the reduction of the free ε-amino groups of HP lysines following the isopeptide bond formation catalyzed by mTGase (Tang, Jiang, Wen & Yang, 2005; Kaewprachu et al., 2017; Masamba et al., 2016). Similar results were obtained by analyzing the film water solubility, indicating that also this reduction was dependent on the formation of a stronger structure in the film network due to the enzyme-catalyzed crosslinks. Nevetherless, it is worthy to point out that, by visual observation, all the films appeared still intact even after 1 h immersion in water. Also the swelling ratio of the developed films revealed the same lowering trend (Fig. 5), confirming previous results (Schmid, Sängerlaub, Wege & Stäbler, 2014; Kaewprachu et al., 2017) reporting a reduction in swelling ratio of films made with mTGase-modified whey proteins and fish myofibrillar proteins, respectively. Therefore, all these findings could be attributed to the high degree of crosslinking in the film matrix (Schmid et al., 2014). Finally, the increase in film hydrophobicity was also assessed by measuring film contact angle which was double when HPs were previously treated with 20 U/g of enzyme. In conclusion, all the measured parameters reported in Fig. 5 clearly indicate a decrease in film hydrophylicity with a maximal effect observed when 20 U/g of mTGase were used. In fact, the treatment with higher enzyme amounts (40 U/g) did not give rise to a further decrease of film hydrophylicity, suggesting that, although the further increase in isopeptide bonds formed significantly modified film mechanical properties, it did not influence at all moisture content, water solubility and swelling ratio of the films, reverting slightly the observed increase of their contact angle values. This latter result might be explained from the SEM experiments illustrated in Fig. 3, since the surface of mTGase-crosslinked films appeared more compact by using 20 U/g of mTGase than that observed in the analysis of films prepared with lower or higher enzyme concentrations.

3.5.4. Water vapor and gas permeability

WV permeability is an important parameter for food packaging being a well known drawback of most hydrocolloid films. It is generally affected by several factors such as the material crystallinity and porosity, the type and amount of plasticizer added, as well as the matrix crosslinking and density (Han & Scanlon, 2005; Jasse, Seuvre and Mathlouthi, 1994; Miller & Krochta, 1997). Reduced WV permeability was evidenced in the films made with HPs previously treated with concentrations of mTGase up to 20 U/g (80% decrease), whereas an opposite trend was observed by analyzing the barrier effect of the crosslinked HPs films toward O_2 and CO_2 (Table 3). In fact, the O_2 and CO_2 transfer rate was found to significantly increase with increasing concentrations of

42.7 MPa and 12.1%, respectively, and these values were further reduced by increasing the enzyme concentration. Similar findings were obtained by Yayli et al. (2017), who reported that TS increased in films made with deboned chicken meat proteins treated with low concentrations (3%) of mTGase (increase from 2.4 MPa to 4.0 MPa), whereas the same parameter was observed to decrease (2.3 MPa) when the proteins were pretreated with higher amounts (4%) of enzyme. Moreover, Kaewprachu et al. (2017) reported that TS of myofibrillar protein films treated with mTGase increased when enzyme content was increased from 0% to 4%. Anchovy by-product protein films showed the highest TS and lowest EB when proteins were pretreated with 5% mTGase, that was the highest concentration of enzyme used in that study (Yilmaz et al., 2020), whereas their EB decreased. These results may be due to the formation of covalent crosslinks between protein chains, catalyzed by mTGase, and the consequent formation of high molecular weight polymers leading to an increase of the resistance of the derived films and to a decrease of their extensibility (Kaewprachu et al., 2017; Yilmaz et al., 2020; Yayli et al., 2017). However, although opposite effects on film EB, YM and WV permeability were often observed, the main measured parameters indicated that, most of the time, an increase in both film resistance and hydrophobicity was detected when comparison was carried out between the films prepared with mTGase-treated proteins with respect to the untreated counterparts (Table S1).

4. Conclusions

HPs were isolated from the hemp OC and demonstrated to effectively act *in vitro* as acyl donors and acceptors for mTGase, as well as to produce handleable films in the presence of plasticizer. Moreover, the enzymatically crosslinked HPs were showed to be able to give rise to bioplastics with improved performances. The scale up of these new materials on industrial scale might open new horizons to produce one time or short-term use items suitable for food packaging. For example, as the obtained bio-plastics are endowed with low water vapor permeability, they could be useful to protect and extend the shelf-life of fresh fruits, as apricots and persimmons, in order to allow their respiration. In this respect, the brownish appearance of the proposed packaging material should not negatively influence the customer acceptance, being of the same colour of that of mentioned food products and for the possible food protection from photooxidation by amber coloured films (Intawiwat et al., 2010). More in general, these findings encourage further investigations since hemp OC seems a potential renewable bio-source capable to partially substitute the highly pollutant petroleum-derived polymers, the production of which is continuing to exponentially increase. In fact, from an environmental and economic point of view, it is worthy to note that petroleum is becoming significantly expensive and a progressively limited resource expected to decline over the next few decades. Therefore, an early transition to renewable sources, such as that represented by hemp OCs, might be a valuable milestone at least for some specific sectors of food packaging industry.

CRediT authorship contribution statement

S.F.M., R.D.G., C.V.L.G., R.P.: Conceptualization; S.F.M., R.D.G., C.V.L.G.: Data curation; F S.F.M., C.V.L.G., R.P.: Investigation; S.F.M., R.D.G., M.F.: Methodology; C.V.L.G., R.P.: Supervision; C.V.L.G., S.F.M.: Writing-original draft; S.F.M., C.V.L.G., R.P.: Writing - review & editing; R.P.: Funding acquisition.

Acknowledgments

This research was funded by the grant PRIN: Progetti di Ricerca di Interesse Nazionale –Bando 2017– "CARDoon valorisation by InteGrAted biorefiNery (CARDIGAN)" of Italian Ministero dell'Università e della Ricerca (COD. 2017KBTK93), Italy.

Author contributions

Seyedeh Fateneh Mirpoor: Investigation; Methodology; Formal analysis; Writing-original draft. C. Valeria L. Giosafatto: Supervision; Conceptualization; Writing review and editing. Rocco Di Girolamo: Methodology; Investigation. Michela Famiglietti: Methodology; Raffaele Porta: Supervision; Conceptualization; Writing review and editing,; Supervision.

Appendix A. Supporting information

Supplementary data associated with this article can be found in the online version at doi:10.1016/j.fpsl.2021.100779.

References

Amadori, S., Torricelli, P., Rubini, K., Fini, M., Panzavolta, S., & Bigi, A. (2015). Effect of sterilization and crosslinking on gelatin films. *Journal of Materials Science: Materials in Medicine, 26*(2), 69.

AACC (2003). Approved Methods of AACC.; The Association: St. Paul, MN, USA. Available at: (https://methods.aaccnet.org/default.aspx).

Arabestani, A., Kadivar, M., Shahedi, M., Goli, S. A. H., & Porta, R. (2013). Properties of a new protein film from bitter vetch (*Vicia ervilia*) and effect of $CaCl_2$ on its hydrophobicity. *International Journal of Biological Macromolecules, 57*, 118–123.

ASTM E88-07a. (2007). Standard test method for seal strength of flexible barrier materials. F88-07. *Annual book of American standard testing method*, 768–777.

ASTM D3985–05 (2010). Standard test method for oxygen gas transmission rate through plastic film and sheeting using a colorimetric sensor; West Conshohocken, PA, USA.

ASTM F2476–13 (2013). Standard test method for the determination of carbon dioxide gas transmission rate through barrier materials using an infrared detector; West Conshohocken, PA, USA.

Basiak, E., Lenart, A., & Debeaufort, F.. (2018). How glycerol and water contents affect the structural and functional properties of starch-based edible films.. *Polymers, 10 (4)*, 412.

Bhattacharjee, S. (2016). DLS and zeta potential–what they are and what they are not? *Journal of Controlled Release, 235*, 337–351.

Callaway, J. C. (2004). Hempseed as a nutritional resource: An overview. *Euphytica, 140*, 65–72.

Crescente, G., Piccolella, S., Esposito, A., Scognamiglio, M., Fiorentino, A., & Pacifico, S. (2018). Chemical composition and nutraceutical properties of hempseed: an ancient food with actual functional value. *Phytochemistry Reviews, 17*, 733–749.

Cruz-Diaz, K., Cobos, Á., Fernández-Valle, M. E., Díaz, O., & Cambero, M. I. (2019). Characterization of edible films from whey proteins treated with heat, ultrasounds and/or transglutaminase. Application in cheese slices packaging. *Food Packaging and Shelf Life, 22*, Article 100397.

Dapčević-Hadnađev, T., Dizdar, M., Pojić, M., Krstonošić, V., Zychowski, L. M., & Hadnađev, M. (2019). Emulsifying properties of hemp proteins: Effect of isolation technique. *Food Hydrocolloids, 89*, 912–920.

de Oliveira Filho, J. G., Rodrigues, J. M., Valadares, A. C. F., de Almeida, A. B., de Lima, T. M., Takeuchi, K. P., … Dyszy, F. H. (2019). Active food packaging: alginate films with cottonseed protein hydrolysates. *Food Hydrocolloids, 92*, 267–275.

FAOSTAT (2020). Food and agriculture organization of the united Nations. Countries by commodity (http://www.fao.org/faostat/en/#rankings/countries_by_commodity). Accessed on 16 June 2021.

Fathi, N., Almasi, H., & Pirouzifard, M. K. (2018). Effect of ultraviolet radiation on morphological and physicochemical properties of sesame protein isolate based edible films. *Food Hydrocolloids, 85*, 136–143.

Fathi, N., Almasi, H., & Pirouzifard, M. K. (2019). Sesame protein isolate based bionanocomposite films incorporated with TiO_2 nanoparticles: study on morphological, physical and photocatalytic properties (doi.org/) *Polymer Testing, 77*, Article 105919. https://doi.org/10.1016/j.polymertesting.2019.105919.

Fetzer, A., Hintermayr, C., Schmid, M., Stäbler, A., & Eisner, P. (2020). Effect of acylation of rapeseed proteins with lauroyl and oleoyl chloride on solubility and film-forming properties (doi.org/) *Waste and Biomass Valorization*. https://doi.org/10.1007/s12649-020-01012-6.

Fike, J. (2016). Industrial hemp: renewed opportunities for an ancient crop. *Critical Reviews in Plant Sciences, 35*, 406–424.

Gaspar, A. L. C., & Góes-Favoni, S. P. D. (2015). Action of microbial transglutaminase (MTGase) in the modification of food proteins: A review. *Food Chemistry, 171*, 315–322.

Geyer, R., Jambeck, J. R., & Law, K. L. (2017). Production, use, and fate of all plastics ever made. *Science Advances, 3*(7), Article e1700782.

Giosafatto, C. V. L., Al-Asmar, A., D'Angelo, A., Roviello, V., Esposito, M., & Mariniello, L. (2018). Preparation and characterization of bioplastics from grass pea flour cast in the presence of microbial transglutaminase. *Coatings, 8*(12), 435.

Giosafatto, C. V. L., Fusco, A., Al-Asmar, A., & Mariniello, L. (2020). Microbial transglutaminase as a tool to improve the features of hydrocolloid-based bioplastics. *International Journal of Molecular Sciences, 21*(10), 3656.

Gómez-Estaca, J., Gavara, R., Catalá, R., & Hernández-Muñoz, P. (2016). The potential of proteins for producing food packaging materials: A review. *Packaging Technology and Science, 29*(4–5), 203–224.

González, A., Gastelú, G., Barrera, G. N., Ribotta, P. D., & Igarzabal, C. I.Á. (2019). Preparation and characterization of soy protein films reinforced with cellulose nanofibers obtained from soybean by-products. *Food Hydrocolloids, 89*, 758–764.

Hadnadev, M., Dapčević-Hadnadev, T., Lazaridou, A., Moschakis, T., Michaelidou, A.-M., Popović, S., & Biliaderis, C. G. (2018). Hempseed meal protein isolates prepared by different isolation techniques. Part I. physicochemical properties. *Food Hydrocolloids, 79*, 526–533.

Haghighi, H., Leugoue, S. K., Pfeifer, F., Siesler, H. W., Licciardello, F., Fava, P., & Pulvirenti, A. (2020). Development of antimicrobial films based on chitosan-polyvinyl alcohol blend enriched with ethyl lauroyl arginate (LAE) for food packaging applications. *Food Hydrocolloids, 100*, Article 105419.

Han, J. H., & Scanlon, M. G. (2005). Mass transfer of gas and solute through packaging materials. In J. H. Han (Ed.), *In Innovations in Food Packaging. Oxford* (pp. 12–23). Oxford: Elsevier Science & Technology.

Hosseini, S. F., Rezaei, M., Zandi, M., & Ghavi, F. F. (2013). Preparation and functional properties of fish gelatin–chitosan blend edible films. *Food Chemistry, 136*, 1490–1495.

House, J. D., Neufeld, J., & Leson, G. (2010). Evaluating the quality of protein from hemp seed (*Cannabis sativa* L.) products through the use of the protein digestibility-corrected amino acid score method. *Journal of Agricultural and Food Chemistry, 58*, 11801–11807.

Intawiwat, N., Pettersen, M. K., Rukke, E. O., Meier, M. A., Vogt, G., Dahl, A. V., … Wold, J. P. (2010). Effect of different colored filters on photooxidation in pasteurized milk. *J. Dairy Sci., 93*, 1372–1382.

Jahed, E., Khaledabad, M. A., Bari, M. R., & Almasi, H. (2017). Effect of cellulose and lignocellulose nanofibers on the properties of *Origanum vulgare* ssp. gracile essential oil-loaded chitosan films. *Reactive and Functional Polymers, 117*, 70–80.

Jasse, B., Seuvre, A. M., & Mathlouthi, M. (1994). Permeability and structure in polymeric packaging materials. In M. Mathlouthr (Ed.), *Food Packaging and Preservation* (pp. 1–22). Blackie.

Jiang, S., Zou, L., Hou, Y., Qian, F., Tuo, Y., Wu, X., … Mu, G. (2020). The influence of the addition of transglutaminase at different phase on the film and film forming characteristics of whey protein concentrate-carboxymethyl chitosan composite films. *Food Packaging and Shelf Life, 25*, Article 100546.

Jiménez-Rosado, M., Bouroudian, E., Perez-Puyana, V., Guerrero, A., & Romero, A. (2020). Evaluation of different strengthening methods in the mechanical and functional properties of soy protein-based bioplastics. *Journal of Cleaner Production, 262*, Article 121517.

Kaewprachu, P., Osako, K., Benjakul, S., Tongdeesoontorn, W., & Rawdkuen, S. (2016). Biodegradable protein-based films and their properties: a comparative study. *Packaging Technology and Science, 29*(2), 77–90.

Kaewprachu, P., Osako, K., Tongdeesoontorn, W., & Rawdkuen, S. (2017). The effects of microbial transglutaminase on the properties of fish myofibrillar protein film. *Food Packaging and Shelf life, 12*, 91–99.

Karimian, Z., Tabatabaee Bafroee, A. S., & Sharifan, A. (2019). Physico-mechanical and antimicrobial properties of isolated soy protein film incorporated with peppermint essential oil on raw hamburger. *Journal of Agricultural Science and Technology, 21*, 1145–1159.

Kitryté, V., Bagdonaité, D., & Venskutonis, P. R. (2018). Biorefining of industrial hemp (*Cannabis sativa* L.) threshing residues into cannabinoid and antioxidant fractions by supercritical carbon dioxide, pressurized liquid and enzyme-assisted extractions. *Food Chemistry, 267*, 420–429.

Laemmli, U. K. (1970). Cleavage of structural proteins during the assembly of the head of bacteriophage T4. *Nature, 227*(5259), 680–685.

Plastic Waste and Recycling: Environmental Impact. In Letcher, T. M. (Ed.), *Societal Issues*, (pp. 1–664). (2020) (pp. 1–664). Academic Press. https://doi.org/10.1016/B978-0-12-817880-5.00004-9.

Liu, Y., Liu, Y., Xu, Z., Shan, M., Ge, X., Zhang, Y., … Lu, F. (2019). Effects of *Bacillus subtilis* transglutaminase treatment on the functional properties of whey protein. *LWT-Food Science and Technology, 116*, Article 108559.

Masamba, K., Li, Y., Hategekimana, J., Zehadi, M., Ma, J., & Zhong, F. (2016). Evaluation of mechanical and water barrier properties of transglutaminase cross-linked zein films incorporated with oleic acid. *International Journal of Food Science & Technology, 51*(5), 1159–1167.

Miller, K. S., & Krochta, J. M. (1997). Oxygen and aroma barrier properties of edible films: A review. *Trends in Food Science & Technology, 8*(7), 228–237.

Ortega-Toro, R., Jiménez, A., Talens, P., & Chiralt, A. (2014). Properties of starch–hydroxypropyl methylcellulose based films obtained by compression molding. *Carbohydrate Polymers, 109*, 155–165.

Pojić, M., Mišan, A., Sakač, M., Dapčevic Hadnadev, T., Šarić, B., Milovanović, I., & Hadnadev, M. (2014). Characterization of byproducts originating from hemp oil processing. *Journal of Agricultural and Food Chemistry, 62*(51), 12436–12442.

Porta, R. (2019). The plastics sunset and the bio-plastics sunrise. *Coatings, 9*, 526. https://doi.org/10.3390/coatings9080526

Porta, R., Di Pierro, P., Rossi-Marquez, G., Mariniello, L., Kadivar, M., & Arabestani, A. (2015). Microstructure and properties of bitter vetch (*Vicia ervilia*) protein films reinforced by microbial transglutaminase. *Food Hydrocolloids, 50*, 102–107.

Riveros, C. G., Martin, M. P., Aguirre, A., & Grosso, N. R. (2018). Film preparation with high protein defatted peanut flour: characterization and potential use as food packaging. *International Journal of Food Science & Technology, 53*, 969–975.

Rostamzad, H., Paighambari, S. Y., Shabanpour, B., Ojagh, S. M., & Mousavi, S. M. (2016). Improvement of fish protein film with nanoclay and transglutaminase for food packaging. *Food Packaging and Shelf Life, 7*, 1–7.

Rouilly, A., & Vaca-Garcia, C. (2013). Industrial use of oil cakes for material applications. In A. Kazmi, & P. Shuttleworth (Eds.), *The Economic Utilisation of Food Co-Products* (pp. 185–213). Royal Society of Chemistry Publ. https://doi.org/10.1039/9781849737326.

Roy, S., & Rhim, J. W. (2020). Preparation of carbohydrate-based functional composite films incorporated with curcumin. *Food Hydrocolloids, 98*, Article 105302.

Roy, S., Rhim, J. W., & Jaiswal, L. (2019). Bioactive agar-based functional composite film incorporated with copper sulfide nanoparticles. *Food Hydrocolloids, 93*, 156–166.

Russo, R., & Reggiani, R. (2015). Evaluation of protein concentration, amino acid profile and antinutritional compounds in hempseed meal from dioecious and monoecious varieties. *American Journal of Plant Sciences, 6*(01), 14.

Sabbah, M., Di Pierro, P., Giosafatto, C. V. L., Esposito, M., Mariniello, L., Regalado-Gonzales, C., & Porta, R. (2017). Plasticizing effects of polyamines in protein-based films. *International Journal of Molecular Sciences, 18*(5), 1026.

Sabbah, M., Altamimi, M., Di Pierro, P., Schiraldi, C., Cammarota, M., & Porta, R. (2020). Black edible films from protein-containing defatted cake of *Nigella sativa* seeds. *International Journal of Molecular Sciences, 21*, 832. https://doi.org/10.3390/ijms21030832

Schmid, M., Sängerlaub, S., Wege, L., & Stäbler, A. (2014). Properties of transglutaminase crosslinked whey protein isolate coatings and cast films. *Packaging Technology and Science, 27*(10), 799–817.

Shojaee-Aliabadi, S., Hosseini, H., Mohammadifar, M. A., Mohammadi, A., Ghasemlou, M., Hosseini, S. M., & Khaksar, R. (2014). Characterization of κ-carrageenan films incorporated plant essential oils with improved antimicrobial activity. *Carbohydrate Polymers, 101*, 582–591.

Sorde, K. L., & Ananthanarayan, L. (2019). Effect of transglutaminase treatment on properties of coconut protein-guar gum composite film. *LWT-Food Science and Technology, 115*, Article 108422.

Tang, C. H., Jiang, Y., Wen, Q. B., & Yang, X. Q. (2005). Effect of transglutaminase treatment on the properties of cast films of soy protein isolates. *Journal of Biotechnology, 120*(3), 296–307.

Tang, C. H., Ten, Z., Wang, X. S., & Yang, X. Q. (2006). Physicochemical and functional properties of hemp (*Cannabis sativa* L.) protein isolate. *Journal of Agricultural and Food Chemistry, 54*(23), 8945–8950.

Weng, W., & Zheng, H. (2015). Effect of transglutaminase on properties of tilapia scale gelatin films incorporated with soy protein isolate. *Food Chemistry, 169*, 255–260.

Wihodo, M., & Moraru, C. I. (2013). Physical and chemical methods used to enhance the structure and mechanical properties of protein films: A review. *Journal of Food Engineering, 114*, 292–302.

Wittaya, T. (2012). Protein-based edible films: Characteristics and improvement of properties (doi.org/) *Structure and Function of Food Engineering*, 43–70. https://doi.org/10.5772/48167.

Xu, W., Liu, B., Yang, H., Liu, K., Jia, S., & Chen, F. (2012). Effect of γ-irradiation on the physicochemical properties of mixed soy protein isolate/starch material. *African Journal of Biotechnology, 11*(28), 7238–7246.

Yayli, D., Turhan, S., & Saricaoglu, F. T. (2017). Edible packaging film derived from mechanically deboned chicken meat proteins: Effect of transglutaminase on physicochemical properties. *Korean Journal for Food Science of Animal Resources, 37*(5), 635.

Yilmaz, K., Turhan, S., Saricaoglu, F. T., & Tural, S. (2020). Improvement of physicochemical, mechanical, thermal and surface properties of anchovy by-product protein films by addition of transglutaminase, and the correlation between secondary structure and mechanical properties. *Food Packaging and Shelf Life, 24*, Article 100483.

Zahedi, Y., Fathi-Achachlouei, B., & Yousefi, A. R. (2018). Physical and mechanical properties of hybrid montmorillonite/zinc oxide reinforced carboxymethyl cellulose nanocomposites. *International Journal of Biological Macromolecules, 108*, 863–873.

Zhao, J., Xu, Y., Wang, W., Griffin, J., Roozeboom, K., & Wang, D. (2020). Bioconversion of industrial hemp biomass for bioethanol production: A review. *Fuel, 281*, 118725–118733.

Zhong, T., Liang, Y., Jiang, S., Yang, L., Shi, Y., Guo, S., & Zhang, C. (2017). Physical, antioxidant and antimicrobial properties of modified peanut protein isolate based films incorporating thymol. *RSC Advances, 7*, 41610–41618.

Zink, J., Wyrobnik, T., Prinz, T., & Schmid, M. (2016). Physical, chemical and biochemical modifications of protein-based films and coatings: An extensive review. *International Journal of Molecular Sciences, 17*(9), 1376.

3- **Mirpoor, S. F.,** Giosafatto, C. V. L., Di Pierro, P., Di Girolamo, R., Regalado-González, C., & Porta, R., 2020. Valorisation of Posidonia oceanica Sea Balls (Egagropili) as a Potential Source of Reinforcement Agents in Protein-Based Biocomposites. Polymers, 12(12), 2788 10.3390/polym12122788

polymers

MDPI

Article

Valorisation of *Posidonia oceanica* Sea Balls (Egagropili) as a Potential Source of Reinforcement Agents in Protein-Based Biocomposites

Seyedeh Fatemeh Mirpoor [1], Concetta Valeria L. Giosafatto [1,*], Prospero Di Pierro [1], Rocco Di Girolamo [1], Carlos Regalado-González [2] and Raffaele Porta [1,*]

[1] Department of Chemical Sciences, University of Naples "Federico II", Montesantangelo Campus, via Cintia 4, 80126 Naples, Italy; seyedehfatemeh.mirpoor@unina.it (S.F.M.); prospero.dipierro@unina.it (P.D.P.); rocco.digirolamo@unina.it (R.D.G.)

[2] Departamento de Investigacion y Posgrado en Alimentos, Facultad de Quimica, Universidad Autonoma de Queretaro, Queretaro 76010, Mexico; carlosr@uaq.mx

* Correspondence: giosafat@unina.it (C.V.L.G.); raffaele.porta@unina.it (R.P.); Tel.: +39-081-2539-473 (R.P.)

Received: 6 November 2020; Accepted: 24 November 2020; Published: 25 November 2020

Abstract: Nanocrystalline cellulose (NC) and a lignin-containing fraction (LF) were obtained from egagropili, the so called sea balls produced from rhizome and stem fragments of *Posidonia oceanica* that accumulate in large amounts along the coastal beaches in the form of tightly packed and dry materials of various dimensions. Both egagropili fractions have been shown to be able to improve the physicochemical properties of biodegradable films prepared from protein concentrates derived from hemp oilseed cakes. These materials, manufactured with a biodegradable industrial by-product and grafted with equally biodegradable waste-derived additives, exhibited an acceptable resistance with a still high flexibility, as well as they showed an effective barrier activity against water vapor and gases (O_2 and CO_2). Furthermore, both NC and LF decreased film moisture content, swelling ability and solubility, thus indicating that both additives were able to improve water resistance of the hydrocolloid films. The exploitation of egagropili, actually considered only an undesirable waste to be disposed, as a renewable source of reinforcing agents to blend with different kinds of polymers is suggested.

Keywords: *Posidonia oceanica*; egagropili; nanocrystalline cellulose; lignin; protein-based biocomposites

1. Introduction

Plastics pollution has become a global threat, mostly to marine ecosystems [1]. Therefore, replacing oil-derived plastics with biodegradable materials is required by a more sustainable life pursuit and, in this respect, polymer matrices derived from bio-renewable polysaccharides and proteins are of highlighted interest. Numerous researches have been carried out in the last twenty years on using polysaccharide fibers derived from agriculture wastes or industrial by-products to develop biodegradable/edible films with improved performance [2].

Biocomposites containing plant- or wood- based fibers have been exploited thus far in an increasing range of items to reinforce plastics, having several advantages over synthetic additives. Plant cell walls consist essentially of rigid cellulosic microfibrils embedded in a soft matrix of hemicellulose and lignin, and cellulose is the major component in lignocellulosic biomass which is localized in the cell wall at around 35–50% [3]. Lignin represents a fairly stable polymer network that acts as a glue to hold the other matrix components (cellulose/hemicellulose) together [4]. Although most of the starting raw materials used are land vegetable sources, aquatic biomass, such as marine plants, may represent a possible effective alternative because the chemical composition of their

fibers is similar to that of other lignocellulosic materials. In particular, *Posidonia oceanica* (PO) is one of the most abundant Mediterranean endemic species, covering 60% of the seabed from 0 to 40 m depth [5] and about fifty thousand km² of coastal sandy areas [6]. One of the largest PO patches in the Mediterranean Sea contains forty undersea meadows stretching over two thousand miles. PO has been demonstrated to be an optimum source for the extraction of lignocellulosic fractions with promising properties for the development of packaging materials or to be used as fillers to enhance the properties of other biopolymers [7–10]. Cellulose extracted from PO, for example, has been proposed as a source of both carboxymethylcellulose [11,12] and sodium cellulose carboxymethylate [13] used as absorption materials. However, whereas stranded PO leaf residues play an important ecological role in protecting of coasts from erosion, other PO fragments accumulate in large amounts along the coastal beaches in the form of tightly packed and ball-shaped (oval or spherical) dry materials of different dimensions, called "egagropili". In fact, what remains of PO fiber-like leaves that are at the base of rhizomes and stems cluster together very closely and generate these characteristic free-floating and brown colored balls. The sea balls, also called sea rissoles or sea potatoes, are similar in texture to rough felt and tend to form by long-wavelength surface waves that run up on flat beaches. Wind and the tide push them together and, once completely dry, they accumulate in huge numbers along the sandy shores (Figure 1). Since egagropili represent a problem, first of all for their negative visual impact [14], the municipalities are forced to remove and dispose them in landfills as municipal wastes with non- negligible costs.

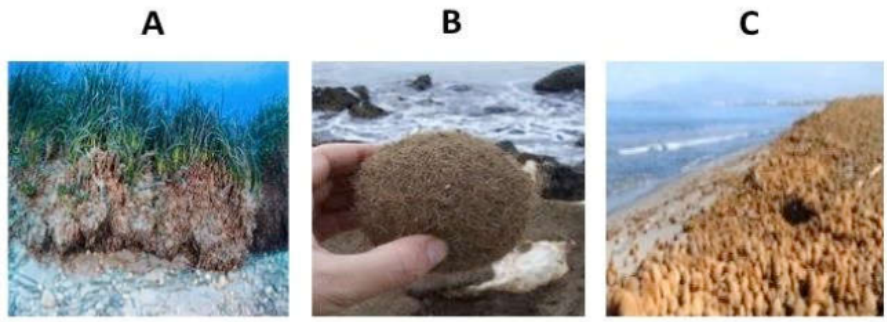

Figure 1. *Posidonia oceanica* rhizomes and stems (**A**) from which ball shaped dry materials called egagropili (**B**) origin and accumulate along the costal beach (**C**).

Therefore, the search for turning egagropili into a resource that provides economic benefits and positive feedback from an environmental point of view is strongly advisable because egagropili do not significantly differ from other lignocellulosic materials [12]. Their small salt content (0.5–2%) allows egagropili to resist decomposition and, being virtually non-flammable, they are currently being studied for insulation use since they markedly reduce heat loss. In addition the dry residue of egagropili is made of holocellulose, lignin and a small amount of ash. Holocellulose is the total carbohydrate component and has been calculated to be 61.8% where cellulose contributes 40%, making this fraction particularly suitable as renewable cellulose source [15]. Among the numerous published studies on the use of lignocellulosic fibers as additives of biodegradable materials [2], Seggiani et al. [16] developed polyhydroxyalkanoate-based bio-composites specifically grafted with PO fibers for potential applications in marine environment, such as natural engineering interventions.

In this paper both cellulose and lignin containing fractions obtained from egagropili fibers were investigated to assess their properties for a possible use as reinforcement additives of protein-based biodegradable/edible films, potentially able to replace oil-based plastics in packaging systems.

2. Materials and Methods

2.1. Materials

Hemp oilseed cakes, a generous gift of prof. Daniele Naviglio, were purchased from Consorzio Goji Italia (Andria, Italy). Egagropili sea balls were collected in the sardinian Poetto beach (Cagliari, Italy) and stored at 4 °C until used. Sodium hydroxide, hydrochloric acid, sodium chlorite, acetic acid glacial, potassium hydroxide, sulfuric acid and glycerol (GLY) were purchased from Sigma Chemical Co (St. Louis, MO, USA). All other chemicals were of analytical grade.

2.2. Egagropili Lignin Containing Fraction and Nanocrystalline Cellulose

Egagropili balls were reshaped to rhizome fibers by hands, then washed and rinsed vigorously in distilled water in order to remove sand, salts and other soil contaminants, and finally dried in an oven at 80 °C for 24 h. The dried egagropili fibers were grinded in a rotary mill (Grindomix GM200, Retsch GmbH, Haan, Germany) at a speed of 1000 rpm for 3 min to a 60-mesh sieve size. Cellulose extraction was carried out as reported by Ilyas et al. [17] with some modifications. In the first step, 20 g of grinded egagropili fibers were dewaxed by means of Soxhlet apparatus, with 440 mL of toluene/ethanol (2:1 *v*/*v*) during 24 h and oven dried overnight at 105 °C. Afterwards, delignification process has been carried out by dispersing at 70 °C for 2 h the dewaxed egagropili powder in 600 mL of 1.7% sodium chlorite solution brought at pH 3.5 by acetic acid. This process was repeated 3 times consecutively until the color changed from brown to white/yellowish. The resulted bleached fibers, known as holocellulose, were filtered by using filter paper and washed with distilled water until the filtrate became neutral. The first filtrate obtained in the delignification step was referred as the lignin containing fraction (LF). A quantitative analysis, carried out by calculating the dry weight of LF, indicated that 152 mg of LF were obtained from 1 g of grinded egagropili powder. To remove hemicellulose and residual pectin, the obtained holocellulose was treated with 5% potassium hydroxide for 24 h at room temperature followed by an exposure for 2 h at 90 °C. Finally, the obtained cellulose fraction was filtered and washed several times until pH neutralization, and finally dried at 55 °C for 18 h.

Nanocrystalline cellulose (NC) was obtained by sulfuric acid hydrolysis of the egagropili cellulose fraction according to the procedure described by Sanyang et al. [18]. Acid hydrolysis started by adding 1 g of cellulose fraction into 10 mL of sulfuric acid solution (65%, *w*/*w*) and by stirring the reaction mixture at 45 °C for 45 min in order to totally hydrolyze the amorphous regions of cellulose. Hydrolysis reaction was stopped by diluting ten-times the suspension by cold distilled water, followed by repeated washing of the pellet obtained by centrifugation at 10,000 rpm for 10 min, until the neutral pH was reached. The resulting precipitate containing NC was finally freeze-dried and, then, the obtained powder was dispersed in distilled water and subjected to ultrasonication for 10 min at 400 W to stabilize NC dispersion by eliminating its excessive aggregation. The quantitative gravimetric determination indicated that 225 mg of NC were obtained from 1 g of grinded egagropili powder. The entire extraction process, summarized in Figure 2, was monitored by Fourier-transform infrared spectroscopy analysis using a model ALPHA spectrometer (Bruker, Leipzig, Germany) equipped with an attenuated total reflectance accessory.

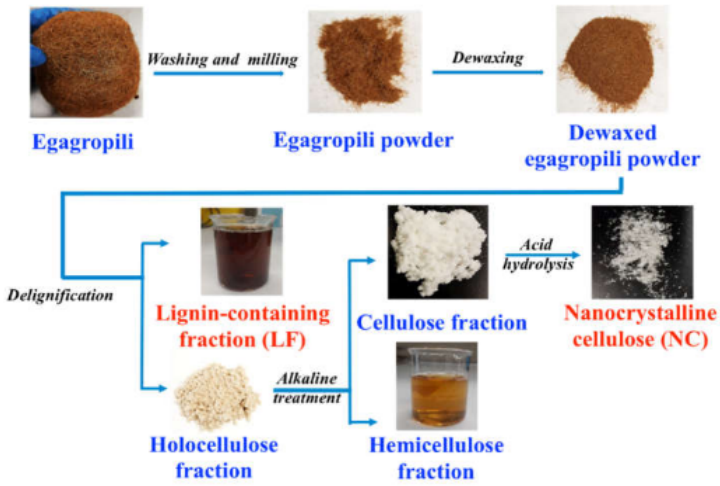

Figure 2. Scheme of the extraction procedure of nanocrystalline cellulose and lignin containing fraction from egagropili.

2.3. Preparation of Protein-Based Composite Films

Hemp proteins (HPs) were extracted from the industrial hemp seed oilcake, a byproduct obtained after the extraction of the hemp seed oil. Defatted hemp seed flour was treated under alkaline conditions (pH 11), and the supernatant obtained after centrifugation was precipitated at acidic pH (5.4). The obtained pellet (HP concentrate) was finally dried and used to obtain hydrocolloid films. The protein content of the derived final HP concentrate was determined by the Kjeldahl's method [19], using a nitrogen conversion factor of 6.25. HP stock solution (2% *v*/*w*) were prepared by dissolving the protein concentrate in distilled water and by adding 1 N NaOH, under constant stirring at room temperature, until the pH of the solution was brought at pH 9 or 12. Film forming solutions (FFSs) (25 mL) were prepared at the two different pH values by using 400 mg of HPs in the presence of 50% GLY, used as plasticizer, and different amounts of either NC (at pH 9) or the extensively dialyzed LF (at pH 12) extracted from egagropili. All kinds of FFSs were cast onto 8 cm diameter polycarbonate Petri dishes and allowed to dry in an environmental chamber at 25 °C and 45% relative humidity (RH) for 24 h. The dried films were peeled, intact, from the casting surface and analyzed after their conditioning at 50% RH and 25 °C by placing them in a desiccator over a saturated solution of $Mg(NO_3)_2 \cdot 6H_2O$ for 24 h.

2.4. Zeta Potential and Particle Size Measurements

The effect of both NC and LF extracted from egagropili on zeta potential and particle size of the HP containing FFSs at pH 9 or 12, respectively, was studied. To this aim each FFS (1.0 mL), containing 50% GLY and 16 mg HPs, was tested in the absence or presence of different amounts of either NC or LF. Zeta potential and particle size values were measured with a Zetasizer Nano-ZSP (Malvern®, Worcestershire, UK) in the wavelength of 633 nm using a helium-neon laser of 4 mW output power. Zeta potential was calculated by the instrument software programmer trough the electrophoretic mobility at a voltage of 200 mV using the Henry equation. Zeta potential and particle size measurements were performed at each pH in triplicate and all the results were reported as mean ± standard deviation.

2.5. Film Mechanical Properties

Film tensile strength (TS), elongation at break (EB) and Young's modulus (YM) were measured by an Instron universal testing instrument (model no. 5543A, Instron Engineering Corp., Norwood, MA, USA). Each prepared film was cut into strips with a width of 10 mm and a length of 60 mm and at least three samples of each film were then tested, by using 1 kN load and 5 mm/min speed, as previously described [20]. Film thickness was determined randomly in five different locations by using a micrometer (IP65 Alpa exacto, Alpa metrology, Pontoglio (BS), Italy) with a precision of 0.001 mm.

2.6. Film Moisture Content, Swelling Ratio and Solubility

Film moisture content was analyzed on 3 × 3 cm^2 samples according to the method described by Zahedi et al. [21]. Films were placed in the aluminum plates and dried at 105 °C in an oven for 24 h. Moisture content of the films was evaluated by calculating the difference between their weight before and after drying using the following equation:

$$\text{Moisture content} = [(W_i - W_a)/W_i] \times 100 \quad (1)$$

where, W_i and W_a represent the film weights before and after drying, respectively.

Film swelling ratio was determined by a gravimetric method [22]. Each film (W_i) was immersed in 30 mL of distilled water at 25 °C for 1 h and, after drying of its surface by an absorbent paper, each film was finally weighed again (W_s). The swelling ratio was calculated using the following equation:

$$\text{Swelling ratio} = [(W_s - W_i)/W_i] \times 100 \quad (2)$$

In order to determine film water solubility, the dried film was weighed (W_i), immersed in 30 mL distilled water and shaken for 24 h at 25 °C. The undissolved film residues were finally dried in the oven at 105 °C to calculate the film dry weights (W_f). Film solubility was determined as the percentage of total weight by using the following equation [23]:

$$\text{Solubility (\%)} = [(W_i - W_f)/W_i] \times 100 \quad (3)$$

All the experiments were repeated at least three times.

2.7. Film Water Vapor, O_2 and CO_2 Permeability

Film water vapor (WV) and gas permeability was investigated, after film conditioning for 24 h at 50% RH, as previously described [24–26] by using a Total Perm apparatus (ExtraSolution s.r.l., Pisa, Italy) and aluminum masks to reduce the film test area to 5 cm^2. All the experiments were repeated at least three times.

2.8. Scanning Electron Microscopy (SEM)

Microstructures of both grinded egagropili fibers and nanocrystalline cellulose were observed by using a Philips-FEI SEM (Nova NanoSem 450-FEI-Thermo Fisher, Scientific, Waltham, MA, USA). The dried samples were coated with thin layers of gold and platinum using a sputter coater at a current of 20 mA for 90 s and then the images were taken at an accelerating voltage of 3 kV, (4.4–5.2) mm working. Further surface and cross-section images were also obtained by analyzing hemp protein films derived from FFSs prepared in the absence or presence of either 6% NC or LF. For cross-section imaging, the samples were previously frozen using liquid nitrogen and then cryofractured.

2.9. Statistical Analysis

SPSS19 (Version 19, SPSS Inc., Chicago, IL, USA) software was used for all statistical analyses. One-way analysis of variance (ANOVA) and Duncan's multiple range tests ($p < 0.05$) were used to determine the significant difference among the samples.

3. Results and Discussion

3.1. Egagropili as Potential Source of Lignin and Nanocrystalline Cellulose

Different fractions of egagropili powder were obtained by preliminary washing, de-waxing, heating and grinding of the starting material and, then, by delignification with sodium chlorite and separation of cellulose from hemicellulose and pectin by potassium hydroxide treatment. Finally, NC was obtained by sulfuric acid hydrolysis of the extracted cellulose to eliminate the amorphous regions of the polysaccharide. It is well known that NC is widely utilized as a reinforcement agent in polymer matrices for its peculiar properties such as a high crystallinity and aspect ratio, large specific surface area, as well as abundance of surface hydroxyl groups able to form hydrogen bonds [27]. Therefore, the aim of the present study was to investigate the possibility to exploit egagropili, until now considered by the local authorities as an undesired waste to be disposed, as a renewable resource to produce reinforced protein-based bioplastics, mainly thanks to their cellulose content. In addition, also the obtained egagropili LF was tested as possible reinforcement of the prepared protein-based films. Lignin is, in fact, the most recalcitrant component in lignocellulosic fibers, being extremely resistant to enzymes and chemical impacts [28] due to its polyphenolic structure which consists of three different phenylpropane monomeric units containing zero, one, and two methoxyl groups, respectively [29–31].

3.2. Surface Microstructure of Egagropili Fibers and the Derived Nanocrystalline Cellulose

The SEM image of surface microstructure of grinded egagropili fibers indicated that egagropili powder has a lignocellulosic fibrous structure and the determined fiber length was in the 1–2 mm range (Figure 3A). On the other hand, NC chains obtained by acidic hydrolysis of the cellulose fraction extracted from egagropili exhibited a rod-like structure of 65–90 nm in diameter with smooth surfaces. In addition, the NC chains appear not to be separated from each other leading to a nebulous morphology (Figure 3B). The observed agglomeration of this material was probably due, as previously reported [32], to the hydrophilic characteristics of cellulose.

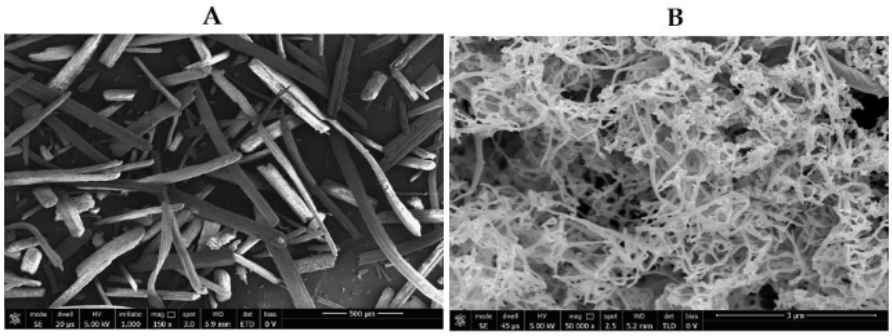

Figure 3. SEM images of both grinded egagropili fibers (**A**) and egagropili nanocrystalline cellulose (**B**).

3.3. Film Forming Solution Zeta Potential and Particle Size Measurements

FFSs containing HPs and different concentrations of NC (2, 4 and 6% with respect to HPs) were prepared at pH 9 and 1 mL of each FFS was analyzed to determine their zeta potential value and the particle size. Table 1 shows that the FFSs prepared in the presence of different amounts of NC exhibited zeta potential values very similar to that measured with the FFS containing only HPs, thus indicating that all the prepared FFSs were relatively stable [33,34]. Conversely, the mean value of the

particle size significantly increased with the increase of NC concentration. This result could be probably due to the hydrogen bond formation between HPs and NC with the consequent formation of particles of higher dimensions. The larger standard deviation detected in the values obtained increasing NC concentration might depend on the variability of the dimension of the particles formed.

Table 1. Mean particle size, zeta potential and polydispersity index (PDI) of different hemp protein film forming solutions (FFSs) containing increasing amounts of either nanocrystalline cellulose (NC) or lignin fraction (LF) and prepared at pH 9 and 12, respectively *.

FFS Additive	Mean Particle Size (d.nm)	Zeta-Potential (mV)	PDI (%)
None, pH 9	374.50 ± 14.50 ^{a}	−22.30 ± 1.55 ^{a}	0.58 ± 0.06 ^{a}
+ 2% NC	397.40 ± 10.40 ^{a,b}	−21.50 ± 1.68 ^{a}	0.56 ± 0.03 ^{a}
+ 4% NC	466.50 ± 14.90 ^{b,c}	−20.20 ± 1.30 ^{a}	0.58 ± 0.03 ^{a}
+ 6% NC	552.20 ± 37.54 ^{c}	−21.80 ± 1.15 ^{a}	0.61 ± 0.02 ^{a}
None, pH 12	324.30 ± 8.83 ^{a}	−28.50 ± 1.15 ^{b}	0.54 ± 0.16 ^{a}
+ 3% LF	389.80 ± 10.69 ^{b}	−27.60 ± 1.06 ^{b}	0.61 ± 0.31 ^{a}
+ 6% LF	394.90 ± 14.35 ^{b}	−27.10 ± 2.38 ^{b}	0.65 ± 0.25 ^{a}
+ 9% LF	312.70 ± 17.18 ^{a}	−28.90 ± 1.76 ^{b}	0.64 ± 0.29 ^{a}

* Different small letters (a–c) indicate significant differences among the values reported in each column ($p < 0.05$). Further experimental details are given in text.

Furthermore, Table 1 also shows that the value of zeta potential of HP-based FFSs prepared at pH 12 in the presence of different concentrations of LF (3%, 6% and 9% with respect to HPs) was almost stable around −28 mV and that, in this case, also the mean particle size was not significantly influenced by the presence of different amounts of LF added to the FFS. It is worthy to note that the polydispersity index (PDI) values did not significantly change in the different FFSs analyzed compared to those of the respective controls.

3.4. Hemp Protein-Based Films

Preliminary experiments carried out by using NC or LF as additives in HP-based FFSs gave rise to manipulable films, whereas the presence of egagropili-derived fibers or holocellulose, hemicellulose and cellulose fractions in FFSs produced films difficult to handle, being fragile or sticky, as well as not homogeneous in their matrix. However, being biodegradable, non-toxic and possessing emulsifying properties, the extracted hemicellulose might find applications in different area of interest, such as papermaking and cosmetics industries.

Therefore, the HP-based composite films under investigation were divided into two groups based on their grafting with only two egagropili-derived additives: NC and LF. It is worthy to note that, in the presence of NC, the optimal pH value of the FFS to give rise to HP films with the best performance was pH 9, whereas the optimal pH was 12 when the reinforcement agent tested was LF.

3.5. Film Mechanical Properties

The HP-based films prepared in the presence of either NC or LF were peeled intact from the casting surface and characterized for their mechanical properties. Figure 4 shows that the thickness of the nanocomposite films significantly increased by increasing the amount of NC incorporated into the film matrix.

Conversely, no significant effect on the film thickness was observed in the films prepared in the presence of different amounts of LF (Figure 5). Moreover, Figures 4 and 5 clearly show that film TS, EB and YM were significantly affected by the addition of either NC or LF to the FFSs. In fact, both kinds of biocomposite films exhibited higher TS and YM values compared to the respective control films, whereas their EB significantly decreased as a function of NC or LF amounts occurring in the FFS. These results indicate that both NC and LF contributed to reinforce HP-based films making them more resistant but still quite flexible to be potentially applied to a variety of packaging

systems. However, it is worthy to note that the addition of the highest lignin amount tested to the FFS caused a decrease of both film resistance and extensibility (Figure 5), likely due to an excessive protein aggregation.

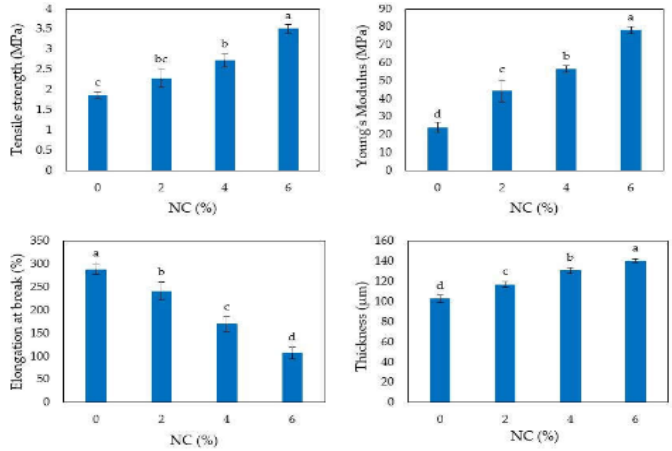

Figure 4. Tensile strength, elongation at break, Young's module and thickness of hemp protein-based films derived from film forming solutions prepared at pH 9 and containing increasing amounts of egagropili nanocrystalline cellulose (NC). Different small letters a–d indicate significant differences among the values reported in each column ($p < 0.05$). Further experimental details are given in text.

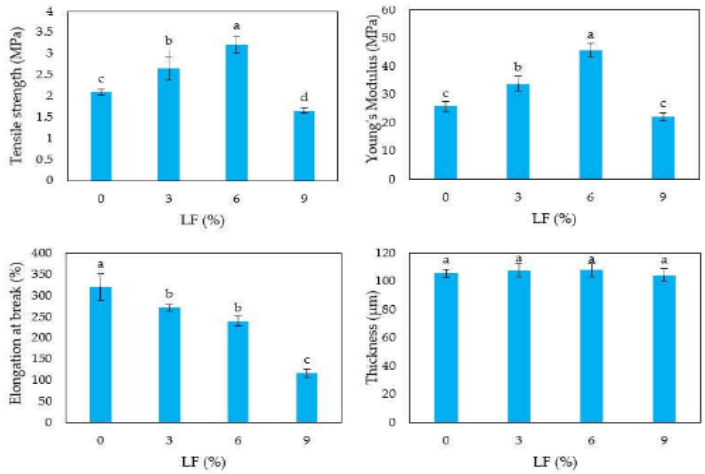

Figure 5. Tensile strength (TS), elongation at break (EB), Young's module (YM) and thickness of hemp protein-based films derived from film forming solutions (FFSs) prepared at pH 12 and containing increasing concentrations of egagropili lignin fraction (LF). Different small letters a–d indicate significant differences among the values reported in each column ($p < 0.05$). Further experimental details are given in text.

These findings are in agreement with those previously reported by Zadeh et al. [35], who investigated the use of commercial lignin to improve the physical properties of films manufactured with transglutaminase-modified soy protein isolate, having observed an improvement in film TS due to intermolecular lignin/soy protein interactions. In addition, Alashwal et al. [36] recently reported the development of keratin-based bioplastics with improved morphology and properties when the protein was blended with nanocrystalline cellulose, envisaging their potential use in biomedical applications and manufacturing of food containers.

3.6. Film Moisture Content, Solubility, Swelling Ratio and Permeability

As water sensitivity is one of the main drawbacks of hydrocolloid bioplastics, the effect of loading NC and LF on film resistance to moisture was investigated by measuring film moisture content, water solubility as well as swelling ratio. As matter of fact, the addition of fillers generally aims not only to enhance film mechanical properties but also to confer them stability for various applications that often require film exposure to a high moisture environment. Thus, Figure 6 shows that the observed mechanical reinforcement due to the presence of either NC or LF in the HP film matrix led also to a decrease of the film moisture content, probably due to a weakened water trapping ability of the biocomposite films as a result of the denser structure of their matrix [37].

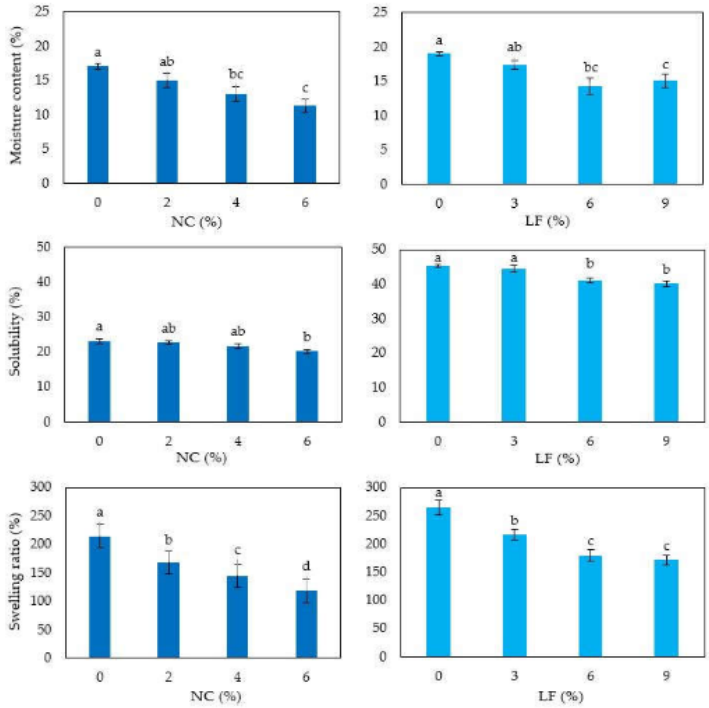

Figure 6. Moisture content, solubility and swelling ratio of hemp protein-based films prepared with film forming solutions containing increasing amounts of either nanocrystalline cellulose (NC) or lignin fraction (LF) and prepared at pH 9 and 12, respectively. Different small letters a–d indicate significant differences among the values reported in each column ($p < 0.05$). Further experimental details are given in text.

In addition, Figure 6 shows that also the swelling ability and solubility of the films significantly decreased, confirming that both egagropili-derived additives were able to improve film water resistance ability, probably through the formation of hydrogen bonds between the blended polymers which enhanced the cohesiveness of the matrix [38]. It is worthy to note that NC was previously exploited for improving also the moisture sensitivity of polysaccharide-based biocomposites. In this respect, Agustin et al. [39] reported that the hydrogen-bond network, formed into a starch-based matrix containing cellulose nanocrystals obtained from rice straw, prevented the formation of voids where water molecules could pass through, thus providing an increase in the resistance to the water uptake by the tested material.

Finally, reduced WV and gas permeability was detected in the films by increasing the concentration of both NC and LF into the FFSs (Figure 7), indicating that the observed reinforcement of the film protein matrix had a significant impact also on the barrier properties of the prepared biocomposite materials.

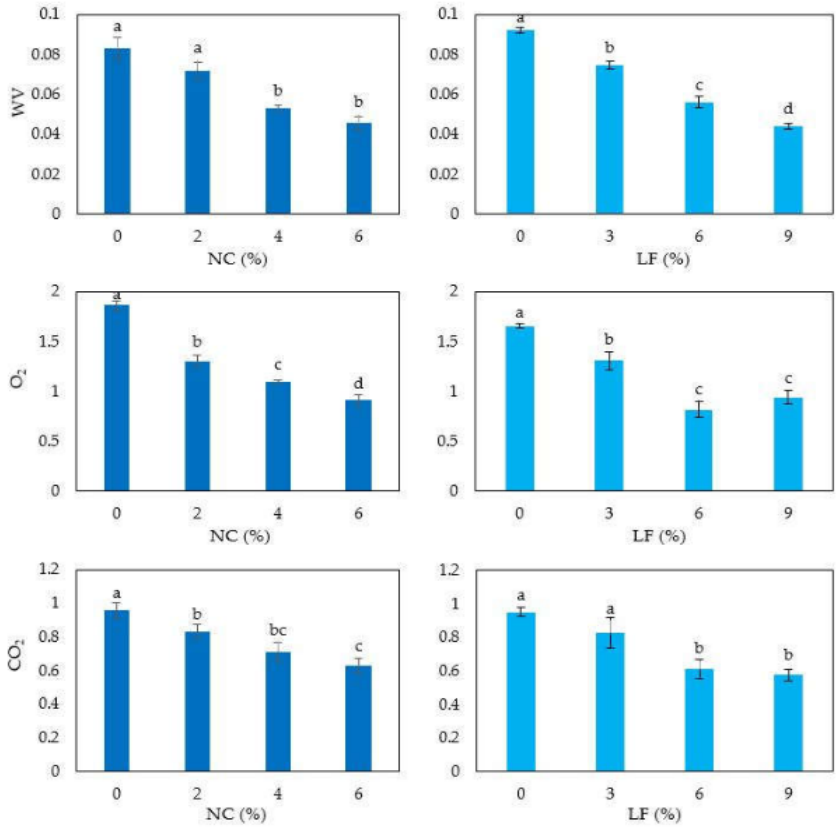

Figure 7. Gas and water vapor permeability of hemp protein-based films prepared with film forming solutions containing increasing amounts of either nanocrystalline cellulose (NC) or lignin fraction (LF) and prepared at pH 9 and 12, respectively. Different small letters a–d indicate significant differences among the values reported in each column ($p < 0.05$). Further experimental details are given in text.

3.7. Film Morphological Properties

SEM analysis was carried out to examine the surface and cross-section microstructure of hemp protein-based bioplastics prepared in the absence or presence of 6% of either NC or LF. Control film, prepared in the absence of egagropili-derived fractions, was found to contain holes that interrupted the continuity of the matrix network, as evidenced in panels 1B and 1C of Figure 8 reporting the images of its cross-section and surface, respectively. Conversely, HP films containing NC (panels 2B and 2C) or LF (panels 3B and 3C) exhibited a more homogenous and uniform aspect. Hence, these results indicate a high compatibility between the film protein matrix and the reinforcement agents isolated from egagropili, consistent with the improved performance exhibited by both grafted films. The present data are in agreement with those reported by Wang et al. [40] who manufactured biocomposites by combining proteins extracted from buckwheat distiller's dried grains with bacterial cellulose that resulted perfectly dispersed in the film matrix and endowed enhanced technological features to the obtained material.

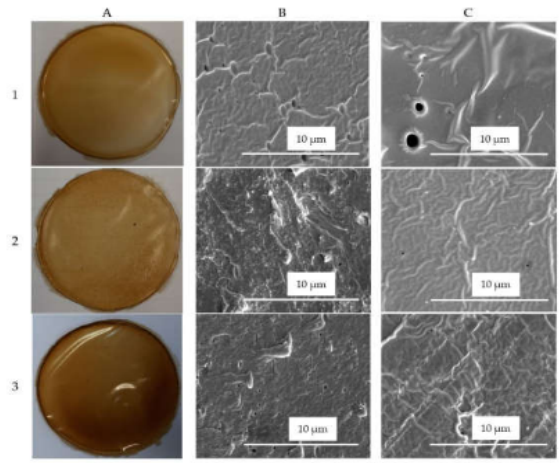

Figure 8. Images of hemp protein films (**A**), and of their SEM cross-sections (**B**, magnification 8000×) and surfaces (**C**, magnification 8000×), containing 50% glycerol and prepared in the absence (1) and presence of either 6% egagropili nanocristalline cellulose (2) or lignin fraction (3). Further experimental details are given in the text.

4. Conclusions

Nanocrystalline cellulose and a lignin enriched fraction were isolated in good yield from egagropili, better known as sea balls, and used as reinforcement additives of a protein-based films. To this aim, new bioplastics composed of proteins extracted from hemp oilseed cakes were prepared. Film microstructure analysis indicated a good interaction of the two additives tested, as both were properly dispersed in the protein film matrix. The improved mechanical and barrier properties, as well as the weakened water trapping ability, exhibited by the grafted biocomposites suggest a potential use of egagropili, presently considered only an undesirable waste to be disposed, as a valuable renewable source for obtaining novel biodegradable materials alternative to the conventional plastics. The possible synergistic effects of nanocrystalline cellulose and lignin enriched fraction, as well as an improvement of their yield in the extraction process, remain intriguing speculations which would deserve to be further investigated.

Author Contributions: Conceptualization, C.V.L.G., P.D., R.P.; Methodology, S.F.M., R.D.; Investigation, S.F.M., R.D.; Writing—original draft preparation, S.F.M., C.V.L.G.; Writing—review and editing, R.P.; Supervision, C.V.L.G., C.R., R.P. All authors have read and agreed to the published version of the manuscript.

Funding: This research was funded by the Italian Ministries of Foreign Affairs and International Cooperation (Cooperazione Italia/Messico, 2018-20 PGR-2020, CUP: E68D20000670001) and by Italian Ministries of University and Research (PRIN: Progetti di Ricerca di Interesse Nazionale –Bando 2017– "CARDoon valorisation by InteGrAted bio-refiNery, CARDIGAN, COD. 2017KBTK93).

Conflicts of Interest: The authors declare no conflict of interest.

References

1. Porta, R. The plastics sunset and the bio-plastics sunrise. *Coatings* **2019**, *9*, 526.
2. Yang, J.; Ching, Y.C.; Chuah, C.H. Applications of lignocellulosic fibers and lignin in bioplastics: A review. *Polymers* **2019**, *11*, 751.
3. Phanthong, P.; Reubroycharoen, P.; Hao, X.; Xu, G.; Abudula, A.; Guan, G. Nanocellulose: Extraction and application. *Carbon Resour. Convers.* **2018**, *1*, 32–43.
4. Keijsers, E.R.P.; Yılmaz, G.; van Dam, J.E.G. The cellulose resource matrix. *Carbohydr. Polym.* **2013**, *93*, 9–21.
5. Den Hartog, C.; Kuo, J. Taxonomy and biogeography of seagrasses. In *Seagrasses: Biology, Ecology and Conservation*; Larkum, A.W.D., Orth, R.J., Duarte, C.M., Eds.; Springer Netherlands: Dordrecht, The Netherlands, 2006; pp. 1–23.
6. Fornes, A.; Basterretxea, G.; Orfila, A.; Jordi, A.; Alvarez, A.; Tintore, J. Mapping *Posidonia oceanica* from IKONOS. *ISPRS J. Photogramm.* **2006**, *60*, 315–322.
7. Benito-Gonzalez, I.; Lopez-Rubio, A.; Martınez-Sanz, M. Potential of lignocellulosic fractions from *Posidonia oceanica* to improve barrier and mechanical properties of bio-based packaging materials. *Int. J. Biol. Macromol.* **2018**, *118*, 542–551.
8. Benito-Gonzalez, I.; Lopez-Rubio, A.; Martınez-Sanz, M. High-performance starch biocomposites with celullose from waste biomass: Film properties and retrogradation behaviour. *Carbohydr. Polym.* **2019**, *216*, 180–188.
9. Bettaieb, F.; Khiari, R.; Hassan, M.L.; Belgacem, M.N.; Bras, J.; Dufresne, A.; Mhenni, M.F. Preparation and characterization of new cellulose nanocrystals from marine bio-mass *Posidonia oceanica*. *Ind. Crops Prod.* **2015**, *72*, 175–182.
10. Fortunati, E.; Luzi, F.; Puglia, D.; Petrucci, R.; Kenny, J.; Torre, L. Processing of PLA nanocomposites with cellulose nanocrystals extracted from *Posidonia oceanica* waste: Innovative reuse of coastal plant. *Ind. Crops Prod.* **2015**, *67*, 439–447.
11. Aguir, C.; M'Henni, M.F. Experimental study on carboxymethylation of cellulose extracted from *Posidonia oceanica*. *J. Appl. Polym. Sci.* **2006**, *99*, 1808–1816.
12. Khiari, R.; Mhenni, M.F.; Belgacem, M.N.; Mauret, E. Valorisation of vegetal wastes as a source of cellulose and cellulose derivatives. *J. Polym. Environ.* **2011**, *19*, 80–89.
13. Khiari, R.; Ferchichi, I.; Mhenni, M.F. Study of liquids absorption and retention capacities of new cellulosic materials and sodium cellulose carboxylmethylate prepared from *Posidonia*. *Fibre Polym.* **2010**, *11*, 593–597.
14. Balestri, E.; Vallerini, F.; Lardicci, C. A qualitative and quantitative assessment of the reproductive litter from Posidonia oceanica accumulated on a sand beach following a storm. Estuar. Coast. Shelf Sci. **2006**, 66, 30–34.
15. Coletti, A.; Valerio, A. and Vismara, E. Posidonia oceanica as a renewable lignocellulosic biomass for the synthesis of cellulose acetate and glycidyl methacrylate grafted cellulose. Materials **2013**, 6, 2043–2058.
16. Seggiani, M.; Cinelli, P.; Mallegni, N.; Balestri, E.; Puccini, M.; Vitolo, S.; Lardicci, C.; and Lazzeri, A. New bio-composites based on polyhydroxyalkanoates and *Posidonia oceanica* fibres for applications in a marine environment. *Materials* **2017**, *10*, 326.
17. Ilyas, R.A.; Sapuan, S.M.; Ishak, M.R. Isolation and characterization of nanocrystalline cellulose from sugar palm fibres (*Arenga Pinnata*). *Carbohydr. Polym.* **2018**, *181*, 1038–1051.
18. Sanyang, M.L.; Sapuan, S.M.; Jawaid, M.; Ishak, M.R.; Sahari, J. Effect of sugar palm-derived cellulose reinforcement on the mechanical and water barrier properties of sugar palm starch biocomposite films. *Bioresources* **2016**, *1*, 4134–4145.
19. *AACC Approved Methods of Analysis, 11th Ed. Method 02-03.Nitrogen AACC Method 46-10.01 (ARCHIVED) Crude Protein-Improved Kjeldahl Method*; Cereals & Grains Association: St. Paul, MN, USA.

20. *ASTM D882-Standard Test Method for Tensile Properties of Thin Plastic Sheeting*; ASTM: Philadelphia, PA, USA, 1997.
21. Zahedi, Y.; Fathi-Achachlouei, B.; Yousefi, A.R. Physical and mechanical properties of hybrid montmorillonite/zinc oxide reinforced carboxymethyl cellulose nanocomposites. *Int. J. Biol. Macromol.* **2018**, *108*, 863–873.
22. Roy, S.; Rhim, J.W.; Jaiswal, L. Bioactive agar-based functional composite film incorporated with copper sulfide nanoparticles. *Food Hydrocolloid.* **2019**, *93*, 156–166.
23. Roy, S.; Rhim, J.W. Preparation of carbohydrate-based functional composite films incorporated with curcumin. *Food Hydrocolloid.* **2020**, *98*, 105302.
24. *ASTM D3985-Standard Test Method for Oxygen Gas Transmission Rate through Plastic Film and Sheeting Using a Coulometric Sensor*; ASTM: Philadelphia, PA, USA, 2005.
25. *ASTM F2476-13 Standard Test Method for the Determination of Carbon Dioxide Gas Transmission Rate (CO2TR) Through Barrier Materials Using an Infrared Detector*; ASTM: Philadelphia, PA, USA, 2013.
26. *ASTM F1249-Standard Test Method for Water Vapor Transmission Rate through Plastic Film and Sheeting Using a Modulated Infrared Sensor*; ASTM: Philadelphia, PA, USA, 2013.
27. Xiao, Y.; Liu, Y.; Wang, X.; Li, M.; Lei, H.; Xu, H. Cellulose nanocrystals prepared from wheat bran: Characterization and cytotoxicity assessment. *Int. J. Biol. Macromol.* **2019**, *140*, 225–233.
28. Tolbert, A.; Akinosho, H.; Khunsupat, R.; Naskar, A.K.; Ragauskas, A.J. Characterization and analysis of the molecular weight of lignin for biorefining studies. *Biofuel. Bioprod. Bior.* **2014**, *8*, 836–856.
29. Isikgor, F.H.; Becer, C.R. Lignocellulosic biomass: A sustainable platform for the production of bio-based chemicals and polymers. *Polym. Chem.* **2015**, *6*, 4497–4559.
30. Azadi, P.; Inderwildi, O.R.; Farnood, R.; King, D.A. Liquid fuels, hydrogen and chemicals from lignin: A critical review. *Renew. Sust. Energ. Rev.* **2013**, *21*, 506–523.
31. Liu, W.J.; Jiang, H.; Yu, H.Q. Thermochemical conversion of lignin to functional materials: A review and future directions. *Green Chem.* **2015**, *17*, 4888–4907.
32. Zhang, J.; Elder, T.J.; Pu, Y.; Ragauskas, A.J. Facile synthesis of spherical cellulose nanoparticles. *Carbohydr. Polym.* **2007**, *69*, 607–611.
33. Flaker, C.H.; Lourenço, R.V.; Bittante, A.M.; Sobral, P.J. Gelatin-based nanocomposite films: A study on montmorillonite dispersion methods and concentration. *J. Food Eng.* **2015**, *167*, 65–70.
34. Bhattacharjee, S. DLS and zeta potential–what they are and what they are not? *J. Control. Release* **2016**, *235*, 337–351.
35. Zadeh, E.M.; O'Keefe, S.F.; Kim, Y.-T. Utilization of Lignin in Biopolymeric Packaging Films. *ACS Omega* **2018**, *3*, 7388–7398.
36. Alashwal, B.Y.; Bala, M.S.; Arun Gupta, Sharma, S.; Mishra, P. Improved properties of keratin-based bioplastic film blended with microcrystalline cellulose: A comparative analysis. *J. King Saud Univ. Sci.* **2020**, *32*, 853–857.
37. Xiao, Y.; Liu, Y.; Kang, S.; Wang, K.; Xu, H. Development and evaluation of soy protein isolate-based antibacterial nanocomposite films containing cellulose nanocrystals and zinc oxide nanoparticles. *Food Hydrocolloid.* **2020**, *106*, 105898.
38. Salari, M.; Khiabani, M.S.; Mokarram, R.R.; Ghanbarzadeh, B.; Kafil, H.S. Development and evaluation of chitosan based active nanocomposite films containing bacterial cellulose nanocrystals and silver nanoparticles. *Food Hydrocolloid.* **2018**, *4*, 414–423.
39. Agustin, M.B.; Ahmmad, B.; Alonzo, S.M.M.; Patriana, F.M. Bioplastic based on starch and cellulose nanocrystals from rice straw. *J. Reinf. Plast. Compos.* **2014**, *33*, 2205–2213.
40. Wang, X.; Niamat, U.; Sun, X.; Guo, Y.; Chen, L.; Li, Z.; Feng, X. Development and characterization of bacterial cellulose reinforced biocomposite films based on protein from buckwheat distiller's dried grains. *Int. J. Biol. Macromol.* **2017**, *96*, 353–360.

Publisher's Note: MDPI stays neutral with regard to jurisdictional claims in published maps and institutional affiliations.

© 2020 by the authors. Submitted for possible open access publication under the terms and conditions of the Creative Commons Attribution (CC BY) license (http://creativecommons.org/licenses/by/4.0/).

4- **Mirpoor, S. F.,** Restaino, O. F., Schiraldi, C., Giosafatto, C. V. L., Ruffo, F., & Porta, R., 2021. Lignin/Carbohydrate Complex Isolated from Posidonia oceanica Sea Balls (Egagropili): Characterization and Antioxidant Reinforcement of Protein-Based Films. International Journal of Molecular Sciences, 22(17), 9147 10.3390/ijms22179147

International Journal of
Molecular Sciences

MDPI

Article

Lignin/Carbohydrate Complex Isolated from *Posidonia oceanica* Sea Balls (Egagropili): Characterization and Antioxidant Reinforcement of Protein-Based Films

Seyedeh Fatemeh Mirpoor [1,†], Odile Francesca Restaino [2,†], Chiara Schiraldi [2], Concetta Valeria L. Giosafatto [1], Francesco Ruffo [1] and Raffaele Porta [1,*]

[1] Department of Chemical Sciences, University of Naples "Federico II", Montesantangelo Campus, via Cintia 4, 80126 Naples, Italy; seyedehfatemeh.mirpoor@unina.it (S.F.M.); giosafat@unina.it (C.V.L.G.); Francesco.ruffo@unina.it (F.R.)

[2] Department of Experimental Medicine, Section of Biotechnology and Molecular Biology, University of Campania "Luigi Vanvitelli", 80138 Naples, Italy; odilefrancesca.restaino@unicampania.it (O.F.R.); chiara.schiraldi@unicampania.it (C.S.)

* Correspondence: raffaele.porta@unina.it; Tel.: +39-081-2539473

† Equally contributing authors.

Abstract: A lignin fraction (LF) was extracted from the sea balls of *Posidonia oceanica* (egagropili) and extensively dialyzed and characterized by FT-IR and NMR analyses. LF resulted water soluble and exhibited a brownish-to-black color with the highest absorbance in the range of 250–400 nm, attributed to the chromophore functional groups present in the phenylpropane-based polymer. LF high-performance size exclusion chromatography analysis showed a highly represented (98.77%) species of 34.75 kDa molecular weight with a polydispersity index of 1.10 and an intrinsic viscosity of 0.15. Quantitative analysis of carbohydrates indicated that they represented 28.3% of the dry weight of the untreated egagropili fibers and 72.5% of that of LF. In particular, eight different monosaccharides were detected (fucose, arabinose, rhamnose, galactose, glucose, xylose, glucosamine and glucuronic acid), glucuronic acid (46.6%) and rhamnose (29.6%) being the most present monosaccharides in the LF. Almost all the phenol content of LF (113.85 ± 5.87 mg gallic acid eq/g of extract) was water soluble, whereas around 22% of it consisted of flavonoids and only 10% of the flavonoids consisted of anthocyanins. Therefore, LF isolated from egagropili lignocellulosic material could be defined as a water-soluble lignin/carbohydrate complex (LCC) formed by a phenol polymeric chain covalently bound to hemicellulose fragments. LCC exhibited a remarkable antioxidant activity that remained quite stable during 6 months and could be easily incorporated into a protein-based film and released from the latter overtime. These findings suggest egagropili LCC as a suitable candidate as an antioxidant additive for the reinforcement of packaging of foods with high susceptibility to be deteriorated in aerobic conditions.

Keywords: lignin; egagropili; *Posidonia oceanica*; protein-based films; antioxidant

check for updates

Citation: Mirpoor, S.F.; Restaino, O.F.; Schiraldi, C.; Giosafatto, C.V.L.; Ruffo, F.; Porta, R. Lignin/Carbohydrate Complex Isolated from *Posidonia oceanica* Sea Balls (Egagropili): Characterization and Antioxidant Reinforcement of Protein-Based Films. *Int. J. Mol. Sci.* **2021**, *22*, 9147. https://doi.org/10.3390/ijms22179147

Academic Editor: Ana María Díez-Pascual

Received: 19 July 2021
Accepted: 20 August 2021
Published: 24 August 2021

Publisher's Note: MDPI stays neutral with regard to jurisdictional claims in published maps and institutional affiliations.

Copyright: © 2021 by the authors. Licensee MDPI, Basel, Switzerland. This article is an open access article distributed under the terms and conditions of the Creative Commons Attribution (CC BY) license (https://creativecommons.org/licenses/by/4.0/).

1. Introduction

Lignocellulosic biomass derived from woody and non-woody dry matter, such as grasses, trees, as well as harvest residues from food crops, is the largest amount of sustainable carbon-containing resources on earth that are annually produced (around 181.5 billion tons) [1–6]. Lignocellulosic material contained in plant cell walls is mainly constituted by three kinds of polymers, i.e., cellulose, hemicellulose and lignin, the content of which is affected by various factors, such as the different species, source and type (hardwood, softwood or grass) of the original biomass [7,8]. Cellulose is a homogeneous and linear polysaccharide consisting of repeating units of cellobiose monomer, β-1,4-linked anhydro-D-glucose, tightly packed in the crystalline parts of cellulose fibrils via intra- and inter-molecular hydrogen bonds [9]. Hemicellulose is an amorphous, short chain

and heterogeneously branched polymer constituted by both pentoses and hexoses, mainly xylans (arabinoxylans and 4-O-methyl-glucuronoxylans), galactomannans, glucomannans and xyloglucans (4-linked β-D-glucans with attached side chains) [10]. The dominant polymers occurring in hemicellulose extracted from hardwood are xylans, while those present in softwood are glucomannans [11,12]. Hemicellulose and cellulose polymers are linked by hydrogen bridges and Van der Waal's interactions, while hemicellulose adheres to the lignin through phenyl glycoside as well as through esters and benzyl ether covalent bonds, giving rise to lignin-carbohydrate complexes (LCCs) [13,14]. Extracted hemicellulose easily degrades to its constituent sugar units, mainly xylose (Xyl), mannose, arabinose (Arab), glucose (Glc), glucuronic acid (GlcA) under acid hydrolysis [15].

Lignin, a highly branched and amorphous biomacromolecule, is the second most abundant aromatic biopolymer in nature [16]. It consists of three different phenylpropane monomers known as p-hydroxyphenyl, coniferyl and sinapyl alcohols, containing zero, one, or two methoxyl groups, respectively [17,18]. The constituent structure and the amount of lignin occurring in plant cell wall depend on the origin, amount of different mono-lignols, chemical bonds in the polymer structure and on the source of the lignocellulosic biomass [19,20]. Coniferyl alcohol is the dominant structure occurring in the softwood lignin, while in the hardwood lignin commonly exist both coniferyl and sinapyl alcohols, the second one being dominant [21]. Lignin monomers are linked by several types of carbon–oxygen (aryl-ether) and carbon–carbon interactions, 50% of which are β-O-4′ ether linkages, whereas the others are β-5 phenylcoumaran, β-β′ resinol, α-O-4′ ether, 4-O-5′ diphenyl ether, 5-5 biphenyl and β-1′ diphenyl methane bonds [22–24]. The monomer random distribution gives rise to heterogeneous lignin structures difficult to isolate, standardize and characterize [25].

Lignin plays a key role in protecting plants against possible environmental stresses by providing a marked mechanical support to their cell walls [26]. Due to the aromatic structure and multiple functional groups, lignin possesses also several physicochemical and biological properties, such as fire resistance, wettability, biodegradability, as well as antioxidant, antifungal and antimicrobial activities [27–31]. All these features might be affected by the method of extraction of the different lignin polymers present in the different lignocellulosic sources [1,2,24,32], since, during the isolation process, lignin fragments into products with different lower molecular weight (Mw) [1,2]. Thus, temperature, pH and pressure of the system, as well as the capacity of the solvent to dissolve the extracted polymer fragments, may significantly affect their physicochemical and biological properties [24,33,34]. However, lignin extraction from lignocellulosic biomass is generally performed by gradually breaking down the polymer into lower Mw products [1,2]. Around 85% of the produced lignin is obtained through the "kraft pulping process", able to break down the majority of hemicellulose covalently bound to lignin and to give rise to LCCs that are different depending on the specific lignocellulosic biomass used [35,36] (Figure 1A).

In the present study, LCCs were extracted from egagropili (fibrous balls from *Posidonia oceanica* detritus), considered as a waste since they accumulate in huge numbers along sandy shores, by using a sodium chlorite extraction procedure at acidic pH [37]. With this procedure, as shown in Figure 1B, coniferyl aldehyde and aromatic ketones present in the lignin originally linked to hemicellulose undergo to oxidative and ring-opening reactions to form acidic groups, making lignin fragments more soluble in water [38]. The isolated LCCs were then characterized and used as reinforcement of protein-based films with the aim to replace oil-based polymers in packaging systems.

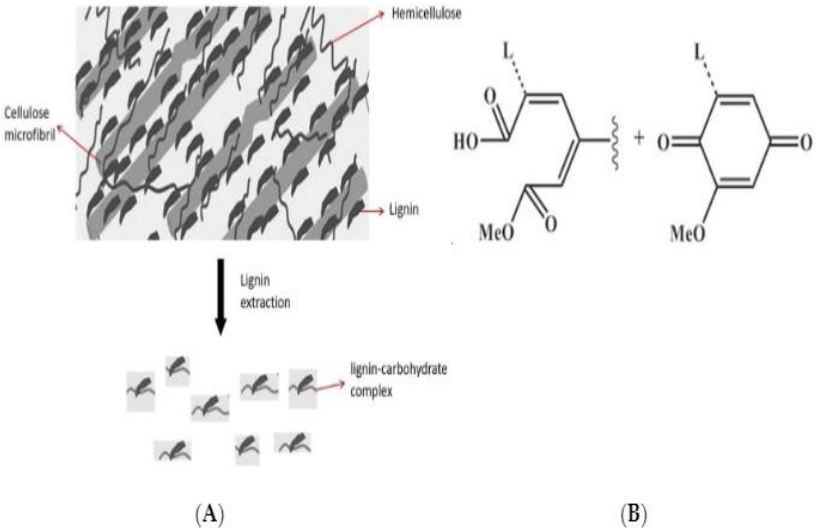

Figure 1. Lignin-carbohydrate complex formation during lignin extraction from a lignocellulosic biomass (**A**). Lignin main fragments obtained from lignocellulosic biomass following $NaClO_2$ treatment (Li et al., 2017) (**B**).

2. Results and Discussion

2.1. Egagropili Powder Fractionation and Fourier-Transform Infrared Spectroscopy Analysis

In order to separate lignin, holocellulose and cellulose fractions, egagropili powder was preliminarily washed, grinded, dewaxed and heat-dried. Fourier-transform infrared (FT-IR) spectroscopy was utilized to determine the chemical structure of egagropili fibers, as well as that of both holocellulose and cellulose fractions [39]. FT-IR spectra reported in Figure 2 show the presence of lignin signals only in the spectrum corresponding to the untreated egagropili fibers (Figure 2A: 1457 cm^{-1} attributed to the CH_2 and CH_3 of C-H bending of lignin; 1507 cm^{-1}, 1595 cm^{-1} and 1630 cm^{-1} ascribed to the in plane stretching vibration of the C=C and C=O of lignin aromatic ring) [39–41].

In addition, the C=O ester peak signaled at 1735 cm^{-1} represents the stretching vibration of the carbonyl and acetyl groups occurring in the Xyl probably present in both lignin and unconjugated hemicellulose [41–44]. It is worthy to note that none of the abovementioned peaks were present in the obtained cellulose spectrum (Figure 2C). Furthermore, the absorption band observed around 1032 cm^{-1} in the holocellulose spectrum (Figure 2B), but absent in the cellulose spectrum (Figure 2C), is probably due to the C-O stretching in pyranose ring that is an indicator of the presence of hemicellulose [43,44], whereas the peak at around 1247 cm^{-1}, present in the spectrum shown in Figure 2C, confirms the removal of hemicellulose from the cellulose fraction. Finally, the peaks at around 898 cm^{-1} and 1105 cm^{-1}, associated with the characteristics of the β-(1→4)glycosidic bond and C-O-C glycosidic ether bond, respectively, are strictly related to cellulose [44,45]. Therefore, cellulose typical peaks appeared in all three spectra, whereas their intensity increased in each step of the chemical bleaching treatment.

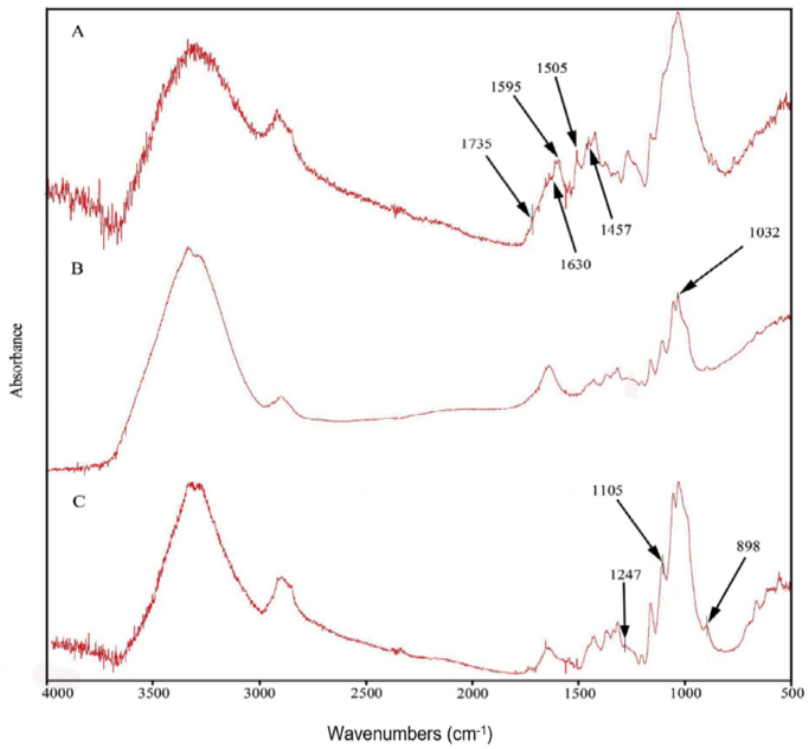

Figure 2. Fourier-transform infrared spectra of fibers (**A**), holocellulose (**B**) and cellulose (**C**) extracted from egagropili dewaxed powder. Further experimental details are given in the text.

2.2. *Egagropili Lignin Fraction Characterization*

Lignin represents a class of complex aromatic polymers built up of phenylpropane units and is one of the most abundant organic materials and renewable resources in Nature. Its composition varies among species, phylogenetic groups, cell types and developmental stages. Lignin is a by-product of several industries and bio-refinery processes and may have different structures and functional groups, as well as different physicochemical and biological properties, according to the extraction procedure that it undergoes. In fact, the native structure of lignin degrades during its extraction from the original lignocellulosic material and smaller polymer molecules endowed with new functional groups are formed. Lignin fraction (LF) obtained from egagropili by sodium chlorite oxidation technique [37] was water soluble and exhibited a brownish-to-black color, probably due to the presence of unsaturated functional groups, including conjugated carbonyl groups, aromatic rings and carbon–carbon double bonds, produced during such harsh chemical treatment [46–48]. As shown in Figure 3, the highest absorbance of the extensively dialyzed LF is in the range of 250–400 nm that could be attributed to the different chromophore functional groups present in the extracted phenylpropane-based polymer. Similar results have been reported by Rukmanikrishnan et al. [49] and Lee et al. [50], who used lignin as a UV blocker component in biopolymers, such as gellan gum or 2-hydroxyethyl cellulose, and as an active ingredient for sunscreens.

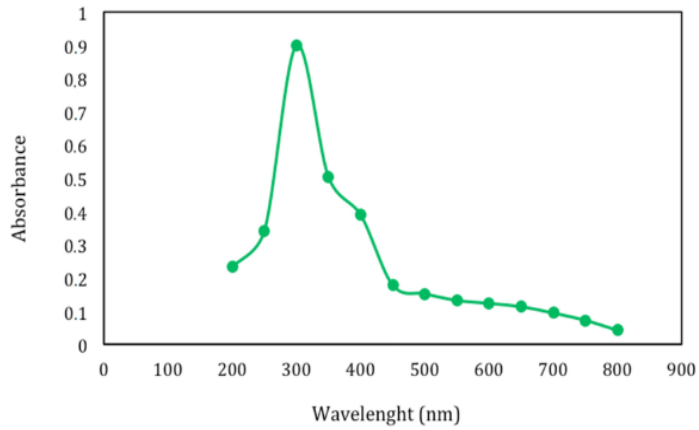

Figure 3. Absorbance at wavelengths between 200 and 800 nm of extensively dialyzed lignin fraction (0.15 mg) extracted from dewaxed egagropili powder.

A proton NMR spectrum of egagropili LF was also recorded in D_2O at pH 12, and the relative spectrum, reported in Figure 4, shows that the prevailing signals are broad peaks in the aromatic (6.5–7.5 ppm) and alkoxide (3.5–4.5 ppm) regions. The latter signal, which is due to the -OCH_3 groups on the syringyl and guaiacyl units, appeared relatively intense. This observation, indicative of the presence of additional protons of alkoxy nature, suggested checking for the possible existence of sugar residues in this fraction.

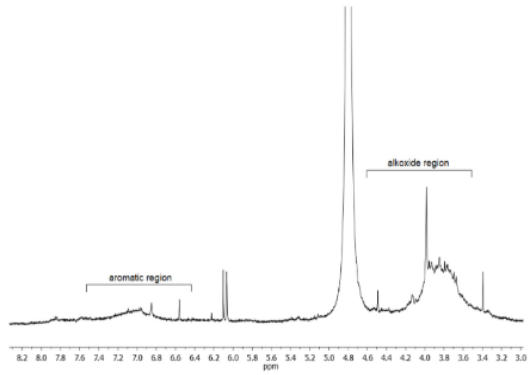

Figure 4. Portion of ^1H NMR spectrum of the egagropili lignin fraction in D_2O (pH 12) at 298 K and 500 MHz. The intense peak at δ 4.8 ppm is due to non-deuterated water taken as reference.

Therefore, to investigate whether hemicellulose-deriving carbohydrate fragments remained linked, either through phenyl glycoside, esters or benzyl ether covalent bonds, to the phenolic polymer during lignin extraction from the egagropili lignocellulosic material, monosaccharide composition analyses were carried out on the egagropili-derived fibers, LF, hollocellulose and cellulose. Figure 5 shows that eight different monosaccharides were detected in the untreated egagropili fiber sample: neutral sugars like fucose (Fuc), Arab, rhamnose (Rham), galactose (Gal), Glc and Xyl were identified, as well as an amino-sugar,

glucosamine (GlcN), and an uronic acid such as GlcA (Figure 5A–D). Their representativity ranged from 51.0% of Glc to the 0.6% of Fuc (panels A and D). The same monosaccharide composition was also found in the LF (panels B and D) but with different percentages, as Glc presence was greatly reduced. Conversely, only Glc was detected in the hollocellulose and cellulose samples (panels C and D). Quantitative analyses indicated that carbohydrates were 28.3% of the dry weight of the untreated egagropili fibers and 72.5% of the LF dry weight. Fuc, Arab, Rham, Gal, Glc, Xyl, and GlcA were previously found also in the water extracts of *Posidonia oceanica* leaves, together with other sugars like mannose and galacturonic acid, even though their relative abundance was quite different with percentages that varied up to 80% for Gal and up to 50% and 45% for Glc and Xyl, respectively [51]. Therefore, we conclude that LF obtained from egagropili contained one or more LCC(s) (27.5 lignin:72.5 carbohydrate).

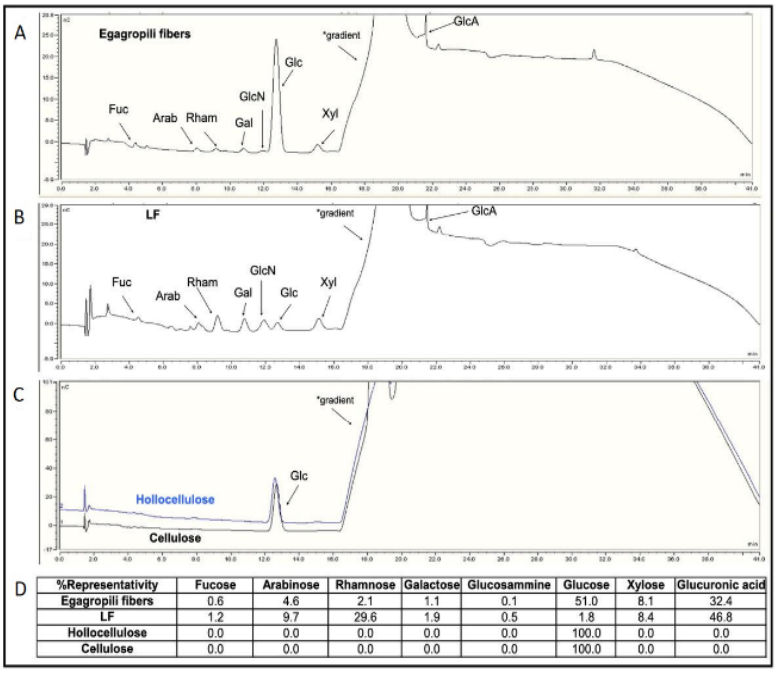

D

%Representativity	Fucose	Arabinose	Rhamnose	Galactose	Glucosammine	Glucose	Xylose	Glucuronic acid
Egagropili fibers	0.6	4.6	2.1	1.1	0.1	51.0	8.1	32.4
LF	1.2	9.7	29.6	1.9	0.5	1.8	8.4	46.8
Hollocellulose	0.0	0.0	0.0	0.0	0.0	100.0	0.0	0.0
Cellulose	0.0	0.0	0.0	0.0	0.0	100.0	0.0	0.0

Figure 5. High-performance anion-exchange chromatograms of egagropili fibers (**A**), lignin fraction (LF) (**B**), hollocellulose and cellulose samples (**C**). The different monosaccharide peaks are indicated by the arrows. The representativity percentage of each monosaccharide is reported in the panel (**D**). * Increasing concentration of NaOH used as eluent. Further experimental details are given in the text.

Furthermore, total phenol content (TPC) as well as flavonoid and anthocyanin content of egagropili LF were investigated. It is well known that phenolic compounds are the largest group of phytochemicals that are responsible for antioxidant activity in plants and in their derived products. They possess an aromatic ring with one or more hydroxyl groups with a wide range of biological properties, such as anti-mutagenic, antioxidant and anti-carcinogenic activities [52,53]. The TPC value determined for egagropili LF (113.85 $\pm$ 5.87 mg gallic acid eqs/g of extract), reported in Table 1, was meaningful, being in the same range of that (92.7 to 181.6 mg gallic acid eqs/g) measured by Faustino et al. [54]

in the industrial black liquors obtained by two cooking processes (kraft and sulphite) to produce *Eucalyptus globulus* pulp. Moreover, it is worthy to note that almost all the phenol content occurring in the LF was water soluble since only a small amount of it was extracted by hexane (Table 1). However, as it was previously reported [55], lignin TPC is affected by several factors such as the plant age and harvesting time, the specific method of lignin extraction, as well as the storage period of the extracted lignin.

Table 1. Phenol, flavonoid and anthocyanin content of lignin fraction extracted from egagropili.

Total Phenols (*mg gallic acid eqs./g extract*)	113.85 ± 5.87
Hexan-extracted Phenols (*mg gallic acid eqs./g extract*)	1.19 ± 0.63
Flavonoids (*mg quercetin eqs./g extract*)	24.5 ± 0.32
Anthocyanins (*mg cyanidin-3-glucoside/g extract*)	2.60 ± 0.51

The contribution of both flavonoids and anthocyanins in the egagropili LF TPC was also evaluated. Flavonoids represent the main group of phenolic compounds present in plants either as glycosides or in free state, being constituted by two benzene rings separated by a propane unit. They possess several biological activities, such as antiulcer, anti-arthritic, anti-angiogenic, anticancer and antimicrobial, as well as antioxidant properties due to their polyphenolic nature, which enable them to scavenge free radicals [56]. The data reported in Table 1 indicate that almost 22% of the TPC of egagropili LF is constituted by flavonoids and that, in particular, only 10% of them are anthocyanins, water-soluble but unstable pigments, because they easily decompose during the extraction, purification, and storage processes [57,58].

Finally, in order to determine the Mw of egagropili LF component(s), a size-exclusion chromatographic analysis with triple detector array system (SEC-TDA) was carried out. The SEC-TDA molecular separation showed a particularly homogeneous sample containing a highly represented (98.77%) species of 34.75 kDa with a polydispersity index of 1.10 and an intrinsic viscosity of 0.15 (Figure 6A,B). Although there are numerous studies reported in literature on the Mw of lignin originating from different biomass sources, this is the first time to our knowledge that the Mw of a LF that contains one or more LCC, from egagropili, has been determined; as well, it is also the first Mw analysis in which a SEC-TDA method has been applied to lignin polymer(s). Lignin Mw values reported so far range from 5.9 to 74.8 kDa, and it is known that they could change according to the lignin extractive methods used, such as milled wood process, enzymatic hydrolysis and/or mild acidolysis, as well as according to the origin of the biomass (e.g., from soft or hard wood) and the different instrumental techniques [59]. Gel permeation chromatography (GPC) and SEC have been frequently employed to determine the Mw values of different types of lignin polymers of different origins [59]. In particular, GPC coupled with a detector based on low-angle laser light scattering resulted more precise and accurate in determining lignin Mw than GCP-MALDI-TOFMS methods [59]. However, no data have been reported so far on the use of SEC-TDA as a tool to determine the Mw of lignin-containing fractions. In particular, with regard to the egagropili, literature data have reported so far only the analysis of the Mw of a "milled-wood" LF" extracted from *P. oceanica* sea balls by using a classic gel-permeation chromatography method. Compared to the Mw data obtained for LF described in the present study, this "milled-wood" lignin sample showed lower Mw (6.1 kDa) but higher polydispersity (Mw/Mn = 2.2) [60]. That difference is probably due to the different extractive method used leading to a LF containing only lignin and not to a water-soluble lignin/carbohydrate complex [60].

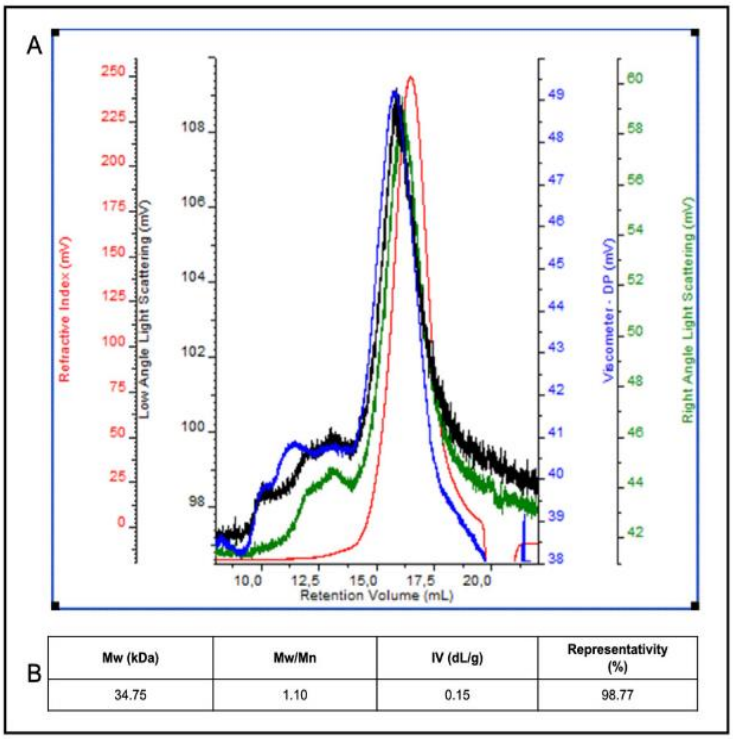

B

Mw (kDa)	Mw/Mn	IV (dL/g)	Representativity (%)
34.75	1.10	0.15	98.77

Figure 6. SEC-TDA analysis of egagropili lignin fraction (LF). Panel A shows the chromatogram of overlaid signals of the refractive index (red line), the right and low angle laser scattering (green and black line) and the viscometer (blue line) detectors (**A**). LF component averaged molecular weight (Mw), polydispersity index (Mw/Mn), intrinsic viscosity (IV) and peak representativity values are reported in the panel (**B**). Further experimental details are given in the text.

2.3. *Egagropili Lignin Fraction Antioxidant Activity*

The significant phenol content observed in the egagropili LF suggested to investigate the antioxidant activity by hydrogen donation and single-electron transfer reactions [55]. As shown in Figure 7, antioxidant activity of LF was found to linearly increase by increasing its concentration from 0.03 to 0.15 mg up to 15 min, then the curves reached the plateau indicating 45 and 75% of the 2,2-diphenyl-1-picrylhydrazyl (DPPH) scavenging activities at 90 min of sample incubation by using the lowest and the highest LF amount, respectively. It is noteworthy that even a very small amount of egagropili LF exhibited a remarkable antioxidant activity similar to that of lignin obtained from spruce and pine [61].

Furthermore, the effect of LF storage on the antioxidant activity was studied over time. Figure 8 reveals that LF antioxidant activity remained quite stable during 6 months since the DPPH scavenging activity slightly changed, under the experimental conditions selected, only from 83 to 79%. These findings strongly suggest the potential exploitation of egagropili LF as a stable and prominent antioxidant agent. Similar results were obtained by Alzagameem et al. [55] and Dizhbite et al. [61], who reported that DPPH sca-venging activity of different fractions of Kraft lignin from different sources slightly decreased after their storing for 6 months. However, the antioxidant activities exhibited by all the

previously extracted LFs resulted lower in comparison with that of LF isolated in the present study from egagropili by oxidation with sodium chlorite.

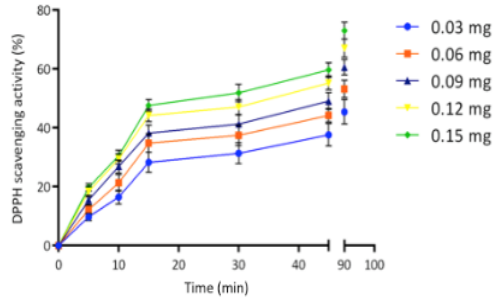

Figure 7. 2,2-diphenyl-1-picrylhydrazyl (DPPH) scavenging activity of different concentrations of egagropili lignin fraction during 90 min of incubation of samples at room temperature and dark. Further experimental details are given in the text.

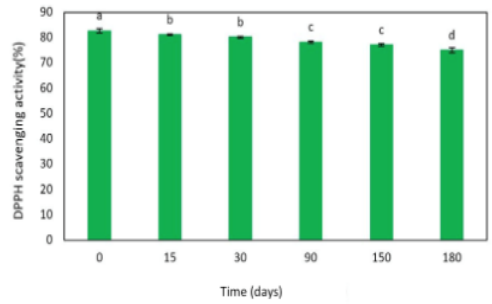

Figure 8. Effect of 6-month time storage of egagropili lignin fraction (0.15 mg) on 2,2-diphenyl-1-picrylhydrazyl (DPPH) scavenging activity during 90 min of sample incubation. Values with different small letters (a–d) were significantly different ($p < 0.05$). Further experimental details are given in the text.

2.4. *Antioxidant Activity of Hemp-Protein-Based Films Containing Egagropili Lignin Fraction*

The effect of different concentrations of egagropili LF on the mechanical and barrier properties of hemp-protein (HP)-based films has been previously investigated [37]. Since it was demonstrated that the presence of 6% LF (*w*/*w* protein) in the film-forming solution (FFS) gave rise to films with improved performances, the antioxidant activity of both FFSs and derived films was studied by measuring their DPPH radical scavenging activity in the presence of the same amount of egagropili LF (Figure 9).

The obtained results indicate that both FFSs and the derived films prepared with HPs in the absence of LF exhibited a very low antioxidant activity measured at different times of incubation with DPPH solution. Conversely, when both HP-based FFSs and films were obtained in the presence of 6% egagropili LF, their DPPH scavenging activities strongly increased (about 10 times). It is worthy to note that the antioxidant activity of the films, as well as that of their corresponding FFSs, increased as a function of the increasing incubation times of the samples. Similar results were obtained by Mohammad Zadeh et al. [62] with soy protein isolate-based films added with lignosulfonate lignin.

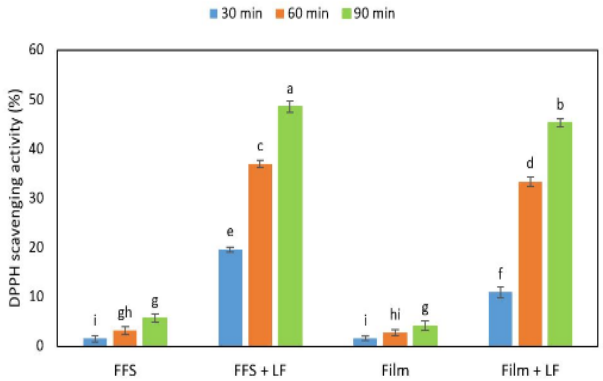

Figure 9. Antioxidant activity of hemp-protein-based film-forming solutions (FFSs) and films prepared in the absence or presence and of egagropili lignin fraction (LF) measured by 2,2-diphenyl-1-picrylhydrazyl (DPPH) assay at different times of incubation. Values with different small letters (a–i) were significantly different ($p < 0.05$). Further experimental details were given in the text.

Finally, Figure 10 shows the release of antioxidant compounds from the matrix of HP-based films containing 6% LF into the DPPH solution during 24 h incubation at both dark and room temperature. Of note, 30% of the antioxidant activity seems to have been released from the films after 2 h, whereas 50% of the DPPH scavenging activity was measured only after 22 h from the moment in which the films were immersed into the DPPH solution.

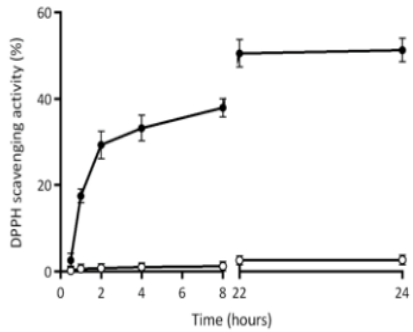

Figure 10. Profile of antioxidant agent release during 24 h in the 2,2-diphenyl-1-picrylhydrazyl (DPPH) solution from the matrix of hemp-protein-based films prepared in the absence (-○-) or presence (-●-) of egagropili lignin fraction (6% *w*/*w* protein). Further experimental details were given in the text.

As is shown in Figure 10, the control films prepared in the absence of egagropili LF were not able to release into DPPH solution any antioxidant agent, since no DPPH scavenging activity was detected at all over time. Therefore, taking also into account the increased barrier effect of LF-containing protein-based films [37], egagropili LF might be considered a suitable candidate as an antioxidant additive for reinforced packaging of food products with high susceptibility to be deteriorated in aerobic conditions.

3. Materials and Methods

3.1. Materials

Hemp oilseed cakes, a generous gift of prof. Daniele Naviglio, were purchased from Consorzio Goji Italia (Andria, Italy). Egagropili sea balls were collected in the sardinian Poetto beach (Cagliari, Italy) and stored at 4 °C until used. N-hexane (99%), sodium carbonate, potassium chloride and Folin-Ciocalteau reagent were supplied by Carlo Erba Reagents (Val de Reuil, France). Sodium hydroxide, hydrochloric acid, sodium chlorite, acetic acid glacial, potassium hydroxide, sulfuric acid that were used for extracting the lignin fraction from egagropili were purchased from Sigma Chemical (St Louis, MO, USA), as well as aluminum chloride, quercetin, glycerol and DPPH. The sodium nitrate used in high-performance size exclusion chromatography SEC-TDA analyses and the sodium acetate used in high-performance anion-exchange chromatography with pulsed amperometric detection (HPAE-PAD) analyses were from Sigma-Aldrich (St. Louis, MO, USA), as well as all the monosaccharide standards used to identify the peaks in HPAE-PAD analyses. The NaOH solution used to prepare the HPAE-PAD buffers was from J.T. Baker (Rijstenborgherweg, Netherlands), while the hydrochloric acid used for the sample hydrolysis was from Carlo Erba (Milano, Italy).

3.2. Egagropili Lignin Containing Fraction Preparation

LF was extracted from egagropili by sodium chlorite oxidation technique as previously described [37]. In particular, egagropili balls were first reshaped to rhizome fibers, washed and rinsed vigorously in distilled water and finally dried in an oven at 80 °C for 24 h. The dried egagropili fibers (10 g) were then grinded in a rotary mill (Grindomix GM200, Retsch GmbH, Haan, Germany) at a speed of 1000 rpm for 3 min to a 60-mesh sieve size, dewaxed by means of Soxhlet apparatus, with 200 mL toluene/ethanol (2:1 v/v) during 24 h and oven-dried overnight at 105 °C. The dewaxed egagropili powder was dispersed at 70 °C for 2 h in 300 mL of 1.7% sodium chlorite solution, brought at pH 3.5 by acetic acid, and the resulting bleached fibers (known as holocellulose) were separated by using filter paper. The obtained filtrate, subjected to extensive dialysis against distilled water, was referred as LF and stored at 4 °C until used. A quantitative analysis, carried out by calculating the dry weight of LF, indicated that 150 mg of LF were obtained from 1 g of grinded egagropili powder. Holocellulose and cellulose fractions were also prepared as previously described [37], and their extraction process was monitored by FT-IR analysis at room temperature by using a FTIR Nicolet 5700 spectrophotometer (Thermo Fisher Scientific, Waltham, MA, USA) equipped with attenuated total reflectance accessory. Infrared spectra analysis was performed using the Omnic software, in the range of 4000–500 cm^{-1} with a spectral resolution of 2 cm^{-1} and by 64 average scan. Light-barrier properties of LF were analyzed by measuring sample absorbance at different wavelengths ranging from 200 nm to 800 nm by using a Spectrophotometer SmartSpec 3000 Bio-Rad (Segrate, Milan, Italy). Finally, a 20 mg sample of the fraction was dissolved in 600 µL of D_2O at pH 12 and the ^1H NMR spectrum was recorded at 298 K with a Varian Inova 500 spectrometer (HDO δ 4.8 as internal reference).

3.3. Molecular Weight Analysis by Size-Exclusion Chromatography with Triple Detector Array

To analyze the average Mw, polydispersity index (Mw/Mn) and intrinsic viscosity (IV) of LF component(s), LF was concentrated five times on a 3-kDa centrifugal filter device (Centricon, Amicon, USA) at 12,000 rpm and 4 °C (Centifuge Z216MK, Hermle Labortechnik, Wehingen, Germany). Analyses were performed by using a high-performance SEC-TDA (Viscotek, Malvern, Italy), equipped with a gel permeation chromatography system (GPCmax VE 2001, Viscotek, Malvern, Italy) and with a triple detector array module that included a refractive index detector (RI), a four-bridge viscosimeter (VIS), and a laser detector (LS) made of a right-angle light scattering (RALS) and a low-angle light scattering (LALS) detector. Runs were performed by injecting, as previously described [63], 0.1 mL of the LF sample onto two gel-permeation columns (TSK-GEL GMPWXL, 7.8 × 30.0 cm, Tosoh

Bioscience, Italy), put in series and equipped with a guard column (TSK-GEL GMPWXL, 6.0 × 4.0 cm, Tosoh Bioscience, Italy) and, by eluting in isocratic conditions at a flow rate of 0.6 mL·min^{-1} with 0.1 M $NaNO_3$, pH 7.0, at 40 °C for 50 min. Data were acquired and analysed by using a OmniSEC software program (Viscotek, Malvern, Italy). The instrument was calibrated by using a polyethylene oxide (PEO) standard (22 kDa PolyCAL, Viscotek, Malvern, Italy) [60]. The values of the average Mw of the LF component(s), as well as of both LF polidispersity index (Mw/Mn) and IV, were determined on the basis of all the detector signals by applying the equations reported by the manufacturer (data from Viscotek) and on the basis of the lignin dn·dc^{-1} value (0.1875) reported in literature (data from Viscotek).

3.4. Monosaccharide Determination by High-Performance Anion-Exchange Chromatography with Pulsed Amperometric Detection

The monosaccharide composition of egagropili fibers and of LF, hollocellulose and cellulose fractions was determined by high-performance anion-exchange chromatography with HPAE-PAD by improving a previously reported method [64]. The samples were hydrolyzed by 5 M HCl treatment for 6 h at 100 °C and 600 rpm (Thermomixer comfort, Eppendorf, Germany) and then analyzed by using a high-pressure ion chromatography system (ICS3000; Thermo Fisher Scientific, Italy), equipped with an anion exchange column (Carbopac PA1; Thermo Fisher Scientific, Italy) and a pulsed amperometric detector (reference electrode Ag-AgCl; measuring electrode Au). Runs were performed by eluting in gradient conditions with 1 to 4 mM NaOH and 100 mM NaOH containing 20 mM sodium acetate (0–12 min from 1 to 4 mM NaOH, 12–14 min 4 mM NaOH, 14–16 min from 4 to 100 mM NaOH, 16–30 min 100 mM NaOH + 20 mM $NaCH_3COOH$, 30–39 min from 100 mM NaOH + 20 mM $NaCH_3COOH$ to 1 mM NaOH; 39–41 min 1 mM NaOH), at a flow rate of 1 mL/min for 41 min, by injecting 25 µL of the sample, as previously described [64]. The identity of each monosaccharide peak was determined on the basis of the elution times by comparison with standard solutions of different monosaccharides (Fuc, Arab, Rham, Gal, GlcN, Glc, Xyl, GlcA). Calibration curves of the monosaccharide standards were built in the range from 0.002 to 0.008 g/L (for Fuc, Gal, GlcN, Glc), from 0.02 to 0.08 g/L (for Arab, Rham, Xyl), and from 0.2 to 0.8 g/L (for GlcA) after their acid hydrolysis performed at 2.5 mg/mL as described above. The percentage of representativity of each monosaccharide was calculated according to the following formula:

$$\%X = \%[X\ (g/L)/(\Sigma Xn\ (g/L) \times 100] \quad (1)$$

where X is the n monosaccharide, whereas the total carbohydrate content percentage with respect to the dry weight of the samples was calculated according to the following formula:

$$\%\text{carbohydrate content} = \%[\Sigma Xn\ (g)/(\text{dry weight}\ (g) \times 100] \quad (2)$$

3.5. Phenol, Flavonoid and Anthocyanin Determination

LF TPC was determined by the Folin–Ciocalteau method as described by Velderrain-Rodríguez et al. [65], with some modifications. An aliquot (0.1 mL) of gallic acid solutions prepared at different concentrations (0.01–0.25 mg/mL) was mixed with 0.75 mL of 2 N Folin–Ciocalteau reagent and 0.65 mL of freshly prepared 7.5% (*w*/*v*) Na_2CO_3 solution to obtain a calibration curve for quantifying TPC. Absorbance of the samples was measured after 30 min at 765 nm using UV/visible Spectrophotometer (SmartSpec 3000 Bio-Rad, Segrate, Milan, Italy). Then, 100 µL of LF sample (1.5 mg/mL) were mixed with the same reagents and incubated for 30 min, as performed for the calibration curve, and the absorbance was determined at 765 nm. To measure the polarity of the phenolic content, 100 µL of LF were mixed with 200 µL of n-hexane, vortexed gently and then centrifuged. Then, 100 µL of each obtained phase were mixed with the reagent in the same conditions mentioned for LF sample and the absorbance was recorded. Results were expressed as mg of gallic acid equivalents/g of dried LF.

Flavonoid content determination was performed by the aluminum chloride colorimetric method [66]. Two solutions of 3.5 mg/mL of $NaNO_2$ (solution A) and of 18.18 mg/mL of NaOH (solution B), respectively, were preliminarily prepared and, then, 0.1 mL of either LF (1.5 mg/mL) sample or quercetin solution at different concentrations (0.01–2.5 mg/mL) were mixed with 0.43 mL of solution A. After incubation for 5 min, 30 µL of 10% anhydrous $AlCl_3$ solution were added and, at the end of a further 1 min incubation, also 0.44 mL of solution B was mixed with the samples. Finally, the absorbance was measured at 415 nm using UV/visible Spectrophotometer (SmartSpec 3000 Bio-Rad, Segrate, Milan, Italy) and the total flavonoid content, expressed as mg of quercetin/g of dried LF, was determined from the obtained quercetin calibration curve.

LF anthocyanin content was determined by the pH-differential method [67]. Then, 25 mM of potassium chloride/0.4 M sodium acetate buffer were prepared at both pH 1.0 and 4.5, respectively. LF was mixed with these two different buffers at a 3:1 buffer/LF ratio and the absorbance of the samples measured at 515 and 700 nm by using distilled water as blank. The anthocyanin content (mg cyanidin-3-gucoside/g of extract) was calculated on the basis of the following equation:

$$\text{Anthocyanin content} = [(A_{515} - A_{700})\ \text{pH 1.0} - (A_{515} - A_{700})\ \text{pH 4.5}] \times Mw \times DF \times 1000/\varepsilon \times L \quad (3)$$

where A_{515} and A_{700} are the absorbances recorded at 515 nm and 700 nm, respectively, Mw is the molecular weight of cyanidin-3-glucoside (449.2 g/mol), DF is the dilution factor, L is the cell path length (cm), and ε is the molar extinction coefficient for cyanidin-3-glucoside (26,900 L mol^{-1} cm^{-1}).

3.6. Antioxidant Activity Analysis

LF activity to scavenge DPPH was carried out according to Parveen et al. [68], with some modifications. Variously diluted solutions of LF (0.1 mL), containing different amounts of LF components (0.03–0.15 mg), were mixed with 0.9 mL of methanol DPPH solution (0.005%, *w*/*v*) and then incubated in dark at room temperature for different times (5–90 min). In addition, the antioxidant activity of LF (0.15 mg) was investigated by adding 0.1 mL of the sample to 0.9 mL of freshly prepared DPPH solution and incubating the aliquots in dark for 90 min during 6 months. Absorbance was measured at 517 nm using UV/visible Spectrophotometer (SmartSpec 3000 Bio-Rad, Segrate, Milan, Italy). Methanol was used as blank, while water (100 µL) added to DPPH solution (900 µL) was used as the control sample. DPPH radical scavenging activity was calculated by the following equation:

$$\text{DPPH scavenging activity (\%)} = (A_0 - As)/A_0 \times 100 \quad (4)$$

where A_0 is the absorbance of the control sample and As the absorbance of the sample. HP-based films, derived from FFSs containing 400 mg of HPs and 50% glycerol as a plasticizer, were prepared in the absence and presence of 6% (*w*/*w* with respect to HP) LF, as previously described [37], and the antioxidant activity of both FFSs and films was evaluated. The films (20 mg) were dissolved in 1.0 mL methanol, whereas the respective FFSs (0.01 mL) were mixed with 1 mL of methanol. Then, 0.1 mL of film and FFS samples, both containing 0.12 mg of LF, were mixed with 0.9 mL of DPPH solution (0.005%, *w*/*v*). The absorbance of each sample was measured at 517 nm after incubation in darkness for 30, 60 and 90 min at room temperature according to Equation (2).

Additional experiments were carried out by immersing pieces of each film (100 mg) in 5 mL of methanol DPPH solution (0.005%, *w*/*v*) and the samples were kept in a dark room without any shaking in order to investigate the profile of LF release in the DPPH solution. Aliquots (0.1 mL) of the solutions were taken at different times, from 0.5 to 24 h, and mixed with 0.9 mL of DPPH solution. The absorbance of the collected samples was finally measured at 517 nm. All the experiments were carried out in triplicate.

3.7. Statistical Analysis

SPSS19 (Version 19, SPSS Inc., Chicago, IL, USA) software was used for all statistical analyses. One-way analysis of variance (ANOVA) and Duncan's multiple range tests ($p < 0.05$) were used to determine the significant difference among the samples. All treatments were analyzed in triplicate and in a completely randomized design.

4. Conclusions

A water soluble lignin (27.5%)/carbohydrate (72.5%) complex (LCC) of 34.75 kDa Mw, formed by a phenol polymeric chain covalently bound to hemicellulose fragments, was extracted from *Posidonia oceanica* sea balls (egagropili) and characterized. Glucuronic acid (46.6%) and rhamnose (29.6%) were the most present monosaccharides in the isolated LCC, whereas 22% of the LCC total phenol content was constituted by flavonoids, 10% of which were anthocyanins. LCC exhibited a remarkable and stable antioxidant activity that is possible to incorporate into protein-based films from which it is easily released over time. Egagropili LCC is proposed as an effective antioxidant additive for the reinforcement and the improvement of gas barrier properties of biodegradable materials potentially useful for the packaging of perishable foods sensitive to oxidation.

Author Contributions: C.S., C.V.L.G. and R.P. planned and designed the work. O.F.R., S.F.M. and F.R. extracted lignin samples and analyzed chemical structure and antioxidant properties. C.S., C.V.L.G. and R.P. administered the project. O.F.R., S.F.M. and R.P. wrote the article. All authors have read and agreed to the published version of the manuscript.

Funding: This research was funded by the grant PRIN: Progetti di Ricerca di Interesse Nazionale—Bando 2017—"CARDoon valorisation by InteGrAted biorefiNery (CARDIGAN)" of Italian Ministero dell'Università e della Ricerca (COD. 2017KBTK93).

Institutional Review Board Statement: This study did not require ethical approval because leftover samples after routine analysis were used.

Informed Consent Statement: Informed consent was obtained from all subjects involved in the study.

Data Availability Statement: The data presented in this study are available on request from the corresponding author.

Conflicts of Interest: The authors declare no conflict of interest.

Abbreviations

Arab	arabinose
DPPH	2,2-diphenyl-1-picrylhydrazyl
FFSs	film forming solutions
FT-IR	fourier-transform infrared
Fuc	Fucose
Gal	galactose
Glc	glucose
GLcA	glucuronic acid
GlcN	glucosamine
GPC	gel permeation chromatography
HP	hemp protein
HPAE-PAD	anion-exchange chromatography with pulsed amperometric detection
LCC	lignin/carbohydrate complex
LF	lignin fraction
Mw	molecular weight
PEO	polyethylene oxide
Rham	rhamnose
SEC	size-exclusion chromatograph
SEC-TDA	size-exclusion chromatographic analysis with triple detector array system
TPC	total phenol content
Xyl	xylose

References

1. Doherty, W.O.; Mousavioun, P.; Fellows, C.M. Value-adding to cellulosic ethanol: Lignin polymers. *Ind. Crop. Prod.* **2011**, *33*, 259–276. [CrossRef]
2. Bruijnincx, P.C.; Weckhuysen, B.M. Biomass conversion: Lignin up for break-down. *Nat. Chem.* **2014**, *6*, 1035–1036. [CrossRef] [PubMed]
3. Paul, S.; Dutta, A. Challenges and opportunities of lignocellulosic biomass for anaerobic digestion. *Resour. Conserv. Recycl.* **2018**, *130*, 164–174. [CrossRef]
4. Lin, C.L.; Wang, C.C.; Chang, S.C.; Stephen Inbaraj, B.; Chen, B.H. Antioxidative activity of polysaccharide fractions isolated from Lycium barbarum Linnaeus. *Int. J. Biol. Macromol.* **2009**, *45*, 146–151. [CrossRef] [PubMed]
5. Chang, S.C.; Hsu, B.Y.; Chen, B.H. Structural characterization of polysaccharides from Zizyphus jujuba and evaluation of antioxidant activity. *Int. J. Biol. Macromol.* **2010**, *47*, 445–453. [CrossRef]
6. Inbaraj, B.S.; Chen, B.Y.; Liao, C.W.; Chen, B.H. Green synthesis, characterization and evaluation of catalytic and antibacterial activities of chitosan, glycol chitosan and poly(γ-glutamic acid) capped gold nanoparticles. *Int. J. Biol. Macromol.* **2020**, *161*, 1484–1495. [CrossRef]
7. Agbor, V.B.; Cicek, N.; Sparling, R.; Berlin, A.; Levin, D.B. Biomass pretreatment: Fundamentals toward application. *Biotechnol. Adv.* **2011**, *29*, 675–685. [CrossRef]
8. Langan, P.; Petridis, L.; O'Neill, H.M.; Pingali, S.V.; Foston, M.; Nishiyama, Y.; Schulz, R.; Lindner, B.; Leif Hanson, B.; Harton, S.; et al. Common processes drive the thermochemical pretreatment of lignocellulosic biomass. *Green Chem.* **2014**, *16*, 63–68. [CrossRef]
9. Phanthong, P.; Reubroycharoen, P.; Hao, X.; Xu, G.; Abudula, A.; Guan, G. Nanocellulose: Extraction and application. *Carbon Resour. Convers.* **2018**, *1*, 32–43. [CrossRef]
10. Yang, J.; Ching, Y.C.; Chuah, C.H. Applications of lignocellulosic fibers and lignin in bioplastics: A review. *Polymers* **2019**, *11*, 751. [CrossRef]
11. Gírio, F.M.; Fonseca, C.; Carvalheiro, F.; Duarte, L.C.; Marques, S.; Bogel-Łukasik, R. Hemicelluloses for fuel ethanol: A review. *Bioresour. Technol.* **2010**, *101*, 4775–4800. [CrossRef]
12. Sella Kapu, N.; Trajano, H.L. Review of hemicellulose hydrolysis in softwoods and bamboo. *Biofuels Bioprod. Biorefin.* **2014**, *8*, 857–870. [CrossRef]
13. Balakshin, M.; Capanema, E.; Gracz, H.; Chang, H.M.; Jameel, H. Quantification of lignin-carbohydrate linkages with high-resolution NMR spectroscopy. *Planta* **2011**, *233*, 1097–1110. [CrossRef]
14. Christopher, L.P. Adding value prior to pulping: Bioproducts from hemicellulose. *Glob. Perspect. Sustain. For. Manag.* **2012**, 225–246. [CrossRef]
15. Sjostrom, E. *Wood Chemistry: Fundamentals and Applications*; Academic Press: London, UK, 1993; pp. 1–293.
16. Zhang, Y.; Zhou, S.; Fang, X.; Zhou, X.; Wang, J.; Bai, F.; Peng, S. Renewable and flexible UV-blocking film from poly(butylene succinate) and lignin. *Eur. Polym. J.* **2019**, *116*, 265–274. [CrossRef]
17. Isikgor, F.H.; Becer, C.R. Lignocellulosic biomass: A sustainable platform for the production of bio-based chemicals and polymers. *Polym. Chem.* **2015**, *6*, 4497–4559. [CrossRef]
18. Liu, W.J.; Jiang, H.; Yu, H.Q. Thermochemical conversion of lignin to functional materials: A review and future directions. *Green Chem.* **2015**, *17*, 4888–4907. [CrossRef]
19. Lennartsson, P.R.; Niklasson, C.; Taherzadeh, M.J. A pilot study on lignocelluloses to ethanol and fish feed using NMMO pretreatment and cultivation with zygomycetes in an air-lift reactor. *Bioresour. Technol.* **2011**, *102*, 4425–4432. [CrossRef] [PubMed]
20. Thakur, V.K.; Thakur, M.K. Recent advances in green hydrogels from lignin: A review. *Int. J. Biol. Macromol.* **2015**, *72*, 834–847. [CrossRef]
21. Holmgren, A.; Brunow, G.; Henriksson, G.; Zhang, L.; Ralph, J. Non-enzymatic reduction of quinone methides during oxidative coupling of monolignols: Implications for the origin of benzyl structures in lignins. *Org. Biomol. Chem.* **2006**, *4*, 3456–3461. [CrossRef]
22. Xu, C.; Arancon, R.A.D.; Labidi, J.; Luque, R. Lignin depolymerisation strategies: Towards valuable chemicals and fuels. *Chem. Soc. Rev.* **2014**, *43*, 7485–7500. [CrossRef]
23. Li, C.; Zhao, X.; Wang, A.; Huber, G.W.; Zhang, T. Catalytic transformation of lignin for the production of chemicals and fuels. *Chem. Rev.* **2015**, *115*, 11559–11624. [CrossRef]
24. Upton, B.M.; Kasko, A.M. Strategies for the conversion of lignin to high-value polymeric materials: Review and perspective. *Chem. Rev.* **2016**, *116*, 2275–2306. [CrossRef] [PubMed]
25. Cline, S.P.; Smith, P.M. Opportunities for lignin valorization: An exploratory process. *Energy Sustain. Soc.* **2017**, *7*, 1–12. [CrossRef]
26. Liu, Q.; Luo, L.; Zheng, L. Lignins: Biosynthesis and biological functions in plants. *Int. J. Mol. Sci.* **2018**, *19*, 335. [CrossRef]
27. Ciobanu, C.; Ungureanu, M.; Ignat, L.; Ungureanu, D.; Popa, V.I. Properties of lignin-polyurethane films prepared by casting method. *Ind. Crop. Prod.* **2004**, *20*, 231–241. [CrossRef]
28. Kai, D.; Ren, W.; Tian, L.; Chee, P.L.; Liu, Y.; Ramakrishna, S.; Loh, X.J. Engineering poly(lactide)-lignin nanofibers with antioxidant activity for biomedical application. *ACS Sustain. Chem. Eng.* **2016**, *4*, 5268–5276. [CrossRef]
29. Zhang, Y.; Liao, J.; Fang, X.; Bai, F.; Qiao, K.; Wang, L. Renewable high-performance polyurethane bioplastics derived from lignin-poly(ε-caprolactone). *ACS Sustain. Chem. Eng.* **2017**, *5*, 4276–4284. [CrossRef]
30. Wang, J.; Tian, L.; Luo, B.; Ramakrishna, S.; Kai, D.; Loh, X.J.; Yang, H.I.; Deen, G.R.; Mo, X. Engineering PCL/lignin nanofibers as an antioxidant scaffold for the growth of neuron and Schwann cell. *Colloids Surf. B Biointerfaces* **2018**, *169*, 356–365. [CrossRef]

31. Figueiredo, P.; Lintinen, K.; Hirvonen, J.T.; Kostiainen, M.A.; Santos, H.A. Properties and chemical modifications of lignin: Towards lignin-based nanomaterials for biomedical applications. *Prog. Mater. Sci.* **2018**, *93*, 233–269. [CrossRef]
32. Norgren, M.; Edlund, H. Lignin: Recent advances and emerging applications. *Curr. Opin. Colloid Interface Sci.* **2014**, *19*, 409–416. [CrossRef]
33. Zakzeski, J.; Bruijnincx, P.C.; Jongerius, A.L.; Weckhuysen, B.M. The catalytic valorization of lignin for the production of renewable chemicals. *Chem. Rev.* **2010**, *110*, 3552–3599. [CrossRef]
34. Galkin, M.V.; Samec, J.S. Lignin valorization through catalytic lignocellulose fractionation: A fundamental platform for the future biorefinery. *ChemSusChem* **2016**, *9*, 1544–1558. [CrossRef]
35. Saska, M.; Ozer, E. Aqueous extraction of sugarcane bagasse hemicellulose and production of xylose syrup. *Biotechnol. Bioeng.* **1995**, *45*, 517–523. [CrossRef]
36. Al-Dajani, W.W.; Tschirner, U.W. Pre-extraction of hemicelluloses and subsequent kraft pulping, Part I: Alkaline extraction. *Tappi J.* **2008**, *7*, 3–8.
37. Mirpoor, S.F.; Giosafatto, C.V.L.; Di Pierro, P.; Di Girolamo, R.; Regalado-González, C.; Porta, R. Valorisation of *Posidonia oceanica* sea balls (egagropili) as a potential source of reinforcement agents in protein-based biocomposites. *Polymers* **2020**, *12*, 2788. [CrossRef]
38. Li, Y.; Fu, Q.; Rojas, R.; Yan, M.; Lawoko, M.; Berglund, L. Lignin-retaining transparent wood. *ChemSusChem* **2017**, *10*, 3445–3451. [CrossRef]
39. Garside, P.; Wyeth, P. Identification of cellulosic fibres by FTIR spectroscopy-thread and single fibre analysis by attenuated total reflectance. *Stud. Conserv.* **2003**, *48*, 269–275. [CrossRef]
40. Neto, W.P.F.; Silvério, H.A.; Dantas, N.O.; Pasquini, D. Extraction and characterization of cellulose nanocrystals from agro-industrial residue-soy hulls. *Ind. Crop. Prod.* **2013**, *42*, 480–488. [CrossRef]
41. Hinterstoisser, B.; Salmén, L. Two-dimensional step-scan FTIR: A tool to unravel the OH-valency-range of the spectrum of cellulose I. *Cellulose* **1999**, *6*, 251–263. [CrossRef]
42. Silvério, H.A.; Neto, W.P.F.; Dantas, N.O.; Pasquini, D. Extraction and characterization of cellulose nanocrystals from corncob for application as reinforcing agent in nanocomposites. *Ind. Crop. Prod.* **2013**, *44*, 427–436. [CrossRef]
43. Rosli, N.A.; Ahmad, I.; Abdullah, I. Isolation and characterization of cellulose nanocrystals from *Agave angustifolia* fibre. *BioResources* **2013**, *8*, 1893–1908. [CrossRef]
44. Lun, L.W.; Gunny, A.A.N.; Kasim, F.H.; Arbain, D. Fourier transform infrared spectroscopy (FTIR) analysis of paddy straw pulp treated using deep eutectic solvent. *AIP Conf. Proc.* **2017**, *1835*, 20049. [CrossRef]
45. Alemdar, A.; Sain, M. Isolation and characterization of nanofibers from agricultural residues–wheat straw and soy hulls. *Bioresour. Technol.* **2008**, *99*, 1664–1671. [CrossRef] [PubMed]
46. Fernández-Costas, C.; Gouveia, S.; Sanromán, M.A.; Moldes, D. Structural characterization of kraft lignins from different spent cooking liquors by 1D and 2D nuclear magnetic resonance spectroscopy. *Biomass Bioenergy* **2014**, *63*, 156–166. [CrossRef]
47. Polcin, J.; Rapson, W.H. Effects of bleaching agents on the absorption spectra of lignin in groundwood pulps, Part 2. Oxidative-Reductive Bleaching. *Pulp Pap. Mag. Can.* **1971**, *72*, 80–91.
48. Paulsson, M.; Parkas, J. Review: Light-induced yellowing of ligninocellulosic pulps-mechanism and preventive methods. *Bioresources* **2012**, *7*, 5995–6040. [CrossRef]
49. Rukmanikrishnan, B.; Ramalingam, S.; Rajasekharan, S.K.; Lee, J.; Lee, J. Binary and ternary sustainable composites of gellan gum, hydroxyethylcellulose and lignin for food packaging applications: Biocompatibility, antioxidant activity, UV and water barrier properties. *Int. J. Biol. Macromol.* **2020**, *153*, 55–62. [CrossRef] [PubMed]
50. Lee, S.C.; Yoo, E.; Lee, S.H.; Won, K. Preparation and application of light-colored lignin nanoparticles for broad-spectrum sunscreens. *Polymers* **2020**, *12*, 699. [CrossRef] [PubMed]
51. Benito-González, I.; López-Rubio, A.; Martínez-Abad, A.; Ballester, A.-R.; Falcó, I.; González-Candelas, L.; Sánchez, G.; Lozano-Sánchez, J.; Borrás-Linares, I.; Segura-Carretero, A.; et al. In-depth characterization of bioactive extracts from *Posidonia oceanica* waste biomass. *Mar. Drugs* **2019**, *17*, 409. [CrossRef] [PubMed]
52. Marinova, D.; Ribarova, F.; Atanassova, M. Total phenolics and total flavonoids in Bulgarian fruits and vegetables. *J. Univ. Chem. Tech. Metall.* **2005**, *40*, 255–260.
53. Okpuzor, J.; Ogbunugafor, H.; Kareem, G.K.; Igwo-Ezikpe, M.N. In vitro investigation of antioxidant phenolics compounds in extract of Senne alata. *Res. J. Phytochem.* **2009**, *3*, 68–76.
54. Faustino, H.; Gil, N.; Baptista, C.; Duarte, A.P. Antioxidant activity of lignin phenolic compounds extracted from kraft and sulphite black liquors. *Molecules* **2010**, *15*, 9308–9322. [CrossRef]
55. Alzagameem, A.; Khaldi-Hansen, B.E.; Büchner, D.; Larkins, M.; Kamm, B.; Witzleben, S.; Schulze, M. Lignocellulosic biomass as source for lignin-based environmentally benign antioxidants. *Molecules* **2018**, *23*, 2664. [CrossRef]
56. Bhat, S.V.; Bhat, S.V.; Nagasampagi, B.A.; Sivakumar, M. *Chemistry of Natural Products*; Narosa Publishing House: New Delhi, India, 2005.
57. Hubbermann, E.M.; Heins, A.; Stockmann, H.; Schwarz, K. Influence of acids, salt, sugars and hydrocolloids on the colour stability of anthocyanin rich black currant and elderberry concentrates. *Eur. Food Res. Technol.* **2006**, *223*, 83–90. [CrossRef]
58. Le, X.T.; Huynh, M.T.; Pham, T.N.; Than, V.T.; Toan, T.Q.; Bach, L.G.; Trung, N.Q. Optimization of total anthocyanin content, stability and antioxidant evaluation of the anthocyanin extract from Vietnamese *Carissa carandas* L. fruits. *Processes* **2019**, *7*, 468. [CrossRef]

59. Tolbert, A.; Akinosho, H.; Khunsupat, R.; Naskar, A.K.; Ragauskas, A.J. Characterization and analysis of the molecular weight of lignin for biorefining studies. *Biofuels Bioprod. Biorefin.* **2014**, *8*, 836–856. [CrossRef]
60. Rencoret, J.; Marques, G.; Serrano, O.; Kaal, J.; Martínez, A.T.; del Río, J.C.; Gutíerrez, A. Deciphering the unique and acylation pattern of *Posidonia oceanica* lignin. *ACS. Sustain. Chem. Eng.* **2020**, *8*, 12521–12533. [CrossRef]
61. Dizhbite, T.; Telysheva, G.; Jurkjane, V.; Viesturs, U. Characterization of the radical scavenging activity of lignins—Natural antioxidants. *Bioresour. Technol.* **2004**, *95*, 309–317. [CrossRef]
62. Mohammad Zadeh, E.; O'Keefe, S.F.; Kim, Y.T. Utilization of lignin in biopolymeric packaging films. *ACS Omega* **2018**, *3*, 7388–7398. [CrossRef] [PubMed]
63. Restaino, O.F.; D'Ambrosio, S.; Cassese, E.; Barbuto Ferraiuolo, S.; Alfano, A.; Ventriglia, R.; Marrazzo, A.; Schiraldi, C.; Cimini, D. Molecular weight determination of heparosan- and chondroitin-like capsular polysaccharides: Figuring out differences between wild-type and engineered Escherichia coli strains. *Appl. Microbiol. Biotechnol.* **2019**, *103*, 6771–6782. [CrossRef]
64. Restaino, O.F.; Finamore, R.; Stellavato, A.; Diana, P.; Bedini, E.; Trifuoggi, M.; de Rosa, M.; Schiraldi, C. European chondroitin sulfate and glucosamine food supplements: A systematic quality and quantity assessment compared to pharmaceuticals. *Carbohydr. Polym.* **2019**, *222*, 114984. [CrossRef] [PubMed]
65. Velderrain-Rodríguez, G.R.; Salvia-Trujillo, L.; González-Aguilar, G.A.; Martín-Belloso, O. Interfacial activity of phenolic-rich extracts from avocado fruit waste: Influence on the colloidal and oxidative stability of emulsions and nanoemulsions. *Innov. Food Sci. Emerg. Technol.* **2021**, *69*, 102665. [CrossRef]
66. Sagar, N.A.; Pareek, S.; Gonzalez-Aguilar, G.A. Quantification of flavonoids, total phenols and antioxidant properties of onion skin: A comparative study of fifteen Indian cultivars. *J. Food Sci. Technol.* **2020**, *57*, 2423–2432. [CrossRef] [PubMed]
67. Teixé-Roig, J.; Oms-Oliu, G.; Velderrain-Rodríguez, G.R.; Odriozola-Serrano, I.; Martín-Belloso, O. The effect of sodium carboxymethylcellulose on the stability and bioaccessibility of anthocyanin water-in-oil-in-water emulsions. *Food Bioprocess Technol.* **2018**, *11*, 2229–2241. [CrossRef]
68. Parveen, S.; Chaudhury, P.; Dasmahapatra, U.; Dasgupta, S. Biodegradable protein films from gallic acid and the cataractous eye protein isolate. *Int. J. Biol. Macromol.* **2019**, *139*, 12–20. [CrossRef]

5- **Mirpoor, S. F.,** Varriale, S., Porta, R., Naviglio, D., Spennato, M., Gardossi, L., Giosafatto, C. V. L., & Pezzella, C., 2022. A biorefinery approach for the conversion of Cynara cardunculus biomass to active films. Food Hydrocolloids, 122, 107099 https://doi.org/10.1016/j.foodhyd.2021.107099

Food Hydrocolloids 122 (2022) 107099

Contents lists available at ScienceDirect

Food Hydrocolloids

journal homepage: www.elsevier.com/locate/foodhyd

A biorefinery approach for the conversion of Cynara cardunculus biomass to active films

Seyedeh Fatemeh Mirpoor [a,1], Simona Varriale [a,1], Raffaele Porta [a,d], Daniele Naviglio [a], Mariachiara Spennato [b], Lucia Gardossi [b], C. Valeria L. Giosafatto [a,d,*], Cinzia Pezzella [c]

[a] Department of Chemical Sciences, University of Naples "Federico II", Complesso Universitario di Monte Sant'Angelo, Naples, 80126, Italy
[b] Dipartimento di Scienze Chimiche e Farmaceutiche, Università Degli Studi di Trieste, Via Licio Giorgieri 1, 34127, Trieste, Italy
[c] Department of Agricultural Sciences, University Federico II, Via Università 100, 8055, Portici, Italy
[d] Center for Studies on Bioinspired Agro-Environmental Technology (BAT), University of Naples "Federico II", Naples, Italy

ARTICLE INFO

Keywords:
Cynara cardunculus
Biorefinery
Bio-plastics
Cardoon seed proteins
Phenolic compounds

ABSTRACT

Cardoon (*Cynara cardunculus*), an herbaceous perennial plant able to grow with high productivity in dry and hot regions, as well as in unproductive soils, was used as a biomass source for the production of both bioactive compounds derived from leaves and proteins extracted from seeds. Naviglio® technology was found as an efficient method to obtain a cardoon leaf extract (CLE) characterized by high phenol content and oxygen scavenging activity. On the other hand, cardoon proteins (CPs) were demonstrated to give rise to handleable greenish films endowed with promising mechanical and barrier properties in the presence of glycerol used as plasticizer. Hence, the CLE was used to functionalize the films that were further characterized. Film microstructure observed by SEM revealed a good compatibility among CPs and CLE, showing a uniform distribution of the leaf extract components throughout the film network that reflected, in turn, an improvement in the mechanical and barrier properties of the obtained material. In addition, the CLE containing films exhibited higher hydrophobicity, as indicated by the contact angle measurement and by the evaluation of water solubility and swelling degree experiments. Finally, CLE-containing films showed a marked antioxidant activity, highlighting the potential of *Cynara cardunculus* to be exploited as a biorefinery where different low-value renewable biomass materials are turned in several higher value bio-based products.

1. Introduction

Cynara cardunculus L., commonly named cardoon, is a perennial dicotyledonous plant widely distributed in the Mediterranean area that grows naturally in harsh habitat conditions with high temperature, elevated salinity and arid summer (Benlloch-González, Fournier, Ramos, & Benlloch, 2005). This plant is part of the Asteraceae (or Compositae) family, including the globe artichoke [var. *scolymus* (L.) Fiori], the cultivated cardoon (var. *altilis*), and the wild cardoon [var. *sylvestris* (Lamk) Fiori], considered to be their common ancestor (Pesce, Negri, Bacenetti, & Mauromicale, 2017). Although native from the Mediterranean area, cardoon has been spread to several other countries like the United States of America, Mexico, Australia, and New Zealand (https://www.cabi.org/isc/datasheet/17584). Due to its natural habitat, cardoon can grow in ash and poor conditions, with high temperatures, severe drought, and in infertile stony soils (Fernández, Curt, & Aguado, 2006), and, therefore, it is a very cheap and accessible crop. Besides, cardoon is a pollinator-supporting industrial crop, so that it is beneficial for the biodiversity. The high biomass productivity of cardoon has been exploited for multiple purposes, ranging from traditional uses to industrial applications. Mauromicale, Sortino, Pesce, Agnello, and Mauro (2014) studied the potential ability of cultivated and wild cardoons to produce energy in terms of biomass, achenes, and energy yield. The authors concluded that both cultivated and wild cardoon are potential energy crops and improved the soil fertility characteristics by increasing organic matter, total nitrogen, available phosphorus, and exchangeable potassium content. The annual average outcome of cultivated cardoon is 14.6 t/ha of dry biomass, 550 kg/ha of achenes, and 275 Gj/ha yields, while for wild cardoon, the outcome is 7.4 t/ha of dry biomass, 240 kg/ha of achenes, and 138 Gj/ha of energy yield. Cardoon has been popularly used by Greeks and Romans as food

* Corresponding author. Department of Chemical Sciences, University of Naples "Federico II", Complesso Universitario di Monte Sant'Angelo, Naples, 80126, Italy.
E-mail address: giosafat@unina.it (C.V.L. Giosafatto).
[1] Equally contributing authors.

https://doi.org/10.1016/j.foodhyd.2021.107099
Received 10 May 2021; Received in revised form 14 July 2021; Accepted 8 August 2021
Available online 9 August 2021
0268-005X/© 2021 Elsevier Ltd. All rights reserved.

Abbreviations

DPPH	2,2-diphenyl-1-picrylhydrazyl
ABTS	2,2′-azino-bis(3-ethylbenzothiazoline-6-sulfonic acid)
TPC	total phenolic content
GAE	gallic acid equivalent
CLE	cardoon leaf extract
FFS	film forming solution
CP	cardoon protein
COC	cardoon oilseed cake
DW	dry weight
FW	fresh weight
TE	Trolox equivalent
TS	tensile strength
YM	Young's modulus
EB	elongation at break
WV	water vapor

and medicine and is part of the Mediterranean diet for the preparation of several dishes. In fact, cardoon flowers are used in soups, stews and salads (Fratianni, Tucci, Palma, Pepe, & Nazzaro, 2007), while the leaves are known for their therapeutic potential as a diuretic, choleretic, cardiotonic, antidiabetic and anti-hemorrhoidal agent (Ramos et al., 2017; Velez et al., 2012). Beside its application as functional food, cardoon biomass has been used as lignocellulosic feedstock for biodiesel and biomethane production (Pesce et al., 2017; Toscano, Sollima, Genovese, Melilli, & Raccuia, 2016, pp. 429–442). Nevertheless, cardoon has been reported as a source of bioactive compounds such as flavonoids, chlorogenic acids and anthocyanins, which have been used for medicinal and cosmetic purposes (Ierna, Sortino, & Mauromicale, 2020; Lattanzio et al., 2009; Mandim et al., 2020; Petropoulos et al., 2019). The environmental sustainability of this plant, together with its bioactive components have made cardoon a recognised key multipurpose crop in biorefinery by processing all the non-edible parts to produce a variety of interesting compounds for potential application in green chemistry (Gominho, Dolores, Lourenço, Fernández, & Pereira, 2018; Pappalardo, Toscano, Puglia, Genovese, & Raccuia, 2020; Turco et al., 2019). Thanks to its adaptability to dry regions, cardoon can be considered a good candidate as a perennial field crop able to grow on marginal lands, thus, it does not compete with food crops (Fagnano, Impagliazzo, Mori, & Fiorentino, 2015). From cardoon seeds it is possible to extract an oil characterized by a very nutritious profile, rich in unsaturated fatty acids, adapted for the production of alternative vegetable oils and herbal formulations for human consumption (Mirpoor, Giosafatto, & Porta, 2021). The remaining by-product after oil extraction is a valuable source of fibers, proteins as well as of bioactive compounds (Genovese et al., 2016). As far as the leaves, many studies have focused on the antioxidant potential of their extracts, strictly related to the polyphenol fraction, mainly composed of hydroxycinnamic derivatives, such as mono- and dicaffeoylquinic acids, and flavonoids, such as apigenin and luteolin (Dias et al., 2018; Falleh et al., 2008; Pandino, Lombardo, Mauromicale, & Williamson, 2011; Scavo, Pandino, et al., 2019). Recent studies (Barbosa et al., 2020) have indicated that cardoon leaves are rich in several polyphenol compounds, with several health benefits. As matter of fact, cardoon leaves contain antimicrobial and antioxidant compounds that have been suggested for use as natural additives for extending the shelf life of food products. Moreover, as leaves are considered cardoon by-products, they can have economic benefits if their natural antioxidants, with benefits to human health, are extracted and applied in food packaging to increase shelf life. Nevertheless, cardoon by-products and their potential for application in food packaging is still not entirely known and it would be worthy to investigate.

Several protocols for the extraction of bioactive molecules from cardoon leaves have been previously described; dried or fresh leaves are mixed with a solvent (ethanol, methanol, acetone or alcoholic solutions) and incubated with shaking (Falleh et al., 2008; Fratianni et al., 2007; Kukić et al., 2008; Pandino et al., 2011). An alternative to these traditional extraction methods could be the use of the Naviglio® extractor, based on a solid-liquid dynamic extraction. By using a suitable solvent, the generation of a negative gradient pressure between the outlet and the inlet of a solid matrix containing some extractable material, followed by a sudden restoration of the initial equilibrium conditions, induces the forced extraction of substances not chemically bonded to the principal structure of which the solid is formed (Naviglio, 2003). This would result in a shorter extraction time, higher extraction yields and preservation of integrity of the components. Naviglio® extraction has already been reported as an innovative technology for the recovery of phenolic compounds from different types of solid matrixes, emerging as a greener alternative to the latest solid-liquid extraction techniques (Naviglio, Scarano, Ciaravolo, & Gallo, 2019; Panzella et al., 2020; Scarano et al., 2020). The Naviglio® extractor is scalable up to 400 L capacity, and is economically feasible due to the following reasons: *i)* the total consumption of this equipment, mainly related to the compressed air, is very negligible, being about 50 W/h; *ii)* it does not require any increase in temperature; *iii)* the extraction method alternates static phase, where the consumption of energy is quite zero, to dynamic one in which consumption reaches the maximum (about 100 W/h). Furthermore, many studies have been done in recent years on binding and conjugating flavonoids and polyphenols with proteins in order to improve the functionality of proteins as well as for developing active protein-based films (Mirpoor, Hosseini, & Nekoei, 2017; Mirpoor, Hosseini, & Yousefi, 2017; Quan, Benjakul, Sae-leaw, Balange, & Maqsood, 2019; Taghavi Kevij, Salami, Mohammadian, & Khodadadi, 2020). Generally, biopolymers from agricultural sources are an interesting option for biodegradable/edible plastics production since agricultural industry generates a high quantity of different by-products containing biomacromolecules, such as proteins and polysaccharides, considered good candidates for the production of hydrocolloid bio-plastics. In fact, proteins from soy and different legumes as well as several carbohydrates, such as pectins, chitosan and starch are extensively used in this sector (Giosafatto, Fusco, Al-Asmar, & Mariniello, 2020). However, despite the huge worldwide production of these agricultural biomasses, they are basically used for animal feeding and on a small amount for bio-plastic production. In this respect, seed oilcakes might be considered valuable by-products for biobased materials development as they are endowed with high amount of fiber, polysaccharides and proteins that can be further utilized. In this paper the phenols were extracted from *Cynara cardunculus* leaves, comparing Naviglio® extractor and maceration methods, using ethanol as solvent. The leaf extracts from both methods were analysed in terms of phenolic content and antioxidant activity. Further towards a development of a cardoon-based biorefinery, in the present work for the first time the seed proteins obtained following the oil removal were exploited for the production of novel bio-plastics potentially able to become candidates for replacing a portion of the petroleum-derived plastics highly pollutant for the environment. In this scenario, it is worth to say that actually Novamont company (https://agro.novamont.com/en/the-innovative-agricultural-system) is trying to exploit cardoon biomass for the development of a biorefinery for the production of low environmental impact bioproducts, even though the company is not exploiting the proteins from cardoon seeds for the manufacturing of bio-plastics. The bio-plastics obtained in this study were then functionalized with cardoon leaf-derived extracts and the obtained materials were finally characterized according to their physico-chemical characteristics, such as mechanical, barrier, morphological and hydrophobicity features, as well as antioxidant properties by evaluating film radical scavenging activity.

2. Materials and methods

2.1. Materials

Ethanol (100%) was supplied by VWR International (Fontenay-sous-Bois, France), 2,2′-azino-bis(3-ethylbenzothiazoline-6-sulfonic acid) (ABTS) was purchased from AppliChem GmbH (Darmstadt, Germany). Trolox was purchased from Sigma-Aldrich, Inc. (St. Louis, MO). *N*-Hexane (99%) and Folin-Ciocalteau reagent were supplied by Carlo Erba Reagents (Val de Reuil, France). Glycerol (GLY) (−99%) and 2,2-diphenyl-1-picrylhydrazyl (DPPH) were purchased from Sigma Chemical Co. (USA). All other chemicals and reagents used were of analytical grade.

Cardoon was recovered in April from a field experiment made in Sant'Angelo dei Lombardi (Avellino, Italy), a hilly area about 700 m above sea level, characterized by cold and rainy winters and low-fertility soil. The soil was composed by 38.5% clay, 25% silt and 36.5% sand, with a pH 8.1 and a content of 0.1% N and 1.3% organic matter (Ottaiano et al., 2017). The leaves were separated from the fresh plants and stored in vacuum sealed plastic bags at −20 °C. For extract preparation, cardoon leaves were thawed at room temperature and cut into 1 cm^2 pieces. Cardoon seeds were obtained from the same field.

2.2. Cardoon leaf extract preparation

A cardoon leaf extract (CLE) was obtained by filling a filter bag (porosity 100 μm) with 40 g of cut cardoon leaves and then, by inserting it into the Naviglio® extractor chamber (Lab. model 500 cm3 capacity). Extraction was performed using 625 mL of 100% ethanol (96% v/v) at room temperature and at pressure value of 9 bar (static phase 2 min; dynamic phase 2 min, with 12 s stop piston). Liquid samples (10 mL) were collected at 2, 4, 8 and 24 h. The CLE was kept at 4 °C until it was analysed. Moreover, further 40 g of cut cardoon leaves were placed in a bottle kept under dark conditions and subjected to maceration at room temperature with constant shaking for the same times of extraction carried out with Naviglio® extractor. The CLEs were filtered through a Whatman filter paper and supernatants were kept at 4 °C until they were analysed.

2.2.1. Naviglio® method

Filter bag (porosity of 100 μm) was filled with 40 g of cut cardoon leaves and then it was inserted into extraction chamber of Naviglio® extractor Lab. model 500 cm^3 capacity. Extractions were conducted using 625 mL of anhydrous ethanol at room temperature at pressure value of 9 bar, static phase 2 min; dynamic phase 2 min, with 12 s stop piston. Liquid samples (10 mL) were collected at 2, 4, 8 and 24 h (Naviglio, 2003). The leaf extracts (CLE) were kept at 4 °C until analysis. Ethanol was chosen as solvent for phenols extraction as described in literature (Kukić et al., 2008; Pinelli et al., 2007; Scavo, Pandino, et al., 2019).

2.2.2. Maceration method

40 g of cut cardoon leaves were used for the comparative analysis with maceration, which was placed in a bottle kept under dark conditions at room temperature with constant shaking. Samples were taken at the same times as extraction using Naviglio® extractor. The CLE were filtered through a Whatman filter paper and supernatants were kept at 4 °C until analysis.

2.3. Total phenolic content analysis

The total phenolic content (TPC) was determined using the Folin-Ciocalteau reagent as previously described (Siddiqui, Rauf, Latif, & Mahmood, 2017) with small changes. The calibration curve was plotted by mixing 100 μL of 10–250 μg/mL gallic acid solutions in ethanol with 500 μL of Folin-Ciocalteu reagent (diluted 10-fold with water) and allowed to stand at room temperature for 5 min. Then, 400 μL of 7.5% w/v Na_2CO_3 solution were added to the mixture and the absorbance was measured after 30 min at 765 nm using UV-1600PC Spectrophotometer (VWR, Leuven, Belgium). For CLEs, 100 μL of each sample were mixed with the same reagent, as performed for constructing the calibration curve and, after 3 h, the absorbance was measured to determine the total CLE phenolic contents. The results were expressed as gallic acid equivalents (GAE). All determinations were carried out in triplicate.

2.4. Antioxidant activity determination

2.4.1. ABTS radical cation decolourisation assay

ABTS activity was quantified in terms of percentage inhibition of the $ABTS^{\bullet+}$ radical cation by antioxidants in each sample. ABTS radical cation ($ABTS^{\bullet1}$) was produced by reacting 7 mM ABTS stock solution (dissolved in water) with 2.45 mM potassium persulfate and allowing the mixture to stand in the dark at room temperature for 12–16 h before use (Re et al., 1999). For the study of CLE phenolic compounds, the $ABTS^{\bullet1}$ solution was diluted with water to an absorbance of 0.70 at 734 nm. After addition of 1 mL of diluted $ABTS^{\bullet1}$ solution to 10 μL of CLE, the absorbance reading was taken exactly 1 min after the initial mixing and up to 10 min using a UV-1600PC Spectrophotometer (VWR, Leuven, Belgium). CLEs were diluted two-times prior the analysis and 10 μL of ethanol in 1 mL of diluted $ABTS^{\bullet1}$ solution was used as control. Inhibition of the $ABTS^{\bullet+}$ radical cation was expressed as Scavenging effect (S) and calculated using the equation:

$$S\ (\%) = 100 \times (A_0 - A_s)/A_0 \quad (1)$$

where A_0 is the absorbance of the control (containing all reagents except the sample to be tested), and A_s is the absorbance of the tested sample. All determinations were carried out in triplicate.

2.4.2. In vitro antioxidant and free radical scavenging activity

$DPPH^{\bullet}$ radical scavenging activity was quantified in terms of percentage inhibition of a pre-formed free radical by antioxidants in each sample. 0.005% (w/v) DPPH radical was prepared in methanol as previously described (Kukić et al., 2008) with some modifications. For the study of phenolic compounds, DPPH solution was diluted with methanol to an absorbance of 0.70 at 517 nm 100 μL of CLE were mixed with 900 μL of diluted DPPH solution, shaken and left for 30 min in the dark. CLEs and film forming solutions (FFSs) were diluted two-times and 20-times, respectively, prior the analysis. Absorbance was measured at 517 nm using UV-1600PC Spectrophotometer (VWR, Leuven, Belgium); 1 mL methanol was used as blank, while 100 μL of ethanol in 900 μL of DPPH solution were used as control. Neutralisation of DPPH radical was calculated using the equation:

$$S\ (\%) = 100 \times (A_0 - A_s)/A_0 \quad (2)$$

where S is the Scavenging effect, A_0 is the absorbance of the control (containing all reagents except the sample to be tested), and A_s is the absorbance of the tested sample. Results were compared with the activity of 6-hydroxy-2,5,7,8-tetramethylchroman-2-carboxylic acid (Trolox). All determinations were carried out in triplicate.

For the evaluation of scavenging activity of film containing CLE, 0.005% (w/v) DPPH radical was prepared in methanol. 10 mg of film were incubated in 5 mL of DPPH solution, shaken and left for 30 min in the dark. 5 mL of DPPH solution were used as control. Absorbance was measured in a 6-wells plate at 517 nm using Benchmark Plus Microplate Spectrophotometer (Bio-Rad Laboratories, Hercules, CA).

2.5. Characterisation of cardoon leaf extract

The volatile triterpenes and sesquiterpenes, known for their antioxidant activity, were identified by GC-MS. The sample was prepared by dissolving 1 mg of CLE obtained by Naviglio® method in 1 mL of diethyl

ether and GC-MS analysis was carried out by a Shimazu gas chromatograph. The gas chromatograph was equipped with a 30 m × 0.25 mm fused-silica capillary column (SLB5ms) coated with 0.25 μm film of poly (5% phenyl, 95% dimethyl siloxane). The temperature was monitored from 50 °C to 280 °C. The mass spectrometer was set to scan 33–700 m/z. Samples were injected (1 μL) with a splitting ratio 1:20 and the injector temperature was set to 280 °C. The column oven was initially at 50 °C and was held for 2 min after the injection, followed by temperature ramping at 8 °C/min up to 250 °C, and 250–280 °C at 3 °C/min. The total run time was 63.33 min (Mathe, Culioli, Archier, & Vieillescazes, 2004).

The NMR analysis was performed in order to confirm the presence of the bioactive molecules observed by GC-MS analysis (see section 3.2) and for carrying out a semi-quantitative evaluation of the content of cynaropicrin respect to the other components of the CLE (see section 3.2). The NMR analysis was performed by dissolving 10 mg of CLE in 0.7 mL of deuterated chloroform. Samples were analysed on a Varian VNMRS 500 MHz NMR spectrometer at 500 MHz.

Finally, an aliquot of CLE was diluted in 70% ethanol and loaded on Vivaspin® (3 kDa and 10 kDa cut-off) ultrafiltration devices in order to determine the presence of high molecular weight molecules. The eluate fraction was recovered and dried at 60 °C overnight and the dry weight (DW) determined.

2.6. Extraction of cardoon seed proteins

Cardoon seeds were grinded at a speed of 1000 rpm for 3 min in a Knife Mill Grindomix GM 200 (Grindomix GM200, Retsch GmbH, Haan, Germany) and then defatted for 6 h by using a soxhlet apparatus (3:1, v/w hexane:grinded seeds) and, finally, the obtained cardoon oilseed cake (COC) was dried at 50 °C in an oven for 2 h. Isoelectric-precipitation technique was used for extracting cardoon proteins (CPs) from COC, according to Dapčević-Hadnađev, Hadnađev, Lazaridou, Moschakis, and Biliaderis (2018) with minor modifications. COC was suspended in water at 1:10 ratio (w/v) and 1.0 N NaOH was added under constant stirring to adjust the pH to 11. After 1 h of stirring, the suspension was centrifuged for 15 min at 5000 rpm and the pH of the collected supernatant was adjusted to 5.4 using 1.0 N HCl. Then, the precipitate was separated by another centrifugation at 5000*g* for 15 min and the obtained pellet collected and dried in an environmental chamber at 25 °C and 45% relative humidity. The protein content of the obtained CP powder was determined by the Kjeldahl's method (AACC, 2003) using a nitrogen conversion factor of 6.25.

2.7. Preparation of cardoon protein-based films

CP was dispersed in distilled water (2% w/v), the pH was adjusted to 12.0 by 1 N NaOH and the dispersion was stirred for 2 h at room temperature for complete CP dissolution. The preliminary attempts to produce CP-based films have been carried out by using 200, 300 and 400 mg of CPs added with different concentrations of GLY (10–50%, w/w protein) as plasticizer, in order to find the optimum conditions for developing handleable films.

CLE obtained as described above by Naviglio® method was dried and resuspended in ethanol up to get a final concentration of 16 mg/mL. This extract was added to the CP solution at different concentrations and the mixture was stirred for 1 h. GLY was then added to obtain a final concentration of 50% (w/w protein) and the solution was stirred for further 30 min. The prepared FFSs were cast on plastic petri dishes (8 cm diameter) and finally dried in an environmental chamber at 25 °C and 45% relative humidity (RH) for 24 h. The dried films were peeled off and conditioned at 25 °C and 50% RH, by saturated magnesium nitrate solution, for 24 h before the analyses.

2.8. Zeta potential, particle size and contact angle measurements

The effect of different concentrations of CPs, GLY and CLE on the mean hydrodynamic diameter (particle size) and the electric charge (zeta potential) values of the FFSs, as well as of CPs diluted in alkaline water (0.1 mg/mL, pH 12) by using 0.1 N NaOH, was measured by a zetasizer (Nano-ZSP, Malvern, Worcestershire, UK) at 25 °C. The effect of pH on both zeta potential and particle size of CP dissolved in water at pH 12.0 was studied by transferring 1 mL solution into the autotitrator and adjusting the pH to different values starting from pH 12.0 to pH 2.0 by adding 1.0, 0.1, and 0.01 N HCL. All measurements were performed in triplicate.

Contact angle values of the FFSs prepared in the presence or absence of CLE were determined using a homemade goniometer and parafilm (Bemis Co., Inc., Neenah, WI, USA) stripes as hydrophobic surfaces. 10 μL of each FFS were deposited on the surface of parafilm strip fixed on the horizontal stage, and the images of each FFS drop were captured using a fixed digital microscopic camera (PS Pro, China) at the moment of contact of the drop with the surface (0 time) and after 30 s. Contact angles between baseline of the FFS drops and the surfaces were then measured using Image J software. Five measurements for each FFS was reported as the average of its contact angle value.

2.9. Cardoon seed protein-based film characterization

2.9.1. Colour, opacity and density measurements

The colour parameters of CP-based films prepared in the absence or presence of different concentrations of CLEs were measured using a Mightex® HRS series compact CCD spectrometer HRS-VIS-025 (Mightex, Toronto, ON). All measurements were made at 5 random positions of each film. The colour parameters, including L as well as "a" and "b" values, indicate lightness/darkness (0–100), greenness/redness (−60 to +60) and blueness/yellowness (−60 to +60), respectively, of the materials tested. Total colour difference (ΔE) was determined by the following equation:

$$\Delta E = \sqrt{(L^* - L)^2 + (a^* - a)^2 + (b^* - b)^2} \quad (3)$$

where L* (99.94), a* (−1.07) and b* (3.74) were the colour parameter values of the standard white tile (Bai et al., 2019).

Film opacity was evaluated by a spectrophotometer according to the method described by Taghavi Kevij et al. (2020). The film specimens (4 cm × 1 cm) were attached to the cell and inserted into a spectrophotometer. The empty cell was used as a blank and the absorbance of each film specimen was read at 600 nm. The opacity of the films was calculated as a ratio between the obtained absorbance value and the film thickness (mm).

Density was determined according to the procedure described by Cruz-Diaz, Cobos, Fernández-Valle, Díaz, and Cambero (2019) with some modifications. The film samples (2 cm × 2 cm) were weighed, their thickness measured at three random places and, finally, the dry matter density was calculated as the ratio between the weight and volume of each film (thickness × film surface area). All the analyses were carried out in triplicate.

2.9.2. Fourier transform infrared (FTIR) spectroscopy

The interactions between CLE and CP in the film matrix were investigated by recording the FT-IR spectra using FTIR Nicolet 5700 spectrophotometer (Thermo Fisher Scientific, Waltham, MA, USA). Infrared spectra analysis was performed using the Omnic software in the range of 4000–500 cm^{-1} with a spectral resolution of 2 cm^{-1}.

2.9.3. Scanning electron microscopy analyses

Film microstructure was examined by both surface and cross section analysis using a field emission scanning electron microscope (FE-SEM, FEI Nova NanoSEM450, Thermo Fisher, Scientific, MA, USA). In order to

prepare the films for cross-sectional analysis, each sample was cryo-fractured in liquid nitrogen, then coated with a thin layer of gold and platinum using a vacuum sputter coater and, finally, observed at an accelerating voltage of 5 kV.

2.9.4. Mechanical properties and thickness

Film thickness was measured from the average of the thickness determined at five different locations of each film using an electronic digital micrometer (IP65 Alpa Metrology Co., Pontoglio, Italy, sensitivity 0.001 mm). Film tensile strength (TS), Young's modulus (YM) and elongation at break (EB) were determined according to ASTM D882 - 18 (1997) method using an Instron universal testing instrument (Model 5543 A, Instron Engineering Corp., Norwood, MA, USA), with a 1000 N load cell. The film strips (8 cm × 1 cm) were fixed between two grips of the instrument with an initial grip distance and crosshead speed of 40 mm and 5 mm/min, respectively.

2.9.5. Hydrophilicity properties

Film moisture content was evaluated by the method of Roy and Rhim (2020) by weighing each film sample (2 cm × 2 cm) before and after drying in an oven at 105 °C for 24 h. Moisture content was calculated as the percentage of the film weight loss with respect to the initial weight of the film.

Water solubility of the films was measured according to the procedure of Adilah, Jamilah, Noranizan, and Hanani (2018) with some slight modifications. The initial weight (W_i) of each film sample (2 cm × 2 cm) was obtained by oven drying at 105 °C for 24 h. The dried films were then immersed in 30 mL of distilled water and stirred in a shaker incubator at 25 °C for 24 h. After that, the final weight (W_f) of the samples were obtained by separating the non-soluble parts of the films and drying in oven at 105 °C for another 24 h. Finally, water solubility was calculated using the following equation:

$$\text{Water solubility (\%)} = [(W_i - W_f)/W_i] \times 100 \quad (4)$$

Film swelling ratio was measured according to the method of Roy, Rhim, and Jaiswal (2019). The initial weight (Wi) of each film sample (2 cm × 2 cm) was measured and, then, the films were immersed in 30 mL distilled water at 25 °C for 1 h. After that, the excess water was drained with filter paper, the surface water of films was dried with an absorbent paper and, finally, the films were weighed again (W_s). Film swelling ratio was calculated using the following equation:

$$\text{Swelling ratio (\%)} = (W_s - W_i) \times 100/Wi \quad (5)$$

The surface wettability of film samples was studied using a home-made water contact analyser. Each film strip was placed on the horizontal stage and then made in contact with 10 μL of distilled water. The image of the water drop was immediately captured using a fixed digital microscopic camera (PS Pro, China). The contact angle between water drop and the film surface was measured by an Image J software and five measurements were performed to calculate the average of the contact angle value of each film sample.

2.9.6. Gas and water vapor permeability

Film permeability to WV water vapor, O_2 and CO_2 was measured in duplicate for each film, according to the modified method ASTM D3985 - 05 (2010), ASTM F 2476-05 (2005), ASTM F1249-13, 2013 using a MultiPerm instrument (ExtraSolutions s.r.l., Pisa, Italy). After conditioning the film samples for 24 h at 50% RH, they were placed into the aluminium masks and their exposed surface area was reduced to 5 cm^2.

2.9.7. Statistical analysis

The experiments were always performed in triplicate and in a completely randomized design. In order to determine the significant difference between treatments, one-way analysis of variance (ANOVA) and Duncan's multiple range tests ($p < 0.05$) were done using the Statistical Package for the Social Sciences (SPSS19, SPSS Inc., Chicago, IL, USA) software. Pearson correlation (r) to measure the strength of the linear relationship between TPC and antioxidant activity were calculated using the same software.

3. Results and discussion

3.1. Cardoon leaf extract preparation and evaluation of phenol content and antioxidant activity

CLE was obtained by two different methods: conventional maceration and Naviglio® extraction. Both processes were carried out using 100% ethanol as solvent, collecting samples after 2, 4, 8 and 24 h. The extracts were analysed and compared in terms of total phenol content (TPC) using Folin-Ciocalteau assay. Naviglio® extracts were characterised by a higher TPC than maceration extracts regardless the extraction time (Fig. 1, A). In particular, Naviglio® CLE showed an increase in the TPC over the time, from 86.8 ⊥ 3.5 mg GAE/L (corresponding to 140 mg GAE/100 g (fresh weight FW) of leaves at 2 h to 147.2 ⊥ 4.4 mg GAE/L (corresponding to 230 mg GAE/100 g (FW fresh weight) of leaves at 24 h.

These results are in agreement with TPC of leaves of several artichoke cultivars, ranging from 141.7 ⊥ 20.5 to 264.5 ⊥ 44.7 mg GAE/100 g (FW fresh weight) of leaves extracted using hydro methanolic solution (Rouphael et al., 2016). On the contrary, TPC did not change significantly in leaf samples obtained by the maceration method at the different extraction times. In particular, the highest value of TPC obtained by maceration after 24 h was lower than that detected after 2 h by Naviglio® extraction. Furthermore, no further increase in TPC was observed over 24 h extraction by both methods.

It is worth noting that, by using Naviglio® extractor, the values of mg GAE/L and mg/mL of extract showed a positive correlation with time increase ($r = 0.915$), since an increase in TPC content was achieved by prolonging the extraction time. In fact, the amount of GAE/g (dry weight DW) in the extracts did not significantly change with the time (Fig. 1, B). On the contrary, in the case of CLE obtained by maceration, no linear correlation was determined between mg GAE/L and mg/mL ($r = 0.067$): the highest amount of GAE/g (DW dry weight) was achieved after 2 h and significantly decreased thereafter, indicating an increase of components in the extracts other than phenols. Naviglio® extraction has been recently applied reported as a green technology for the to the recovery of phenolic compounds from different sources types of solid matrix (Naviglio et al., 2019; Panzella et al., 2020). Up to 69.9 ⊥ 7.3 mg GAE/g of extract have been obtained from the flowering aerial parts of *Schizogyne sericea* using both water and ethanol as solvents (Caprioli et al., 2017), whereas Posadino et al. (2018) have reported the extraction of phenols from wine waste (*Cagnulari* Grape Marc) using water: ethanol (60:40 v/v) as solvent with a recovering of 4000 mg/L ⊥ 0.05 TPC containing specific anthocyanins. Moreover, the extraction of 9210.4 ⊥ 45.8 mg GAE/L has been reported from crushed, dried and shredded grapes using water as solvent (Gallo et al., 2019) and aqueous vine shoot extracts, resulting into high phenolic content, have been obtained by Naviglio® method (Sánchez-Gómez, Zalacain, Alonso, & Salinas, 2014). Djeridane et al. (2006) reported that TPC in plants of Asteraceae family was higher than that detected in several other plants reported in literature, probably due to the ability to grow in harsh habitat conditions. Polyphenols extraction from cardoon leaves has been carried out by using different solvents such as ethanol, methanol or hydroalcoholic mixtures (Barbosa et al., 2020). According to Ramos et al. (2014), 22.6 GAE/g (DW dry weight) of extract were obtained from *C. cardunculus* L. var. altilis using methanol/water/acetic acid (49.5:49.5:1) after removing the lipophilic fraction. Similarly, 14.79 mg GAE/g (DW dry weight) of extract were obtained by using methanol (Falleh et al., 2008), and 50 mg GAE/g (DW dry weight) of extract were obtained by subsequent extraction with ethanol (Kukić et al., 2008). These differences in TPC reported in literature may be related to

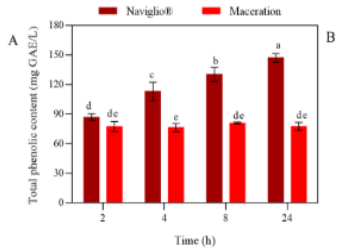

Sample	Naviglio® Extraction		Maceration Extraction	
	mg/mL extract	mg GAE/ g DW extract	mg/mL extract	mg GAE/ g DW extract
2 h	1.6	58.0	1.0	80.8
4 h	1.9	61.1	1.2	64.2
8 h	2.0	68.2	1.3	64.9
24 h	2.9	53.8	1.6	51.9

Fig. 1. A) Total phenolic content in cardoon leaves extracted by Naviglio® and maceration methods. CLE were analysed by using the Folin-Ciocalteau reagent. Values with different small letters (a–e) are significantly different (Duncan's multiple range tests, $p < 0.05$). B) Comparison of extraction efficiency of the two methods. Gallic acid equivalent (GAE), dry weight (DW). Further experimental details are given in the text.

intrinsic factors, such as genetics, as well as extrinsic ones, including geographical location, handling methodologies, storage, and extraction procedures (Fratianni et al., 2007). In addition, the distribution of secondary metabolites, such as polyphenols, may be dependent on the life cycle stage of the plant (Del Baño et al., 2003). The values of GAE/g (DW dry weight) detected in this work by using Naviglio® extractor fall within the range reported in literature, demonstrating the applicability of this method to the cardoon leaves.

Antioxidant activity of samples collected at different extraction times with both methods was evaluated using ABTS radical cation decolourisation and DPPH radical scavenging activity assays. Both methodologies are based on the reaction of the radicals ($DPPH^{\bullet}$ and $ABTS^{\bullet 1}$) with the antioxidant molecules which can be determined by spectrophotometric analysis (Dawidowicz, Wianowska, & Olszowy, 2012; Re et al., 1999). ABTS assay is commonly used for both hydrophilic and hydrophobic antioxidants, whereas DPPH is more efficient for hydrophobic systems as it is dissolved in organic solution (Bitencourt, Fávaro-Trindade, Sobral, & Carvalho, 2014; Floegel, Kim, Chung, Koo, & Chun, 2011). Regardless the assay method applied, Naviglio® extracts showed higher scavenging activity than the samples obtained by maceration (Fig. 2).

In particular, all the samples obtained by Naviglio® extractor displayed up to two and three fold the antioxidant activity with respect to the samples obtained by maceration, measured with either DPPH or ABTS assays, respectively. Furthermore, Naviglio® extract showed an increasing antioxidant activity as the extraction time increased, ranging from 41.2% ⊥ 3.4 at 2 h of extraction to 64.5% ⊥ 0.4 at 24 h of extraction using DPPH assay. These results reflect the same trend observed for the TPC determination, since the antioxidant activity of Naviglio® extract evaluated over the extraction time correlates with the TPC measured in the extract, showing highly significant correlation coefficients (r) (0.994 and 0.71) in both DPPH and ABTS assays. The observed correlation between TPC and antioxidant activity supports the hypothesis that this class of compounds directly contributes to the free

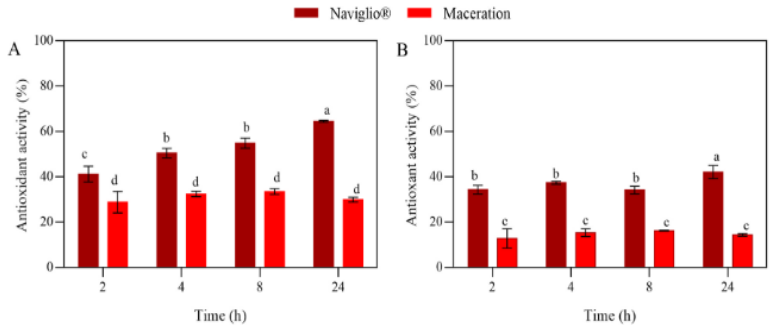

C

Sample	Naviglio® Extraction		Maceration Extraction	
	μg TE/g FW	μmol TE/ 100g FW	μg TE/g FW	μmol TE/ 100g FW
2 h	912.4	364.5	652.9	306.7
4 h	1107.8	442.6	728.3	333.0
8 h	1199.4	479.2	750.5	305.5
24 h	1401.9	560.1	676.0	372.3

Fig. 2. Antioxidant activity of cardoon leaf extracts obtained by Naviglio® and maceration methods detected following DPPH (A) and ABTS (B) assays. Values with different small letters (a–d) are significantly different (Duncan's multiple range tests, $p < 0.05$)). Comparison of antioxidant activity of the extracts are expressed as ratio of Trolox equivalents (TE) and fresh weight (FW) of extracts (C).

radical scavenging activity of the extracts.

It is worthy to note that the extract obtained by maceration does not follow the trend exhibited by the Naviglio® extract, showing an almost constant scavenging activity over the time (Fig. 2), in agreement with the TPC data. The antioxidant activity values measured in Naviglio CLEs are consistent with those reported in literature for the extracts of leaves of other species of *Cynara* genus. A radical scavenging activity in the range of 28.7%–94% has been reported for Green Globe and Violet artichoke (*Cynara scolymus* L.) varieties (Ben Salem et al., 2017; Biel, Witkowicz, Piątkowska, & Podsiadło, 2020). When referred to the Trolox standard, the antioxidant activities of the samples obtained with Naviglio® extractor were higher than those reported for methanolic extracts of leaves from *Cynara cardunculus* var. *ferocissima* (Madeira cardoon), expressed in the same way (176 μmol eq. Trolox/100 g) (Gouveia & Castilho, 2012).

3.2. Characterization of cardoon leaf extract

The characterization of the components of the Naviglio® extracts at 24 h was carried out by GC-MS and ^{1}H NMR spectroscopy. The panel a) of Fig. 3 shows a typical chromatogram of the extract, where the peaks were identified by comparing their mass spectra with the NIST14s database and with literature data (Mathe et al., 2004; Ramos et al., 2013). The GC-MS chromatogram provides qualitative information on the chemical composition of the CLE. The volatile pentacyclic triterpenes and sesquiterpenes, known for their antioxidant activity, are the main families of lipophilic components previously identified in the CLE (Ramos et al., 2013; Scavo, Rial, et al., 2019). In particular, cynaropicrin ($C_{19}H_{22}O_6$) and grosheimin ($C_{15}H_{18}O_4$) (RT = 35.61–37.25 min) have been identified in higher amount in the leaves than in other parts of cardoon and globe artichoke (Eljounaidi et al., 2015; Ramos et al., 2013; Rouphael et al., 2016). Grosheimin has also been previously reported in globe artichoke (Bernhard, 1982). Since the structures of the two sesquiterpene lactones are similar, it was not possible to identify their specific molecular fragmentation. Fatty acids (RT = 19.17 min), long-chain aliphatic alcohols (RT = from 19.50 to 22 min) and some aromatic compounds were also detected in traces. In particular, linoleic acid was identified, as also confirmed by ^{1}H NMR characterization (Fig. 3, panel b) (Ramos et al., 2013; Sobolev, Brosio, Gianferri, & Segre, 2005). The signal at 31.26 min is ascribable to squalene, whereas the signals corresponding to pentacyclic triterpenes fall in the range 23.45–29.73 min. Finally, the signals of hydrophobic long chain alkanes is visible at the range 40–42.5 min. Pentacyclic triterpenes have been identified as the main liphophilic constituents of *C. cardunculus* L. var. *altilis*, although less present in the leaves, where they represent only 8% of total detected compounds. On the other hand, fatty acids are reported to be mainly concentrated in the leaves, especially the saturated ones (Ramos et al., 2013). Furthermore, Rouphael et al. (2016) reported a wide range of phenolic compounds, including flavonoids, hydroxycinnamic acids, tyrosols, and lignans, in the extracts of leaves of different cultivars of artichoke. The characterization by ^{1}H NMR spectroscopy confirmed the presence of lupeol (Reynolds et al., 1986), and pheophytins (Sobolev et al., 2005) (Fig. 3, panel b). The cynaropicrin, a well known bioactive molecule endowed with antioxidant activity, was clearly identified by means of ^{1}H NMR in the extract, because of its typical signals. A semi-quantitative evaluation of its content respect to all other components was carried out because it was possible to integrate the signals of cynaropicrin by taking as a reference the signal of -CH2 protons at 4′ position, having a theoretical integral value of 2 and an observed experimental integral value of 0.85. When considering that the integral value of all protons present in the spectrum (range 0.5–6.5 ppm) is 84.14, it results that the proton of cynaropicrin correspond to the 11% of the protons present in the mixture (Fig. 3, panel c).

Finally, CLE was further analysed by ultrafiltration to determine the average molecular weight of its components. No retention of high molecular weight molecules was determined after ultrafiltration with neither 10 kDa nor 3 kDa cut-off membranes, indicating that CLE contained molecules smaller than 3 kDa.

3.3. Cardoon protein-based films

3.3.1. Zeta potential and particle size of film forming solutions

The data reported in Fig. 4 show that CPs were positively charged in the acidic pH range, since the detected zeta potential was found to increase from a value of about −40.00 mV at pH 12 to that of about −30 mV at pH 7.0 and 0 mV just under pH 4.0, indicating that the electrostatic repulsion pattern was gradually modified as a result of the gradual deprotonation of carboxyl groups and protonation of the amino groups of each CPs present in the sample. As far as the CP particle size, it also varied, like zeta potential, as a function of pH. In fact, at pH $\leq$ 5 high molecular mass protein species were present in the solution, likely because the isoelectric point of CPs was between pH 4 and 5 where the zeta potential value was around 0 mV. CP zeta potential and particle size were measured also in FFSs prepared at pH 12 by varying the concentrations of both proteins and GLY, used as plasticizer. All the FFSs tested were quite stable, regardless of protein and GLY concentration, zeta potential value fluctuating between −28 mV and −33 mV (Table 1).

As far as the particle size, it did not change by varying the GLY content, but it significantly increased by enhancing CP concentration, likely as a consequence of protein aggregation. However, the observed size distribution in the range of 300–400 nm is in agreement with previous results obtained with protein-based FFSs prepared by using other oilcakes (Mirpoor et al., 2020, 2021).

3.3.2. Thickness and mechanical properties of cardoon protein-based films

FFSs previously analysed for the particle size and zeta potential have been used for the preparation of bio-plastics by the casting method. It is worthy to note that the minimum GLY concentration to obtain handleable films under the described experimental conditions was 30% (w/w of CP), since the films cast in the absence or lower amount (10 and 20%) of plasticizer were brittle and not able to be peeled off from the plates. The handleable films were thus characterized for their thickness and mechanical properties (e.g. tensile strength, elongation at break and YMYoung's modulus) (Fig. 5).

As expected, the film thickness was found to increase by enhancing CP concentration independently on GLY amount present in the FFSs. Conversely, all the parameters characterising the mechanical properties of the films changed by varying both CP and plasticizer concentrations. In fact, TS tensile strength and YM Young's modulus decreased whereas EB elongation at break increased by enhancing GLY amounts at all the CP concentrations used. On the other hand, the investigated mechanical properties increased as function of CP amount. This effect was the result of the well known capacity of the plasticizer to increase the free volume and the polymer mobility by decreasing the attractive intermolecular forces into the protein matrix. Porta, Di Pierro, Roviello, and Sabbah (2017) also observed a similar effect for bitter vetch protein-based films prepared with two different plasticizers, such as GLY and spermidine. Sun et al. (2019) demonstrated that such phenomenon occurs also with carbohydrate-based materials, since they reported that chitosan/starch blended films had a greater extensibility when plasticizing components were added. In conclusion, among the different films produced, the one obtained from 400 mg of CP and 50% GLY was selected for the further investigations, possessing the highest EB elongation at break (154.19 ± 8.25) and acceptable TS tensile strength (1.69 ± 0.33) and YM Young's modulus (53.59 ± 6.89) (Fig. 5).

3.3.3. Zeta potential, particle size, contact angle and antioxidant activity of cardoon protein-based film forming solutions containing cardoon leaf extract

FFSs, prepared with 400 mg CPs and 50% GLY, were added with different amounts of CLE in order to test their zeta potential, particle size, contact angle and antioxidant activity as well as the properties of the derived films. Regarding the particles, it should be mentioned that

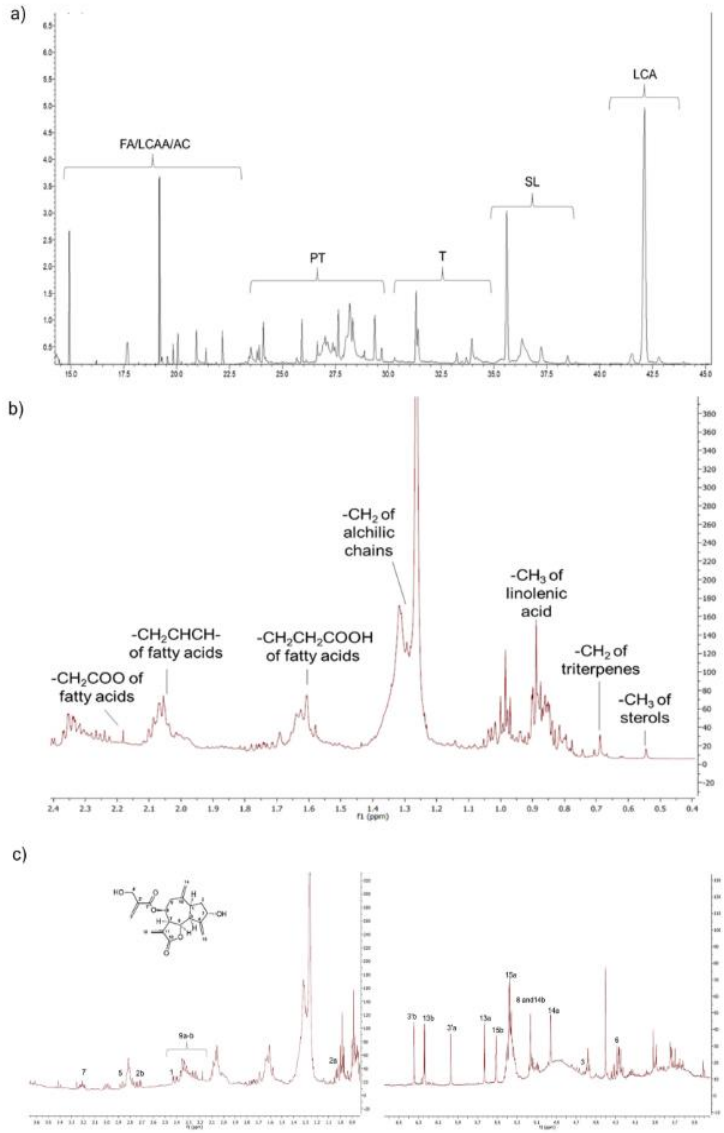

Fig. 3. a) GC-MS chromatogram; b) ^{1}H NMR spectrum of a cardoon leaf extract obtained by Naviglio® method. The GC-MS peaks represent the total ion current (TIC) of the compounds: FA = fatty acids; LCAA = long chains aliphatic alcohols, AC = aromatic compounds; PT = pentacyclic triterpenes; T = triterpene; SL = sesquiterpene lactones; LCA = long chain alkanes. ^{1}H NMR spectrum was detected in the range of 0.4–2.4 ppm. Further experimental details are given in the text. c) Signals of cynaropicrin in the range of 0.9–3.6 ppm (on the left) and signals of cynaropicrin in the range of 3.5–6.5 ppm (on the right). ^{1}H NMR (500 MHz, CD3OD): 1 δ: 2.43, dt; 2a δ: 1.09, ddd; 2b δ:2.07, dt; 3 δ:4.62, tt; 5 δ:2.84,dd; 6, δ:4.27,dd; 7 3.27, tt; 8 and 14b δ:5.17,ttt; 9a-b δ:2.25–2.45, dd; 13a δ:5.62,d; 13b, δ:6.25,d; 14a δ:4.96,d; 15a δ: 5.43,t; 15b δ:5.52,t; 3′a δ:5.9,m; 3′b δ:6.35, m.

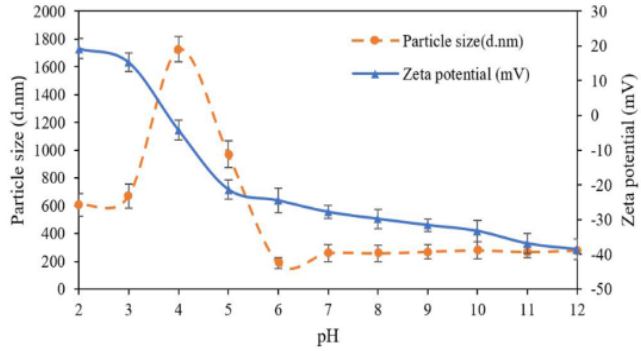

Fig. 4. Cardoon protein zeta potential and particle size measurements vs different pH values.

Table 1
Effect of different concentrations of cardoon proteins (CPs) and glycerol (GLY) on particle size and zeta potential on CP film forming solutions prepared at pH 12[a].

CPs (mg)	GLY (% w/w)	Particle size (d.nm)	Zeta Potential (mV)	PDI
200	30	312.7 ± 3.7^{e}	−31.50 ± 1.49^{cd}	0.44 ± 0.03^{e}
	40	309.2 ± 3.5^{e}	−31.63 ± 0.58^{cd}	0.43 ± 0.02^{e}
	50	310.6 ± 2.7^{e}	−32.56 ± 1.42^{d}	0.42 ± 0.02^{e}
300	30	379.3 ± 7.1^{b}	−29.63 ± 1.61^{bc}	0.52 ± 0.04^{b}
	40	379.0 ± 10.2^{b}	−29.70 ± 0.85^{bc}	0.51 ± 0.02^{b}
	50	381.8 ± 16.5^{b}	−29.45 ± 1.52^{ab}	0.53 ± 0.03^{b}
400	30	436.2 ± 4.8^{a}	−28.51 ± 0.40^{a}	0.60 ± 0.02^{a}
	40	435.0 ± 6.3^{a}	−28.78 ± 0.86^{a}	0.61 ± 0.04^{a}
	50	433.3 ± 5.9^{a}	−29.17 ± 0.46^{a}	0.60 ± 0.02^{a}

[a] Different small letters (a–d) indicate significant differences among the values reported in each column (Duncan's multiple range tests, $p < 0.05$). Poly-dispersion index (PDI). Further experimental details are given in text.

they consist of different kinds of proteins, some fibres and phenols (coming from the seed oilcakes), glycerol used as plasticizer and finally, as far as the activated FFSs, the CLE. From the performed experiments, it is possible to note that particle size of CPs FFS increased by incorporation of higher concentration of antioxidant in the FFS compared to the control sample, as reported in Table 2. These results could be attributed to the interactions between the CP functional groups and the phenolic hydroxyl groups of antioxidants that formed larger CPs polymers that increase the polydispersity index (PDI), that is an indicator of relative variance in the particle size distribution. These results are in agreement with a linear increase in polydispersity index. The protein surface charges were also affected by the addition of antioxidants and all the FFSs were stable with negative zeta potential higher than −28 mV shows the high stability of solution (Bhattacharjee, 2016). As shown in Table 2, zeta potential of CPs FFS decreased as a function of increasing the concentration of antioxidants due to the participation of negative functional groups of CPs in protein-polyphenols interaction and/or interactions between the CPs surface and CLE that can modify the surface charge of the proteins. The same results were reported for changing the surface charge of soy protein isolate and whey protein isolate based films loaded by curcumin by Chen, Li, and Tang (2015) and Taghavi Kevij et al. (2020), respectively.

The contact angle of the different FFSs was measured on parafilm, the semi-transparent, flexible film composed of a proprietary blend of waxes and polyolefins currently used in research laboratories. The results reported in Fig. 6 clearly show that the addition of increasing amounts of CLE significantly decreased the contact angle value of the CP FFS in comparison to the control sample, thus indicating that the hydrophobicity of CP FFS significantly increased in the presence of increasing CLE concentrations (Fig. 6).

The higher hydrophobicity of the FFS prepared in the presence of CLE might be dependent on the decrease in the number of free hydrophilic groups of CPs involved in the interactions between protein and CLE components (Fathi, Almasi, & Pirouzifard, 2019).

Furthermore, FFS antioxidant activity was preliminarily evaluated using the DPPH radical scavenging activity assay with the aim of choosing the right amount of CLE to graft in the CP-based films. CP containing FFS had a marked antioxidant activity also in the absence of CLE and, whereas the antioxidant activity of the samples added with an amount of CLE up to 3% were at the same level of the control, it progressively increased in the presence of 5, 10, 15 and 30% (w/w) CLE (Fig. 7). For this reason, CP-based films were manufactured by preparing FFSs containing 15% and 30% CLE.

3.3.4. *FT-IR spectra of CP-based films incorporated wit CLE*

The FT-IR spectra of CP-based films incorporated or not with CLE are shown in Fig. 8. The sharp peaks in the spectrum of neat CP-based film in the range of 1649 cm^{-1} are attributed to the amide I (C=O stretching vibrations) and in the range of 1544 cm^{-1} to the amide II (N–H bending with C–N groups stretching vibrations) are the regions that employed to study the secondary structure properties of proteins (Mohammadian et al., 2019). The FT-IR results of the films incorporated with different amounts of CLE showed a significant shift in the position of these peaks to the lower wavenumbers. These alterations in the peak positions could be attributed to new molecular arrangement in the film matrix due to the interactions between the polypeptide chain of the protein and CLE molecules (Moghadam, Salami, Mohammadian, Khodadadi, & Emam-Djomeh, 2020). Moreover, there are the characteristic peaks around 2878 cm^{-1} and 3270 cm^{-1} in the CP-based films, that correspond to the aliphatic C–H stretching vibrations of CH_2 functional groups and O–H stretching overlapping N–H stretching vibrations, respectively. The incorporation of CLE in the CP-based films matrix caused a considerable shift in the position of these peaks (Chentir et al., 2019; Taghavi Kevij et al., 2020). A common peak observed in the spectra of all the

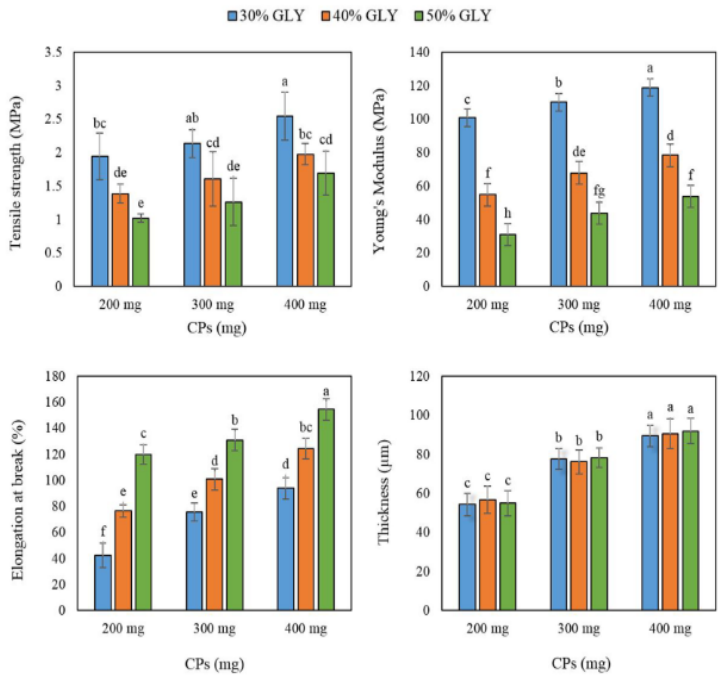

Fig. 5. Effect of different amounts of cardoon proteins (CPs) on the thickness and mechanical properties of films prepared at pH 12 and containing different glycerol (GLY) concentrations. Different small letters (a–g) indicate significant differences among the values reported in each bar (Duncan's multiple range tests, $p < 0.05$). Further experimental details are given in the text.

Table 2
Effect of different concentrations of cardoon leaf extract (CLE) on Z-average and zeta potential of cardoon proteins (400 mg) film forming solutions prepared at pH 12 in the presence of 50% glycerol (GLY)[a].

CLE (% w/w)	Mean particle size (d.nm)	Zeta potential (mV)	PDI (%)
0	411.00 ± 8.20^{c}	−34.35 ± 1.41^{c}	0.47 ± 0.01^{c}
15	441.4 ± 10.08^{b}	−31.69 ± 0.95^{b}	0.52 ± 0.03^{b}
30	512.10 ± 12.22^{a}	−28.84 ± 1.12^{a}	0.58 ± 0.02^{a}

[a] Different small letters (a–d) indicate significant differences among the values reported in each column (Duncan's multiple range tests, $p < 0.05$). Polydispersion index (PDI). Further experimental details are given in text.

investigated samples at around 1040 cm^{-1} is related to OH group of glycerol, indicating the incorporation of glycerol into the film matrix (Moghadam et al., 2020).

3.3.5. *Physicochemical, morphological and mechanical properties of cardoon protein-based films containing cardoon leaf extract*

Films containing different ratios of CP/CLE amounts were manufactured to investigate the effects of CLE on the formation of CP-based materials. To this aim FFSs containing a constant presence of 400 mg of total mass were prepared by increasing the percentage of CLE and parallely decreasing the CP amount. The data reported in Table 3 indicate that thinner films were obtained by reducing the content of CPs until 70% and a concurrent increase in the CLE amount to 30%.

At the same time the mechanical performance of the obtained materials was found to get worse having been observed a progressive decrease of all the parameters (TS, tensile strength, elongation at break EB and YM Young's modulus). Therefore, these findings suggested to test the influence of increasing CLE concentrations on the films manufactured with a constant CP amount (400 mg). Fig. 9 shows that the film thickness slightly increased as a function of CLE amount present in the film matrix, probably due to the interaction of CLE component(s) with the CP polymeric chains, via

Hydrogen bonding and hydrophobic forces (Arciello et al., 2021). In fact, polyphenols may lead to protein crosslinking, thus, increasing the film thickness. These findings were consistent with the results of Hanani, Yee, and Nor-Khaizura (2019) and Moghadam et al. (2020) who observed the effects of pomegranate peel powder on fish gelatin and mung bean protein films, respectively. In addition, both TS tensile strength and YM Young's modulus of films containing 15% CLE were found markedly increased, whereas only a lower, but significant, reduction of the elongation at break EB value was detected in the films prepared in the presence of the same amount of CLE compared to the control samples. However, it should be noted that, by enhancing CLE concentration to 30%, both ~~TS~~ tensile strength and ~~YM~~ Young's modulus values decreased, whereas elongation at break EB slightly increased, with respect to the values detected with films containing 15% CLE. These findings suggest that hydrogen bonding and/or hydrophobic interactions between some CLE components, possibly polyphenols, and CP reactive groups might be responsible for the observed reinforcement of the film network at lower CLE concentrations (Moghadam et al., 2020). Conversely, higher amounts of CLE active molecules could reduce TS tensile strength and increase the flexibility of the CP-based films due to

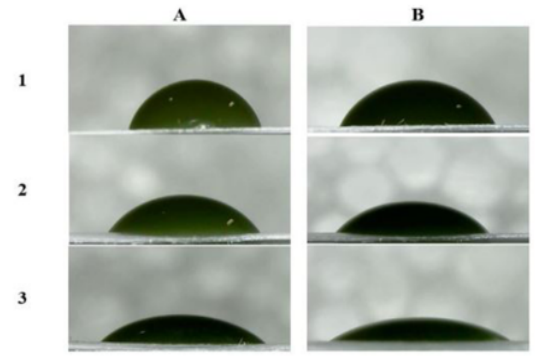

Fig. 6. Images of drops on parafilm surface, captured immediately (A) and after 30 s (B), and contact angle (θ) values of film forming solution (FFS), containing cardoon protein (CP) and 50% glycerol, prepared at pH 12 in the absence (1) or presence of 15% (2) and 30% (3) of cardoon leaf extract (CLE). Different small letters (a–c) indicate significant differences among the values reported in each column (Duncan's multiple range tests, $p < 0.05$). Further experimental details are given in the text.

FFS	0 *(sec)*	30 *(sec)*
CP	66.20 ± 0.12 [a]	58.60 ± 0.31 [a]
CP + 15% CLE	50.33 ± 1.15 [b]	41.53 ± 0.63 [b]
CP+ 30% CLE	40.70 ± 1.65 [c]	28.50 ± 1.27 [c]

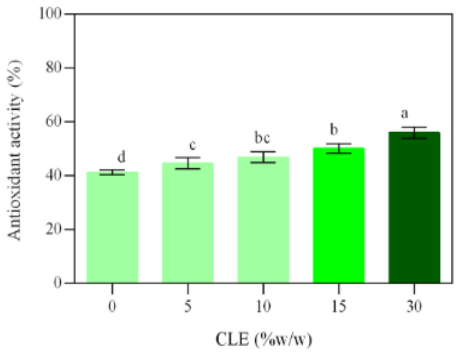

Fig. 7. Antioxidant activity of cardoon protein-based film forming solutions containing different concentrations of cardoon leaf extract (CLE) determined by DPPH assay. Values with different small letters (a–d) are significantly different (Duncan's multiple range tests, $p < 0.05$). Further experimental details are given in the text.

their possible plasticizing effects, as previously reported for bitter vetch protein-based films added with different polyphenol containing extracts (Arabestani, Kadivar, Shahedi, Goli, & Porta, 2016) or for whey protein- and fish gelatin-based films in which curcumin and mango peel extracts were, respectively, incorporated (Adilah et al., 2018; Taghavi Kevij et al., 2020). The films functionalized with 15% CLE were slightly less flexible than the ones prepared in the absence of the phenolic components showing a lower elongation at break, however a significant increase in tensile strength and Young's modulus was observed as a result of CLE incorporation. The same observations were reported by Arciello et al. (2021) who studied whey protein-based bio-plastics prepared with the addition of phenolic extracts from Pecan nuts.

Furthermore, it is well known that color parameters and opacity of the films play a key role in consumers' willingness to choose packed food products, and, in addition, these parametes can affect food quality, specially for the foods that are sensitive to the light (Baek, Kim, & Song, 2018). As shown in Fig. 10 and inferred from the data reported in Table 4, all the CP-based films had low L*, b* and a* values determining a dark greenish-yellow color of the films. The presence of CLE in the CP-based films increased their opacity and the a* and b* values by increasing its concentrations. The higher a* and b* values of films obtained in the presence of higher amount of CLE indicate that the films were more close to green and yellow colors, compared to the control film, probably due to the natural pigments present in CLE. Moreover, also the lightness (L* value) of the film samples was reduced by increasing CLE concentrations. The density of CP-based films significantly increased by increasing CLE concentration, suggesting that the formation of hydrogen and hydrophobic bonds between proteins and CLE components increased by increasing CLE concentrations and led to a more compact film microstructure. Similar behaviour has been previously reported by Riaz et al. (2018) who observed an increasing trend in the density of chitosan-based films by increasing its polyphenols content.

As ar fas as the structural morphology, the films prepared in the absence of CLE exhibited some irregularities and large pores in both surface and matrix (Fig. 10, B1 and C1), whereas the microstructural images of the CLE containing films appeared more homogeneous, continuous and smooth. On the other hand, the film prepared in the presence of 15% CLE seems smoother and more compact than that cast with 30% CLE especially in the cross-section where several holes, voids and discontinuities are quite visible (Fig. 10, B2 and C2 and B3 and C3).

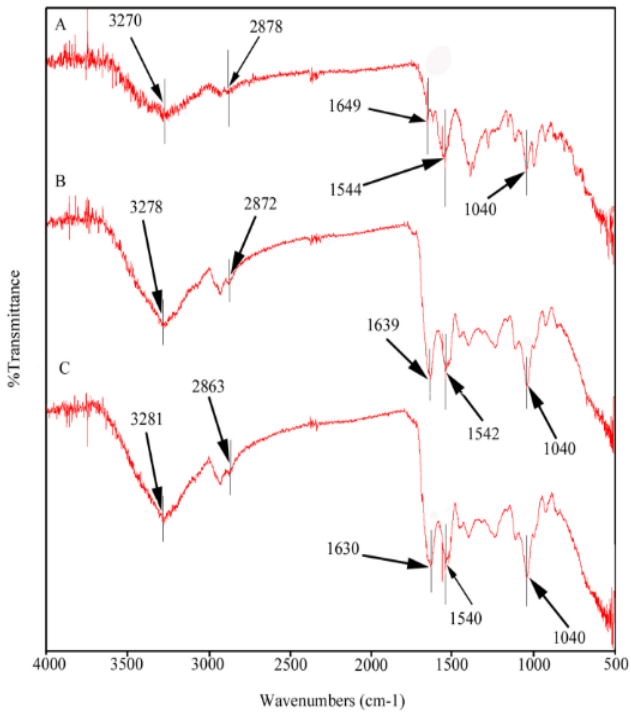

Fig. 8. FT-IR spectra of films prepared in the absence (A) and the presence of 15% (B) and 30% (C) of cardoon leaf extract (CLE).

Table 3
Effect of different cardoon protein (CP)/cardoon leaf extract (CLE) ratios on the thickness and mechanical properties of films prepared at pH 12[a].

CP/CLE (% w/w)	TS (MPa)	EB (%)	YM (MPa)	Thickness (μm)
100	1.86 ± 0.23[a]	141.21 ± 6.14[a]	62.39 ± 7.74[a]	86.84 ± 5.92[a]
90/10	1.64 ± 0.31[a]	132.83 ± 5.27[a]	56.47 ± 6.31[ab]	77.31 ± 5.47[a]
80/20	1.29 ± 0.17[ab]	107.62 ± 7.41[b]	49.93 ± 4.71[bc]	65.72 ± 6.28[ab]
70/30	1.17 ± 0.06[b]	92.43 ± 6.08[b]	34.15 ± 5.73[c]	49.32 ± 4.88[c]

[a] Tensile strength (TS), elongation at break (EB), Young's module (YM). Different small letters (a–c) indicate significant differences among the values reported in each column (Duncan's multiple range tests, $p < 0.05$). Further experimental details are given in text.

3.3.6. Water resistance of cardoon protein-based films containing cardoon leaf extract

The moisture content, solubility, swelling ratio and contact angle values of CP-based films containing different amount of CLE are reported in Fig. 11. It is well known that the moisture content of the protein-based films is related to the free volume occupied by water molecules that is in turn influenced by the conformation of the protein and the number of exposed polar groups, and the consequent surface polarity of the polymeric matrix (Sarıcaoglu & Turhan, 2020). The CP-based films revealed a declining tendency for moisture content after incorporation of CLE components, probably due to their hydrophobic properties that limited the water retention in the film matrix (Emam-Djomeh, Moghaddam, & Yasini Ardakani, 2015; Sarıcaoglu & Turhan, 2020). Similar results were obtained by Shams, Ebrahimi, & Khodaiyan (2019) who studied the effects of the orange peel extract added to nanocomposite films made with whey protein and gelatin. Also the reduced tendency for water content of chitosan films observed after incorporation of apple peel polyphenols (Riaz et al., 2018) seems in agreement with the present results.

Furthermore, since both water solubility and swelling of the protein-based films are considered as important factors for their possible applications, mainly in the humid enviroment (Batista, Araújo, Peixoto Joele, Silva, & Lourenço, 2019; Haghighi et al., 2019), also the effect of CLE on these film features was analysed. The data reported in Fig. 11 clearly indicate that both water solubility and swelling ratio of the CLE containing films significantly decreased in comparison with the control CP films. In fact, the hydrophobic nature of several molecules present in CLE might be responsible for the formation of a more compact protein matrix able to maintain the integrity of the films upon their immersion in water, as well as for the reduced interactions among protein and water molecules.

In agreement with these results, Nur Hanani, Aelma Husna, Nurul Syahida, Nor Khaizura, and Jamilah (2018) showed that the water solubility of gelatin/polyethylene bilayer films markedly improved after their enrichment with different fruit peels.

Finally, it is well known that the contact angle is a valid indicator of hydrophobicity of the film surface and that this parameter is affected by different factors such as heterogeneity, surface roughness, particle and

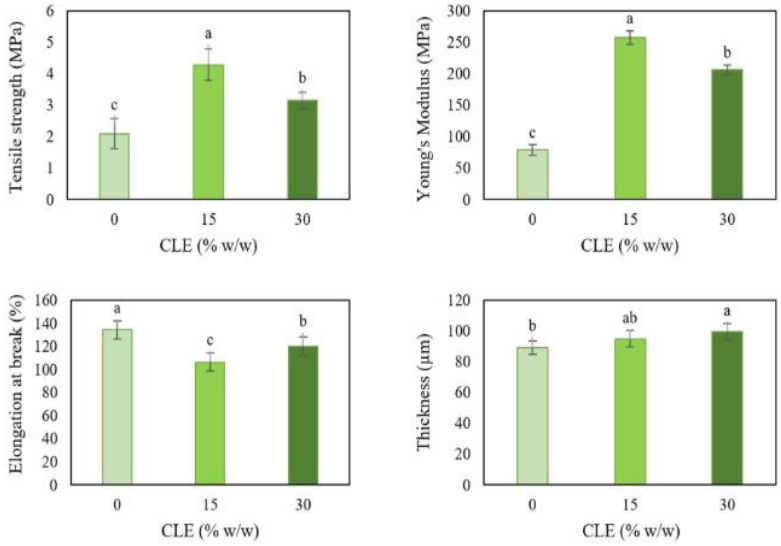

Fig. 9. Thickness and mechanical properties of cardoon protein-based films containing different concentrations of cardoon leaf extract (CLE). Values with different small letters (a–c) are significantly different (Duncan's multiple range tests, $p < 0.05$). Further experimental details are given in the text.

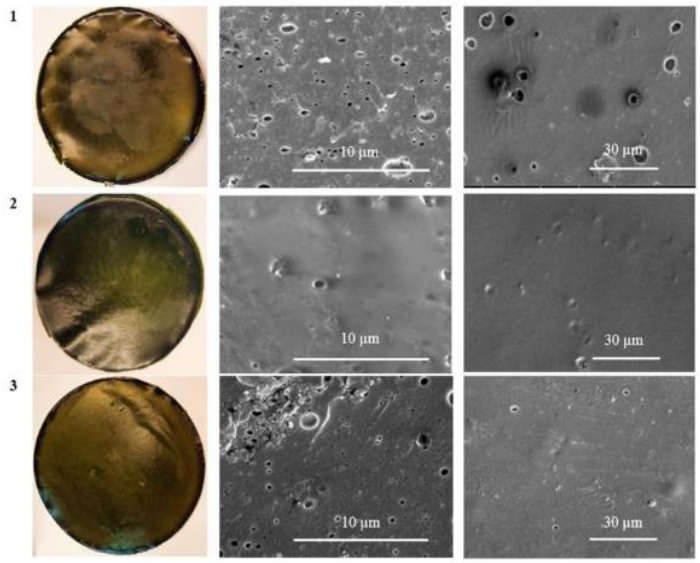

Fig. 10. Images of films (A), prepared in the absence (1) and presence of either 15% (2) or 30% (3) of cardoon leaf extract, and of their SEM cross sections (B, magnification 8000 ×) and surfaces (C, magnification 4000 ×). Further experimental details are given in the text.

pore size of the film matrix (Abdelhedi et al., 2018; Hebbar, Isloor, & Ismail, 2017). As shown in Fig. 11, the incorporation of CLE into CP-based films significantly increased their contact angle values compared to those of control films. These findings suggest that the presence of CLE components in the CP film matrix might increase the smothness of the film surface leading to an increase in the

Table 4
Colour parameters, opacity and density of cardoon proteins-based films containing different concentrations of cardoon leaf extracts (CLE).

CLE (%, w/w)	L	a	b	ΔE	Opacity (mm^{-1})	Density (g/cm^3)
0	28.42 ± 0.87[a]	−2.25 ± 0.10[a]	13.82 ± 0.69[c]	72.22 ± 1.54[c]	14.89 ± 0.17[c]	1.19 ± 0.01[c]
15	23.64 ± 1.03[b]	−2.81 ± 0.07[b]	15.51 ± 0.84[b]	77.20 ± 1.08[b]	16.14 ± 0.35[b]	1.28 ± 0.02[b]
30	20.44 ± 0.57[c]	−3.29 ± 0.15[c]	20.04 ± 0.56[a]	81.16 ± 1.12[a]	17.61 ± 0.28[a]	1.34 ± 0.01[a]

[a] L, a and b values indicate lightness/darkness (0–100), greenness/redness (−60 to +60) and blueness/yellowness (−60 to +60), respectively; ΔE, total color difference. Values with different small letters (a-c) are significantly different (Duncan's multiple range tests, $p < 0.05$). Further experimental details are given in the text.

hydrophobicity of their surface, as a consequence of the interactions between CPs and CLE components able to decrease the number of protein hydrophilic groups. Increasing of the surface hydrophobicity of mung bean protein-based films enriched with pomegranate peel powder was previously reported by Moghadam et al. (2020).

3.3.7. Film barrier properties of cardoon protein-based films containing cardoon leaf extract

The resistance to water vapor (WV) permeation of CP-based films prepared in the presence or absence of two different CLE concentrations is reported in Table 5. CP-based films containing 15% CLE exhibited WV water vapor permeability values lower than those observed by testing CP films prepared in CLE absence, while WV water vapor permeability was found significantly increased with respect to control samples in the films obtained in the presence of CLE double concentration (30%). The enhancement of WV water vapor barrier properties of films containing a lower CLE amount could be attributed to the decrease of the free space among the CP chains due to the formation of hydrogen bonds and/or hydrophobic interactions among protein and CLE components that could probably decrease the penetration and diffusion of WV water vapor through the film matrix.

Conversely, the addition of higher amounts of CLE to the CP-based FFS probably prevented an homogeneous distribution of the same components in the film matrix, thus determining an opposite effect on the WV water vapor permeability of the resulting films. In this regard, Moghadam et al. (2020) reported that WV water vapor barrier properties of mung bean protein-based films increased in the presence of pomegranate peel powder, whereas Adilah et al. (2018) did not observe any significant change in WV water vapor permeability of the fish gelatin films by adding increasing amounts of mango peel.

Furthermore, as shown in Table 5, even the permeabilities to both O_2 and CO_2 of the CP films containing CLE were observed to significantly decrease with respect to those of control films, probably as a consequence of the lower number of pores observed by SEM in the film surface and cross-section images (Fig. 10). More in particular, the interactions between CP and CLE components might be responsible for the reduced diffusion paths of the gas molecules through the film networks (Laufer, Kirkland, Cain, & Grunlan, 2013). However, also the O_2 and CO_2

Table 5
Water vapor (WV) and gas permeability of cardoon protein (CP)-based films containing different concentrations of cardoon leaf extract (CLE)[a].

CLE (% w/w of CP)	WV	O_2	CO_2
	(cm^3 mm m^{-2} d^{-1} kPa^{-1})		
0	0.05 ± 0.01[a]	2.24 ± 0.01[a]	6.53 ± 0.42[a]
15	0.02 ± 0.01[b]	1.19 ± 0.06[b]	1.89 ± 0.37[b]
30	0.08 ± 0.01[c]	1.64 ± 0.08[c]	3.47 ± 0.82[c]

[a] Different small letters (a–c) indicate significant differences among the values reported in each column (Duncan's multiple range tests, $p < 0.05$). Further experimental details are given in text.

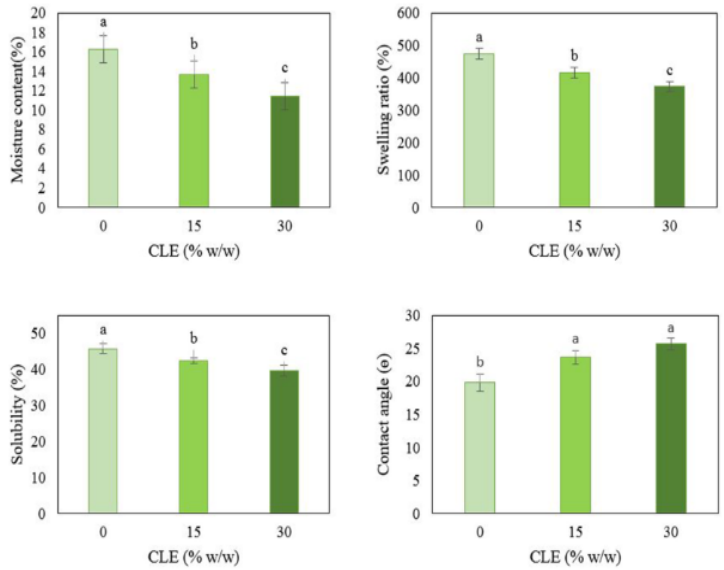

Fig. 11. Moisture content, water solubility, swelling and contact angle of cardoon protein-based films containing different concentrations of cardoon leaf extract (CLE). Values with different small letters (a–c) are significantly different (Duncan's multiple range tests, $p < 0.05$). Further experimental details are given in the text.

permeability values of CP films containing higher aumounts of CLE were found to be higher than those containing 15% CLE. Similar findings were obtained by Galus and Kadzińska (2016) who reported an increase in gas permeabilities by increasing almond and walnut oil concentrations in the whey protein films. Therefore, also these data seem to reflect the microstructure of the prepared films, since an increase in pores and voids in the film network was observed in the films prepared with the highest (30%) CLE concentration (Fig. 10, B3). Similar results were reported by Bai et al. (2019) who studied the effects of different amounts of quercetin on carboxymethyl chitosan based films. Nevertheless, it is worthy to note that the behaviour in terms of barrier properties of the films containing CLE is not far from that observed for another protein-based bio-plastic, such as the one produced by using whey proteins functionalized with a phenolic extract (30% w/w of proteins) obtained from Pecan nutshell (Arciello et al., 2021). In fact, the authors found out that the permeabilities towards water vapor and the two types of gases performed by the whey protein film prepared with the extract were found to be significantly lower compared to those of the unfunctionalized one. The authors concluded that these results are useful for a potential application of such bio-plastics in the food sector, since, to keep food fresh, the water vapor permeability value should be maintained as low as possible. Furthermore, a higher O_2 barrier property is also important since oxygen causes, for example, the rancidity of fatty acids (Arciello et al., 2021).

3.3.8. *Antioxidant activity of cardoon protein-based films containing cardoon leaf extract*

CP-based films containing CLE were tested for DPPH radical scavenging activity over time. Fig. 12 shows that the films freshly manufactured in the absence of CLE exhibited a marked antioxidant activity and that the addition of 30% CLE improved this property since the observed scavenging activity against DPPH radical of the films increased form 30% up to 60%. The antioxidant activity of all films remained quite stable after 30 days at room temperature, suggesting their potential exploitation as active packaging for shelf life extension of foodstuffs. Similar results were obtained by Moghadam et al. (2020) who described a range of scavenging activity from 14% to 65% for mung bean protein-based films enriched with different amounts of pomegranate peel powder, whilst Adilah et al. (2018) and Hanani et al. (2019) reported an enhancement of the scavenging activity up to 89% and up to 72% for fish gelatin films added with mango kernel extract and pomegranate peel powder, respectively. From Fig. 12 it also possible to note that over a period of 70 days the antioxidant activity decreased roughly of 25% for all the bio-plastics tested, likely because of the oxidation of the phenolic compounds responsible of conferring the films with this biological activity. Nevertheless, the materials functionalized with the highest amount of CLE seem to be still endowed with the highest antioxidant activity (45%) even after a period of 70 days, suggesting their possible application in protecting some foods from the oxidation.

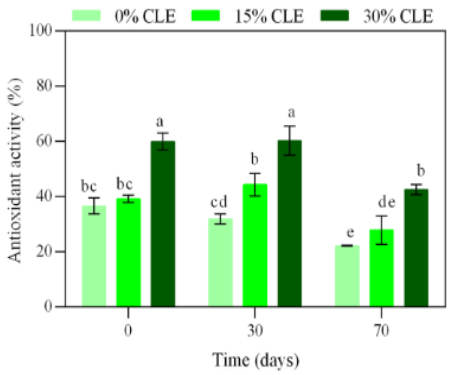

Fig. 12. Effect of different concentrations of cardoon leaf extract (CLE) on the antioxidant activity of cardoon protein-based films measured by DPPH assay at different times of storage. Values with different small letters (a–e) are significantly different (Duncan's multiple range tests, $p < 0.05$). Further experimental details are given in the text.

4. Conclusions

The objective of this paper was to valorise different *Cynara cardunculus* segments by extracting bio-based products useful for an integrated application. A method for recovery of a functional cardoon leaf extract (CLE) was set up and its composition analysis revealed the presence of several low molecular weight molecules (such as two sesquiterpene lactone, cynaropicrin and grosheimin) of potential attractiveness as bioactive compounds. In addition, proteins extracted from cardoon seeds were tested as raw material for producing, in the presence of glycerol, manipulable bio-plastics endowed with promising mechanical and barrier features, as well as antioxidant properties. Towards the development of a *Cynara cardunculus* biorefinery, the obtained CLE was added to the protein-based film forming solutions and the characterization of the derived films showed a significant improvement of all the properties of the manufactured material. The CLE-containing films appeared smoother and more homogenous, and showed also a higher and lasting antioxidant activity that conferred a higher value to the obtained bio-plastics. Therefore, all the presented data envisage *Cynara cardunculus* as a potential biomass resource for the development of a plant biorefinery devoted to the production of innovative bio-based products according to the principles of the circular bio-economy. In particular, the produced bio-plastics may be exploited for extending the shelf-life of different kinds of foodstuffs due to the fact that, besides showing good mechanical and barrier properties, they are endowed with antioxidant features that are of a paramount importance for food protection. Nevertheless, a potential use of such biomaterials as mulching sheets is also advisable.

Author contributions

Seyedeh Fatemeh Mirpoor: Investigation; Methodology; Formal analysis; Writing-original draft. Simona Varriale: Investigation; Methodology; Formal analysis; Writing-original draft. Raffaele Porta: Supervision; Funding acquisition; Conceptualization; Writing review and editing. Daniele Naviglio: Methodology; Investigation. Mariachiara Spennato: Methodology; Investigation. Lucia Gardossi: Methodology; Investigation. C. Valeria L. Giosafatto: Supervision; Conceptualization; Writing review and editing. Cinzia Pezzella: Supervision; Conceptualization; Writing review and editing.

Declaration of competing interest

None.

Acknowledgments

We thank Prof. Rocco Di Girolamo for performing microscopy analyses and Prof. Massimo Fagnano for providing Cardoon in April 2019. This research was funded by the grant PRIN: Progetti di Ricerca di Interesse Nazionale –Bando 2017– "CARDoon valorisation by InteGrAted bioreñiNery (CARDIGAN)" of Italian Ministero dell'Università e della Ricerca (COD. 2017KBTK93).

References

AACC. (2003). *Approved methods of AACC*. St. Paul, MN, USA: The Association. Available at: https://methods.aaccnet.org/default.aspx. (Accessed 5 May 2021).

Abdelhedi, O., Nasri, R., Jridi, M., Kchaou, H., Nasreddine, B., Karbowiak, T., et al. (2018). Composite bioactive films based on smooth-hound viscera proteins and gelatin: Physicochemical characterization and antioxidant properties. *Food Hydrocolloids, 74*, 176–186. https://doi.org/10.1016/j.foodhyd.2017.08.006

Adilah, A. N., Jamilah, B., Noranizan, M. A., & Hanani, Z. A. N. (2018). Utilization of mango peel extracts on the biodegradable films for active packaging. *Food Packaging and Shelf Life, 16*, 1–7. https://doi.org/10.1016/j.fpsl.2018.01.006

Arabestani, A., Kadivar, M., Shahedi, M., Goli, S. A. H., & Porta, R. (2016). Characterization and antioxidant activity of bitter vetch protein-based films containing pomegranate juice. *Lebensmittel-Wissenschaft und -Technologie- Food Science and Technology, 74*(74), 77–83. https://doi.org/10.1016/j.lwt.2016.07.025

Arciello, A., Panzella, L., Dell'Olmo, E., Abdalrazeq, M., Moccia, F., Gaglione, R., et al. (2021). Development and characterization of antimicrobial and antioxidant whey protein-based films functionalized with Pecan (*Carya illinoinensis*) nut shell extract. *Food Packaging and Shelf Life, 29*, Article 100710. https://doi.org/10.1016/J.FPSL.2021.100710

ASTM F1249 - 13: Standard test method for water vapor transmission rate through plastic film and sheeting using a modulated infrared sensor. Retrieved from https://www.astm.org/DATABASE.CART/HISTORICAL/F1249-13.htm, (2013).

ASTM D3985 - 05. (2010). Standard test method for oxygen gas transmission rate through plastic film and sheeting using a coulometric sensor. Retrieved from https://www.astm.org/DATABASE.CART/HISTORICAL/D3985-05.htm.

ASTM D882 - 18. (1997). Standard test method for tensile properties of thin plastic sheeting - ANSI blog. Retrieved from https://www.astm.org/Standards/D882.

ASTM F 2476-05. (2005). Standard test method for the determination of carbon dioxide gas transmission rate (CO2 TR) through barrier materials using an infrared detector. Retrieved from https://www.astm.org/DATABASE.CART/HISTORICAL/F2476-05.htm.

Baek, S.-K., Kim, S., & Song, K. (2018). Characterization of *Ecklonia cava* alginate films containing cinnamon essential oils. *International Journal of Molecular Sciences, 19*(11), 3545. https://doi.org/10.3390/ijms19113545

Bai, R., Zhang, X., Yong, H., Wang, X., Liu, Y., & Liu, J. (2019). Development and characterization of antioxidant active packaging and intelligent Al 3+ -sensing films based on carboxymethyl chitosan and quercetin. *International Journal of Biological Macromolecules, 126*, 1074–1084. https://doi.org/10.1016/j.ijbiomac.2018.12.264

Barbosa, C. H., Andrade, M. A., Vilarinho, F., Castanheira, I., Fernando, A. L., Loizzo, M. R., et al. (2020). A new insight on cardoon: Exploring new uses besides cheese making with a view to zero waste. *Foods, 9*(5), 1–22. https://doi.org/10.3390/foods9050564

Batista, J. T. S., Araújo, C. S., Peixoto Joele, M. R. S., Silva, J. O. C., & Lourenço, L. F. H. (2019). Study of the effect of the chitosan use on the properties of biodegradable films of myofibrillar proteins of fish residues using response surface methodology. *Food Packaging and Shelf Life, 20*, Article 100306. https://doi.org/10.1016/j.fpsl.2019.100306

Ben Salem, M., Affes, H., Athmouni, K., Ksouda, K., Dhouibi, R., Sahnoun, Z., et al. (2017). Chemicals compositions, antioxidant and anti-inflammatory activity of *Cynara scolymus* leaves extracts, and analysis of major bioactive polyphenols by HPLC. *Evidence-based Complementary and Alternative Medicine, 2017*, 4951937. https://doi.org/10.1155/2017/4951937, 2017.

Benlloch-González, M., Fournier, J. M., Ramos, J., & Benlloch, M. (2005). Strategies underlying salt tolerance in halophytes are present in *Cynara cardunculus*. *Plant Science, 168*(3), 653–659. https://doi.org/10.1016/j.plantsci.2004.09.035

Bernhard, H. (1982). Quantitative determination of bitter sesquiterpenes from *Cynara scolymus* L. (artichoke) and *Cynara cardunculus* L. (Kardone) (Compositae). *Section Title: Plant Biochemistry, 57*(7), 179–180.

Bhattacharjee, S. (2016, August 10). DLS and zeta potential - what they are and what they are not? *Journal of Controlled Release, 235*, 337–351. https://doi.org/10.1016/j.jconrel.2016.06.017

Biel, W., Witkowicz, R., Piątkowska, E., & Podsiadło, C. (2020). Proximate composition, minerals and antioxidant activity of artichoke leaf extracts. *Biological Trace Element Research, 194*(2), 589–595. https://doi.org/10.1007/s12011-019-01806-3

Bitencourt, C. M., Fávaro-Trindade, C. S., Sobral, P. J. A., & Carvalho, R. A. (2014). Gelatin-based films additivated with curcuma ethanol extract: Antioxidant activity and physical properties of films. *Food Hydrocolloids, 40*, 145–152. https://doi.org/10.1016/j.foodhyd.2014.02.014

Caprioli, G., Iannarelli, R., Sagratini, G., Vittori, S., Zorzetto, C., Sánchez-Mateo, C. C., et al. (2017). Phenolic acids, antioxidant and antiproliferative activities of Naviglio® extracts from *Schizogyne sericea* (Asteraceae). *Natural Product Research, 31*(5), 515–522. https://doi.org/10.1080/14786419.2016.1195383

Chen, F. P., Li, B. S., & Tang, C. H. (2015). Nanocomplexation between curcumin and soy protein isolate: Influence on curcumin stability/bioaccessibility and in vitro protein digestibility. *Journal of Agricultural and Food Chemistry, 63*(13), 3559–3569. https://doi.org/10.1021/acs.jafc.5b00448

Chentir, I., Kchaou, H., Hamdi, M., Jridi, M., Li, S., Doumandji, A., et al. (2019). Biofunctional gelatin-based films incorporated with food grade phycocyanin extracted from the Saharian cyanobacterium *Arthrospira sp*. *Food Hydrocolloids, 89*, 715–725. https://doi.org/10.1016/J.FOODHYD.2018.11.034

Cruz-Díaz, K., Cobos, Á., Fernández-Valle, M. E., Díaz, O., & Cambero, M. I. (2019). Characterization of edible films from whey proteins treated with heat, ultrasounds and/or transglutaminase. Application in cheese slices packaging. *Food Packaging and Shelf Life, 22*, Article 100397. https://doi.org/10.1016/j.fpsl.2019.100397

Dapčević-Hadnađev, T., Hadnađev, M., Lazaridou, A., Moschakis, T., & Biliaderis, C. G. (2018). Hempseed meal protein isolates prepared by different isolation techniques. Part II. gelation properties at different ionic strengths. *Food Hydrocolloids, 81*, 481–489. https://doi.org/10.1016/j.foodhyd.2018.03.022

Dawidowicz, A. L., Wianowska, D., & Olszowy, M. (2012). On practical problems in estimation of antioxidant activity of compounds by DPPH method (Problems in estimation of antioxidant activity). *Food Chemistry, 131*(3), 1037–1043. https://doi.org/10.1016/j.foodchem.2011.09.067

Del Baño, M. J., Lorente, J., Castillo, J., Benavente-García, O., Del Río, J. A., Ortuño, A., et al. (2003). Phenolic diterpenes, flavones, and rosmarinic acid distribution during the development of leaves, flowers, stems, and roots of *Rosmarinus officinalis*. Antioxidant activity. *Journal of Agricultural and Food Chemistry, 51*(15), 4247–4253. https://doi.org/10.1021/jf0300745

Dias, M. I., Barros, L., Barreira, J. C. M., Alves, M. J., Barracosa, P., & Ferreira, I. C. F. R. (2018). Phenolic profile and bioactivity of cardoon (*Cynara cardunculus* L.) inflorescence parts: Selecting the best genotype for food applications. March *Food Chemistry, 268*, 196–202. https://doi.org/10.1016/j.foodchem.2018.06.081.

Djeridane, A., Yousfi, M., Nadjemi, B., Boutassouna, D., Stocker, P., & Vidal, N. (2006). Antioxidant activity of some algerian medicinal plants extracts containing phenolic compounds. *Food Chemistry, 97*(4), 654–660. https://doi.org/10.1016/j.foodchem.2005.04.028

Eljounaidi, K., Comino, C., Moglia, A., Cankar, K., Genre, A., Hehn, A., et al. (2015). Accumulation of cynaropicrin in globe artichoke and localization of enzymes involved in its biosynthesis. *Plant Science, 239*, 128–136. https://doi.org/10.1016/j.plantsci.2015.07.020

Emam-Djomeh, Z., Moghaddam, A., & Yasini Ardakani, S. A. (2015). Antimicrobial activity of pomegranate (*Punica granatum* L.) peel extract, physical, mechanical, barrier and antimicrobial properties of pomegranate peel extract-incorporated sodium caseinate film and application in packaging for ground beef. *Packaging Technology and Science, 28*(10), 869–881. https://doi.org/10.1002/pts.2145

Fagnano, M., Impagliazzo, A., Mori, M., & Fiorentino, N. (2015). Agronomic and environmental impacts of giant reed (*Arundo donax* L.): Results from a long-term field experiment in hilly areas subject to soil erosion. *Bioenergy Research, 8*(1), 415–422. https://doi.org/10.1007/s12155-014-9532-7

Falleh, H., Ksouri, R., Chaieb, K., Karray-Bouraoui, N., Trabelsi, N., Boulaaba, M., et al. (2008). Phenolic composition of *Cynara cardunculus* L. organs, and their biological activities. *Comptes Rendus Biologies, 331*(5), 372–379. https://doi.org/10.1016/j.crvi.2008.02.008

Fathi, N., Almasi, H., & Pirouzifard, M. K. (2019). Sesame protein isolate based bionanocomposite films incorporated with TiO2 nanoparticles: Study on morphological, physical and photocatalytic properties. *Polymer Testing, 77*, Article 105919. https://doi.org/10.1016/j.polymertesting.2019.105919

Fernández, J., Curt, M. D., & Aguado, P. L. (2006). Industrial applications of *Cynara cardunculus* L. for energy and other uses. *Industrial Crops and Products, 24*(3), 222–229. https://doi.org/10.1016/J.INDCROP.2006.06.010

Floegel, A., Kim, D. O., Chung, S.-J., Koo, S. I., & Chun, O. K. (2011). Comparison of ABTS DPPH assays to measure antioxidant capacity in popular antioxidant-rich US foods. *Journal of Food Composition and Analysis, 24*, 1043–1048. https://doi.org/10.1016/j.jfca.2011.01.008

Fratianni, F., Tucci, M., Palma, M. De, Pepe, R., & Nazzaro, F. (2007). Polyphenolic composition in different parts of some cultivars of globe artichoke (*Cynara cardunculus* L. var. *scolymus* (L.) Fiori). *Food Chemistry, 104*(3), 1282–1286. https://doi.org/10.1016/j.foodchem.2007.01.044

Gallo, M., Formato, A., Giacco, R., Riccardi, G., Lungo, D., Formato, G., et al. (2019). Mathematical optimization of the green extraction of polyphenols from grape peels through a cyclic pressurization process. *Heliyon, 5*(4), Article e01526. https://doi.org/10.1016/j.heliyon.2019.e01526

Galus, S., & Kadzińska, J. (2016). Whey protein edible films modified with almond and walnut oils. *Food Hydrocolloids, 52*, 78–86. https://doi.org/10.1016/j.foodhyd.2015.06.013

Genovese, C., Platania, C., Venticinque, M., Calderaro, P., Argento, S., Scandurra, S., et al. (2016). Evaluation of cardoon seeds presscake for animal feeding. *Acta Horticulturae, 1147*, 323–328. https://doi.org/10.17660/ActaHortic.2016.1147.45

Giosafatto, C. V. L., Fusco, A., Al-Asmar, A., & Mariniello, L. (2020). Microbial transglutaminase as a tool to improve the features of hydrocolloid-based bioplastics, 2020, Vol. 21, Page 3656 *International Journal of Molecular Sciences, 21*(10), 3656. https://doi.org/10.3390/IJMS21103656.

Gominho, J., Dolores, M., Lourenço, A., Fernández, J., & Pereira, H. (2018). Biomass and bioenergy *Cynara cardunculus* L . as a biomass and multi-purpose crop : A review of 30 years of research. December 2017 *Biomass and Bioenergy, 109*, 257–275. https://doi.org/10.1016/j.biombioe.2018.01.001.

Gouveia, S. C., & Castilho, P. C. (2012). Phenolic composition and antioxidant capacity of cultivated artichoke, Madeira cardoon and artichoke-based dietary supplements. *Food Research International, 48*(2), 712–724. https://doi.org/10.1016/j.foodres.2012.05.029

Haghighi, H., Biard, S., Bigi, F., De Leo, R., Bedin, E., Pfeifer, F., et al. (2019). Comprehensive characterization of active chitosan-gelatin blend films enriched with different essential oils. *Food Hydrocolloids, 95*, 33–42. https://doi.org/10.1016/j.foodhyd.2019.04.019

Hanani, Z. A. N., Yee, F. C., & Nor-Khaizura, M. A. R. (2019). Effect of pomegranate (*Punica granatum* L.) peel powder on the antioxidant and antimicrobial properties of fish gelatin films as active packaging. *Food Hydrocolloids, 89*, 253–259. https://doi.org/10.1016/j.foodhyd.2018.10.007

Hebbar, R. S., Isloor, A. M., & Ismail, A. F. (2017). Contact angle measurements. In *Membrane characterization* (pp. 219–255). https://doi.org/10.1016/B978-0-444-63776-5.00012-7

Ierna, A., Sortino, O., & Mauromicale, G. (2020). Biomass, seed and energy yield of *Cynara cardunculus* L. As affected by environment and season, 2020, Vol. 10, Page 1548 *Agronomy*, *10*(10), 1548. https://doi.org/10.3390/AGRONOMY10101548.

Kukić, J., Popović, V., Petrović, S., Mucaji, P., Ćirić, A., Stojković, D., et al. (2008). Antioxidant and antimicrobial activity of *Cynara cardunculus* extracts. *Food Chemistry*, *107*(2), 861–868. https://doi.org/10.1016/j.foodchem.2007.09.005

Lattanzio, V., Kroon, P. A., Linsalata, V., Cardinali, A., Agro-ambientali, D. S., & Vegetale, D. (2009). Globe artichoke : A functional food and source of nutraceutical ingredients. *Journal of Functional Foods*, *1*(2), 131–144. https://doi.org/10.1016/j.jff.2009.01.002

Laufer, G., Kirkland, C., Cain, A. A., & Grunlan, J. C. (2013). Oxygen barrier of multilayer thin films comprised of polysaccharides and clay. *Carbohydrate Polymers*, *95*(1), 299–302. https://doi.org/10.1016/j.carbpol.2013.02.048

Mandim, F., Inês, M., Pinela, J., Barracosa, P., Ivanov, M., & Ferreira, I. C. F. R. (2020). Chemical composition and in vitro biological activities of cardoon (*Cynara cardunculus* L . var . *altilis* DC .) seeds as influenced by viability. November 2019 *Food Chemistry*, *323*, Article 126838. https://doi.org/10.1016/j.foodchem.2020.126838.

Mathe, C., Culioli, G., Archier, P., & Vieillescazes, C. (2004). Characterization of archaeological frankincense by gas chromatography-mass spectrometry. *Journal of Chromatography A*, *1023*(2), 277–285. https://doi.org/10.1016/j.chroma.2003.10.016

Mauromicale, G., Sortino, O., Pesce, G. R., Agnello, M., & Mauro, R. P. (2014). Suitability of cultivated and wild cardoon as a sustainable bioenergy crop for low input cultivation in low quality Mediterranean soils. *Industrial Crops and Products*, *57*, 82–89. https://doi.org/10.1016/J.INDCROP.2014.03.013

Mirpoor, S. F., Giosafatto, C. V. L., Di Pierro, P., Di Girolamo, R., Regalado-González, C., & Porta, R. (2020). Valorisation of *Posidonia oceanica* sea balls (egagropili) as a potential source of reinforcement agents in protein-based biocomposites. *Polymers*, *12*(12), 2788. https://doi.org/10.3390/polym12122788

Mirpoor, S. F., Giosafatto, C. V. L., & Porta, R. (2021). Biorefining of seed oil cakes as industrial co-streams for production of innovative bioplastics. A review. *Trends in Food Science & Technology*, *109*, 259–270. Retrieved from https://www.sciencedirect.com/science/article/pii/S0924224421000194.

Mirpoor, S. F., Hosseini, S. M. H., & Nekoei, A. R. (2017a). Efficient delivery of quercetin after binding to beta-lactoglobulin followed by formation soft-condensed core-shell nanostructures. *Food Chemistry*, *233*, 282–289. https://doi.org/10.1016/j.foodchem.2017.04.126

Mirpoor, S. F., Hosseini, S. M. H., & Youseft, G. H. (2017b). Mixed biopolymer nanocomplexes conferred physicochemical stability and sustained release behavior to introduced curcumin. *Food Hydrocolloids*, *71*, 216–224. https://doi.org/10.1016/j.foodhyd.2017.05.021

Moghadam, M., Salami, M., Mohammadian, M., Khodadadi, M., & Emam-Djomeh, Z. (2020). Development of antioxidant edible films based on mung bean protein enriched with pomegranate peel. *Food Hydrocolloids*, *104*, Article 105735. https://doi.org/10.1016/j.foodhyd.2020.105735

Mohammadian, M., Salami, M., Momen, S., Alavi, F., Emam-Djomeh, Z., & Moosavi-Movahedi, A. A. (2019). Enhancing the aqueous solubility of curcumin at acidic condition through the complexation with whey protein nanofibrils. *Food Hydrocolloids*, *87*, 902–914. https://doi.org/10.1016/J.FOODHYD.2018.09.001

Naviglio, D. (2003). Naviglio's principle and presentation of an innovative solid-liquid extraction technology: Extractor Naviglio®. *Analytical Letters*, *36*(8), 1647–1659. https://doi.org/10.1081/AL-120021555

Naviglio, D., Scarano, P., Ciaravolo, M., & Gallo, M. (2019). Rapid solid-liquid dynamic extraction (rslde): A powerful and greener alternative to the latest solid-liquid extraction techniques. *Foods*, *8*(7), 245. https://doi.org/10.3390/FOODS8070245, 2019, Vol. 8, Page 245.

Nur Hanani, Z. A., Aelma Husna, A. B., Nurul Syahida, S., Nor Khaizura, M. A. B., & Jamilah, B. (2018). Effect of different fruit peels on the functional properties of gelatin/polyethylene bilayer films for active packaging. *Food Packaging and Shelf Life*, *18*, 201–211. https://doi.org/10.1016/j.fpsl.2018.11.004

Ottaiano, L., Di Mola, I., Impagliazzo, A., Cozzolino, E., Maiucci, F., Mori, M., et al. (2017). Yields and quality of biomasses and grain in *Cynara cardunculus* L. grown in southern Italy, as affected by genotype and environmental conditions. *Italian Journal of Agronomy*, *12*(4), 375–382. https://doi.org/10.4081/ija.2017.954

Pandino, G., Lombardo, S., Mauromicale, G., & Williamson, G. (2011). Phenolic acids and flavonoids in leaf and floral stem of cultivated and wild *Cynara cardunculus* L. genotypes. *Food Chemistry*, *126*(2), 417–422. https://doi.org/10.1016/j.foodchem.2010.11.001

Panzella, L., Moccia, F., Nasti, R., Marzorati, S., Verotta, L., & Napolitano, A. (2020). Bioactive phenolic compounds from agri-food wastes: An update on green and sustainable extraction methodologies. May *Frontiers in Nutrition*, *7*, 1–27. https://doi.org/10.3389/fnut.2020.00060.

Pappalardo, H. D., Toscano, V., Puglia, G. D., Genovese, C., & Raccuia, S. A. (2020). March. *Cynara cardunculus L . As a multipurpose crop for plant secondary metabolites production in marginal stressed lands*, *11* pp. 1–14). https://doi.org/10.3389/fpls.2020.00240.

Pesce, G. R., Negri, M., Bacenetti, J., & Mauromicale, G. (2017). The biomethane, silage and biomass yield obtainable from three accessions of *Cynara cardunculus*. September 2016 *Industrial Crops and Products*, *103*, 233–239. https://doi.org/10.1016/j.indcrop.2017.04.003.

Petropoulos, S. A., Fernandes, Â., Tzortzakis, N., Sokovic, M., Ciric, A., Barros, L., et al. (2019). Bioactive compounds content and antimicrobial activities of wild edible Asteraceae species of the Mediterranean fl ora under commercial cultivation conditions. October 2018 *Food Research International*, *119*, 859–868. https://doi.org/10.1016/j.foodres.2018.10.069.

Pinelli, P., Agostini, F., Comino, C., Lanteri, S., Portis, E., & Romani, A. (2007). Simultaneous quantification of caffeoyl esters and flavonoids in wild and cultivated cardoon leaves. *Food Chemistry*, *105*(4), 1695–1701. https://doi.org/10.1016/j.foodchem.2007.05.014

Porta, R., Di Pierro, P., Roviello, V., & Sabbah, M. (2017). Tuning the functional properties of bitter vetch (*Vicia ervilia*) protein films grafted with spermidine. *International Journal of Molecular Sciences*, *18*(12). https://doi.org/10.3390/ijms18122658

Posadino, A. M., Biosa, G., Zayed, H., Abou-Saleh, H., Cossu, A., Nasrallah, G. K., et al. (2018). Protective effect of cyclically pressurized solid–liquid extraction polyphenols from cagnulari grape pomace on oxidative endothelial cell death. *Molecules*, *23*(9), 1–12. https://doi.org/10.3390/molecules23092105

Quan, T. H., Benjakul, S., Sae-leaw, T., Balange, A. K., & Maqsood, S. (2019). September 1). Protein–polyphenol conjugates: Antioxidant property, functionalities and their applications. *Trends in Food Science & Technology*, *91*, 507–517. https://doi.org/10.1016/j.tifs.2019.07.049

Ramos, P. A. B., Guerra, A. R., Guerreiro, O., Freire, C. S. R., Silva, A. M. S., Duarte, M. F., et al. (2013). Lipophilic extracts of *Cynara cardunculus* L. var. *altilis* (dc): A source of valuable bioactive terpenic compounds. *Journal of Agricultural and Food Chemistry*, *61*(35), 8420–8429. https://doi.org/10.1021/jf402253a

Ramos, P. A. B., Guerra, Â. R., Guerreiro, O., Santos, S. A. O., Oliveira, H., Freire, C. S. R., et al. (2017). Antiproliferative effects of *Cynara cardunculus* L. Var. *altilis* (DC) lipophilic extracts. *International Journal of Molecular Sciences*, *18*(1). https://doi.org/10.3390/ijms18010063

Ramos, P. A. B., Santos, S. A. O., Guerra, Â. R., Guerreiro, O., Freire, C. S. R., Rocha, S. M., et al. (2014). Phenolic composition and antioxidant activity of different morphological parts of *Cynara cardunculus* L. var. *altilis* (DC). *Industrial Crops and Products*, *61*, 460–471. https://doi.org/10.1016/j.indcrop.2014.07.042

Re, R., Pellegrini, N., Proteggente, A., Pannala, A., Yang, M., & Rice-Evans, C. (1999). Antioxidant activity applying an improved ABTS radical cation decolorization assay, 2007 *Free Radical Biology & Medicine*, *26*, 51.

Reynolds, W. F., McLean, S., Poplawski, J., Enriquez, R. G., Escobar, L. I., & Leon, I. (1986). Total assignment of 13C and 1H spectra of three isomeric triterpenol derivatives by 2D NMR: An investigation of the potential utility of 1H chemical shifts in structural investigations of complex natural products. *Tetrahedron*, *42*(13), 3419–3428. https://doi.org/10.1016/S0040-4020(01)87309-9

Riaz, A., Lei, S., Akhtar, H. M. S., Wan, P., Chen, D., Jabbar, S., et al. (2018). Preparation and characterization of chitosan-based antimicrobial active food packaging film incorporated with apple peel polyphenols. *International Journal of Biological Macromolecules*, *114*, 547–555. https://doi.org/10.1016/j.ijbiomac.2018.03.126

Rouphael, Y., Bernardi, J., Cardarelli, M., Bernardo, L., Kane, D., Colla, G., et al. (2016). Phenolic compounds and sesquiterpene lactones profile in leaves of nineteen artichoke cultivars. *Journal of Agricultural and Food Chemistry*, *64*(45), 8540–8548. https://doi.org/10.1021/acs.jafc.6b03856

Roy, S., & Rhim, J. W. (2020). Preparation of carbohydrate-based functional composite films incorporated with curcumin. *Food Hydrocolloids*, *98*, Article 105302. https://doi.org/10.1016/j.foodhyd.2019.105302

Roy, S., Rhim, J. W., & Jaiswal, L. (2019). Bioactive agar-based functional composite film incorporated with copper sulfide nanoparticles. *Food Hydrocolloids*, *93*, 156–166. https://doi.org/10.1016/j.foodhyd.2019.02.034

Sánchez-Gómez, R., Zalacain, A., Alonso, G. L., & Salinas, M. R. (2014). Vine-shoot waste aqueous extracts for re-use in agriculture obtained by different extraction techniques: Phenolic, volatile, and mineral compounds. *Journal of Agricultural and Food Chemistry*, *62*(45), 10861–10872. https://doi.org/10.1021/jf503929v

Sarıcaoglu, F. T., & Turhan, S. (2020). Physicochemical, antioxidant and antimicrobial properties of mechanically deboned chicken meat protein films enriched with various essential oils. *Food Packaging and Shelf Life*, *25*, Article 100527. https://doi.org/10.1016/j.fpsl.2020.100527

Scarano, P., Naviglio, D., Prigioniero, A., Tartaglia, M., Postiglione, A., Sciarrillo, R., et al. (2020). Sustainability: Obtaining natural dyes from waste matrices using the prickly pear peels of *Opuntia ficus-indica* (L.) miller, 2020, Vol. 10, Page 528 *Agronomy*, *10*(4), 528. https://doi.org/10.3390/AGRONOMY10040528.

Scavo, A., Pandino, G., Restuccia, C., Parafati, L., Cirvilleri, G., & Mauromicale, G. (2019). Antimicrobial activity of cultivated cardoon (*Cynara cardunculus* L. var. *altilis* DC.) leaf extracts against bacterial species of agricultural and food interest. December 2018 *Industrial Crops and Products*, *129*, 206–211. https://doi.org/10.1016/j.indcrop.2018.12.005.

Scavo, A., Rial, C., Varela, R. M., Molinillo, J. M. G., Mauromicale, G., & Macias, F. A. (2019). Influence of genotype and harvest time on the *Cynara cardunculus* L. Sesquiterpene lactone profile. *Journal of Agricultural and Food Chemistry*, *67*(23), 6487–6496. https://doi.org/10.1021/acs.jafc.9b02313

Shams, B., Ebrahimi, N. G., & Khodaiyan, F. (2019). Development of antibacterial nanocomposite: Whey protein-gelatin-nanoclay films with orange peel extract and tripolyphosphate as potential food packaging. *Advances in Polymer Technology*, *2019*. https://doi.org/10.1155/2019/1973184

Siddiqui, N., Rauf, A., Latif, A., & Mahmood, Z. (2017). Spectrophotometric determination of the total phenolic content, spectral and fluorescence study of the herbal Unani drug Gul-e-Zoofa (*Nepeta bracteata* Benth). *Journal of Taibah University Medical Sciences*, *12*(4), 360–363. https://doi.org/10.1016/j.jtumed.2016.11.006

Sobolev, A. P., Brosio, E., Gianferri, R., & Segre, A. L. (2005). Metabolic profile of lettuce leaves by high-field NMR spectra. *Magnetic Resonance in Chemistry*, *43*(8), 625–638. https://doi.org/10.1002/mrc.1618

Sun, K. Q., Li, F. Y., Li, J. Y., Li, J. F., Zhang, C. W., Chen, S., et al. (2019). Optimisation of compatibility for improving elongation at break of chitosan/starch films. *RSC Advances*, *9*(42), 24451–24459. https://doi.org/10.1039/c9ra04053f

Taghavi Kevij, H., Salami, M., Mohammadian, M., & Khodadadi, M. (2020). Fabrication and investigation of physicochemical, food simulant release, and antioxidant properties of whey protein isolate-based films activated by loading with curcumin through the pH-driven method. *Food Hydrocolloids, 108*, Article 106026. https://doi.org/10.1016/j.foodhyd.2020.106026

Toscano, V., Sollima, L., Genovese, C., Melilli, M. G., & Raccuia, S. A. (2016). *Pilot plant system for biodiesel and pellet production from cardoon : Technical and economic feasibility*. https://doi.org/10.17660/ActaHortic.2016.1147.60

Turco, R., Tesser, R., Cucciolito, M. E., Fagnano, M., Ottaiano, L., Mallardo, S., et al. (2019). Cynara cardunculus biomass recovery: An eco-sustainable, nonedible resource of vegetable oil for the production of poly(lactic acid) bioplasticizers. *ACS Sustainable Chemistry & Engineering, 7*(4), 4069–4077. https://doi.org/10.1021/acssuschemeng.8b05519

Velez, Z., Campinho, M. A., Guerra, Â. R., García, L., Ramos, P., Guerreiro, O., et al. (2012). Biological characterization of *Cynara cardunculus* l. Methanolic extracts: Antioxidant, anti-proliferative, anti-migratory and anti-angiogenic activities. *Agriculture, 2*(4), 472–492. https://doi.org/10.3390/agriculture2040472

6- Qazanfarzadeh, Z., **Mirpoor, S. F**., Kadivar, M., Shekarchizadeh, H., Di Girolamo, R., Giosafatto, C. V. L., Di Pierro, P., & Porta, R. (2021). Potential use of glycerol-and/or spermidine-plasticized secalin films as leaf surface coatings for sustainable plant disease management. *Journal of Cleaner Production*, *328*,129461 https://doi.org/10.1016/j.jclepro.2021.129461

Journal of Cleaner Production 328 (2021) 129461

Contents lists available at ScienceDirect

Journal of Cleaner Production

journal homepage: www.elsevier.com/locate/jclepro

Potential use of glycerol- and/or spermidine-plasticized secalin films as leaf surface coatings for sustainable plant disease management

Zeinab Qazanfarzadeh [a,b,1], Seyedeh Fatemeh Mirpoor [b,1], Mahdi Kadivar [a], Hajar Shekarchizadeh [a], Rocco Di Girolamo [b], C. Valeria L. Giosafatto [b,c,**], Prospero Di Pierro [b,c], Raffaele Porta [b,c,*]

[a] Department of Food Science and Technology, College of Agriculture, Isfahan University of Technology, Isfahan, Iran
[b] Department of Chemical Sciences, University of Naples "Federico II", Complesso Universitario di Monte Sant'Angelo, Naples, 80126, Italy
[c] Center for Studies on Bioinspired Agro-Environmental Technology (BAT), University of Naples "Federico II", Naples, Italy

ARTICLE INFO

Handling editor: M.T. Moreira

Keywords:
Secalin
Spermidine
Biodegradable film
Film-forming spray
Leaf coating

ABSTRACT

The effects of spermidine (SPD) on the properties of both secalin (SCL)-based film-forming solutions (FFSs) and their resultant films were studied in the absence or presence of glycerol (GLY) used as primary plasticizer. The average size of SCL particles significantly increased with the increase of SPD concentration, mainly in the presence of GLY, while the negative zeta potential values parallely decreased suggesting a greater stability of the FFSs containing SPD concentrations lower than 1.0 mM. In addition, the decreased contact angle value, compared to water and ethanol solution, indicated that SCL FFSs were highly hydrophobic and that it might be spreaded easily on hydrophobic biological surfaces. SPD could replace GLY in obtaining handleable, homogeneous and performing SCL-based films. The film tensile strength and the Young's module strongly increased in the absence of GLY, reaching values higher than 5 times with respect to controls, whereas elongation at break value of GLY-plasticized films containing 5.0 mM SPD was twice of that of the films prepared without SPD. Conversely, the film moisture content, water solubility and swelling ratio progressively decreased, both in the presence and absence of GLY, up to a SPD concentration of 1.0 mM, whereas the film contact angle increased, confirming the enhancement of its hydrophobicity determined by SPD incorporation. SPD also increased the film barrier properties to gases and water vapor, while the presence of GLY hindered these effects. Finally, SEM analysis of the cross-sections of the SPD containing films showed heterogeneous microstructures, whereas their surfaces appeared rougher than those of the control films. Preliminary experiments carried out by *Rosa chinensis* Jacq. leaf coating suggest the potential use of SCL-based FFSs spraying in plant disease control. High spreading of the SCL-based FFSs on the entire leaf surfaces, both in the presence and absence of Bordeaux mixture tested as agrochemical, was observed, and the SEM images showed the formation of an evident coating of the leaves. Therefore, these findings suggest the possibility to coat the leaf surface also *in vivo* with different SCL-based FFSs, giving rise to films possessing tailored functional properties and able to carry and release different agrochemicals.

1. Introduction

Renewable materials provide promising alternatives to conventional plastics, which cause serious environmental pollution (Porta, 2019). In fact, the replacement of synthetic polymers by bio-based and biodegradable macromolecules, obtained from different sources such as microorganisms, plants or animals, has become a highly attractive research trend (Reddy et al., 2013; Petkoska et al., 2021). Recently, the development of edible films and coatings has increasingly attracted the attention of both researchers and consumers, mainly as a consequence of the potential large variety of applications afforded by these materials and, among the different biopolymers used, polysaccharides and

* Corresponding author. Department of Chemical Sciences, University of Naples "Federico II", Complesso Universitario di Monte Sant'Angelo, Naples, 80126, Italy.
** Corresponding author. Department of Chemical Sciences, University of Naples "Federico II", Complesso Universitario di Monte Sant'Angelo, Naples, 80126, Italy.
E-mail addresses: giosafat@unina.it (C.V.L. Giosafatto), raffaele.porta@unina.it (R. Porta).
[1] Equally contributing authors.

https://doi.org/10.1016/j.jclepro.2021.129461
Received 7 April 2021; Received in revised form 5 October 2021; Accepted 22 October 2021
Available online 25 October 2021
0959-6526/© 2021 Elsevier Ltd. All rights reserved.

proteins are the most common group of macromolecules under investigation as food packaging systems (Petkoska et al., 2021; Galus et al., 2020). More in particular, there is a great research effort focused on developing and investigating new film formulations in which novel components and additives are used, as well as on processing systems to optimize the composition and the functional properties of tailored edible films and coatings (Galus et al., 2020; Zink et al., 2016). An important research trend in this field is the development of inexpensive biopolymer sources as well as of additives as potential new components of film matrices (Galus et al., 2020). Composite films generally derive from the combination of multiple film-forming substances and additives with the aim to obtain structures with better physical, mechanical and/or barrier properties, for specific applications, than those exhibited by the material made with only one basic component (Galus et al., 2020; Bealer et al., 2020). Thus, various compounds, such as plasticizers, crosslinkers, reinforcement agents or emulsifiers are added to the film-forming formulation to improve the basic functionality of the material. Also different bioactive substances, such as antimicrobials, antioxidants, nutraceuticals or color and flavor agents may be incorporated into film-forming solutions (FFSs) to improve the quality, stability and safety of packed products (Azeredo and Waldron, 2016; Galus et al., 2020; Kouhi et al., 2020; Kritchenkov et al., 2020; Petkoska et al., 2021; Tyagi and Bhattacharya, 2019). Furthermore, being the protein-based films quite hydrophilic, various types of oils and fats, such as waxes, essential oils, triglycerides or free fatty acids, are often incorporated into the protein hydrocolloid matrix to reduce their water vapor (WV) permeability (Reichert et al., 2020).

Secalin (SCL), an alcohol soluble protein fraction extracted from rye grains, has been recently studied and its interesting functional properties and capability to give rise to edible films have been highlighted (Qazanfarzadeh et al., 2020, 2021a, 2021b). Consequently, its potential use both as protein additive in food preparations and as low cost biosource of edible packaging materials has been suggested. In the present paper the effects of the addition of spermidine (SPD; N-(3-aminopropyl)-1,4-diaminobutane) to the SCL FFSs and the physicochemical properties of the derived edible films were investigated. SPD is a small aliphatic polycation widely distributed in varying concentrations in different unicellular microorganisms and higher eukaryotes (Gevrekci, 2017). This biogenic polyamine is positively charged under pH 8, which enables its interaction under physiological conditions with polyanionic molecules and, thus, it can readily bind to acidic sites on cellular components, including nucleic acids, proteins and membranes. In addition to a multitude of biological functions suggested for polyamines, including the protective effects on the membrane structure/function and on the nucleic acid structure and stability, SPD is also gathering an increasing attention in biotechnology. SPD was recently used in manufacturing carbon fiber surfaces (Bäumgartner et al., 2017) and films produced with both proteins (Porta et al., 2017; Sabbah et al., 2017) and polysaccharides (Esposito et al., 2016; Sabbah et al., 2019) potentially useful as coating materials. In fact, the low toxicity of SPD, attested by an acute oral toxicity of 600 mg/kg in rats (Til et al., 1997) would allow its presence as additive at low concentrations into hydrocolloid FFSs to prepare safe coatings. Therefore, the present study was aimed not only to produce and characterize SPD containing SCL films, but also to investigate the possibility to give rise with glycerol- (GLY) and/or SPD-plasticized SCL films to leaf surface coatings finalized to the time-releasing of agrochemicals for the control of pests and disease. In fact, it has been reported that around 4 million tons of pesticides are applied worldwide each year and it is estimated that at least 90% of the total amount of the applied pesticides do not reach their final target (Zhang, 2018). Conversely, most of their amount is wasted through spray drift, off target deposition, leaching into the soil, as well as due to the wind, run-off, evaporation, photodegradation and microbial activity (Castro et al., 2014). Thus, there is an urgent need for innovative managements of plant disease solutions and to improve the resiliency of agriculture globally. The approaches adopted thus far to overcome the negative impacts of the agrochemicals include, other than precision agriculture (Mahlein et al., 2012), the use of biopesticides (Lorsbach et al., 2019), encapsulating agents (Nuruzzaman et al., 2016) and seed coatings (Farias et al., 2019). Therefore, a leaf coating with a protein-based film forming solution containing low amounts of agrochemicals might represent an innovative green technology for plant disease control.

2. Materials and methods

2.1. Materials

SCL was extracted from rye flour (*Secale cereale* L. cv. Danko) using aqueous solution of 70% (w/w) ethanol containing 2% (w/w protein) sodium metabisulfite as previously described (Qazanfarzadeh et al., 2020), whereas SPD hydrochloride was purchased from Sigma Chemical Co. (MO, USA). *Rosa chinensis* Jacq. leaves were cut off from plants purchased from a local plant nursery and tested within 30 min. Bordeaux mixture (BM), containing the same amount of pentahydrated $CuSO_4$ and $Ca(OH)_2$, was obtained from a local farmers market. All other reagents and solvents were of the highest purity available from Carlo Erba (Milan, Italy).

2.2. Secalin-based film forming solution and film preparation

FFSs were prepared by dispersing SCL (7.0%, w/v) in an aqueous ethanol solution (70%, w/w), then adjusting the pH to 10 by 0.5 N NaOH, and finally stirring the solution at 60 °C by a magnetic heating stirrer for 30 min. SPD and or BM were then added at different concentrations to FFS aliquots (10 mL) and incubated at 60 °C for 30 min. Where indicated, after cooling down at room temperature GLY (20% w/w protein) was added to the FFS samples under continuous stirring for further 30 min and all FFSs were then cast into polyester Petri dishes (8 cm diameter) and finally dried at 25 °C and 45% RH for 12 h. The obtained films were conditioned in a glass chamber containing saturated magnesium nitrate solution for 24 h before to be analyzed. The film average thickness was measured using an electronic digital micrometer (IP65 Alpa Metrology Co., Pontoglio, Italy, sensitivity 0.001 mm).

2.3. Zeta potential and particle size measurements of film forming solutions

The effect of different concentrations of either SPD or BM on both zeta potential and the mean hydrodynamic diameter (Z-average) of the SCL FFSs, prepared in the presence or absence of GLY, were studied using a zeta-sizer (Nano-ZSP, Malvern, Worcestershire, UK). All the measurements were carried out on the FFSs were previously diluted, by using ethanol solution (70% w/w) at pH 10, to obtain 1 mg/mL concentrations of SCL.

2.4. Determination of contact angle of film forming solutions

The hydrophobicity or hydrophilicity behavior of the FFSs was determined using a homemade goniometer. Either parafilm (Bemis Co., Inc., Neenah, WI, USA) strips or *Rosa chinensis* Jacq. leaves, used as hydrophobic surfaces, were placed on the horizontal stage and 10 μl of each FFS were dropped on their surface. The image of each FFS drop was captured using a fixed digital microscopic camera (PS Pro, China) immediately and at different times (0.5–5 min) and the angles between FFS drops and the parafilm or leaf surfaces were then measured using ImageJ software. Five measurements of the contact angle of each sample were reported as the average of hydrophobicity of the different FFSs.

2.5. Film opacity and mechanical properties

The transparency of the different films was determined by using a

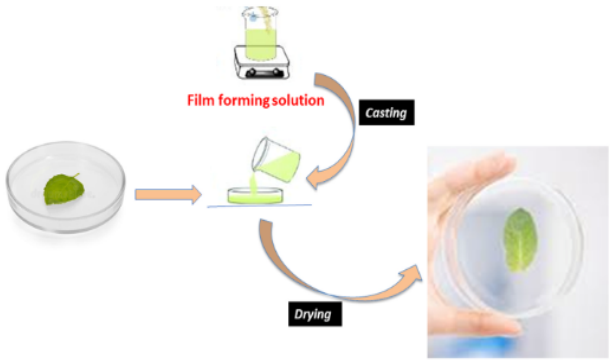

Fig. 1. Leaf coating by casting and drying with secalin-based film forming solutions.

previously described method (Galus et al., 2016). The film samples were cut into rectangular strips (1 cm × 4 cm) and placed on the inner side of the transparent plastic cuvette. Light absorption at a wavelength of 600 nm was measured using an UV-VIS spectrophotometer (Santa Clara, CA, USA) by an empty test cuvette as a blank. Opacity of the films was calculated as following equation:

$$\text{Opacity} = A_{600\ nm}/t \quad (1)$$

Where A_{600nm} is the absorbance at 600 nm and t is the film thickness (mm).

Film tensile strength (TS), elongation at break (EB) and Young's modulus (YM) were determined according to the ASTM D882-18 method (1998) using an Instron universal testing instrument (Model 5543 A, Instron Engineering Corp., Norwood, MA, USA). Film strips were cut (1 cm × 8 cm) and placed between two grips of the instrument. The initial grip separation and crosshead speed were set to 40 mm and 5 mm/min, respectively.

2.6. Film hydrophilicity

Moisture content, swelling ratio, and water solubility of the film samples were analyzed as previously described (Roy and Rhim, 2020). Moisture content was measured by weighing the film samples (2 cm × 2 cm) before and after drying in oven at 105 °C for 24 h. Moisture content was calculated as the percentage of the dried film weight with respect to the initial weight of the film.

In order to determine the water solubility, the initial weight (W_i) of the film samples (2 cm × 2 cm) was determined by their drying in the oven at 60 °C for 24 h. The dried samples were then immersed in 30 mL of distilled water and stirred in a shaker incubator (Kühner Shaker, ISF-1-W, Basel, Switzerland) at 25 °C for 24 h. The final weight (W_f) was obtained by drying the insoluble film samples in the oven at 105 °C for another 24 h. Finally, water solubility was calculated using the following equation:

$$\text{Water solubility (\%)} = (W_i - W_f) \times 100/W_i \quad (2)$$

Swelling ratio of the films was determined by weighing the film samples (2 cm × 2 cm) (W_i) and immersing them in 30 mL distilled water at 25 °C for 1 h. Then, the surface water of the films was dried with absorbent paper and the films were weighed again (W_s). Film swelling ratio was calculated using the following equation:

$$\text{Swelling ratio (\%)} = (W_s\text{-}W_i) \times 100/W_i \quad (3)$$

The surface hydrophobicity of the films was measured using a homemade water contact angle analyzer. Film strips were placed on the horizontal stage and 10 μl of distilled water was dropped on the surface of each film. The images of the water drop were captured using a fixed digital microscopic camera (PS Pro, China) after 30 s and the angles between water drop and film surfaces were measured using ImageJ software. The mean values of contact angles were measured carefully from five drops for the upper side of each film.

2.7. Film water vapor and gas permeability

WV permeability was measured gravimetrically according to the ASTM E96/E96M-16 method (1995) using glass cups (4.5 cm height and 1.5 cm diameter) containing 3 g anhydrous calcium chloride. The surface of the cups was covered and sealed with the film samples. The initial weight of the cups with their contents was measured and then placed in a desiccator containing 1 L distilled water at 25 °C. The weight changes of the cups were measured every 12 h during one week, in order to obtain WV transmission rate (WVTR; g/s), and WV permeability (g m/Pa s m2) was calculated according to the following equation:

$$\text{WV permeability} = (\text{WVTR} \times X)/A\ \Delta P \quad (4)$$

where X is the film thickness (m), A is the exposed area of the film (m^2) and ΔP is the partial WV pressure difference (Pa).

The film permeability to both O_2 and CO_2 was measured according to the modified ASTM D3985-17 method (1995) using a MultiPerm instrument (ExtraSolutions s.r.l., Pisa, Italy). Duplicates of each film sample were conditioned for 48 h at 50% RH. Aluminum masks were used to reduce the film test area to 2 cm^2. The analysis was performed at 25 °C and 50% RH.

2.8. Bordeaux mixture spraying onto Rosa chiniensis Jacq. leaves

Both BM aqueous and 70% ethanol/water solutions (1% w/v) were sprayed vertically on different leaves of *Rosa chiniensis* Jacq. employing a plastic container with a dip tube diameter of 1.2 mm and an aperture size of 0.3 mm. The spray angle produced was about 80° and the amount of the sprayed solution was about 0.1 mL. The leaves were subsequently dried at 25 °C without forced air convection and the images of each leaf surface were captured also using a fixed digital microscopic camera (PS Pro, China) for magnification.

2.9. Rosa chiniensis Jacq. leaf coating

The leaves from *Rosa chiniensis* Jacq. were washed by dipping in distilled water, immediately after their cutting, and then placed into

Table 1
Effect of different concentrations of spermidine (SPD) on Z-average and zeta potential of secalin (700 mg) film forming solutions prepared at pH 10 in the absence or presence of 20% glycerol (GLY).

Addition	GLY	Z-Average (*d. nm*)	Zeta Potential (*mV*)	PDI
None	+	262.9 ± 5.9 ^{a}	−50.9 ± 1.4 ^{a}	0.25 ± 0.03 ^{a}
	-	284.3 ± 7.6 ^{a}	−48.9 ± 1.8 ^{a}	0.24 ± 0.04 ^{a}
SPD (*0.05 mM*)	+	286.7 ± 1.8 ^{a,b,c}	−34.6 ± 1.6 ^{b}	0.41 ± 0.03 ^{b}
	-	304.7 ± 9.8 ^{b,c}	−24.9 ± 3.5 ^{c}	0.41 ± 0.01 ^{b}
SPD (*0.1 mM*)	+	284.1 ± 5.5 ^{a,c}	−23.1 ± 3.4 ^{c}	0.40 ± 0.05 ^{b}
	-	317.8 ± 4.9 ^{b,c,d}	−19.4 ± 1.6 ^{d}	0.31 ± 0.01 ^{a}
SPD (*1.0 mM*)	+	291.8 ± 3.2 ^{a,b,c}	−15.4 ± 0.9 ^{c}	0.73 ± 0.08 ^{c}
	-	326.6 ± 6.7 ^{b,d}	−10.3 ± 1.0 ^{f,g,h}	0.79 ± 0.04 ^{c,d}
SPD (*5.0 mM*)	+	302.0 ± 7.5 ^{a,b,c}	−11.7 ± 0.4 ^{h}	0.82 ± 0.02 ^{d,e}
	-	346.6 ± 4.7 ^{d}	−8.5 ± 0.7 ^{f,g}	0.91 ± 0.05 ^{f}
SPD (*10 mM*)	+	306.8 ± 8.3 ^{b,c}	−10.9 ± 0.3 ^{g,h}	0.86 ± 0.05 ^{e,f}
	-	623.5 ± 23.6 ^{e}	−7.8 ± 0.5 ^{f}	1 ^{g}
SPD (*20 mM*)	+	468.5 ± 23.8 ^{f}	−9.1 ± 0.1 ^{f,g,h}	1 ^{g}
	-	1014.1 ± 69.6 ^{g}	−4.2 ± 0.2 ^{i}	1 ^{g}

*Different small letters (a-h) indicate significant differences among the values reported in each column ($p < 0.05$). Further experimental details are given in the text.

Table 2
Contact angle (θ) on parafilm surface of water, aqueous ethanol solution (70%) and secalin (SCL, 700 mg) film forming solutions prepared at pH 10 in the absence or presence of 20% glycerol (GLY) and different spermidine (SPD) concentrations.

Sample	+GLY (*time 0*)	+GLY (*after 0.5 min*)	-GLY (*time 0*)	-GLY (*after 0.5 min*)
Water	96.95 ± 0.50 ^{a}	95.95 ± 0.78 ^{a}	105.06 ± 1.36 ^{a}	102.98 ± 0.87 ^{a}
70% Ethanol	39.25 ± 0.10 ^{b}	36.45 ± 0.21 ^{b}	47.07 ± 1.23 ^{b}	43.37 ± 1.44 ^{b}
SCL	31.01 ± 0.06 ^{c,d}	28.17 ± 0.67 ^{c}	25.85 ± 0.80 ^{c,d}	24.67 ± 0.65 ^{c}
SCL + SPD (*0.05 mM*)	29.57 ± 0.77 ^{d}	25.46 ± 1.61 ^{c}	24.43 ± 0.45 ^{d,e}	19.34 ± 0.97 ^{d}
SCL + SPD (*0.1 mM*)	30.19 ± 0.91 ^{c,d}	26.06 ± 0.62 ^{c}	22.16 ± 0.46 ^{e,f}	18.46 ± 0.61 ^{d,e}
SCL + SPD (*1.0 mM*)	30.21 ± 0.79 ^{c,d}	26.20 ± 1.24 ^{c}	19.40 ± 1.14 ^{f,g}	14.04 ± 1.30 ^{f,g}
SCL + SPD (*5.0 mM*)	30.67 ± 0.57 ^{c,d}	25.88 ± 2.21 ^{c}	17.48 ± 1.09 ^{g}	12.15 ± 0.41 ^{g}
SCL + SPD (*10 mM*)	31.76 ± 1.30 ^{c}	26.32 ± 0.54 ^{c}	17.90 ± 0.89 ^{g}	16.21 ± 1.26 ^{e,f}
SCL + SPD (*20 mM*)	31.21 ± 0.62 ^{c,d}	26.62 ± 0.86 ^{c}	28.13 ± 1.11 ^{c}	23.79 ± 1.05 ^{c}

*Different small letters (a-g) indicate significant differences among the values reported in each column ($p < 0.05$). Further experimental details are given in the text.

Petri dishes, with their under surface well fixed by a double face tape. SCL-based FFSs, prepared as described above and containing 20% GLY and/or 1 mM SPD, were added or not with 0.2% (w/v) BM and then cast into the Petri dishes (8 cm diameter) by completely covering the upper surface of the leaves (Fig. 1). The Petri dishes were finally placed in the climatic chamber and the FFSs were dried at 25 °C and 45% RH for 12 h. The obtained films were conditioned in a glass chamber containing saturated magnesium nitrate solution for additional 12 h before the analyses of the coated and uncoated leaves by SEM.

2.10. Scanning electron microscopy

The surface microstructure and cross-section images of the prepared films were examined using a field emission scanning electron microscope (FE-SEM, FEI Nova NanoSEM450, Thermo Fisher, Scientific, MA, USA). In order to prepare the films for cross-sectional analysis, the film samples were cryo-fractured in liquid nitrogen or were gently cut with a razor blade in the case of *Rosa chinensis* Jacq. leaves. The samples were then coated with a thin layer of gold-palladium alloy using a vacuum sputter coater and observed at different magnifications with an accelerating voltage of 5 kV by using an ETD detector.

2.11. Statistical analysis

The effect of the spermidine in the presence or absence of GLY on the SCL-based film properties was analyzed in a completely randomized design with three replications. In order to determine the significant difference between treatments, one-way analysis of variance (ANOVA) and Duncan's multiple range tests ($p < 0.05$) were done using the Statistical Package for the Social Sciences (SPSS19, SPSS Inc., Chicago, IL, USA) software.

3. Results and discussion

3.1. Effect of spermidine on zeta potential, particle size and contact angle of secalin film forming solutions

Previous studies reported that alkaline pH was optimal for preparing SCL-based films (Qazanfarzadeh et al., 2020) and, since the pKa values of the triamine SPD are in the range of pH 8–11, SPD could be able to link to SCL at alkaline pH basically both through hydrogen bonds and hydrophobic interactions (Esposito et al., 2016; Porta et al., 2017). Moreover, it is worthy to note that intermolecular hydrogen bonds between GLY and protein electronegative atoms might decrease the interaction between SPD and SCL. Therefore, the effects of different SPD concentrations on zeta potential and Z-average size of the particles occurring in the SCL FFSs were investigated at pH 10 both in the presence and absence of GLY.

As shown in Table 1, the average size of SCL particles significantly increased with the increase of SPD concentration, both in the absence and presence of GLY, even though the observed enhancements were more marked in the FFSs prepared without GLY.

Further analyses showed that also the zeta potential values of the SCL FFS were significantly affected by the addition of increasing SPD amounts, both in the absence and presence of GLY, since the negative zeta potential values decreased parallelly with the enhancement of SPD concentration. However, the measurement of the polydispersity index (PDI) values, showing the width of molecular weight distributions in the different samples, suggested a greater stability of the FFSs containing SPD concentrations lower than 1.0 mM (PDI <0.7) whereas, in the presence of higher SPD amounts, the PDI >0.7 signaled the presence of highly polydisperse samples with multiple particle size populations.

With the aim to investigate the effect of SPD on the hydrophobicity of SCL FFS for its possible use in coating applications, the contact angle of the different SCL FFSs was measured by using a parafilm surface. As reported in Table 2, SCL FFS showed a significantly decreased contact angle value at time 0 and after 0.5 min, compared to water and ethanol solution, both in the absence and presence of GLY. These data demonstrated that SCL FFS was highly hydrophobic and, thus, that it might be spreaded easily also on hydrophobic biological surfaces.

Furthermore, Table 2 indicates that such a feature was significantly amplified by increasing SPD concentrations in the FFS up to 5.0 mM, even though only in the absence of GLY. Fig. 2 shows the images of the spread of the drops of SCL FFSs containing or not 1.0 mM SPD and 20% GLY.

The higher hydrophobicity of the SCL FFS prepared in the presence of SPD might be due to the decreased polarity of SCL following the interaction of SPD, probably hindered by GLY, with reactive groups present in the protein lateral chains. This explanation is in agreement with the results reported in Table 1 indicating a higher decrease of the negative zeta potential values observed by analyzing the SCL FFS

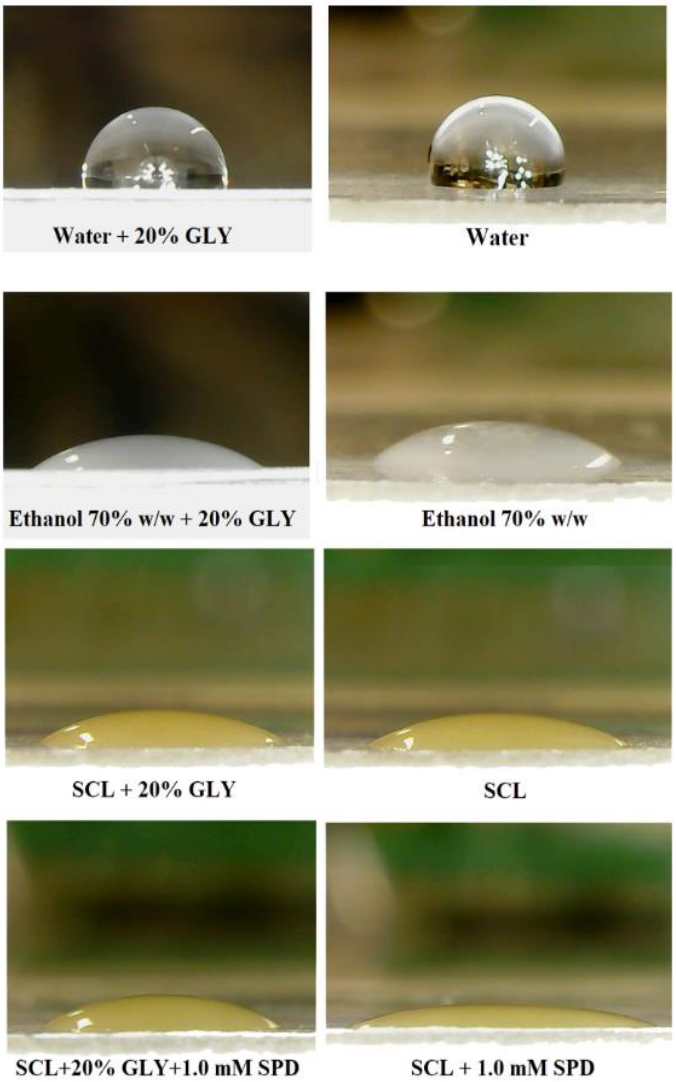

Fig. 2. Images of drops of secalin (SCL) film forming solutions (FFSs) on parafilm surfaces captured using a fixed digital microscopic camera after 0.5 min. FFSs were prepared at pH 10 in the absence or presence of glycerol (GLY) and/or spermidine (SPD). Drops of both distilled water and aqueous ethanol solution containing or not 20% GLY were used as control. Further experimental details are given in the text.

prepared in the presence of SPD but in the absence of GLY.

All these findings suggest a possible application of SPD-containing SCL FFS to coat high-fat foods, such as dairy products and nuts, or to vehicle pesticides, antimicrobial and repellents onto the hydrophobic and superhydrophobic fruit and leaf surfaces to protect plants against insects, worms, fungi, microbes, and other pathogens (Walters, 2006; Koch and Barthlott, 2009; Valdes et al., 2017; Pirzada et al., 2020; Spielman-Sun et al., 2020).

3.2. Macro and micro-structure of secalin-based films containing spermidine

The ability of SCL to give rise to GLY-plasticized films has been recently demonstrated (Qazanfarzadeh et al., 2020). In the attempt to improve the performances of SCL-based films, FFSs prepared at pH 10 in the presence of different SPD concentrations, both with and without GLY, were cast and the obtained films were analyzed. Fig. 3 shows that

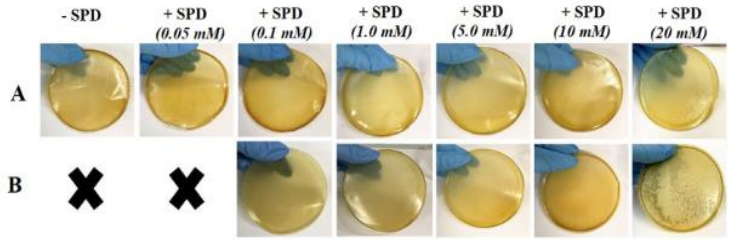

Fig. 3. Secalin-based films obtained at pH 10 in the presence (A) or absence (B) of 20% glycerol and different spermidine (SPD) concentrations. X indicates not handleable brittle films. Further experimental details are given in the text.

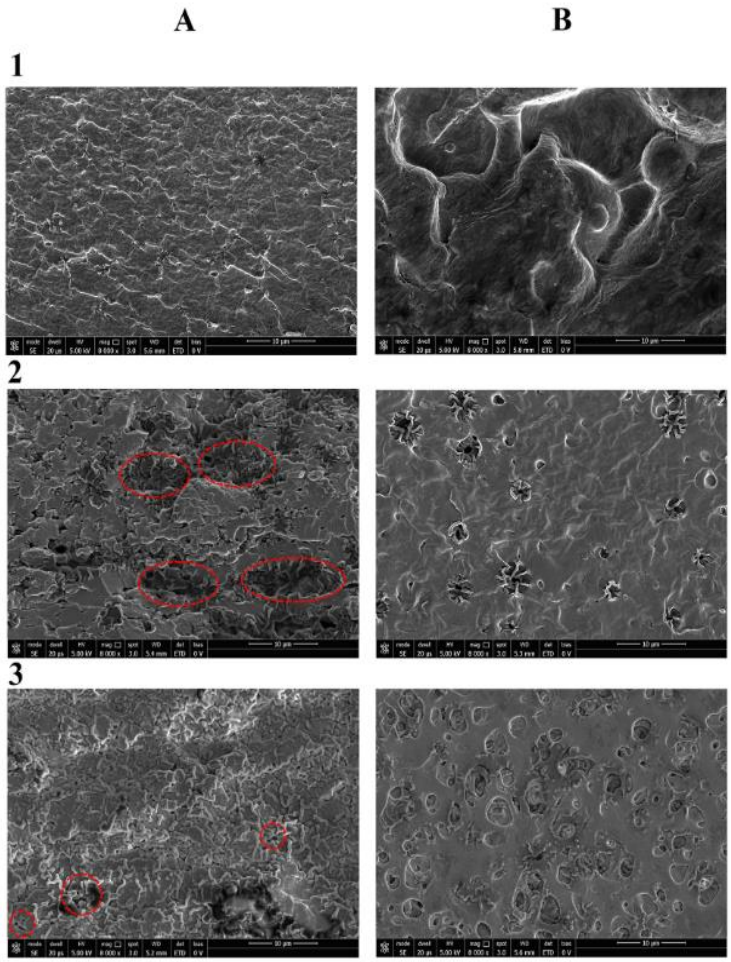

Fig. 4. Images of SEM cross-sections (panels A, at 8000 ×) and surfaces (panels B, at 8000 ×) of secalin-based films containing 20% glycerol (A1-2; B1-2) and/or 1 mM spermidine (A2-3; B2-3). The observed microvoids are circled in red. Further experimental details are given in the text.

Table 3
Opacity, thickness and mechanical properties of secalin-based films (700 mg) obtained at pH 10 in the absence or presence of 20% glycerol (GLY) and different concentrations of spermidine (SPD)*.

Addition	GLY	Opacity (mm^{-1})	Thickness (μm)	Mechanical properties		
				TS (MPa)	EB (%)	YM (MPa)
None	+	7.35 ± 0.85 ^{a}	93.8 ± 1.3 ^{a}	3.83 ± 0.27 ^{a}	102.84 ± 5.06 ^{a}	242.2 ± 6.2 ^{a}
	-	ND	ND	ND	ND	ND
SPD (0.05 mM)	+	7.43 ± 0.15 ^{a}	105.3 ± 1.5 ^{b}	2.82 ± 0.17 ^{b}	125.91 ± 5.11 ^{b}	184.9 ± 17.2 ^{b}
	-	ND	ND	ND	ND	ND
SPD (0.1 mM)	+	8.53 ± 0.26 ^{a}	112.7 ± 2.3 ^{c}	2.46 ± 0.16 ^{b}	173.15 ± 4.28 ^{c}	83.8 ± 3.0 ^{c}
	-	10.20 ± 0.87 ^{b}	82.2 ± 1.0 ^{d}	16.39 ± 0.92 ^{c}	1.17 ± 0.02 ^{d}	1662.9 ± 20.5 ^{d}
SPD (1.0 mM)	+	10.32 ± 0.38 ^{b}	128.2 ± 1.6 ^{e}	2.31 ± 0.20 ^{b}	188.55 ± 6.03 ^{e}	42.4 ± 2.7 ^{e,c}
	-	13.22 ± 0.34 ^{c}	86.2 ± 1.3 ^{f}	19.86 ± 1.79 ^{d}	1.62 ± 0.09 ^{d}	1758.6 ± 28.5 ^{f}
SPD (5.0 mM	+	14.99 ± 0.38 ^{d}	131.0 ± 1.0 ^{g}	0.87 ± 0.06 ^{e}	206.21 ± 5.00 ^{f}	36.4 ± 2.3 ^{e}
	-	17.41 ± 0.27 ^{e}	90.2 ± 1.3 ^{h}	17.63 ± 1.14 ^{f}	1.85 ± 0.07 ^{d}	1712.4 ± 21.6 ^{g}
SPD (10 mM)	+	15.00 ± 0.22 ^{d}	132.8 ± 0.8 ^{g,i}	0.13 ± 0.01 ^{e}	95.17 ± 0.45 ^{g}	27.4 ± 0.9 ^{e}
	-	18.90 ± 0.10 ^{f}	94.0 ± 1.0 ^{a}	14.93 ± 0.91 ^{g}	2.33 ± 0.34 ^{d}	1688.6 ± 63.5 ^{d,g}
SPD (20 mM)	+	16.65 ± 0.47 ^{e}	134.2 ± 1.3 ^{i}	0.10 ± 0.09 ^{e}	82.92 ± 4.07 ^{h}	24.2 ± 2.3 ^{e}
	-	20.86 ± 0.70 ^{g}	96.0 ± 0.5 ^{a}	7.34 ± 0.32 ^{h}	2.96 ± 0.04 ^{d}	1369.3 ± 49.2 ^{h}

*Different small letters (a-i) indicate significant differences among the values reported in each column ($p < 0.05$). ND, not detectable. Further experimental details are given in the text.

Table 4
Effect of spermidine (SPD) on different parameters of hydrophilicity of secalin-based films obtained at pH 10 in the absence or presence of 20% glycerol (GLY)*.

Addition	GLY	Moisture content (%)	Solubility (%)	Swelling ratio (%)	Contact angle (θ)
None	+	15.34 ± 0.91 ^{a}	49.33 ± 1.42 ^{a}	308.17 ± 9.80 ^{a}	46.45 ± 1.59 ^{a}
	-	ND	ND	ND	ND
SPD (0.05 mM)	+	14.39 ± 0.38 ^{a,b}	46.45 ± 1.59 ^{a}	274.09 ± 12.65 ^{b,c}	47.59 ± 2.65 ^{a,b}
	-	ND	ND	ND	ND
SPD (0.1 mM)	+	13.09 ± 1.03 ^{b,c}	39.69 ± 2.23 ^{b}	231.78 ± 17.57 ^{d,c}	46.12 ± 0.95 ^{a}
	-	10.41 ± 0.54 ^{d,e}	27.07 ± 1.06 ^{c,d}	195.53 ± 6.83 ^{f}	49.65 ± 0.65 ^{a,b}
SPD (1.0 mM)	+	11.39 ± 0.43 ^{d,e,f}	24.12 ± 1.62 ^{d,e}	218.61 ± 9.54 ^{e,f}	49.85 ± 1.06 ^{a,b}
	-	10.17 ± 0.45 ^{e}	22.72 ± 2.38 ^{e}	163.59 ± 10.28 ^{g}	55.32 ± 1.45 ^{e,d}
SPD (5.0 mM)	+	13.03 ± 0.93 ^{b,c}	22.97 ± 0.90 ^{e}	139.91 ± 4.75 ^{g,h}	51.29 ± 1.65 ^{b,d}
	-	11.64 ± 0.44 ^{c,f}	19.14 ± 1.15 ^{f}	121.57 ± 15.24 ^{h}	56.36 ± 0.85 ^{e}
SPD (10 mM)	+	14.49 ± 0.24 ^{a}	31.54 ± 0.73 ^{g}	261.58 ± 22.94 ^{e,d}	49.25 ± 0.56 ^{a,b}
	-	12.37 ± 0.41 ^{c,f}	23.54 ± 0.73 ^{e}	227.22 ± 11.33 ^{c}	56.02 ± 1.41 ^{e}
SPD (20 mM)	+	15.48 ± 0.63 ^{a}	39.06 ± 1.35 ^{b}	298.18 ± 16.72 ^{a,b}	50.01 ± 1.04 ^{a,b}
	-	12.85 ± 0.28 ^{c}	28.42 ± 0.88 ^{e,g}	244.13 ± 16.79 ^{e,d,c}	55.58 ± 0.91 ^{e,d}

*Different small letters (a-h) indicate significant differences among the values reported in each column ($p < 0.05$). ND, not detectable. Further experimental details are given in the text.

handleable SCL-based films were produced also in the absence of GLY, used as plasticizer, by adding at least 0.1 mM SPD. All films, except those prepared at high SPD concentrations, appeared visually homogenous, with a yellowish color quite similar to the GLY-plasticized films normally obtained in the absence of SPD. These findings were in agreement with previous data indicating that SPD could act as a primary plasticizer for both pectin-based and bitter vetch protein-based films (Porta et al., 2017; Sabbah et al., 2017, 2019).

The microstructure of the SCL-based films prepared in the absence or presence of 1.0 mM SPD, as well as of 20% GLY, is shown in Fig. 4. SEM analysis of the cross-sections of the films containing SPD, both with (A2) and without (A3) GLY, showed a more heterogeneous microstructure, compared to the counterpart obtained in the absence of SPD (A1), with microvoids formed near the fractured surfaces.

In addition, also the surfaces of films containing SPD (B2-3) appeared rougher compared to the one of the control film (B1), and all these differences resulted more marked in the SPD-containing films prepared in the absence of GLY (B3), indicating an interfering role played by the plasticizer on the SPD structuring effect of the biopolymer matrix.

3.3. Effect of spermidine on the opacity, thickness and mechanical properties of secalin-based films

The results reported in Table 3 showed that the opacity of SCL-based films increased significantly when SPD was added to the FFS both in the presence and absence of GLY, even though all the films prepared in the presence of plasticizer were always more transparent. This effect, due to a significant decrease in the light transmission observed in the SPD-containing films, could be explained by the more heterogeneous structure of the biopolymer matrix produced by SPD through both hydrogen and hydrophobic interactions with SCL. These interactions were partially hindered by GLY, as indicated by the SEM cross-section images showing more free volume in the GLY-plasticized films. Furthermore, an increase in the SCL film thickness was observed parallelly with the increasing SPD amounts present in the FFS. But, unlike opacity, the thickness did not significantly change when the films were not concurrently plasticized by GLY. Conversely, in this case, the film thickness was found to slightly decrease at low SPD concentrations with respect to control samples. As far as the effect of SPD on the mechanical properties of SCL-based films, although the films prepared in the presence of SPD alone exhibited a very low EB and a very high YM, it is worthy to note that SPD conferred a minimal plasticity to the material able to give rise to manipulable and resistant films exhibiting a high TS. In fact, at very low SPD concentration (0.05 mM), as well as in its absence, it was impossible to obtain films (Table 3). More in detail, film TS and YM strongly increased in the absence of GLY, reaching at 1.0 mM SPD values (about 20 and 1760 MPa) higher than 5 and 7 times, respectively, than those of the control films manufactured in the presence of GLY and in the absence of SPD. Moreover, the presence in the SCL FFS of SPD concentrations higher than 1.0 mM progressively reduced both TS and YM of the derived films, probably leading to the formation of an excessive SPD-protein aggregation and to a consequent weakening of the film matrix. Finally, the film EB dramatically decreased in the presence of SPD, reaching, already at very low SPD concentrations, values corresponding to less than 2% of those detected with GLY-plasticized SCL films.

Opposite results were obtained when films containing both GLY and SPD were analyzed. In fact, in this case, lower TS and YM, as well as higher EB, values of the produced films were detected by adding increased amounts of SPD to GLY-containing FFSs. The highest EB value, double of the control sample one, was observed for the GLY-plasticized films containing 5.0 mM SPD whereas, by further increasing SPD concentration, the EB parallelly decreased. Conversely, the TS and YM values progressively decreased by increasing SPD concentrations.

Therefore, two different supramolecular organizations of the SCL biopolymeric matrix, due to the SPD-SCL hydrophobic interactions and hydrogen bonds, can be hypothesized when SPD is added either in the

Table 5
Gas and water vapor (WV) permeabilities of secalin-based films obtained at pH 10 in the absence or presence of 20% glycerol (GLY) and different concentrations of spermidine (SPD)*.

Addition	GLY	O_2 ($\times 10^{-10}$ cm^3 m/Pa s m^2)	CO_2 ($\times 10^{-10}$ cm^3 m/Pa s m^2)	WV ($\times 10^{-10}$ g m/Pa s m^2)
None	+	0.98 ± 0.04 [a]	1.03 ± 0.03 [a]	1.315 ± 0.002 [a]
	-	ND	ND	ND
SPD (0.05 mM)	+	0.75 ± 0.04 [b]	0.92 ± 0.01 [a, b]	1.179 ± 0.001 [b]
	-	ND	ND	ND
SPD (0.1 mM)	+	0.78 ± 0.04 [b]	0.87 ± 0.03 [b, c]	1.299 ± 0.003 [a]
	-	0.57 ± 0.03 [c]	0.81 ± 0.01 [b, c]	1.011 ± 0.002 [c]
SPD (1.0 mM)	+	0.90 ± 0.02 [d]	1.04 ± 0.01 [a]	1.454 ± 0.001 [d]
	-	0.25 ± 0.01 [e]	0.72 ± 0.02 [c, d]	0.788 ± 0.120 [e]
SPD (5.0 mM)	+	0.92 ± 0.01 [a,d]	1.66 ± 0.13 [e]	1.785 ± 0.032 [f]
	-	0.20 ± 0.01 [e]	0.63 ± 0.04 [d]	0.619 ± 0.001 [g]
SPD (10 mM)	+	1.16 ± 0.02 [f]	1.99 ± 0.05 [f]	1.854 ± 0.021 [f]
	-	0.56 ± 0.03 [c]	0.92 ± 0.01 [a, b]	0.693 ± 0.017 [e,g]
SPD (20 mM)	+	1.36 ± 0.08 [g]	3.64 ± 0.18 [g]	1.883 ± 0.003 [f]
	-	0.80 ± 0.02 [b]	1.08 ± 0.03 [a]	0.723 ± 0.009 [e,g]

*Different small letters (a-g) indicate significant differences among the values reported in each column ($p < 0.05$). ND, not detectable. Further experimental details are given in the text.

absence or presence of GLY. In fact, when GLY is present, SPD seems to facilitate the GLY-dependent reduction of the intermolecular forces along the SCL chains, consequently improving film extensibility and flexibility (EB, >200%). In this case, SPD might be considered a "secondary" plasticizer since it is able to enhance the performance of a "primary" plasticizer, such as GLY is. Conversely, when SPD is present alone, its behavior seems to be like that of a typical primary plasticizer, i.e. able to transform the SCL solution into a FFS from which a film extremely resistant (TS, about 20 MPa), but still quite flexible to be manipulable, is originated. Similar results are in agreement with previously reported data on bitter vetch protein films obtained at alkaline pH and plasticized with GLY and/or SPD (Porta et al., 2017).

3.4. Effect of spermidine on the hydrophilicity properties of secalin-based films

The low water sensitivity of edible films and coatings is one of the most important requirements in food packaging and pharmaceutical applications (da Silva et al., 2009). The results reported in Table 4 indicate that the moisture sensitivity properties of SCL-based films, including the moisture content, water solubility, and swelling ratio values, were significantly affected by the presence of SPD into the FFSs.

The moisture content of the SCL-based films containing SPD progressively decreased, both in the presence and absence of GLY, up to a SPD concentration of 1.0 mM, whereas further increase of SPD amounts led to a reversal of the observed effect. However, it is worthy to note that the GLY-free films exhibited, at all the SPD concentrations, a moisture content lower than those containing the plasticizer, confirming that the moisture affinity of hydrocolloid films was markedly influenced by the presence of hydrophilic and hygroscopic compounds, such as GLY is (da Silva et al., 2009). Also the water solubility and swelling ratio of the SPD-containing films showed similar behaviors, even though the lowest values were obtained with SCL films containing 5.0 mM SPD. It is worthy to note that the films prepared in the absence of SPD (control samples), as well as the films containing both SPD and GLY, swelled quickly after their immersion in distilled water and lost their shape and integrity, whereas the films containing only SPD maintained their integrity during soaking.

Furthermore, the data reported in Table 4 showing that the film surface contact angle significantly increased in the presence of SPD, both in the GLY-plasticized films and in those prepared without GLY, clearly confirmed the increase in film hydrophobicity determined by the SPD incorporation.

3.5. Effect of spermidine on gas and water vapor permeabilities of secalin-based films

The changes in permeability properties exhibited by the SCL films

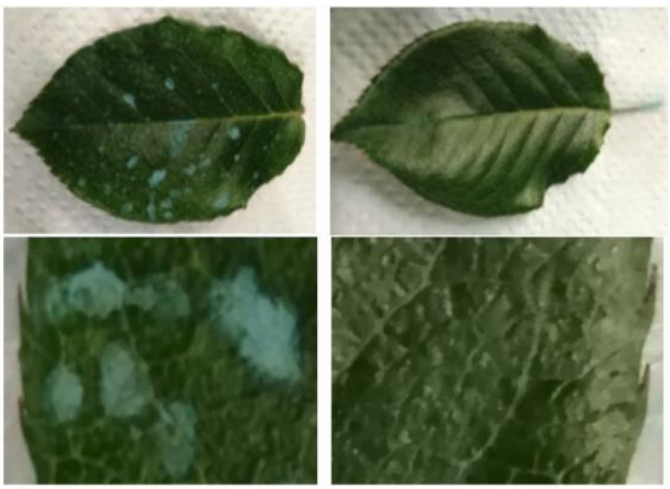

Fig. 5. Images of *Rosa chinensis* Jacq. leaves sprayed with 1% Bordeaux mixture dissolved either in water (left) or in 70% ethanol (right). The images below were obtained using a fixed digital microscopic camera to magnify the leaf surface. Further experimental details are given in the text.

Table 6
Effect of 1.0 mM spermidine (SPD) on contact angle (θ) of secalin (SCL, 700 mg) film forming solution, prepared at pH 10 in the absence or presence of both 20% glycerol (GLY) and Bordeaux mixture (1% BM), on *Rosa chinensis* Jacq. leaf surface*.

Sample	*(time 0)*	*(after 0.5 min)*	Contact angle (θ) *(after 1 min)*	*(after 3 min)*	*(after 5 min)*
Water	89.83 ± 0.31^{a}	83.15 ± 0.12^{a}	80.37 ± 0.69^{a}	67.30 ± 1.05^{a}	63.01 ± 0.56^{a}
Water + BM	69.59 ± 1.03^{b}	66.33 ± 0.80^{b}	64.39 ± 0.98^{b}	53.30 ± 1.20^{b}	48.93 ± 0.75^{b}
70% Ethanol	38.34 ± 1.43^{c}	33.23 ± 0.79^{c}	28.83 ± 0.85^{d}	21.68 ± 0.51^{c}	14.71 ± 1.01^{e,d}
70% Ethanol + BM	37.55 ± 0.63^{c}	34.55 ± 0.52^{c}	31.85 ± 0.44^{c}	21.04 ± 0.12^{c}	14.43 ± 0.57^{e,d}
SCL + GLY	33.07 ± 0.04^{d}	24.83 ± 1.23^{f}	21.20 ± 1.73^{g}	17.98 ± 1.27^{d}	15.11 ± 1.24^{c}
SCL + GLY + BM	34.41 ± 0.64^{d}	29.37 ± 0.36^{d}	26.21 ± 0.33^{c}	19.96 ± 0.40^{d}	15.13 ± 0.28^{c}
SCL + SPD + GLY	28.27 ± 0.04^{e}	24.57 ± 1.93^{f}	20.83 ± 0.47^{g}	16.90 ± 0.97^{f}	14.27 ± 0.23^{e,d}
SCL + SPD + GLY + BM	29.31 ± 0.67^{e}	27.64 ± 0.29^{e}	23.07 ± 0.29^{f}	18.31 ± 0.55^{e}	14.25 ± 0.18^{e,d}
SCL + SPD	26.87 ± 0.25^{f}	23.48 ± 0.73^{f,g}	19.88 ± 0.49^{i}	14.76 ± 0.84^{g}	11.53 ± 1.97^{d}
SCL + SPD + BM	26.93 ± 0.65^{f}	24.79 ± 0.27^{f,g}	21.45 ± 0.50^{h}	17.93 ± 0.17^{f}	11.74 ± 0.34^{d}

*Different small letters (a-i) indicate significant differences among the values reported in each column ($p < 0.05$). Further experimental details are given in the text.

obtained in the presence of different SPD concentrations confirmed the marked influence of the grafted polyamine on the film matrix structure and its functional features (Table 5). In fact, a significant increase in the barrier effect towards both O_2 and CO_2 was observed by analyzing SCL films manufactured with SPD concentration up to 0.1 mM in the presence of GLY, whereas the further increase of SPD up to 20 mM resulted in an opposite effect. These findings were more evident when the films were manufactured in the absence of GLY. But, in this case, the maximal barrier effect towards the two gases was observed with the films containing 5.0 mM SPD. Similar effects were determined by SPD on WV permeability. In fact, the barrier capacity towards WV decreased in the presence of SPD up to 10 mM in the GLY-containing films, whereas it increased in the presence of a SPD concentration up to 5.0 mM when SCL films were prepared in the absence of plasticizer. The addition of GLY is known to reduce the intermolecular forces in the film matrix and increases the protein chain mobility along with enhancing permeability to WV (Jiang et al., 2012). Moreover, as shown by the SEM images, the hydrophobic interactions and hydrogen bonds between SCL and SPD led to reduce the free hydrophilic groups of the SCL matrix, as well as to create a film network with a tortuous path for the diffusion of WV through the film network, thereby decreasing WV permeability. In conclusion, SPD was confirmed to increase the film barrier properties to both gases and WV, while GLY led to hinder this effect up to its marked reversal at highest SPD concentrations. It is worthy to note that the same effect was previously observed by testing films prepared with bitter vetch proteins in the presence of SPD (Porta et al., 2017). Therefore, the hypothesis previously advanced to consider SPD not only as a "primary plasticizer" (i.e. a compound able to make a material flexible, softer and easier to be processed), but also an "extender" able to enhance the plasticizing performance of a GLY-containing material (Porta et al.,

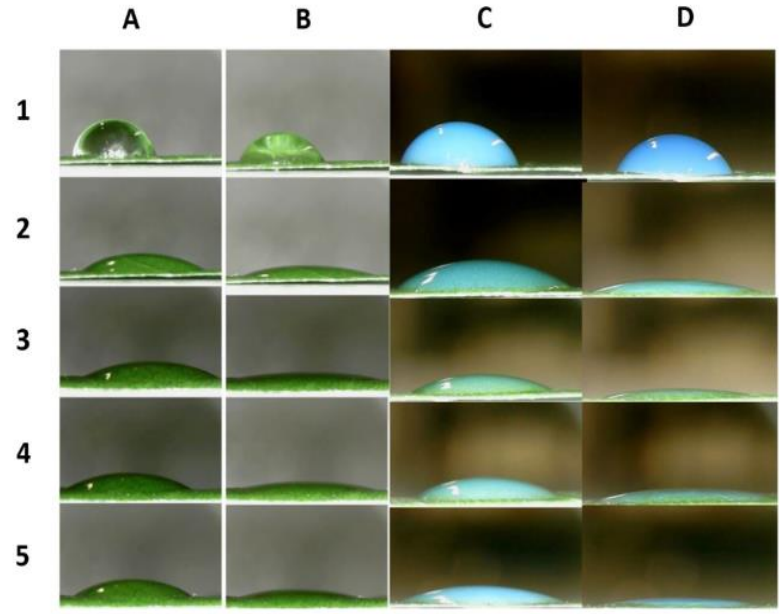

Fig. 6. Images of drops of secalin (SCL) film forming solutions (FFSs), without (A, B) or with (C, D) 1% Bordeaux mixture, on *Rosa chinensis* Jacq. leaf surfaces captured using a fixed digital microscopic camera at time 0 (A,C) and after 5 min (B,D). FFSs were prepared at pH 10 in the presence (4,5) or absence (3) of 1.0 mM spermidine and with (3,4) or without (5) 20% glycerol. Drops of both distilled water (1) and aqueous ethanol solution (2) containing 20% GLY were used as controls. Further experimental details are given in the text.

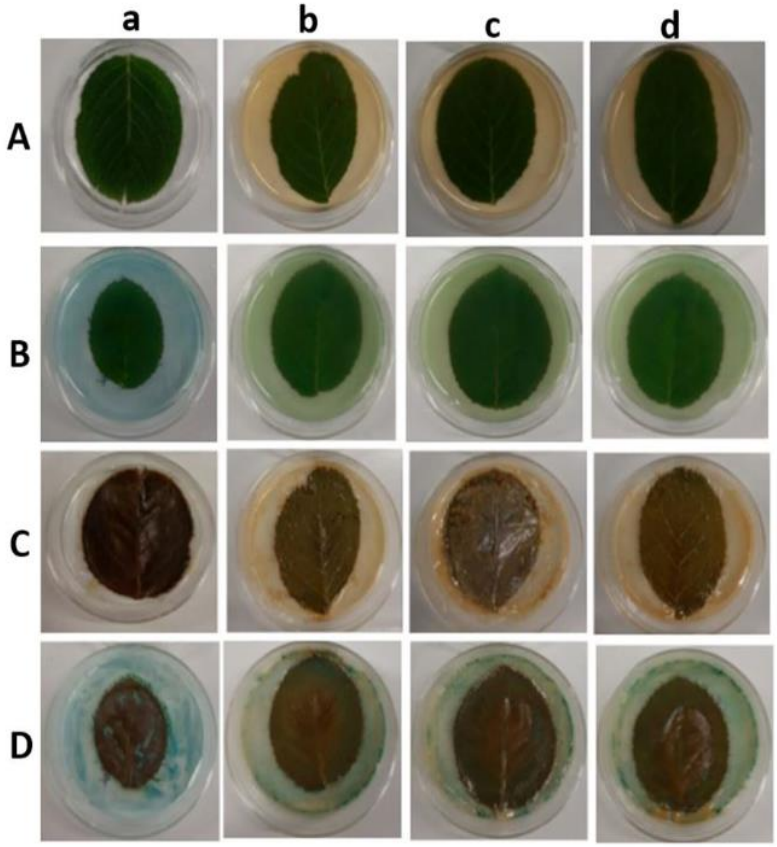

Fig. 7. Ethanol (70%) (a) and secalin film forming solutions, containing 20% glycerol (b), 1.0 mM spermidine (c) or both (d), cast onto the upper surface of *Rosa Chinensis* Jacq. leaves before (A and B) and after (C and D) drying. Bordeaux mixture (0.2%) was present in the cast solutions shown in the panels B and D. Further experimental details are given in the text.

2017; Sothornvit and Krochta, 2005), seems to be confirmed by the permeability analyses of the SCL films manufactured with SPD in the absence and presence of GLY.

3.6. Leaf coating with secalin-based film forming solutions

The development of easily volatile solutions as biodegradable carriers containing natural polymers, such as SCL, and able to deliver low volumes and amounts of agrochemicals on the leaf surfaces overtime, might represent a promising alternative to the spray application of high volumes of aqueous solutions containing large amounts of pesticides. In fact, the leaf coating with hydrophobic biopolymers dissolved in organic solvents might improve both the distribution and adhesion of specific agrochemicals on the leaf surfaces, as well as might control diseases by acting as an extra barrier to prevent plant infections (Valdes et al., 2017; Pirzada et al., 2020). With the aim to realize a targeted delivery of fungicides with low environmental impact by using an eco-friendly vehicle, the coating of *Rosa chinensis* Jacq. leaves with SCL-based films was investigated. *Rosa chinensis* Jacq. was selected both for its wide diffusion as an ornamental plant and for the quite hydrophobic surface of its leaves suitable to be sprayed with a 70% ethanol-based FFS containing SCL and either GLY (20%), SPD (1.0 mM) or both. BM (0.2%), an agrochemical widely sprayied at higher concentrations (>1%) in aqueous solution in fruit-farms and gardens to prevent infestations of downy mildew, powdery mildew and other fungi, was also added to the FFSs. It is well known that repeated applications of BM dissolved in water cause a soil buildup of copper that can be toxic to plants. Therefore, new technologies aimed at reducing the amount of BM used, by giving greater adhesion and $CuSO_4$ concentration capacity to the material sprayed on the leaf surface, are highly desirable. Preliminary experiments were carried out by spraying leaves cut off from *Rosa chinensis* Jacq. with BM dissolved either in water or in 70% ethanol, solvent used in preparing SCL-based FFSs, to obtain solutions containing 0.2–1% BM. The left images of Fig. 5 clearly show the presence of single blue spots on the *Rosa chinensis* Jacq. leaf sprayed with 1% BM dissolved in water, due to the repulsion of the BM aqueous solution by the hydrophobic leaf surface and to the consequent aggregation and evaporation of the water droplets in well bordered leaf areas. Conversely, the right images of

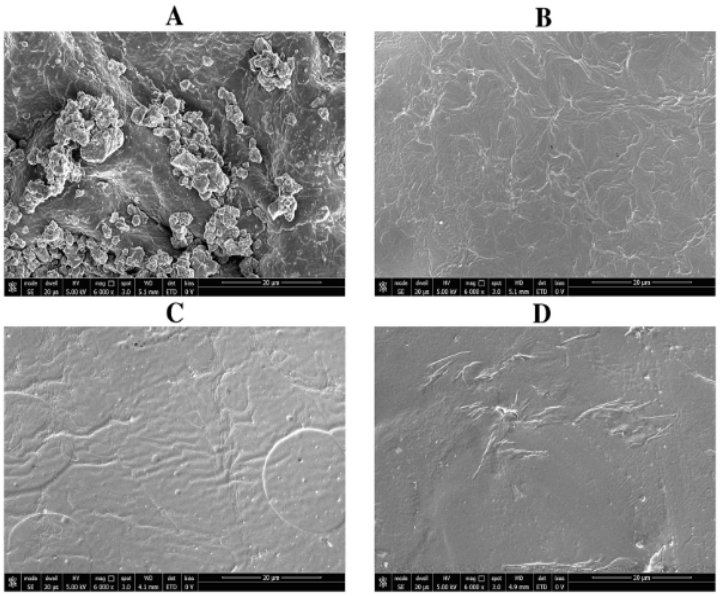

Fig. 8. SEM images at 6000 × of the leaf surfaces after casting and drying with either 70% ethanol (A) or secalin-based film forming solutions containing 0.2% Bordeaux mixture and either 20% glycerol (B), 20% glycerol and 1.0 mM spermidine (C) or 1.0 mM spermidine alone (D). After casting the leaves were dried for 12 h, conditioned for additional 12 h, and finally analyzed. Further experimental details are reported in the text.

Fig. 5 indicate that, when the leaf was sprayed with BM dissolved in 70% ethanol, a high spreading of $CuSO_4$ on the entire leaf surface occurred.

Therefore, experiments of contact angle measurements of SCL-based FFSs, by using upper side of the *Rosa chinensis* Jacq. leaf as hydrophobic surface, were carried out. The results reported in both Table 6 and Fig. 6 confirmed the data previously obtained by measuring the contact angles of the SCL-based FFSs using parafilm as hydrophobic contact surface (Fig. 1 and Table 2), and showed a high spreading of all the SCL-based FFSs, mostly those containing SPD, on the entire leaf surfaces independently on the presence or absence of BM. In addition, the data reported in Table 6 demonstrate that the presence of 1% BM in the SCL-based FFSs did not influence at all the hydrophobicity behavior of FFSs prepared with 70% ethanol, being reduced significantly only the contact angle values of the BM dissolved in water.

Moreover, also the zeta potential and average size values of the different SCL-based FFSs containing BM did not differ from those obtained in its absence and previously reported in Table 1, as well as the mechanical properties of the derived films obtained after FFS drying were not significantly influenced by the presence of BM.

Therefore, the different SCL-based FFSs, containing or not different concentrations (0.2–1%) of BM, were cast onto Petri dishes where fresh leaves of *Rosa chinensis* Jacq. were placed and fixed in such a way that the FFSs could not infiltrate under the leaves. Fig. 7 shows the images of the leaves before (panels A and B) and after (panels C and D) that the FFSs, containing (panels B and D) or not (panels A and C) 0.2% BM, were dried and the derived films on the upper leaf surface were formed.

From the SEM images of the leaf surfaces obtained after casting with the different SCL-based FFSs containing BM, it was possible to observe that an evident leaf coating occurred (Fig. 8, panels B, C and D), whereas the own structure of the leaf surface was clearly visible only when 70% ethanol was cast and left to evaporate on the leaf (Fig. 8, panel A). In addition, the film surface appeared smoother when the leaves were coated with SCL-based FFSs containing SPD alone as plasticizer (Fig. 8, panel D). Finally, it is worthy to note that coatings of very similar aspect were obtained also when FFSs prepared in the absence of BM were applied, thus indicating that, at least at the BM concentration used (0.2%), the leaf coating was not significantly influenced by the contained copper.

Furthermore, the SEM images of the cross-sections of the different samples (Fig. 9) showed leaf coatings of both aspect and thickness (60–65 μm) apparently similar, independently on the type of SCL-based FFS used. It is fair to point out that the observed separation between the coating and the leaf surface, evident in Fig. 9 (panel B, C and D), is not representative of the real morphology since it has been caused during sample preparation for SEM analysis despite the good adhesion between the two layers.

Therefore, these findings suggest the possibility to coat the leaf surface also *in vivo* with different SCL-based FFS, each capable to give rise to films possessing different and tailored functional properties. In fact, the reported results demonstrate ways to realize a leaf coating with a more resistant film (high TS value) and less repelled by the leaf surface (film derived from FFSs with low contact angle), as well as with a lower permeability to gas and WV, by spraying a SCL-based FFS containing only SPD. Conversely, a FFS containing both SPD and GLY could be useful whether a leaf coating with a film possessing a greater extensibility (high EB value) and higher gas and WV permeabilities would be needed, whereas FFSs obtained in the presence of GLY, but in the absence of SPD, would be able to produce a leaf coating thinner as well as more transparent and hydrophilic than the others.

Hydrophobic film-forming sprays can offer important advantages in comparison with the conventional topical aqueous solutions, since they might provide an uniform distribution, as well as a strong reduction of the drug amount normally used. However, the described strategy, focused on a targeted delivery of BM using FFSs derived from a naturally

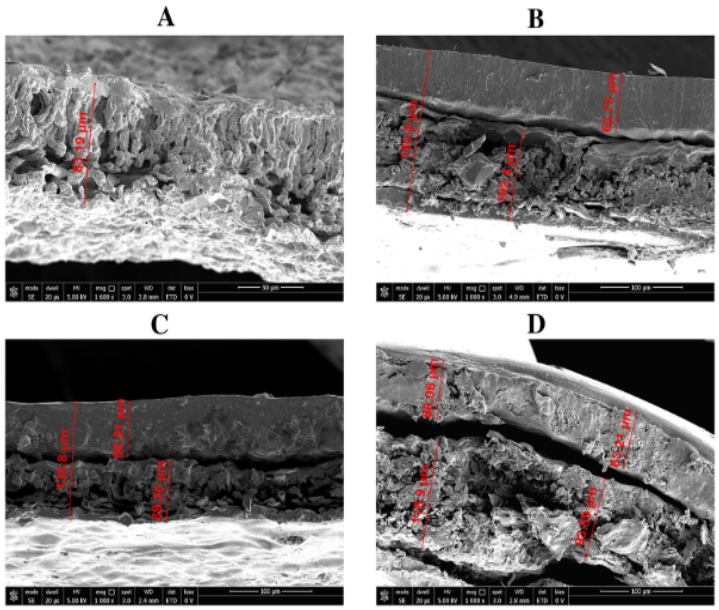

Fig. 9. SEM images of the leaf cross-sections after casting and drying with either 70% ethanol (A, at 1600x) or secalin-based film forming solutions containing 20% glycerol (B, 1000x), 20% glycerol and 1.0 mM spermidine (C, 1000x) or 1.0 mM spermidine alone (D, 1000x). The upper layer in B, C and D refers to the coating films. The thickness (μm) of both coating films and leaves is indicated in red. Further experimental details are reported in the text.

available source, deserves further studies. In this respect, experiments carried out in field with living plants are needed both (i) to optimize topical $CuSO_4$ release and (ii) to investigate the actual performance of the leaf coatings obtained by spraying a lower amount of protein in order to coat the leaves with thinner (few micrometers) films. In fact, possible interferences of the coating with the normal vital functions of the leaves, such as photosynthesis and respiration, are possible and could be prevented by a leaf coating with thinner films possessing shorter life times. In this respect, the degradation mechanisms of films of different thickness following their deposition on the plant leaves, due to photoxidative and hydrolytic agents as well as to microbial proteolytic enzymes, deserve to be investigated. As well as the life times of the films deposited on the leaves, that certainly depend on the specific environmental and climatic conditions of the treated plants, would be worthy of further studies. Furthermore, it would be of great interest also to determine the extent of reduction of the amount of agrochemical used, by spraying it dissolved in the 70% ethanol FFS instead than in a simple solvent (water or other) and, consequently, to calculate the actual decrease of its off-target deposition. However, further extensive *in vivo* leaf coating experiments are needed to verify the effective possibility to quantitatively reduce the agrochemicals to be used, with respect to the normal spraying of them through the conventional procedures, in order to reach a similar prevention or treatment of specific diseases through such a proposed greener technology.

4. Conclusions

Different 70% ethanol-based FFSs, containing SCL and either GLY, SPD or both plasticizers, were prepared and demonstrated to give rise to potentially biodegradable films with different properties and, thus, useful to be tailored for different applications. Among these, the SCL-based FFS spraying onto *Rosa chinensis* Jacq. plants has been suggested to be a promising technology to develop leaf coatings by protein films with multiple features and able to act as eco-friendly carriers of agrochemicals. The preliminary experiments carried out with different SCL-based FFSs containing BM showed the formation and uniform distribution of eco-friendly films onto the cut off leaves of *Rosa chinensis* Jacq.. These results stimulate further *in vivo* experiments to confirm that the leaf coating realized by using SCL as a naturally available source can be an effective green technology to reduce the normally used amount of agrochemicals, with a consequent decrease of their off-target deposition, and their possible release continuous and overtime.

CRediT authorship contribution statement

Zeinab Qazanfarzadeh: Conceptualization, Formal analysis, Methodology. **Seyedeh Fatemeh Mirpoor:** Data curation, Formal analysis, Methodology. **Mahdi Kadivar:** Methodology, Validation. **Hajar Shekarchizadeh:** Investigation. **Rocco Di Girolamo:** Methodology. **C. Valeria L. Giosafatto:** Project administration, Writing – original draft. **Prospero Di Pierro:** Investigation, Methodology. **Raffaele Porta:** Funding acquisition, Writing – review & editing, Project administration, Supervision.

Declaration of competing interest

The authors declare that they have no known competing financial interests or personal relationships that could have appeared to influence the work reported in this paper.

Acknowledgements

This work was supported by Italian Ministries of University and Research (PRIN: Progetti di Ricerca di Interesse Nazionale –Bando 2017– "CARDoon valorization by InteGrAted bio-refiNery, CARDIGAN, COD. 2017KBTK93).

References

ASTM. D3985, 1995. Standard test method for oxygen gas transmission rate through plastic film and sheeting using a coulometric sensor. In: Annual Book of American Standard Testing Methods. American Society for Testing and Materials, Philadephia, PA, USA, pp. 472–477.

ASTM. D882, 1998. Standard test method for tensile properties of thin plastic sheeting. In: Annual Book of ASTM Standards. American Society for Testing and Materials, Philadephia, PA, USA, pp. 163–171.

ASTM. E96, 1995. Standard test method for water vapor transmission of materials. In: Annual Book of ASTM Standards. American Society for Testing and Materials, Philadephia, PA, USA.

Azeredo, H.M., Waldron, K.W., 2016. Crosslinking in polysaccharide and protein films and coatings for food contact–A review. Trends Food Sci. Technol. 52, 109–122.

Bäumgartner, B., Möller, H., Neumann, T., Volkmer, D., 2017. Preparation of thick silica coatings on carbon fibers with fine-structured silica nanotubes induced by a self-assembly process. Beilstein. J. Nanotechnol. 8, 1145–1155. https://doi.org/10.3762/bjnano.8.116.

Bealer, E.J., Onissema-Karimu, S., Rivera-Galletti, A., Francis, M., Wilkowski, J., Salas-de la Cruz, D., Hu, X., 2020. Protein–polysaccharide composite materials: fabrication and applications. Polymers 12, 464. https://doi.org/10.3390/polym12020464.

Castro, M.J.L., Ojeda, C., Cirelli, A.F., 2014. Advances in surfactants for agrochemicals. Environ. Chem. Lett. 12, 85–95. https://doi.org/10.1007/s10311-013-0432-4.

da Silva, M.A., Bierhalz, A.C.K., Kieckbusch, T.G., 2009. Alginate and pectin composite films crosslinked with Ca^{2+} ions: effect of the plasticizer concentration. Carbohydr. Polym. 77, 736–742.

Esposito, M., Di Pierro, P., Regalado-Gonzales, C., Mariniello, L., Giosafatto, C.V.L., Porta, R., 2016. Polyamines as new cationic plasticizers for pectin-based edible films. Carbohydr. Polym. 153, 222–228. https://doi.org/10.1016/j.carbpol.2016.07.087.

Farias, B.V., Pirzada, T., Mathew, R., Sit, T.L., Opperman, C., Khan, S.A., 2019. Electrospun polymer nanofibers as seed coatings for crop protection. ACS Sustain. Chem. Eng. 7, 19848–19856. https://doi.org/10.1021/acssuschemeng.9b05200.

Galus, S., Kadzińska, J., 2016. Moisture sensitivity, optical, mechanical and structural properties of whey protein-based edible films incorporated with rapeseed oil. Food Technol. Biotechnol. 54, 78–89.

Galus, S., Arik Kibar, E.A., Gniewosz, M., Kraśniewska, K., 2020. Novel materials in the preparation of edible films and coatings—a review. Coatings 10, 674. https://doi.org/10.3390/coatings10070674.

Gevrekci, A.O., 2017. The roles of polyamines in microorganisms. ‰‰‰‰‰World J. Microbiol. Biotechnol. 33, 204. https://doi.org/10.1007/s11274-017-2370-y.

Jiang, X., Jiang, T., Gan, L., Zhang, X., Dai, H., Zhang, X., 2012. The plasticizing mechanism and effect of calcium chloride on starch/poly (vinyl alcohol) films. Carbohydr. Polym. 90, 1677–1684.

Koch, K., Barthlott, W., 2009. Superhydrophobic and superhydrophilic plant surfaces: an inspiration for biomimetic materials. Phil. Trans. R. Soc. A 367, 1487–1509.

Kouhi, M., Prabhakaran, M.P., Ramakrishna, S., 2020. Edible polymers: an insight into its application in food, biomedicine and cosmetics. Trends Food Sci. Technol. 103, 248–263.

Kritchenkov, A.S., Egorov, A.R., Volkova, O.V., Artemjev, A.A., Kurliuk, A.V., Le, T.A., Truong, H.H., Le-Nhat-Thuy, G., Thi, T.V.T., Van Tuyen, N., 2020. Novel biopolymer-based nanocomposite food coatings that exhibit active and smart properties due to a single type of nanoparticles. Food Chem. 343, 128676. https://doi.org/10.1016/j.foodchem.2020.128676.

Lorsbach, B.A., Sparks, T.C., Cicchillo, R.M., Garizi, N.V., Hahn, D.R., Meyer, K.G., 2019. Natural products: a strategic lead generation approach in crop protection discovery. Pest Manag. Sci. 75, 2301–2309. https://doi.org/10.1002/ps.5350.

Mahlein, A.K., Oerke, E.C., Steiner, U., Dehne, H.W., 2012. Recent advances in sensing plant diseases for precision crop protection. Eur. J. Plant Pathol. 133, 197–209. https://doi.org/10.1007/s10658-011-9878-z.

Nuruzzaman, M., Rahman, M.M., Liu, Y., Naidu, R., 2016. Nano- encapsulation, nano-guard for pesticides: a new window for safe application. J. Agric. Food Chem. 64, 1447–1483. https://doi.org/10.1021/acs.jafc.5b05214.

Petkoska, A.T., Daniloski, D., D'Cunha, N.M., Naumovski, N., Broach, A.T., 2021. Edible packaging: sustainable solutions and novel trends in food packaging. Food Res. Int. 140, 109981. https://doi.org/10.1016/j.foodres.2020.109981.

Pirzada, T., de Farias, B.V., Mathew, R., Guenther, R.H., Byrd, M.V., Sit, T.L., Pal, L., Opperman, C.H., Khan, S.A., 2020. Recent advances in biodegradable matrices for active ingredient release in crop protection: towards attaining sustainability in agriculture. Curr. Op. Coll. Interf. Sci. 48, 121–136.

Porta, R., 2019. The plastics sunset and the bioplastics sunrise. Coatings 9, 526. https://doi.org/10.3390/coatings9080526.

Porta, R., Di Pierro, P., Roviello, V., Sabbah, M., 2017. Tuning the functional properties of bitter vetch (*Vicia ervilia*) protein films grafted with spermidine. Int. J. Mol. Sci. 18, 2658. https://doi.org/10.3390/ijms18122658.

Qazanfarzadeh, Z., Kadivar, M., Shekarchizadeh, H., Porta, R., 2020. Rye secalin characterisation and use to improve zein-based film performance. Int. J. Food Sci. Technol. 56, 742–752. https://doi.org/10.1111/ijfs.14718.

Qazanfarzadeh, Z., Kadivar, M., Shekarchizadeh, H., Porta, R., 2021a. Secalin films acylated with capric acid chloride. Food Biosci 40, 100879. https://doi.org/10.1016/j.fbio.2021.100879.

Qazanfarzadeh, Z., Kadivar, M., Shekarchizadeh, H., Porta, R., 2021b. Functional properties of rye prolamin (secalin) and their improvement by protein lipophilization through capric acid covalent binding. Foods 10, 515. https://doi.org/10.3390/foods10030515.

Reddy, M.M., Vivekanandhan, S., Misra, M., Bhatia, S.K., Mohanty, A.K., 2013. Biobased plastics and bionanocomposites: current status and future opportunities. Prog. Polym. Sci. 38, 1653–1689.

Reichert, C.L., Bugnicourt, E., Coltelli, M.-B., Cinelli, P., Lazzeri, A., Canesi, I., Braca, F., Martínez, B.M., Alonso, R., Agostinis, L., 2020. Bio-based packaging: materials, modifications, industrial applications and sustainability. Polymers 12, 1558. https://doi.org/10.3390/polym12071558.

Roy, S., Rhim, J.-W., 2020. Preparation of carbohydrate-based functional composite films incorporated with curcumin. Food Hydrocolloids 98, 105302. https://doi.org/10.1016/j.foodhyd.2019.105302.

Sabbah, M., Di Pierro, P., Giosafatto, C.V.L., Esposito, M., Mariniello, L., Regalado-Gonzales, C., Porta, R., 2017. Plasticizing effects of polyamines in protein-based films. Int. J. Mol. Sci. 18, 1026. https://doi.org/10.3390/ijms18051026.

Sabbah, M., Di Pierro, P., Cammarota, M., Dell'Olmo, E., Arciello, A., Porta, R., 2019. Development and properties of new chitosan-based films plasticized with spermidine and/or glycerol. Food Hydrocolloids 87, 245–252. https://doi.org/10.1016/j.foodhyd.2018.08.008.

Sothornvit, R., Krochta, J.M., 2005. Plasticizers in edible films and coatings. In: Han, J.H. (Ed.), Innovations in Food Packaging, ffrst ed. Elsevier Academic Press, Cambridge, CA, USA, pp. 403–433.

Spielman-Sun, E., Avellan, A., Bland, G.D., Clement, E.T., Tappero, R.V., Acerbo, A.S., Lowry, G.V., 2020. Protein coating composition targets nanoparticles to leaf stomata and trichomes. Nanoscale 12, 3630–3636.

Til, H.P., Falke, H.E., Prinsen, M.K., Willems, M.I., 1997. Acute and subacute toxicity of tyramine, spermidine, spermine, putrescine and cadaverine in rats. Food Chem. Toxicol. 35, 337–348.

Tyagi, V., Bhattacharya, B., 2019. Role of plasticizers in bioplastics. MOJ Food Proc. Technol. 7, 128–130.

Valdes, Ramos, M., Beltran, A., Jimenez, A., Garrigos, M.C., 2017. State of the art of antimicrobial edible coatings for food packaging applications. Coatings 7, 56. https://doi.org/10.3390/coatings7040056.

Walters, D.R., 2006. Disguising the leaf surface: the use of leaf coatings for plant disease control. Eur. J. Plant Pathol. 114, 255–260.

Zhang, W., 2018. Global pesticide use: profile, trend, cost/benefit and more. Proc. Int. Acad. Ecol. Environ. Sci. 8, 1–27.

Zink, J., Wyrobnik, T., Prinz, T., Schmid, M., 2016. Physical, chemical and biochemical modifications of protein-based films and coatings: an extensive review. Int. J. Mol. Sci. 17, 1376. https://doi.org/10.3390/ijms17091376.

➢ List of Communications

1. **S.F. Mirpoor**, C. V. L. Giosafatto, C. Pezzella[2], D. Naviglio[1], L. Gardossi and R.Porta, From *Cynara cardunculus* biomass to active protein-based films. 7th International Conference on Food Chemistry & Technology (FCT-2021) - A Virtual Conference held on November 8-10, 2021.

UNIVERSITÀ DEGLI STUDI DI NAPOLI
"FEDERICO II"

FCT - 2021
Nov 08-10, 2021 | Virtual

From *Cynara cardunculus* biomass to active protein-based films

Seyedeh Fatemeh Mirpoor[1]*, C. Valeria L. Giosafatto[1], Cinzia Pezzella[2], Daniele Naviglio[1], Lucia Gardossi[3] and Raffaele Porta[1]

[1]*Department of Chemical Sciences, University of Naples "Federico II", Complesso Universitario di Monte Sant'Angelo, Naples, 80126, Italy*

[2]*Department of Agricultural Sciences, University Federico II, Via Universita` 100, 8055, Portici, Italy*

[3]*Department of Chemical and Pharmaceutical Sciences, University of Trieste, Via Licio Giorgieri 1, 34127, Trieste, Italy*

Email: seyedehfatemeh.mirpoor@unina.it , +39 3498169875

Abstract:

Cardoon *(Cynara cardunculus)* is a plant that can grow in hot and dry region, as well as in abortive soil with a high productivity. Therefore, bioactive compounds and proteins were extracted from cardoon leaves and seeds. Naviglio® technology was used to extract from leaves bioactive compounds with high phenol content and oxygen scavenging activity. Moreover, cardoon proteins (CPs) revealed the ability to give rise by casting to greenish films, in the presence of glycerol (Gly) used as plasticizer, possessing promising mechanical and barrier properties. Accordingly, to develop a bioactive film, the cardoon leaf extract (CLE) was added to the obtained CP- based films and further characterized. Microstructure of the produced films, studied by scanning electron microscopy, showed an uniform distribution of CLE among the film network. Moreover, the CP-based films developed in the presence of CLE exhibited an improvement in the mechanical and barrier properties, higher hydrophobicity and a marked antioxidant activity in comparison with the film obtained in the absence of CLE. The obtained results revealed the potential of *Cynara cardunculus* to be used as a biorefinery where different low-value renewable biomass materials are turned in several higher value bio-based products.

2. S. F. Mirpoor, Z. Qazanfarzadeh, L. V. C. Giosafattoa ,P. D. Pierro, and R. Porta, Glycerol- and/or spermidine-plasticized secalin films as potential leaf surface coatings for controlling plant diseases. 61° SIB 2021 Congress, Virtual Edition, 23-24 September 2021

UNIVERSITÀ DEGLI STUDI DI NAPOLI
"FEDERICO II"

Glycerol- and/or spermidine-plasticized secalin films as potential leaf surface coatings for controlling plant diseases

Seyedeh Fatemeh Mirpoor[a], Zeinab Qazanfarzadeh[a], L. Valeria C. Giosafatto[ab], Prospero Di Pierro[ab], and Raffaele Porta[ab]

[a]*Department of Chemical Sciences, University of Naples "Federico II", Complesso Universitario di Monte Sant'Angelo, Naples, 80126, Italy*
[b]*Center for Studies on Bioinspired Agro-Environmental Technology (BAT), University of Naples "Federico II", Naples, Italy*
e-mail: seyedehfatemeh.mirpoor@unina.it

It has been reported that around 4 million tons of pesticides are applied worldwide each year and it is estimated that at least 90% of the total amount of the applied pesticides does not reach their final target (1). Conversely, most of them is wasted through spray drift, off target deposition, leaching into the soil, as well as due to the wind, run-off, evaporation, photodegradation and microbial activity (2). Thus, there is an urgent need for innovative managements of plant disease and to improve the resiliency of agriculture globally. The approaches adopted so far to overcome the negative impacts of the agrochemicals include the use of biopesticides (3), encapsulating agents (4) and seed coatings (5). Therefore, a leaf coating with a protein-based film forming solution (FFS) containing low amounts of agrochemicals might represent an innovative green technology for plant disease control. With the aim to realize a targeted delivery of fungicides with low environmental impact by using an ecofriendly vehicle, the coating of *Rosa chinensis* Jacq. leaves with a protein-based film produced by using secalin (SCL), an alcohol soluble protein fraction extracted from rye grains, was investigated (6). Therefore, different 70% ethanol-based FFSs, containing SCL, either glycerol (GLY) or spermidine (SPD) as plasticizers, and Bordeaux Mixture (BM) were prepared. It is worthy to say that BM is an agrochemical widely sprayed at high concentrations (>1%) in aqueous solution in fruit-farms and gardens to prevent infestations of downy mildew, powdery mildew and other fungi. Preliminary experiments carried out on *Rosa chinensis* Jacq. showed the formation and uniform distribution of biodegradable films onto the cut off leaves. Preliminary experiments of contact angle measurements of SCL-based FFSs, by using upper side of the *Rosa chinensis* leaf as hydrophobic surface, showed a high spreading of the SCL-based FFSs, mostly those containing SPD, on the entire leaf surfaces independently on the presence or absence of BM. Hence, different SCL-based FFSs, containing or not different concentrations (0.2-1%) of BM, were cast onto Petri dishes where fresh leaves of *Rosa chinensis* were placed and fixed so that FFSs could not infiltrate under the leaves. SEM analyses of the leaf surfaces obtained after casting with the different SCL-based FFSs containing BM, showed the formation of an evident leaf coating, whereas the own structure of the leaf surface was clearly visible when only 70% ethanol was cast and left to evaporate on the leaf. In addition, the film surface appeared smoother when the leaves were coated with SCL-based FFSs containing SPD alone as plasticizer. Film characterization revealed that the hydrophobicity progressively decreased, both in the presence and absence of GLY, up to a SPD concentration of 1.0 mM, whereas SPD increased also the film barrier properties to gases and water vapor and the presence of GLY hindered these effects. In conclusion, these findings suggest that the leaf surface might be an effective green technology to reduce the normally used amount of agrochemicals as well as their off-target deposition.

3. **S.F. Mirpoor**, C.V.L. Giosafatto, and R.Porta, Seed oilcakes as a promising renewable resources for producing bioplastics**.** 32a RIUNIONE NAZIONALE "*A. Castellani"* DEI DOTTORANDI DI RICERCA IN DISCIPLINE BIOCHIMICHE, Brallo di Pregola (PV) 13 - 16 settembre 2021

SEED OILCAKES AS A PROMISING RENEWABLE RESOURCES FOR PRODUCING BIOPLASTICS

Seyedeh Fatemeh Mirpoor[a], C. Valeria L. Giosafatto[a], Raffaele Porta[a]

[a]*Department of Chemical Sciences, University of Naples "Federico II", Complesso Universitario di Monte Sant'Angelo, Naples, 80126, Italy. e-mail: seyedehfatemeh.mirpoor@unina.it*

One of the most crucial problems that the world is facing these days is disposing of the petroleum-based plastics since they are not biodegradable and only less than 10% of them are recycled. Petroleum-based plastic application has increased enormously in the last years causing huge waste-disposal problems and a consequent environmental pollution such as releasing of small and toxic petro-polymers in oceans and on the lands swallowed by fish and birds[1]. It is worth to say that yearly a huge amounts of waste (almost 600 million tons in 2018/2019, according to USDA) [2] are produced by oil industries and only a small amount of them are utilized as an animal feed, human nutrition, food additives and plant fertilizers, even though most of them are a rich sources of bio-active molecules, fibres, proteins and polysaccharides [3]. In this regards, the proteins existing in the oilseed cakes (SOCs) can be considered as an abundant, biodegradable and inexpensive resources for developing edible and environmental-friendly plastics in order to replace at least a portion of non-biodegradable materials that are currently used in the world.

In our work, biodegradable protein-based films were prepared from the by-product obtained from Argan (*Argania spinosa L.*), hemp (*Cannabis sativa*) and cardoon (*Cynara cardunculus* var. altilis) oilcake following the oil extraction process. Cultivation of industrial hemp with low levels of Δ9-tetrahydrocannabinol has an increasing rate due to its multipurpose utilization for a wide variety of products, such as cellulose and fiber for paper and textile, hemp seed oil and SOC for food, cosmetics and pharmaceutical industries. Although cardoon (*Cynara cardunculus* L.), a native crop belonging to the Mediterranean region, is a minor vegetable crop in most countries (except in Italy, Spain and France where it is produced in few thousands of tons/year and used in traditional dishes), it has recently achieved increasing interest and economic value due to its multipurpose applications. *Argania spinosa* L., known as Argan, belongs to the *Sapotaceae* family and it is an endemic plant of Morocco but it is also cultivated in desert and semi-desert regions such as the south-west of Algeria. SOC chemical composition is affected by different factors, primarily by the plant variety and growing conditions. The protein content in hemp SOCs is between 34 to 47.9 %, 16.5 to 21% and 40 to 48.9% for cardoon and argan, respectively [3]. Our results demonstrated that such SOCs gave rise to manipulable and handeleable films endowed with promising mechanical and water barrier properties allowing their use as good candidates for the production of eco-friendly bioplastics.

4. **S.F. Mirpoor**, Plastic and bioplastic: a sustainable alternative derived from proteins present in the by-product of the oil industry, Webinar as a young member of SIB, virtual, 16th of July 2021

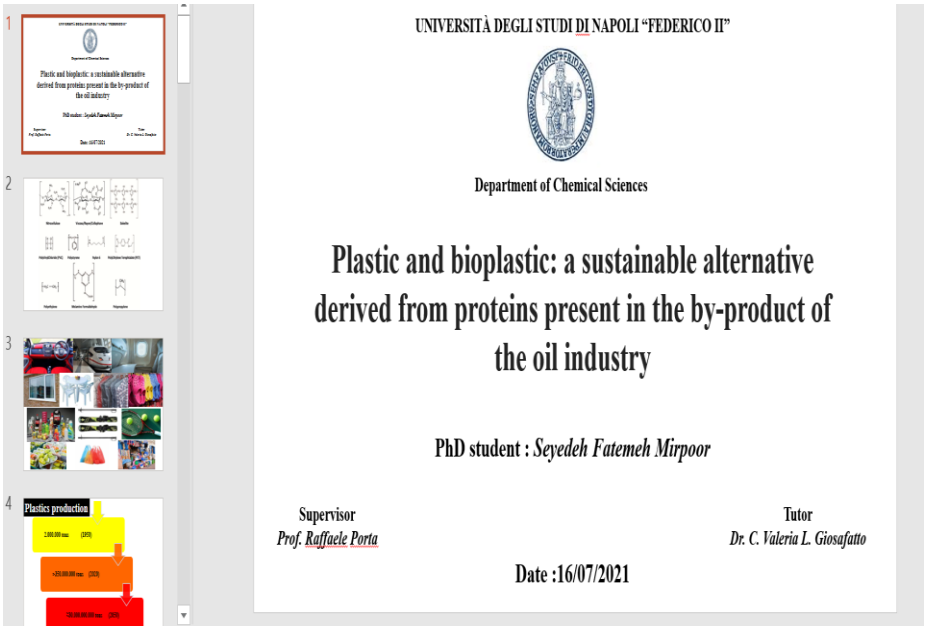

5. **S.F. Mirpoor**, C.V.L. Giosafatto, M. Maisto, G. Santagata, D. Zannini, and R.Porta, Cardoon (Cynara cardunculus) seed oilcake as natural source for bioplastics production. The 45th FEBS congress, virtual, 3-8 July 2021

UNIVERSITÀ DEGLI STUDI DI NAPOLI
"FEDERICO II"

FEBS 2021
THE 45TH FEBS CONGRESS
3-8 JULY 2021
LJUBLJANA SLOVENIA

Cardoon (*Cynara cardunculus)* seed oilcake as natural source for bioplastics production

Mirpoor, S.F., Giosafatto, C.V.L., Maisto, M., Santagata, G., Zannini, D., and Porta, R.

[1]Department of Chemical Sciences, University of Naples "Federico II", 80126 Naples, Italy; [2]Institute for Polymers, Composites and Biomaterials (IPCB) National Council of Research (CNR), Pozzuoli, 80078 Naples, Italy.

The production of innovative environment-friendly materials as substitutes of the high pollutant petroleum-derived plastics is in the spotlight. Oilseed crops produce a huge amount of protein containing by-products known as oilseed cakes, which can be considered as novel bioplastics sources. Protein concentrates (PCs) from cardoon defatted seeds were prepared and used to obtain different film forming solutions (FFSs) containing different amounts of glycerol (GLY) as plasticizer. The FFSs were characterized by dynamic light scattering and zeta-potential and the derived films analysed for mechanical properties. The results showed that the presence of 30% GLY (w/w protein) was strictly needed to provide handleable materials. Both tensile strength (TS) and Young's modulus (YM) of the films containing different amounts of PCs (200-400 mg) decreased as a function of plasticizer concentrations, whereas their elongation at break (EB) simultaneously increased. However, film TS, EB and thickness values were higher, whereas those of YM were lower, when PC concentrations were increased. Thermogravimetric and differential scanning calorimetry analyses showed that plasticized cardoon-based films were more stable than the films obtained in the absence of GLY, shifting the maximum of degradation peaks towards higher temperatures. In the attempt to reinforce film matrix, cardoon PCs were also analyzed as possible substrates of microbial transglutaminase (mTG), an enzyme catalysing the formation of protein intermolecular ε-(γ-glutamyl)-lysine crosslinks. Preliminary results showed that cardoon PC contained effective mTG protein substrates able to act as both acyl donors and acceptors giving rise to high mol.wt. polymers.

Acknowledgements: Authors acknowledge italian Ministero dell'Istruzione, dell'Università e della Ricerca for the financial support (PRIN, Progetti di Ricerca di Interesse Nazionale, 2017, COD. 2017KBTK93).

6. S.F. Mirpoor, C.V.L. Giosafatto, R. Porta, Hemp seed proteins as valuable source to obtain edible food packaging. The NIZO Plant Protein Functionality Conference - Online Edition 21-22 October 2020

UNIVERSITÀ DEGLI STUDI DI NAPOLI
"FEDERICO II"

Hemp seed proteins as valuable source to obtain edible food packaging

Seyedeh Fatemeh Mirpoor, Concetta Valeria Lucia Giosafatto, and Raffaele Porta

Department of Chemical Sciences, University of Naples "Federico II", Naples, Italy

Oilseed crops produce a huge amount of protein containing by-products known as oilseed cakes. Hemp (*Cannabis sativa* L.) is a cultivated crop of great industrial importance and hemp seed proteins (HPs) account for about 25% of total seed mass. The present study reports the ability of HP concentrate obtained from hemp defatted seeds to give rise by casting to edible films in the presence of glycerol (Gly) used as plasticizer. In particular, the effect of protein (200-400 mg) and Gly (0- 50%, w/w protein) concentrations and pH different values (7 and 12) was evaluated. The different film forming solutions (FFSs) prepared were characterized by dynamic light scattering and zeta-potential, and the derived films analysed for mechanical properties. Since the film prepared at pH 12 by using 400 mg HPs in the presence of 50% glycerol exhibited the best mechanical features, these experimental conditions were used for modifying protein structure by transglutaminase (TGase) catalyzed reactions to obtain crosslinked bio-plastics. Herein, it was found that HPs effectively act as both acyl donor and acceptor substrates of the enzyme, as demonstrated from the formation of protein polymers and the concomitant decrease in intensity of HP bands in SDS-PAGE analyses. The thickness and opacity of the films, as well as their surface hydrophobicity and water vapor barrier capacity, increased by increasing TGase amount, whereas the gas barrier properties toward CO_2 and O_2 decreased as a function of the increase of the TGase. Furthermore, it is worth to point out that FFS pretreatment with the enzyme significantly modified the film mechanical properties by increasing both tensile strength and Young's module, as well as by decreasing film elongation at break. Therefore, all these data suggest a possible utilization of proteins contained in hemp oilseed cakes as an useful source for novel food packaging material following TGase-catalyzed crosslinking.

Key words: Hemp (*Cannabis sativa* L.), food packaging, seed oilcakes, transglutaminase

7. S.F. Mirpoor, C.V.L. Giosafatto, L. Mariniello, B. Garcia-Almendarez, R. Porta, Transglutaminase - modified hemp (cannabis sativa, L.) proteins as matrix of novel bioplastics. SIB 2019_60th CONGRESS, Lecce, Italy. 18th – 20th September 2019.

TRANSGLUTAMINASE-MODIFIED HEMP *(CANNABIS SATIVA,* L.) PROTEINS AS MATRIX OF NOVEL BIOPLASTICS

*Fatemeh Mirpoor[1], C.Valeria L. Giosafatto[1], Loredana Mariniello[1], Blanca Garcia-Almendarez[2] and Raffaele Porta[1]**

[1]DEPARTMENT OF CHEMICAL SCIENCES, UNIVERSITY OF NAPLES "FEDERICO II", NAPLES, ITALY
[2]DEPARTAMENTO DE INVESTIGACIÓN Y POSTGRADO EN ALIMENTOS (DIPA), FACULTAD DE QUÍMICA, UNIVERSIDAD AUTÓNOMA DE QUERÉTARO, QUERETARO, MEXICO
**CORRESPONDING AUTHOR: raffaele.porta@unina.it*

Abstract

The huge environmental pollution caused by oil-based plastics highlight the need to produce innovative bio-based materials. Proteins are renewable biopolymers able to give rise to biodegradable/edible films either alone or blended together with polysaccharides. Hemp (*Cannabis sativa* L.) is a cultivated oleaginous crop of great industrial importance and hemp proteins (HPs), as by-product of oil extraction from their seeds, account for about 25%. Hence, HP concentrates were prepared, assayed as possible microbial transglutaminase (mTG) substrates, and used to prepare different film forming solutions (FFSs). mTG is a calcium independent enzyme catalysing the introduction of intermolecular ε-(γ-glutamyl)-lysine crosslinks into proteins via an acyl transfer reaction. In addition, endoprotein reactive lysine may be substituted with small *Mr* compounds containing primary amino groups, such as spermidine (SPD), giving rise to a variety of protein γ-glutamyl-aminoderivatives. Enzymatic mixtures containing HPs and different amounts of mTG and SPD showed that HPs effectively act as both acyl donor and acceptor substrates of the enzyme, as demonstrated from the formation of protein polymers and the concomitant decrease of intensity of HP bands in SDS-PAGE analyses. Furthermore, an evident reduction of HP mTG-catalysed crosslinking was observed in the presence of high concentrations of SPD, which indicated that the polyamine was covalently incorporated into HPs without formation of intermolecular cross-bridges among the different protein chains. Therefore, different HP FFSs were prepared both in the absence and presence of different amounts of mTG and SPD, characterized by dynamic light scattering, and the mechanical properties, as well as the water content and uptake, of the derived films were finally compared. Therefore, the possible utilization of protein containing hemp byproducts, obtained following oil extraction, may represent an useful source for novel bioplastic production.

➢ Memberships

01/02/2019 – Present

Junior Member in Italian Society of Biochemistry and Molecular Biology

15/04/2021 – Present

Member in Mediterranean and Middle East University Network Agreement (MUNA)

➢ Honours and Awards

03-05/12/2019

- Grant from Italian Society of Biological Chemistry (SIB) to participate in the Enzyme Discovery and Engineering for Biotechnological, Monte Sant 'Angelo, University of Naples Federico II, Napoli, Italy.

24-28/05/2021

- Grant from Italian Society of Biological Chemistry (SIB) to participate in the "Bioeconomy school: from basic science to a new economy" *Lake Como School of Advanced Studies*

01/09/2021 – 01/11/2021

- Grant from Italian Society of Biological Chemistry (SIB) for research stays abroad as a financial support for short periods (minimum two months) of stay abroad

01/11/2018 – present

- Ranked 2^{ed} in PhD interview of University of Naples "Federico II" among more than 60 students and won the fellowship for 3 years of PhD program

➢ Conferences

- 7th International Conference on Food Chemistry & Technology (FCT-2021) - A Virtual Conference held on November 8-10, 2021
- 61° SIB 2021 Congress, Virtual Edition, 23-24 September 2021

- 32a RIUNIONE NAZIONALE "*A. Castellani"* DEI DOTTORANDI DI RICERCA IN DISCIPLINE BIOCHIMICHE, Brallo di Pregola (PV) 13 - 16 settembre 2021

- The 45th the Federation of European Biochemical Societies (FEBS) congress, virtual, 3-8 July 2021
- The NIZO Plant Protein Functionality Conference - Online Edition 21-22 October 2020
- II Industrial Biotechnology Congress : BioID&A Biotechnology Identity and Application**,** Naples, Italy, 28th of October 2019
- 60th SIB 2021 Congress, Lecce, Italy, 18th- 20th, September 2019
- 5th Blue sky Conference on catalytic olefin polymerization, Naples, Italy, 24th of June 2019

➢ **Workshops**

- 2° Workshop BIO/10 for SIB society , Aula Magna del Complesso delle Biotecnologie, Naples, Italy, 17 May 2019.
- Tempera workshop5 – Innovative training network, Sala Azzuro, University of Naples Federico II, Napoli, Italy. 18-21 February 2019.
- Speaker in "Migrant women in university and research", Naples, Italy. 7th February 2019

➢ **Schools**

- "Bioeconomy school: from basic science to a new economy" *Lake Como School of Advanced Studies,* Lake Como, Italy, 24-28 May 2021
- School of enzyme discovery and engineering for biotechnological applications, Monte Sant ' Angelo, University of Naples Federico II, Naples, Italy. 3-5 December 2019.